

See discussions, stats, and author profiles for this publication at: <https://www.researchgate.net/publication/270221009>

ChemInform Abstract: Multimetallic Catalysis Based on Heterometallic Complexes and Clusters

ARTICLE *in* CHEMICAL REVIEWS · DECEMBER 2014

Impact Factor: 46.57 · DOI: 10.1021/cr500208k · Source: PubMed

CITATIONS

18

READS

221

3 AUTHORS, INCLUDING:



Pierre Braunstein

University of Strasbourg

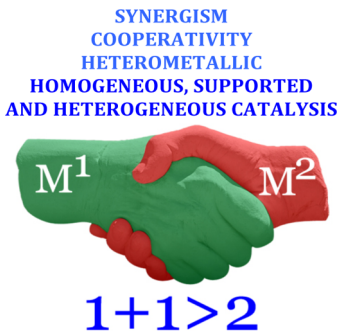
627 PUBLICATIONS 12,199 CITATIONS

[SEE PROFILE](#)

Multimetallic Catalysis Based on Heterometallic Complexes and Clusters

Paulin Buchwalter,* Jacky Rosé,* and Pierre Braunstein*

Laboratoire de Chimie de Coordination (UMR 7177 CNRS), Institut Le Bel - Université de Strasbourg, 4, rue Blaise Pascal F-67081, Strasbourg, France



CONTENTS

1. Introduction	B	2.3.3. Cr–W	J
2. Reactions in the Presence of Heterometallic Catalysts	G	2.3.4. Mo–Rh	J
2.1. Isotopic Exchanges	G	2.4. Hydrocarbon Skeletal Rearrangements	J
2.1.1. Zr–Ir	G	2.4.1. Cr–Pd	J
2.1.2. Hf–Ir	G	2.4.2. Mo–Ir	J
2.1.3. Pt–Au	G	2.4.3. W–Ir	K
2.2. Isomerization of Alkenes and Alkynes	G	2.4.4. W–Pd	K
2.2.1. Ta–Rh	G	2.4.5. Re–Os	K
2.2.2. Ta–Ir	H	2.4.6. Re–Ir	K
2.2.3. Cr–Fe	H	2.4.7. Re–Pt	K
2.2.4. Cr–Pd	H	2.4.8. Fe–Ru	K
2.2.5. Mo–Fe	H	2.4.9. Fe–Rh	K
2.2.6. Mo–Ru–Co	H	2.4.10. Fe–Pt	K
2.2.7. Mo–Pd	H	2.4.11. Ru–Ni	K
2.2.8. W–Fe	H	2.4.12. Ru–Pt	K
2.2.9. W–Ru–Co	H	2.4.13. Co–Rh	K
2.2.10. W–Pd	H	2.4.14. Co–Pt	L
2.2.11. Mn–Fe	H	2.4.15. Rh–Ir	L
2.2.12. Fe–Ru	H	2.4.16. Ir–Pt	L
2.2.13. Fe–Co	I	2.4.17. Pt–Cu	L
2.2.14. Fe–Rh	I	2.4.18. Pt–Au	L
2.2.15. Fe–Pd	I	2.5. Hydrogenation Reactions	L
2.2.16. Ru–Os	I	2.5.1. Hydrogenation of Carbon–Carbon Multiple Bonds	L
2.2.17. Ru–Co	I	2.5.2. Hydrogenation of CO and CO ₂	U
2.2.18. Ru–Ni	I	2.5.3. Hydrogenation of Aldehydes and Ketones	Z
2.2.19. Ru–Cu	I	2.5.4. Hydrogenation of Oxygen	AA
2.2.20. Ru–Au	I	2.6. Dehydrogenation of Alkanes (to Alkenes) and Alcohols (to Aldehydes)	AA
2.2.21. Os–Rh	I	2.6.1. Mo–Pt	AA
2.2.22. Os–Ni	J	2.6.2. Re–Pt	AA
2.2.23. Os–Au	J	2.6.3. Fe–Ru	AA
2.2.24. Co–Rh	J	2.6.4. Ru–Ni, Os–Ni, Os–Ni–Cu	AA
2.2.25. Co–Pt	J	2.6.5. Pt–Au	AA
2.3. Olefin Metathesis	J	2.7. Dehydration of Alcohols	AB
2.3.1. Ti–Ru	J	2.7.1. Mo–Pd	AB
2.3.2. Cr–Mo	J	2.7.2. Os–Ni	AB
	J	2.7.3. Pd–Zn	AB
	J	2.8. Water Gas Shift Reaction	AB
	J	2.8.1. Fe–Ru	AB
	J	2.8.2. Fe–Ir	AB
	J	2.8.3. Ru–Co	AB
	J	2.8.4. Ru–Rh	AB
	J	2.8.5. Co–Rh	AB
	J	2.8.6. Co–Ir	AB

Received: April 14, 2014

2.9. Oxidation Reactions	AB	2.18. Miscellaneous	BA
2.9.1. Oxidation of Alkanes and Alkenes	AB	2.18.1. Ti–Zn	BA
2.9.2. Oxidation of Alcohols	AD	2.18.2. Mo–Co	BA
2.9.3. Oxidation of CO	AE	2.18.3. Mn–Zn	BA
2.9.4. Oxidation of THF	AE	2.18.4. Re–Pt	BB
2.9.5. Oxidation of Phosphines	AE	2.18.5. Fe–Pd	BB
2.10. Carbon–Carbon Bond Formation	AE	2.18.6. Fe–Pt	BB
2.10.1. Homologation Reactions	AE	2.18.7. Co–Rh	BB
2.10.2. Carbonylation Reactions	AF	3. Synthesis of Specific Chemical Functions in the	
2.10.3. Hydroformylation Reactions	AH	Presence of Heterometallic Catalysts	BB
2.10.4. Intramolecular Hydroacylation Reac-	AM	3.1. Synthesis of Alkanes	BB
tions	AM	3.2. Synthesis of Alkenes	BE
2.10.5. Cyclopropanation of Styrene	AN	3.3. Synthesis of Alcohols	BF
2.10.6. Pauson–Khand Reactions	AO	3.4. Synthesis of Ethers	BG
2.10.7. Transformations of Ethylene	AQ	3.5. Synthesis of Aldehydes	BG
2.10.8. Transformations of Other Linear Ole-	AR	3.6. Synthesis of Ketones	BH
fins	AR	3.7. Synthesis of Carboxylic Acids	BH
2.10.9. Transformations of Norbornadiene	AR	3.8. Synthesis of Esters	BH
2.10.10. Trimerization of Alkynes	AR	3.9. Synthesis of Lactones	BI
2.10.11. Coupling Reactions	AR	3.10. Synthesis of Acetals	BI
2.10.12. Other Carbon–Carbon Bond Forma-	AT	3.11. Synthesis of Ketals (by Addition of Alcohols	
tion Reactions	AT	to Alkynes)	BI
2.11. Carbon–Nitrogen Bond Formation	AT	3.12. Synthesis of Isocyanates and Carbamates	
2.11.1. Carbonylation of Organic Nitro Deriv-	AT	(by Carbonylation of Organic Nitro Deriv-	
atives	AU	3.13. Synthesis of Ammonia	BJ
2.11.2. Other Carbon–Nitrogen Bond Forma-	AV	3.14. Miscellaneous	BJ
tion Reactions	AV	4. Conclusion	BJ
2.12. Carbon–Oxygen Bond Formation	AV	Author Information	CI
2.12.1. Addition of Alcohols to Alkynes	AV	Corresponding Authors	CI
2.12.2. Addition of Carboxylic Acids to Al-	AW	Notes	CI
kynes	AW	Biographies	CI
2.12.3. Cycloaddition of CO ₂ and Alkynes	AW	Acknowledgments	CJ
2.12.4. Transesterification	AW	Abbreviations	CJ
2.13. Metal–Carbon Bond Formation	AW	References	CJ
2.13.1. Mo–Pd, W–Pd	AW		
2.14. Silylation Reactions	AX		
2.14.1. Hydrosilylation of Olefins and Alkynes	AX	1. INTRODUCTION	
2.14.2. Hydrosilylation of Ketones	AY	Multimetallic catalysis is based on the combined action of	
2.14.3. Silylformylation Reactions	AY	different metals in a chemical transformation. It has witnessed	
2.15. Reduction of Nitrogenated Compounds	AY	rapidly increasing developments during the past decades in	
2.15.1. Reduction of NO	AZ	numerous areas of chemistry. A close proximity between the	
2.15.2. Reduction of Nitrates and Nitrites	AZ	metal centers thus appears to provide favorable conditions for	
2.15.3. Reduction of Nitrobenzene to Aniline	AZ	the occurrence of enhanced catalytic properties, and this	
2.15.4. Reduction of Hydrazines to Amines	AZ	proximity can result from the existence of direct metal–metal	
2.15.5. Hydrogenation of N ₂	AZ	interactions. It was in 1963–64 that F. A. Cotton first defined	
2.16. Hydrodesulfurization and Hydrodenitroge-	AZ	metal atom clusters as “compounds containing a finite group of	
nation	AZ	metal atoms which are held together entirely, mainly, or at least	
2.16.1. Mo–W–Fe, Mo–W–Co, Mo–W–Ni	AZ	to a significant extent, by bonds directly between the metal	
2.16.2. Mo–Fe	AZ	atoms even though some non-metal atoms may be associated	
2.16.3. Mo–Fe–Co	AZ	intimately with the cluster”, and it is also ca. 50 years ago that	
2.16.4. Mo–Ru	AZ	he reported the ground-breaking discovery of metal–metal	
2.16.5. Mo–Co	AZ	quadruple bonding. ¹ Almost inevitably, the exact nature of a	
2.16.6. Mo–Rh, Mo–Ir	BA	catalytically (very) active species remains usually unknown due	
2.16.7. Mo–Ni	BA	to its elusiveness, whether in homogeneous or in heterogeneous	
2.16.8. Mo–Pd, Mo–Pt	BA	phases. When heterometallic clusters are used as precatalysts, it	
2.16.9. W–Fe, W–Co	BA	remains to be demonstrated whether they retain their integrity	
2.16.10. W–Rh	BA	during the catalytic cycle, and one cannot claim without strong	
2.16.11. W–Ni	BA	evidence that they are the actual catalysts. However,	
2.16.12. Ru–Co	BA	(reversible) cluster fragmentation may well occur to generate	
2.17. Dehydrogenation of Amine-boranes	BA	coordinatively unsaturated species otherwise not accessible, the	
2.17.1. Zr–Fe	BA	cluster acting as a “reservoir” of highly reactive species.	
2.17.2. Zr–Ru	BA	Notwithstanding these considerations, we shall refer in the	
2.17.3. Hf–Ru	BA		

following to the clusters discussed as “catalysts” for commodity. Diverse communities of chemists may employ different definitions, and it is probably appropriate at the onset of this Review to clarify terms that will be used in the following. Some authors apply the term “bimetallic” to hetero- as well as homodinuclear systems, whether metal–metal bonding is present or not; others specify “heterobimetallic” but include heterodi- or polynuclear complexes. In this Review, bimetallic will be used in the sense of heterometallic (metals of a different chemical nature), and the number of metal atoms forming the core of the molecular precursor defines its nuclearity. Particularly attractive features in bi- or multimetallic (more than two chemically different metals) are the possible cooperativity and synergistic effects that can arise from the simultaneous or consecutive action of different metal centers in a homogeneous or heterogeneous medium or in ion–molecule reactions.² Positive cooperativity occurs when the affinity for binding of a substrate with multiple binding sites to a metal is increased upon fixation to another metal. Synergism applied to heterometallic reactivity and catalysis can be considered to occur when the interaction of a substrate with a heterometallic system produces a combined effect greater than the sum of separate effects observed with the corresponding homometallic components of similar nuclearity (mono- or polynuclear). Each metal center may be specifically responsible for elementary steps/transformations contributing to the overall transformation under investigation. Furthermore, a heterometallic metal–metal bond possesses an intrinsic polarity that offers unique reaction pathways. One may thus envisage that the sharing of electrons between the metals forming the bi- or multimetallic system will be at the origin of the specific reactivity observed. This electronic explanation may apply to molecular systems (i.e., homogeneous catalysts) and to surfaces or nanoparticles (i.e., heterogeneous catalysts). However, a metal center may (also) play the role of a ligand toward its neighbors so that considering the overall stereoelectronic consequences of transforming a homometallic into a heterometallic system may be a more relevant approach to discuss bimetallic effects. Substrate binding to M¹ is expected to affect the interaction of this metal with M², and, conversely, metal M² can be viewed as a “ligand” for M¹ and modify its stereoelectronic interactions with the substrate when compared to a mononuclear complex. Obviously, when the substrate occupies a bridging position between two or more metal centers, it will be most sensitive to their nature (Scheme 1). The relative weight of electronic versus ligand effects remains very difficult to assess and has to be discussed on a case-by-case basis.

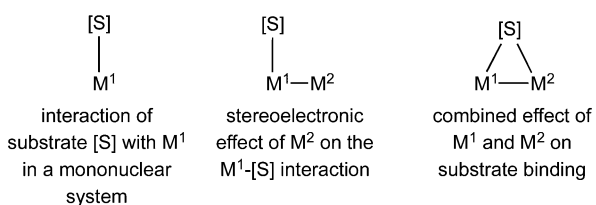
Furthermore, in heterogeneous systems, concepts based on the size of the ensemble formed by the active metal have often supplanted the electronic theory.³ Here, the progressive

addition of a second metal may be viewed as “diluting” the first, leading to smaller ensembles. The strength of the metal–support interactions is also known to considerably influence the catalytic properties. In addition, the structure and composition of a surface will also strongly depend on the interacting substrates, and reconstructions and selective metal migration from the core to the surface, or vice versa, are well-known phenomena. It is striking to see the developments of heterogeneous bimetallic catalysts containing gold, a noble metal known for its lack of reactivity in the bulk state.⁴ Supported gold-containing bi- and trimetallic nanoparticles often display unique catalytic properties,⁵ but such systems will not be discussed here when they are not obtained from molecular, mixed-metal clusters. The often unique properties of transition metal-based heterometallic systems have long been recognized by nature, which uses them as enzymes cofactors to perform diverse chemical reactions. This is the case in, for example, Fe–Mo and V–Fe nitrogenases, Ni–Fe hydrogenases, and Ni-[3Fe-4S]⁺ CO dehydrogenases where the association of a mid- and late-first row transition metal promotes the heterolytic activation of small molecules. In class Ic ribonucleotide reductases, Fe and Mn are responsible for the tuning of the redox properties of the cofactor.⁶ Motivated by the development of the H₂ economy, very efficient mimic complexes of NiFe hydrogenases have been discovered in the past decades, some containing the same metal centers, Fe and Ni, as in the natural active site, other bearing ruthenium and nickel centers.⁷

An example of industrial application of heterometallic systems in homogeneous catalysis is the Cativa process developed by BP Chemicals for the production of acetic acid by carbonylation of methanol.⁸ It involves the use of an iridium iodo-complex as catalyst, [IrI₂(CO)₂]⁻, promoted by a ruthenium iodo-complex, and this combination leads to a catalyst that is superior to the rhodium-based systems developed by Monsanto. Although the (pre)catalyst is not heterometallic, intermediates have been suggested on the basis of ¹³C NMR spectroscopy that contain both metals in the same molecule.⁹ Similarly, the combined positive effect of iridium and platinum in the carbonylation of methanol to acetic acid has been evidenced.¹⁰ Heterogeneous bimetallic catalysts based on the couples Mo–Ni and Mo–Co,¹¹ or Re–Pt–S,¹² are commonly used in industry for hydrodesulfurization and naphtha reforming, respectively.

Synthetic inorganic chemists have shown great skills at creating new metal–metal bonds and building and characterizing novel and fascinating architectures in the field of heterometallic transition metal clusters.¹³ In these complex molecules, the presence of direct metal–metal interactions offers the unique advantage of bringing metal centers of a different nature in close proximity, thus favoring multisite interactions with substrates leading to a molecular activation that mononuclear complexes (or even homomultinuclear clusters) are not able to achieve. It is of course clear that ions of the same metal, even in the same oxidation state, but placed in different coordination environments generated by a multtopic ligand, will acquire different chemical properties and may confer to such di- or polynuclear complexes properties superior to those of the corresponding mononuclear complexes.¹⁴ Such homometallic systems will however not be discussed within the scope of this Review. As specified above, the metals contained in the molecular precursors to the catalysts investigated will be of a chemically different nature,

Scheme 1. Influence of a Second Metal, Chemically Different, on the Binding of a Substrate to a Metal Center^a



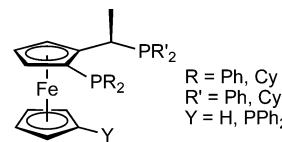
^aSynergism may arise from such interactions.

and we will be dealing here mostly with heterometallic systems displaying metal–metal interactions. In selected cases, we will mention examples of non metal–metal bonded heterometallic systems when relevant synergistic effects have been evidenced. Assembling ligands, such as the popular class of short-bite diphosphines of the dppm- or dppa-type, can be used to favor the direct interaction between different metal centers and thus promote bimetallic reactivity. More generally, ligand design has become an integral part of homogeneous catalysis and allows for tunability of the metal(s) coordination sphere, including the stabilization in the ground state of “masked” coordination sites that may become available in solution for substrate binding during the catalytic cycle, as found in hemilabile systems.¹³ With the emergence and rapidly increasing number of large nuclearity, low oxidation state homo- and heterometallic clusters, from a dozen to a few hundreds of metal atoms, it became clear that the manner in which the ligands, often carbon monoxide, were arranged around the metal centers was clearly reminiscent of the way in which they interact with metal surfaces. Furthermore, when the nuclearity of the cluster increases, the structure adopted by its metal core becomes strikingly similar to that of the same metal in the bulk state.¹⁶ These observations on the bonding modes of small molecules, like CO or arenes, in molecular clusters led to the development of “cluster-surface” structural analogy¹⁷ and to the idea of using heterometallic molecular clusters as precursors to mixed-metal nanoparticles.¹⁸ The possibility emerged to access alloy nanoparticles from mixed-metal clusters after removal of the ligand shell under mild conditions. This approach is particularly appealing for metals that are not miscible in the bulk because it can lead to new, metastable phases endowed with unique chemical properties.¹⁹ For example, Ru and Au do not form alloys, although molecular clusters containing these metals are well-known.²⁰

Mixed-metal clusters have become unique molecular precursors to heterogeneous catalysts that offer the potential of fine-tuning their intermetallic ratio and retaining it in the resulting bimetallic particles. This application extends and complements their use in homogeneous or supported catalysis, where they may behave as intact molecular entities or as reservoirs of reactive moieties upon reversible fragmentation. Examples where bimetallic activation and catalysis have been noted with bimetallic precursors that are outside the scope defined above because of a clear lack of metal–metal interaction will still be mentioned when the corresponding bimetallic couple is otherwise not represented. Other examples are briefly mentioned below to provide the reader with relevant references.

Substituted ferrocenyls constitute a large family of ligands that find applications in homogeneous catalysis, and generally lead to non metal–metal bonded heterometallic complexes (a few exceptions include Zr–Fe or Ti–Fe interactions and the applications of such complexes in olefin polymerization catalysis²¹) when coordinated to metals,²² such as palladium or, to some extent, nickel and platinum. In particular, asymmetric and highly enantioselective reactions can be carried out with such catalysts, and complexes of Josiphos (Scheme 2) are probably the best-known examples. Almost any type of functional group can be introduced on the ferrocenyl skeleton. Other metallacycles can be formed with non-Fe metals, and they are active in asymmetric and enantioselective catalysis as well.²³ Because the literature in this field is very rich and many

Scheme 2. Ferrocenyl-type Ligand Josiphos



aspects have been reviewed recently,²² we shall not deal with those ferrocenyl metallacycles in this Review.

Heterodinuclear complexes in which the metal centers are not directly bonded to each other but connected via bridging ligand(s) have been successfully used as catalysts for a variety of organic transformations and exhibited cooperative effects.^{14,24} Similarly, heterometallic complexes bearing bridging N-heterocyclic carbene ligands have proved to be excellent catalysts in tandem processes.²⁵ Other significant examples of homogeneous catalysis by heterometallic complexes bearing no metal–metal bond have been discussed recently,¹⁴ and will not be included in this Review.

Heterometallic clusters containing group 14 and 15 elements (Sn, Pb, Sb, Bi) have been used in homogeneous and heterogeneous catalysis, because they often improve the activity and the lifetime of the catalysts. In this regard, tin is of particular interest,²⁶ as it appears to greatly enhance the activity of known catalysts, especially heterogenized Pt-based catalysts.²⁷ Tin has also been associated with Ir²⁸ and Ru.²⁹ Thomas et al. have made major contributions in this field.³⁰ They prepared bi- and trimetallic Ru_xSn_y and Ru_xPtSn_y nanoparticles (NPs) with various stoichiometries from organometallic precursors for applications in the hydrogenation of polyenes. Lead has also been used in bimetallic couples with transition metals, but to a lesser extent. For instance, a complex analyzed as [PdPb(OAc)₄] was used in the acyloxylation of benzene derivatives.³¹ Heterogeneous catalysts of compositions Re₂Sb, Re₂Sb₂, and Re₂Bi₂, derived from molecular clusters, have been used in the synthesis of vitamin B3.³² A carbon-supported PdBi catalyst for the oxidation of D-glucose was obtained from the cluster [Bi₂Pd₂(O₂CCF₃)₁₀(HO₂CCF₃)₂].³³ Also, [Ir₃Bi] and [Ir₅Bi₃] NPs, obtained by thermal activation of the clusters [Ir₃(CO)₉(μ₃-Bi)] and [Ir₅(CO)₁₀(μ₃-Bi)₂(μ₄-Bi)], respectively, were used as catalysts for the oxidation of 3-picoline to niacin.³⁴

Heterogeneous supported catalysts have been prepared from double salt metal complexes where no heterometallic bond is present and afforded CoPt and CoRh catalysts for preferential CO oxidation in the presence of H₂,³⁵ and steam reforming, respectively.

The applications of polyoxometallates in catalysis have been reviewed;³⁶ therefore, we shall not deal with those compounds in this Review. Metal–organic frameworks (MOFs) find increasing applications in catalysis as new support materials, because of their high surface areas, tunable compositions, possible substrate size selectivity, and potential enantioselectivity.³⁷ However, much research remains to be developed in this field. Some MOFs can be built from two or more different metals, but very few have actually been used as catalysts. In most cases, one type of metal atoms is meant to be the active site, while the other is only present for structural reasons. Postsynthetic functionalization is also possible for such materials.

In the course of gas-phase studies performed in an ion cyclotron resonance mass spectrometer of “naked” reactants for

Table 1. List of Metal Couples in Molecular Mixed-Metal Clusters Used as Precursors to Homogeneous, Immobilized, and Heterogeneous Catalysts

catalyzed reaction	homogeneous catalysts	immobilized catalysts	heterogeneous catalysts
isotopic exchanges	Zr–Ir, Hf–Ir, Pt–Au	Pt–Au	Pt–Au
isomerization of alkenes and alkynes	Ta–Rh, Ta–Ir Cr–Fe, Cr–Pd Mo–Fe, Mo–Ru–Co, Mo–Pd W–Fe, W–Ru–Co, W–Pd Mn–Fe, Fe–Ru, Fe–Co, Fe–Rh, Fe–Pd Ru–Co, Ru–Ni, Ru–Cu, Ru–Au Os–Rh, Os–Ni, Co–Pt	Ru–Os Os–Rh, Os–Au	Fe–Pd, Ru–Os, Co–Rh
olefin metathesis	Ti–Ru	Cr–Mo, Cr–W	Mo–Rh
hydrocarbon skeletal rearrangements			Cr–Pd, Mo–Ir, W–Ir, W–Pd Re–Os, Re–Ir, Re–Pt Fe–Ru, Fe–Rh, Fe–Pt, Ru–Ni, Ru–Pt Co–Rh, Co–Pt, Rh–Ir, Ir–Pt, Pt–Cu, Pt–Au
hydrogenation of C–C multiple bonds	V–Fe, Ta–Rh, Ta–Ir, Cr–Pd Mo–Fe, Mo–Fe–Co, Mo–Ru–Co Mo–Co, Mo–Co–Ni, Mo–Rh, Mo–Ir Mo–Pd, Mo–Pt W–Fe–Co, W–Os, W–Rh, W–Ir W–Ni, W–Pd, W–Pt Mn–Fe, Mn–Ru Re–Rh, Re–Pt Fe–Ru, Fe–Ru–Co, Fe–Rh, Fe–Pd Ru–Co, Ru–Rh, Ru–Ir, Ru–Ni, Ru–Pt Os–Ni Co–Rh, Co–Pt, Rh–Au, Ir–Pt	Mo–Pd	Ta–Rh, Ta–Ir Mo–W–Fe, Mo–W–Co, Mo–W–Ni Mo–Fe, Mo–Fe–Co, Mo–Ru Mo–Co, Mo–Rh, Mo–Ir Mo–Ni, Mo–Pd, Mo–Pt W–Fe, W–Co, W–Ni, W–Pt Fe–Ru, Fe–Co Ru–Os, Ru–Co, Ru–Ni, Ru–Pd, Ru–Pt Ru–Cu, Ru–Ag Os–Ni, Os–Ni–Cu Co–Rh, Rh–Pt Pt–Cu, Pt–Au Cr–Ru, Cr–Co, Cr–Pt Mo–Fe, Mo–Ru, Mo–Os Mo–Co, Mo–Rh, Mo–Ni W–Os, W–Rh, W–Ir, W–Pt Mn–Fe, Mn–Ru, Mn–Co, Re–Os Fe–Ru, Fe–Os Fe–Co, Fe–Rh, Fe–Ir, Fe–Pd, Fe–Pt Ru–Os, Ru–Co, Ru–Rh, Ru–Ni Os–Rh, Os–Ni, Co–Rh, Co–Cu Mo–Co, Mo–Rh, Ru–Pt Os–Ni, Co–Cu, Co–Zn Pt–Au
hydrogenation of CO and CO ₂	Ti–Rh, Mo–Ru, W–Ru Mn–Rh, Mn–Pd, Re–Rh Fe–Co Ru–Co, Ru–Rh, Ru–Cu, Ru–Ag, Ru–Au Co–Rh Rh–Ir, Rh–Pt, Rh–Cu, Rh–Ag, Rh–Au, Rh–Zn	Co–Rh	Cr–Ru, Cr–Co, Cr–Pt Mo–Fe, Mo–Ru, Mo–Os Mo–Co, Mo–Rh, Mo–Ni W–Os, W–Rh, W–Ir, W–Pt Mn–Fe, Mn–Ru, Mn–Co, Re–Os Fe–Ru, Fe–Os Fe–Co, Fe–Rh, Fe–Ir, Fe–Pd, Fe–Pt Ru–Os, Ru–Co, Ru–Rh, Ru–Ni Os–Rh, Os–Ni, Co–Rh, Co–Cu Mo–Co, Mo–Rh, Ru–Pt Os–Ni, Co–Cu, Co–Zn Pt–Au
hydrogenation of aldehydes and ketones	Cr–Ru, Mo–Ru, W–Ru Fe–Ru, Ru–Rh, Ru–Ir		
hydrogenation of oxygen			
dehydrogenation of alkanes and alcohols			
dehydration of alcohols	Mo–Pd		
water gas shift reaction	Fe–Ru, Fe–Co, Fe–Ir, Ru–Co, Ru–Rh Co–Rh, Co–Ir		Os–Ni, Pd–Zn
oxidation of alkanes and alkenes	Fe–Co, Fe–Co–Cu Co–Cu, Co–Cu–Zn, Pd–Cu	V–Co, V–Rh	Cr–Mn, Cr–Co, Mn–Co, Fe–Au, Pt–Au
oxidation of alcohols	Cr–Ru, Cr–Os, Ru–Ni, Ru–Pd, Ru–Pt	Fe–Cu	Ta–Re, Fe–Au, Ru–Pt, Co–Ni
oxidation of CO		Pt–Au	Fe–Pt, Fe–Au, Pt–Au
oxidation of THF	Mo–Ru		
oxidation of phosphines	Cr–Os, Ru–Pd		
homologation reactions	Mn–Pd, Fe–Co Ru–Co, Ru–Co–Cu, Ru–Co–Au, Ru–Rh Os–Co, Co–Rh, Co–Pd, Co–Pt		
carbonylation of alcohols	Mo–Fe, Fe–Rh, Fe–Ni, Fe–Cu, Fe–Hg, Os–Ir, Ir–Pt		
hydrocarbonylation reactions	Co–Rh		Ru–Co, Co–Pd
carbonylation of olefins	Zr–Rh, Fe–Pd		
other carbonylation reactions	Co–Pd, Co–Pt		Co–Rh
hydroformylation of olefins	Ti–Rh, Zr–Rh, Cr–Ru, Cr–Pd Mo–Fe–Co, Mo–Ru, Mo–Co, Mo–Co–Ni W–Ru, W–Rh, W–Pd, Mn–Rh	Ru–Co Co–Rh Co–Pd	Mo–Rh, Fe–Rh, Fe–Ir, Fe–Pd, Fe–Pt Ru–Co, Co–Rh, Co–Cu

Table 1. continued

catalyzed reaction	homogeneous catalysts	immobilized catalysts	heterogeneous catalysts
other hydroformylation reactions	Fe–Ru, Fe–Co, Fe–Rh, Ru–Co, Ru–Rh Co–Rh, Co–Ni, Co–Pt, Rh–Zn, Ir–Cu		
intramolecular hydroacylation reactions	Co–Rh		
cyclopropanation of styrene	Ti–Rh		
Pauson–Khand reactions			Co–Rh
transformations of ethylene			V–Cr, Cr–Mo, Fe–Ru
transformations of other linear olefins	Ti–Ru, Ta–Ru, Mo–Cu, Fe–Cu Fe–Co, Ru–Co, Co–Pt Ti–Zr, Ti–Cr, Ti–W, Ti–Pd, Ti–Pt Zr–Hf, Zr–Cr, Zr–Mo, Zr–Fe, Zr–Co, Zr–Rh Zr–Ni, Zr–Pd, Hf–Rh, Fe–Co		
transformations of NBD	Ti–Zr, Ti–W, Zr–Hf, Zr–Cr, Zr–Mo, Zr–Fe Zr–Co, Zr–Rh, Zr–Ni, Hf–Rh, Mo–Pd, W–Pd Co–Pt	Cr–Mo	
trimerization of alkynes coupling reactions	Mo–Pt, W–Pt, Fe–Co, Fe–Pt, Co–Pt Co–Zn, Co–Cd, Co–Hg Cr–Rh, Mo–Ru	Fe–Co	
other C–C bond formation reactions	Ti–Pd, Zr–Co, Zr–Pd, Hf–Co, Cr–Ni, Mo–Pd		
carbonylation of organic nitro derivatives	W–Pd, Fe–Pd, Ru–Pd, Co–Pd, Pd–Pt		Mo–Pd, Fe–Pd
other C–N bond formation reactions	Fe–Cu, Co–Zn, Cu–Zn		
addition of alcohols to alkynes	Fe–Rh, Ru–Rh, Os–Rh, Os–Au		
addition of carboxylic acids to alkynes	Mo–Pd, Co–Pd, Pd–Ag	Co–Rh	
cycloaddition of CO ₂ and alkynes	Ir–Pd, Ir–Pt		
transesterification	Ti–Ru, Mo–Ni, Mo–Pd, Re–Ru		
metal–C bond formation reactions	Co–Zn, Co–Cd, Zn–Cd	Fe–Rh	
hydrosilylation of olefins and alkynes	Mo–Pd, W–Pd		
hydrosilylation of ketones	Ti–Rh, Nb–Rh, Ta–Rh, Ta–Ir		
silylformylation reactions	Mo–Fe–Co, Mo–Co, Mo–Co–Ni		
reduction of NO	Mo–Pd, Mo–Pt, W–Co, W–Pd, W–Pt		
reduction of nitrates and nitrites	Fe–Co, Fe–Rh, Fe–Pt, Ru–Pt, Os–Pt		
reduction of nitrobenzene to aniline	Co–Ni, Ir–Pt		
reduction of hydrazines to amines	Zr–Co	Co–Rh	
hydrogenation of N ₂			Mo–Pd, Mn–Fe, Fe–Co, Fe–Ni, Pt–Au
HDS and HDN	Mo–Co, W–Rh, W–Ni	Mo–Fe	
dehydrogenation of amine-boranes	Zr–Fe, Zr–Ru, Hf–Ru	Ru–Pt, Co–Rh	

the thermal activation of methane, a comparison was made between [VNbO₅]^{•+} and [V₂O₅]^{•+}, which emphasized the crucial role of oxygen-centered radicals. Under similar conditions, catalytic redox reactions involving CO and N₂O were carried out in the presence of the couple AlVO₃^{+/2m},³⁸ AlVO₄^{+/2m}. Incorporation of V and Ti ions in the framework of aluminophosphate molecular sieves has been used to study catalytic synergism in selective aerobic oxidation reactions.³⁹ In this Review, we wish to highlight the diversity of catalytic reactions based on the use of heterometallic complexes and clusters in homogeneous, supported, or heterogeneous systems. Heterodinuclear complexes will be included when there is metal–metal bonding and/or close proximity between the metal centers, although bimetallic effects have been observed in

heterometallic complexes in which the metals are far apart from each other (see above). In the latter cases, a consecutive rather than a concerted action of the metals occurs. We realize that this distinction may be somewhat arbitrary because metal–metal interactions can span a large range of distances, in particular in the presence of flexible bridging ligands, and this applies to the molecular precursors as well as to the active species for which there is generally no structural information available.

Sections 2 and 3 provide complementary information, since the former presents, for each catalytic reaction considered, an exhaustive list of the catalysts ranked by metal couple, whereas the latter introduces the metal couples that were successfully used in a given catalytic reaction, thus providing general trends

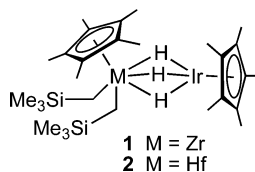
on results and performances of these catalysts. In the following, the metal couples are listed in order of earliest group, and within each group, the earliest metal is given first (e.g., Cr–M will appear before Mo–M and W–M for M in group ≥ 7). This classification will generally be followed throughout, and, as mentioned earlier, only transition metals are considered. Compounds with a 4f valence shell will not be discussed in this Review, although recent examples show that here too intermetallic cooperation plays an important role, for example, in intramolecular C–H activation processes, where the reactivity of the methyl C–H bonds was found to decrease in the sequence $\mu_3\text{-C}(\text{H}_2)\text{-H} > \mu_2\text{-C}(\text{H}_2)\text{-H} > \text{C}(\text{H}_2)\text{-H}$.⁴⁰ For each bimetallic couple, we will generally discuss the catalytic properties in the sequence homogeneous, supported, and heterogeneous.

2. REACTIONS IN THE PRESENCE OF HETEROMETALLIC CATALYSTS

A summary of the various bimetallic couples that have been used for a given chemical transformation in either homogeneous, supported, or heterogeneous catalysis is presented in Table 1. A complete listing of the mixed-metal clusters that have been used as catalyst precursors is given in Table 4 where the metal couples are also listed in order of earliest transition metals they contain.

2.1. Isotopic Exchanges

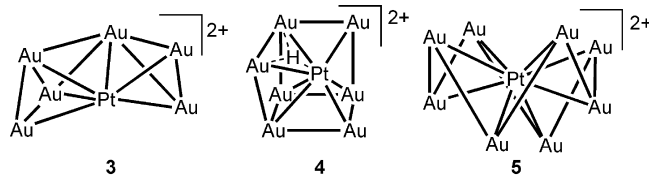
2.1.1. Zr–Ir. H–D exchange reactions were performed with the substrates 1,4-dimethoxybenzene and 2-methoxynaphthalene in the presence of the dinuclear complex $[\text{Cp}^*(\text{Me}_3\text{SiCH}_2)_2\text{Zr}(\mu\text{-H})_3\text{IrCp}^*]$ (**1**) at 373–393 K in C_6D_6 . In both cases, the methoxy groups and the aromatic C–H bonds were all effectively deuterated. This heterobimetallic complex was much more active than its Hf–Ir analogue **2**.⁴¹



2.1.2. Hf–Ir. The heterobimetallic complex $[\text{Cp}^*(\text{Me}_3\text{SiCH}_2)_2\text{Hf}(\mu\text{-H})_3\text{IrCp}^*]$ (**2**) was also used in the H–D exchange reaction between C_6D_6 and the substrates 1,4-dimethoxybenzene and 2-methoxynaphthalene, but it was found to be much less active than the aforementioned Zr–Ir complex **1**.⁴¹

2.1.3. Pt–Au. The clusters $[\text{Pt}(\text{AuPPh}_3)_3(\text{PPh}_3)_2](\text{NO}_3)$ and $[\text{Pt}(\text{AuPPh}_3)_4(\text{PPh}_3)_2](\text{NO}_3)_2$ homogeneously catalyzed $\text{H}_2\text{-D}_2$ equilibration with turnover rates in the range $(3\text{--}5) \times 10^{-2} \text{ s}^{-1}$. Their microcrystalline powders gave even better results (no details available).⁴²

Similarly, many platinum–gold cluster compounds in the form of solid microcrystals showed fast and clean H_2 activation as evidenced by $\text{H}_2\text{-D}_2$ equilibration. Indeed, the clusters $[\text{Pt}(\text{AuPPh}_3)_6(\text{PPh}_3)](\text{NO}_3)_2$ (**3**), $[\text{HPt}(\text{AuPPh}_3)_7(\text{PPh}_3)](\text{NO}_3)_2$ (**4**), and $[\text{Pt}(\text{AuPPh}_3)_8](\text{NO}_3)_2$ (**5**) display rates of $\text{H}_2\text{-D}_2$ equilibration significantly higher (turnover rates ca. $2\text{--}5 \text{ s}^{-1}$) than under homogeneous conditions (turnover rates ca. $2\text{--}8 \times 10^{-2} \text{ s}^{-1}$), mainly due to the low solubility of H_2 in organic solvents. It was suggested that H_2 activation occurs at the Pt–Au sites and leads to the formation of bridging hydrides.^{42,43}

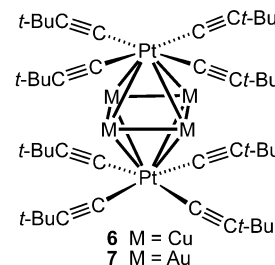


Structure of the dicationic metal core of **3** (left), **4** (middle) and **5** (right)
PPh₃ ligands omitted for clarity

In solution, the cluster $[\text{HPt}(\text{AuPPh}_3)_9](\text{NO}_3)_2$ was found to exhibit slower rates in $\text{H}_2\text{-D}_2$ equilibration reactions than **4**, as a result of slower PPh₃ dissociation rate to afford an open Au site.⁴⁴

Upon adsorption on Al₂O₃ or silica, clusters **3**–**5** were found to remain intact and to be good heterogenized catalysts for $\text{H}_2\text{-D}_2$ equilibration. Adsorbed clusters **3** and **5** gave turnover rates ranging from 10 to 20 s^{-1} when treated at 408 K under vacuum, but these values could be raised up to $85\text{--}200 \text{ s}^{-1}$ by treating the samples at 383 K under H₂ atmosphere instead.⁴⁵ The adsorbed cluster **4**, however, did not need any thermal treatment to exhibit turnover rates of ca. 170 s^{-1} .⁴⁵ These high activities are believed to result from support-promoted partial PPh₃ dissociation that will favor oxidative-addition of the diatomic molecules.⁴⁵ A work performed by another research group confirmed those trends and showed that the silica-adsorbed cluster **3** displayed ca. 30 s^{-1} turnover rates.⁴⁶

Homoexchange of ¹⁶O–¹⁸O was performed with the [Pt₂Au₄] catalysts derived from the silica-supported cluster [Pt₂Au₄(C≡C-t-Bu)₈] (**7**). This system was however less active than catalysts prepared by coimpregnation of mono-metallic salts.⁴⁷

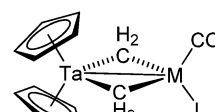


(each acetylenic fragment forms π -interactions with the closest Cu/Au center)

2.2. Isomerization of Alkenes and Alkynes

With the exception of one example of alkyne isomerization with a Ru–Ni cluster, all of the reactions described in this paragraph apply to alkenes.

2.2.1. Ta–Rh. The bridged dinuclear complex $[\text{Cp}_2\text{Ta}(\mu\text{-CH}_2)_2\text{Rh}(\text{CO})(\text{PPh}_3)]$ (**8a**) homogeneously catalyzed the isomerization of 1-butene to a 1:1 mixture of *cis*- and *trans*-2-pentenes, in the absence of H₂. This catalytic system was more active than its Ir-based analogue (see section 2.2.2).⁴⁸

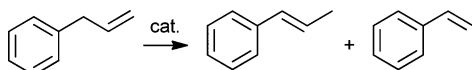


- 8a** M = Rh, L = PPh₃
8b M = Rh, L = CO
9a M = Ir, L = PPh₃
9b M = Ir, L = CO

2.2.2. Ta–Ir. On the contrary, the complex $[\text{Cp}_2\text{Ta}(\mu\text{-CH}_2)_2\text{Ir}(\text{CO})_2]$ (**9b**) catalyzed the isomerization of alkenes heavier than ethylene (substituted or linear) only in the presence of H_2 . The involvement of tantalum in the process remains unclear.⁴⁹

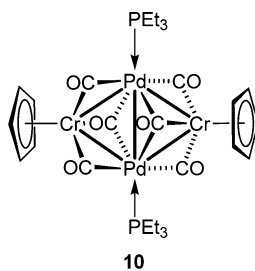
2.2.3. Cr–Fe. Allylbenzene and 1-hexene could be isomerized into internal olefins in the presence of the complex $[\text{PPN}][\text{HCrFe}(\text{CO})_9]$ and light (fluorescent light or mercury vapor lamp; $\lambda > 366 \text{ nm}$). In particular, allylbenzene was converted into *cis*- and *trans*-propenylbenzene (Scheme 3). The

Scheme 3



authors suggested the formation of two fragments: $\text{HFe}(\text{CO})_4^-$ and $[\text{Cr}(\text{CO})_5]$, the former being able to lose a CO ligand to bind the substrate under the reaction conditions. The same applies to the Mo–Fe and W–Fe analogues described below.⁵⁰

2.2.4. Cr–Pd. Isomerization of 1,5-COD was observed when using the planar cluster $[\text{Cr}_2\text{Pd}_2\text{Cp}_2(\text{CO})_6(\text{PEt}_3)_2]$ (**10**) as a homogeneous catalyst in hydrogenation reactions (see section 2.5.1.4). At full conversion, the main product of the isomerization was 1,3-COD (ca. 84%). Traces of 1,4-COD were also observed. The hydrogenation products were COE (ca. 15%) and traces of COA. Comparison with the isostructural Mo–Pd and W–Pd clusters (see sections 2.2.7 and 2.2.10) showed that the $[\text{Cr}_2\text{Pd}_2]$ catalyst was the most selective for 1,3-COD.⁵¹



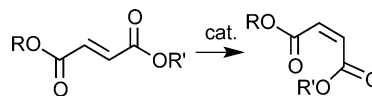
2.2.5. Mo–Fe. Isomerization of 1-hexene and allylbenzene to yield internal olefins was achieved when the complex $[\text{PPN}][\text{HMnFe}(\text{CO})_9]$ was used as a homogeneous catalyst precursor in the presence of light. In particular, allylbenzene was converted into *cis*- and *trans*-propenylbenzene. This system was overall more active than the corresponding Cr–Fe and W–Fe complexes.⁵⁰

The arsenido-bridged complex $[\text{Cp}(\text{OC})_2\text{Mo}(\mu\text{-AsMe}_2)\text{Fe}(\text{CO})_4]$ is an active homogeneous catalyst for 1-octene isomerization to *cis*- and *trans*-2-octene under H_2 pressure. Indeed, *trans*-2-octene is the most favored product (ca. 60% of the product mixture). Octane was also observed as a result of hydrogenation of the C=C double bond. This complex was less active than its Mn–Fe and Fe–Co analogues.⁵²

2.2.6. Mo–Ru–Co. The trimetallic cluster $[\text{HMnRuCo}(\mu_3\text{-CMe})\text{Cp}(\text{CO})_8]$ catalyzed the conversion of various fumaric esters to the corresponding maleic esters with high turnover numbers at 303 K (Scheme 4). The reaction was 3 times faster than that with the often used catalyst HI. The analogous W–Ru–Co cluster had similar catalytic performances.⁵³

2.2.7. Mo–Pd. Isomerization of carbon–carbon double bonds occurred when the planar clusters

Scheme 4

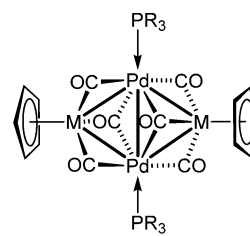


$[\text{Mo}_2\text{Pd}_2\text{Cp}_2(\text{CO})_6(\text{PEt}_3)_2]$ (**11a**) and $[\text{Mo}_2\text{Pd}_2\text{Cp}_2(\text{CO})_6(\text{PPh}_3)_2]$ (**11b**) were used in hydrogenation of 1,5-COD (see section 2.5.1.15). When **11a** was used, COE (ca. 70%) was obtained as the main hydrogenation product, but isomerization products were found in significant proportions: 1,3-COD (ca. 24%), 1,4-COD (ca. 3%), and unreacted 1,5-COD (ca. 3%). On the other hand, **11b** favored isomerization over hydrogenation at lower conversion, since the reacted mixture contained ca. 51% 1,3-COD, 13% 1,4-COD, 13% unreacted 1,5-COD, and only ca. 22% of COE and 1% of COA. Thus, it appears that the PEt₃ ligand is favorable for the hydrogenation route.⁵¹

2.2.8. W–Fe. Isomerization of 1-hexene and of allylbenzene into internal olefins in the presence of light was catalyzed by the complex $[\text{PPN}][\text{HWFe}(\text{CO})_9]$. This system was less active than the Cr–Fe and Mo–Fe analogous complexes described above.⁵⁰

2.2.9. W–Ru–Co. The conversion of some fumaric esters to the corresponding maleic esters was achieved with high turnover numbers using the cluster $[\text{HWRuCo}(\mu_3\text{-CMe})\text{Cp}(\text{CO})_8]$ at 303 K. The reaction was faster than when the common acid catalyst HI was used.⁵³

2.2.10. W–Pd. The planar clusters $[\text{W}_2\text{Pd}_2\text{Cp}_2(\text{CO})_6(\text{PEt}_3)_2]$ (**12a**) and $[\text{W}_2\text{Pd}_2\text{Cp}_2(\text{CO})_6(\text{PPh}_3)_2]$ (**12b**) were used in hydrogenation of olefins (see section 2.5.1), and it appeared that isomerization of 1,5-COD to afford 1,3-COD and 1,4-COD competed strongly. Indeed, the proportions of 1,4-COD were ca. 61% and 79% for **12a** and **12b**, respectively, while the mixture contained 7–8% of 1,3-COD and 7–8% of unreacted 1,5-COD in both cases. The hydrogenation products were COE (ca. 25% and 4% for **12a** and **12b**, respectively) and COA (traces). Overall, with the exception of **11a**, all of the catalysts favored isomerization over hydrogenation under the reaction conditions (see sections 2.2.4 and 2.2.7).⁵¹



11a M = Mo, R = Et
11b M = Mo, R = Ph
12a M = W, R = Et
12b M = W, R = Ph

2.2.11. Mn–Fe. Isomerization of 1-octene to a mixture of *cis*- and *trans*-2-octene happened to compete strongly with hydrogenation in the presence of the arsenido-bridged complex $[(\text{OC})_4\text{Mn}(\mu\text{-AsMe}_2)\text{Fe}(\text{CO})_4]$. The main product was *trans*-2-octene (more than 50% of the product mixture), while octane and *cis*-2-octene accounted for ca. 25% each. This system was more active than the corresponding Mo–Fe analogue, but less active than the Fe–Co one.⁵²

2.2.12. Fe–Ru. The three clusters $[\text{FeRu}_2(\text{CO})_{12}]$, $[\text{Fe}_2\text{Ru}(\text{CO})_{12}]$, and $[\text{H}_2\text{FeRu}_3(\text{CO})_{13}]$ were found to be active in

isomerization of *cis*-stilbene.⁵⁴ Moreover, isomerization of 1-hexene to give a mixture of *cis*- and *trans*-2-hexenes with a turnover number of approximately 4500 mol of hexene/(mol cluster·h) was readily catalyzed by the tetrahedral cluster [$H_2FeRu_3(CO)_{13}$].⁵⁵

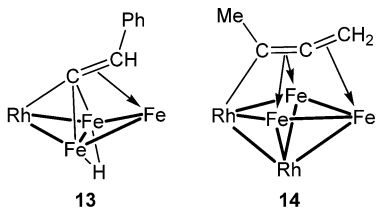
Homogeneous hydrogenation/isomerization of 1,3- and 1,4-cyclohexadiene was catalyzed by $[Fe_2Ru(CO)_{12}]$ and $[H_2FeRu_3(CO)_{13}]$ (see also section 2.5.1.29), but there was evidence for catalysis by metal species rather than by intact clusters. These catalysts showed poor activity in isomerization.⁵⁶

2.2.13. Fe–Co. The arsenido-bridged complex $[(OC)_3Co(\mu\text{-AsMe}_2)Fe(CO)_4]$ was used in the isomerization/hydrogenation of 1-octene. The main product was *trans*-2-octene, while octane and *cis*-2-octene were detected in small amounts. This system was more active than the corresponding Mo–Fe and Mn–Fe analogues.⁵²

The cluster $[Fe_2CoCp(CO)_9]$ was reported in a patent to catalyze the isomerization of 1-pentene in the presence of light.⁵⁷

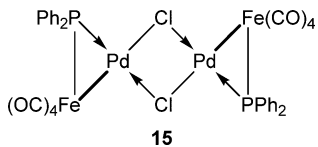
2.2.14. Fe–Rh. Isomerization of 1-heptene to *cis*- and *trans*-2-heptene was achieved with $[HFe_3Rh(CO)_{11}(\mu_4\text{-}\eta^2\text{-C=CHPh})]$ (**13**) at 10 atm of dihydrogen at room temperature. Partial hydrogenation also occurred (see section 2.5.1.32). A fragmentation of the cluster is responsible for the subsequent isomerization of 2-heptene into 3-heptene at a lower rate.⁵⁸ The cluster $[Ph_4P][Fe_3Rh_2(\mu_4\text{-}\eta^3\text{-MeC=C=CH}_2)(\mu\text{-CO})_3(CO)_{10}]$ (**14**) however was far less active toward the isomerization of alkenes. In particular, under the same reaction conditions (10 atm of H_2), it appeared necessary to heat to 333 K to observe some catalytic activity: 1-octene could be converted to 25% octane and 75% of a mixture of octenes.⁵⁹

These are two examples of mixed iron–rhodium systems in which the known hydrogenation ability of rhodium is lowered by iron, thus favoring isomerization over hydrogenation reactions.



Core of the clusters $[HFe_3Rh(CO)_{11}(\mu_4\text{-}\eta^2\text{-C=CHPh})]$ and $[Ph_4P][Fe_3Rh_2(\mu_4\text{-}\eta^3\text{-MeC=C=CH}_2)(\mu\text{-CO})_3(CO)_{10}]$; CO ligands omitted for clarity

2.2.15. Fe–Pd. Selective isomerization of 1-octene to 2-octene was evaluated in the presence of the phosphanido-bridged complex $[(OC)_4Fe(\mu\text{-PPh}_2)Pd(\mu\text{-Cl})_2]$ (**15**).⁶⁰ When entrapped in a SiO_2 sol–gel matrix, this complex was found to lose all of its carbonyl ligands. The resulting catalyst was active in the isomerization of 1-octene with almost 50% selectivity for *trans*-2-octene. The activity decreased for the second run, but sonication and treatment with hot water reactivated the catalyst for several more cycles without loss of activity.⁶¹



2.2.16. Ru–Os. Isomerization of 1-butene to *cis*- and *trans*-2-butene (no other detectable product) was achieved in the presence of the hydride cluster $[Al]^{+}[HRuOs_3(CO)_{13}]^{-}$, obtained after adsorption of $[H_2RuOs_3(CO)_{13}]$ and deprotonation on the surface of alumina. After catalysis, $[Al]^{+}[H_3RuOs_3(CO)_{12}]^{-}$ was the only detectable metal carbonyl species.⁶²

When attached to a polymeric support of the type (poly-NR₃)⁺, the cluster $[Ph_4As][H_3RuOs_3(CO)_{12}]$ was used for 1-hexene hydroformylation. Under the reaction conditions, it appeared that isomerization to 2-hexene competed weakly.⁶³

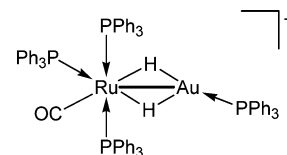
2.2.17. Ru–Co. The clusters $[RuCo_2(\mu_3\text{-S})(CO)_9]$ and $[RuCo_2(\mu_3\text{-Se})(CO)_9]$ catalyzed isomerization of 1-hexene.⁶⁴

2.2.18. Ru–Ni. Isomerization of 1-pentene was catalyzed by the tetrahedral cluster $[Ru_3Ni(\mu\text{-H})_3Cp(CO)_9]$ in the absence of H_2 . This cluster was also fairly active for the isomerization of 1,4-pentadiene to *cis*-1,3-pentadiene.⁶⁵ Introducing a phosphine ligand in this tetrahedral cluster to give $[Ru_3Ni(\mu\text{-H})_3Cp(CO)_8(PR_3)]$ ($R = Ph, Cy$) or $[Ru_3Ni(\mu\text{-H})_3Cp(CO)_7(PPh_3)_2]$ generally led to increased activity for the homogeneous isomerization of dienes rather than their hydrogenation.⁶⁶ Analogous behavior was observed for the C_6 molecules *cis*-1,4-hexadiene, 2,4-hexadiene, 1,5-hexadiene, and *trans*-3-hexene. However, this system was found to be overall less active than its Os–Ni analogue (see section 2.2.22).

2.2.19. Ru–Cu. The cluster complexes $[H_3Ru_4\{Cu(PPh_3)\}(CO)_{12}]$ and $[H_2Ru_4\{Cu(PPh_3)\}_2(CO)_{12}]$ were used in the isomerization of 1-pentene, but were less active than the monometallic precursor $[H_4Ru_4(CO)_{12}]$.⁶⁷

2.2.20. Ru–Au. On the contrary, the clusters $[H_3Ru_4\{Au(PPh_3)\}(CO)_{12}]$ and $[H_2Ru_4\{Au(PPh_3)\}_2(CO)_{12}]$ clearly exhibit higher activity than the parent $[H_4Ru_4(CO)_{12}]$ in the isomerization of 1-pentene. Indeed, while the Ru_4Au_2 cluster afforded a mixture of *cis*-2-pentene (ca. 15%) and *trans*-2-pentene (ca. 33%) at ca. 50% conversion, the Ru_4Au cluster was more efficient: conversion reached 71%, and *cis*-2-pentene and *trans*-2-pentene accounted for ca. 18% and 51% of the product mixture, respectively. Noteworthy is that only ca. 1% pentane was observed in both cases.⁶⁷

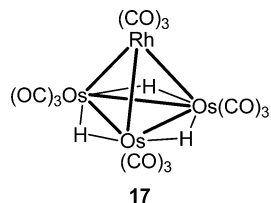
Preliminary results indicate that the isomerization of 1-hexene to *cis*- and *trans*-2-hexene can be achieved in the presence of the dinuclear complex $[(OC)(Ph_3P)_3Ru(\mu\text{-H})_2Au(PPh_3)](PF_6)$ (**16**), and the activity was better than with the parent complex $[H_2Ru(CO)(PPh_3)_3]$. Moreover, the latter appears to be more selective for the *cis* isomer, while the Ru–Au complex is more selective for the *trans* isomer.⁶⁸



Structure of the cation in **16**

2.2.21. Os–Rh. Preliminary experiments showed that in the presence of the hydrido-bridged cluster $[Os_3Rh(\mu\text{-H})_3(CO)_{12}]$ (**17**), isomerization of 1-octene to all isomers was observed at 333 and 373 K, but not at room temperature. The reaction conditions were not optimized.⁶⁹

The immobilized species $[H_2Os_3Rh(acac)(CO)_{10}(Ph_2P\text{-polym})]$ was obtained by anchoring the coordinatively unsaturated cluster $[H_2Os_3Rh(acac)(CO)_{10}]$ on poly(styrene-divinylbenzene). Although the cluster was



initially anchored intact on the support, it fragmented during tests performed for the isomerization of 1-butene to give catalytically active species. In particular, the authors suggest that the activity in isomerization is due to the formation of triosmium carbonyl species. Conversion was less than 2% after 4 h at 383 K. The same system was also used for ethylene hydrogenation (see section 2.5.1.44).⁷⁰

2.2.22. Os–Ni. The cluster $[\text{Os}_3\text{Ni}(\mu\text{-H})_3\text{Cp}(\text{CO})_9]$ was used in the isomerization of alkenes, alkynes, and dienes, including 1-pentene, *trans*-3-hexene, 1-pentyne, 3-hexyne, *cis*-, *trans*-1,3-pentadiene, *cis*-1,4-hexadiene, *cis*- and *trans*-2,4-hexadiene, 1,5-hexadiene, and 3-methylbut-3-en-1-yne.^{65,71} In particular, nonconjugated dienes were first isomerized, and then hydrogenation of terminal C=C bonds occurred. The same applies to its phosphine derivatives $[\text{Os}_3\text{Ni}(\mu\text{-H})_3\text{Cp}(\text{CO})_8\text{L}]$ ($\text{L} = \text{PPh}_2\text{H}$ or $\text{P}(\text{C}_6\text{H}_4\text{Me}-o)_3$).⁷¹ For instance, in isomerization/hydrogenation of *cis*-1,3-pentadiene, depending on the cluster, the reaction mixture contained 0.5–2.5% of pentane, 10–25% of 1-pentene, and 45–49% of *cis*- + *trans*-2-pentene, for activities in the range of 60–75%. Under those conditions, $[\text{Os}_3\text{Ni}(\mu\text{-H})_3\text{Cp}(\text{CO})_8(\text{PPh}_2\text{H})]$ was the most active catalyst with the highest selectivity for 2-pentenes.

2.2.23. Os–Au. The immobilized bimetallic $[\text{Os}_3\text{Au}]$ catalysts $[\text{HOs}_3\text{Au}(\text{CO})_{10}(\text{Ph}_2\text{P}\sim\text{SIL})]$ and $[\text{ClOs}_3\text{Au}(\text{CO})_{10}(\text{Ph}_2\text{P}\sim\text{SIL})]$, prepared by anchoring the PPh_3 clusters onto phosphine-functionalized silica, were not active in 1-butene isomerization below 383 K.⁷² If the former system was slightly active at 383 K, the corresponding homonuclear system $[\text{HOs}_3(\text{CO})_9(\text{Ph}_2\text{P}\sim\text{SIL})]$ was still ca. 10 times more efficient.⁷³

2.2.24. Co–Rh. When entrapped in a silica sol–gel matrix, the cluster $[\text{Co}_2\text{Rh}_2(\text{CO})_{12}]$ was inactive in the isomerization of allylbenzene. However, it became an efficient and reusable catalyst when an alumina sol–gel matrix was used instead. When the reaction was performed at 373 K, a mixture of *cis*-(17.5%) and *trans*-1-phenyl-1-propene (81%) was obtained, along with 1.5% of unreacted species.⁷⁴

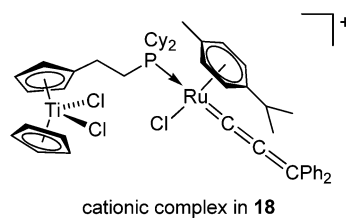
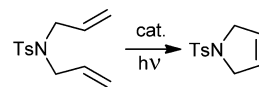
2.2.25. Co–Pt. The cobalt–platinum cluster $[\text{Co}_2\text{Pt}_2(\text{CO})_8(\text{PPh}_3)_2]$ catalyzes the isomerization of 1,3-butadiene.⁷⁵

2.3. Olefin Metathesis

2.3.1. Ti–Ru. Although it does not contain a metal–metal bond, the dinuclear complex $[\text{CpCl}_2\text{Ti}(\mu\text{-}\eta^5\text{:}\eta^1\text{-C}_5\text{H}_4(\text{CH}_2)_2\text{PCy}_2)\text{RuCl}_2(p\text{-cymene})]$ reacts under UV irradiation and in the presence of AgOTf and $\text{HC}\equiv\text{C-CPh}_2\text{OH}$, to afford the allenylidene complex $[\text{CpCl}_2\text{Ti}(\mu\text{-}\eta^5\text{:}\eta^1\text{-C}_5\text{H}_4(\text{CH}_2)_2\text{PCy}_2)\text{Ru}(\equiv\text{C=C=CPh}_2)\text{Cl}(p\text{-cymene})][\text{OTf}]$ (18). It is assumed to be responsible for the excellent activity (complete conversion after 1 h) in the ring-closing metathesis reaction of *N,N*-diallyltosylamide to give 3-tosylamide cyclopentene in toluene at 353 K (Scheme 5). The same complex also catalyzed the cyclization of dimethyl diallylmalonate by ring-closing metathesis with 63% yield.⁷⁶

2.3.2. Cr–Mo. Very active heterogeneous catalysts for olefin metathesis could be obtained by combining a reduced Phillips

Scheme 5

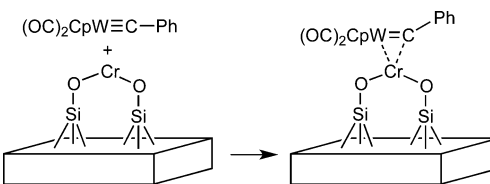


cationic complex in 18

catalyst ($\text{Cr}\sim\text{SIL}$) with a Fischer-type molybdenum carbene or carbyne complex, such as $[(\text{OC})_5\text{Mo}=\text{CPh}(\text{OMe})]$. The resulting active species was described as $[(\text{OC})_4\text{Mo}=\text{CPh}(\text{OMe})\text{Cr}\sim\text{SIL}]$.⁷⁷

2.3.3. Cr–W. Similarly to the Cr–Mo complexes described above, reduced Phillips catalyst were reacted with Fischer-type tungsten carbene complexes such as $[(\text{OC})_5\text{W}=\text{CR}^1\text{R}^2]$ ($\text{R}^1 = \text{Ph}, \text{Tol}, \text{Me}; \text{R}^2 = \text{Ph}, \text{OMe}$),^{77,78} or carbyne complexes like $[\text{X}(\text{OC})_n\text{W}\equiv\text{CPh}]$ ($\text{X} = \text{Cl}, \text{Br}, \text{I}, n = 4$; $\text{X} = \text{Cp}, n = 2$)⁷⁹ to yield very active heterogeneous catalysts $[(\text{OC})_4\text{W}=\text{CR}^1\text{R}^2\text{Cr}\sim\text{SIL}]$ and $[\text{X}(\text{OC})_n\text{W}=\text{CPhCr}\sim\text{SIL}]$ for olefin metathesis (Scheme 6). It should be noted that the olefin polymerization activity of the reduced Phillips catalyst is lost in this new bimetallic catalyst.⁷⁸

Scheme 6



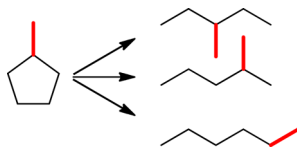
2.3.4. Mo–Rh. Thermal treatment and CO photoreduction on the silica-supported cubane-type clusters $[(\text{Cp}^*\text{Rh})_2\text{Mo}_3\text{O}_9(\text{OMe})_4]$ and $[(\text{Cp}^*\text{Rh})_4\text{Mo}_4\text{O}_{16}]$ yielded very active $[\text{Mo}_3\text{Rh}_2]$ and $[\text{Mo}_4\text{Rh}_4]$ catalysts, respectively, for propene metathesis. More precisely, the $[\text{Mo}_3\text{Rh}_2]$ catalyst was 3 times more active than $[\text{Mo}_4\text{Rh}_4]$, and its selectivity for *trans*-2-pentene was higher (*trans/cis* ratio of 1.7 vs 1.3 for $[\text{Mo}_4\text{Rh}_4]$).⁸⁰

2.4. Hydrocarbon Skeletal Rearrangements

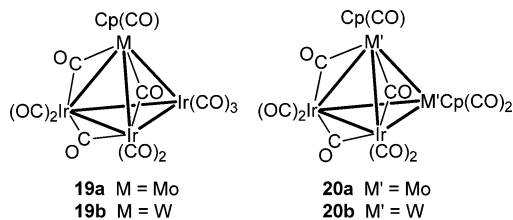
2.4.1. Cr–Pd. The heterogenized $[\text{Cr}_2\text{Pd}_2]$ catalyst derived from the planar cluster $[\text{Cr}_2\text{Pd}_2\text{Cp}_2(\text{CO})_6(\text{PMe}_3)_2]$, analogous to 10, supported on alumina was used for the isomerization of 2-methylpentane to methylcyclopentane. The contribution of the C_5 -cyclic mechanism (see Scheme 7)⁸¹ to this transformation was the same as a conventional Cr–Pd catalyst containing 6.6% Pd.⁸²

2.4.2. Mo–Ir. The alumina-supported $[\text{MoIr}_3]$ and $[\text{Mo}_2\text{Ir}_2]$ heterogeneous catalysts, prepared from $[\text{MoIr}_3\text{Cp}(\text{CO})_{11}]$ (19a) and $[\text{Mo}_2\text{Ir}_2\text{Cp}_2(\text{CO})_{10}]$ (20a), respectively, were used in *n*-butane hydrogenolysis, a structure-sensitive reaction. It was deduced from comparisons with catalysts derived from homometallic clusters or their mixtures that the properties of the MMCD catalysts originated from bimetallic interactions that were retained in the activated materials. The selectivity

Scheme 7. C₆ Products Resulting from the Hydrogenolysis of Methylcyclopentane



toward ethane was about 70–75% for all samples, but the [MoIr₃] catalyst was 5–10 times more active.⁸³

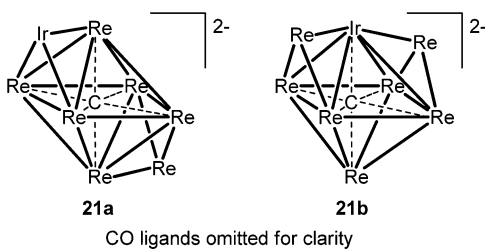


2.4.3. W–Ir. The clusters [WIr₃Cp(CO)₁₁] (**19b**) and [W₂Ir₂Cp₂(CO)₁₀] (**20b**), analogous to the Mo–Ir clusters described above were examined for *n*-butane hydrogenolysis. The [WIr₃] MMCD catalyst showed a selectivity toward ethane production of 70% or more, against less than 50% for the [W₂Ir₂] catalyst.⁸⁴

2.4.4. W–Pd. The heterogeneous [W₂Pd₂] catalyst, prepared from [W₂Pd₂Cp₂(CO)₆(PPh₃)₂], exhibited completely different properties for the isomerization of 2-methylpentane in methylcyclopentane as compared to the corresponding [Cr₂Pd₂] cluster-derived catalyst: it selectively afforded 3-methylpentane.⁸⁵

2.4.5. Re–Os. Alumina-supported [ReOs₃] MMCD catalysts prepared from [H₃ReOs₃(CO)₁₃] were found to be active for *n*-butane hydrogenolysis and resistant to deactivation. In particular, the authors demonstrated that the oxidation state of the rhenium atoms depended on the nature of the pretreatment, under He or H₂ atmosphere, respectively, followed by a treatment under H₂. Low oxidation state (+II/+III) Re-containing systems (i.e., pretreated under H₂ and then activated under H₂) were twice as active as higher oxidation state (+VII) Re catalysts (i.e., pretreated under He and then activated under H₂).⁸⁶

2.4.6. Re–Ir. The isomeric clusters 1,4-[Re₆C(CO)₁₈{μ₃-Re(CO)₃}]{μ₃-Ir(CO)₂}]²⁻ (**21a**) and 1,3-[Re₅IrC(CO)₁₇{μ₃-Re(CO)₃}]₂]²⁻ (**21b**) with different counterions, Et₄N⁺ or PPN⁺, were supported on Al₂O₃ and used to prepare MMCD catalysts. The Et₄N-containing precursors yielded larger nanoparticles than the corresponding PPN-containing precursors. The rate of ethane hydrogenolysis increased with the average cluster size.⁸⁷



2.4.7. Re–Pt. Hydrogenolysis of cyclopentane to yield methane was performed with an alumina-supported [Re₂Pt] catalyst derived from [Re₂Pt(CO)₁₂]. The turnover frequency

for this reaction was over 100 times higher than when a mixture of monometallic complexes was used, most likely because of a direct contact between the Re and Pt atoms on the surface.⁸⁸

2.4.8. Fe–Ru. The [Fe₂Ru] catalyst obtained from [Fe₂Ru(CO)₁₂] showed more than 1 order of magnitude greater activity in ethane hydrogenolysis than the [FeRu₂] catalyst prepared from [FeRu₂(CO)₁₂]. Noteworthy is that these mixed-metal clusters were more active than the corresponding monometallic species [Fe₃(CO)₁₂] and [Ru₃(CO)₁₂]. Also, such results emphasize the benefits resulting from the possibility of changing the intermetallic ratio within a series of analogous clusters.⁸⁹

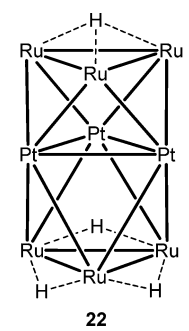
2.4.9. Fe–Rh. Catalysts of the type [Fe₂Rh₄(CO)₁₆]²⁻/NaY zeolite were also investigated for ethane and *n*-butane hydrogenolysis. In particular, hydrogenolysis of the latter showed selectivity for terminal C–C bond scission, thus yielding a mixture of C₁ and C₃ products.⁹⁰

2.4.10. Fe–Pt. The MMCD catalyst [Fe₂Pt] derived from the chain complex *trans*-[Pt{Fe(CO)₃NO}₂{CN(*t*-Bu)}₂] is active in the demethylation of methylcyclopentane. Its properties when lightly loaded with platinum (e.g., 0.3% Pt) are similar to those of highly dispersed Pt catalysts (0.2% Pt/Al₂O₃).^{85,91}

2.4.11. Ru–Ni. The transformation of toluene to cyclohexane via demethylation of the intermediate methylcyclohexane, previously hydrogenated (see section 2.5.1.39), could be achieved in the presence of the cluster [Ru₃Ni(μ-H)₃Cp(CO)₉]. Cracking of methylcyclohexane to *n*-hexane was also observed to a limited extent.⁶⁵

2.4.12. Ru–Pt. A supported complex formulated as [Ru₃Pt(CO)₁₂py₃] was impregnated onto inorganic oxides and found to be poorly selective for toluene in *n*-heptane dehydrocyclization reactions, unlike Ir–Pt clusters (see below).⁹²

The cluster [Ru₆Pt₃(μ₃-H)(μ-H)₃(CO)₂₁] (**22**) was adsorbed onto alumina and magnesia, and then decarbonylated at 573 K under helium. This system was used in the catalytic hydrogenolysis of *n*-butane. With alumina, the selectivity for ethane was superior to 60% (<40% for methane), while magnesia gave selectivities toward methane and ethane in the range 40–60%, depending on the temperature (473–533 K range). Using magnesia resulted in 5 times greater activity than with alumina.⁹³

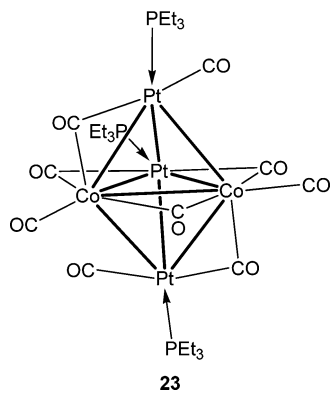


CO ligands omitted for clarity

2.4.13. Co–Rh. An alumina-supported [Co₂Rh₂(CO)₁₂]-derived catalyst was active in hydrogenolysis of methylcyclopentane (Scheme 7), and led to a remarkable specificity for the hydrogenolysis of the methyl-substituted five-membered ring to noncyclic C₆ isomers.⁹⁴

An alumina-supported $[\text{Co}_2\text{Rh}_2(\text{CO})_{12}]$ -derived catalyst was active for hydrocarbon skeletal rearrangement.⁹⁵

2.4.14. Co–Pt. Three Co–Pt complexes, the linear complex *trans*- $[\text{Pt}\{\text{Co}(\text{CO})_4\}_2(\text{CNCy})_2]$, the butterfly $[\text{Co}_2\text{Pt}_2(\text{CO})_8(\text{PPh}_3)_2]$, and the trigonal bipyramidal clusters $[\text{Co}_2\text{Pt}_3(\text{CO})_9(\text{PEt}_3)_3]$ (23), characterized by Co/Pt ratios of 2:1, 2:2, and 2:3, respectively, were adsorbed on alumina and afforded bimetallic heterogeneous catalysts for the hydrogenolysis of methylcyclopentane. The $[\text{Co}_2\text{Pt}_2]$ and $[\text{Co}_2\text{Pt}_3]$ catalysts showed a higher selectivity for demethylation of methylcyclopentane ($\text{C}_6 \rightarrow \text{C}_5 + \text{C}_1$) than the $[\text{Co}_2\text{Pt}]$ catalyst. These effects were tentatively attributed to the different nature of the ligands bound to the molecular precursors (phosphines vs isonitriles) rather than to the change in the Co:Pt ratio. Thus, these ligands might have been difficult to completely eliminate during the thermal activation steps of the catalysts, and this could lead to modifications in the composition and/or structure of the final catalyst.^{81,96}



2.4.15. Rh–Ir. Catalysts of the type $[\text{Rh}_{6-x}\text{Ir}_x(\text{CO})_{16}]/\text{NaY}$ ($x = 1-4$) were tested in ethane and butane hydrogenolysis. Increasing the Ir content suppressed the catalytic activity. The selectivity toward the central C–C bond scission in butane hydrogenolysis was superior to 75%. The cluster-derived catalysts consisted of bimetallic particles of less than 10 Å in diameter, which were uniformly distributed inside the NaY zeolites and had a metal composition similar to that of their molecular precursors.^{90,97}

2.4.16. Ir–Pt. Impregnation of the complexes formulated as $[\text{Ir}_2\text{Pt}(\text{CO})_7\text{py}_2]$ and $[\text{Ir}_6\text{Pt}(\text{CO})_{15}\text{py}_2]$ onto inorganic oxides led to very active and selective catalysts for hydrocarbon conversion. The cluster-derived $[\text{Ir}_6\text{Pt}]$ heterogeneous catalyst was significantly more active in dehydrocyclization of *n*-heptane than the standard catalysts prepared from $[\text{H}_2\text{MCl}_6]$ ($M = \text{Ir}$ or Pt) acid solutions. It led to a range of products, from methane to xylenes. The most desirable products are benzene, toluene, and the isomeric xylenes because of their high research octane number (RON). The $[\text{Ir}_6\text{Pt}]$ catalyst was found to be 5–7% more selective toward toluene than the $[\text{Ir}_2\text{Pt}]$ catalyst. The 30% lower coking rate displayed by the $[\text{Ir}_6\text{Pt}]$ as compared to a conventional catalyst was found to be another advantage of the MMCD catalyst. The $[\text{Ir}_2\text{Pt}]$ and $[\text{Ir}_6\text{Pt}]$ catalysts have been found to be, at least 1.6 and 2.4 times, respectively, more active for naphtha reforming than conventional catalysts, and the $[\text{Ir}_6\text{Pt}]$ catalyst was 1.8 times more active than the $[\text{Ir}_2\text{Pt}]$ catalyst. It was suggested that unique heterometallic sites on the cluster-derived catalysts were more efficient in carrying out aromatization reactions than those present on conventional Ir–Pt catalysts.⁹²

2.4.17. Pt–Cu. The silica-supported cluster $[\text{Pt}_2\text{Cu}_4(\text{C}\equiv\text{C}-t\text{-Bu})_8]$ (6) afforded a $[\text{Pt}_2\text{Cu}_4]$ heterogeneous catalyst for hexane conversion. It was found to be selective for the cracking products (C_1-C_5), with a majority of C_3 (almost 50% at 10% conversion). Unlike its Pt–Au counterpart (see section 2.4.18), this catalyst was not more resistant to deactivation than the usual Pt catalysts.⁹⁸

2.4.18. Pt–Au. The silica-supported cluster $[\text{Pt}_2\text{Au}_4(\text{C}\equiv\text{C}-t\text{-Bu})_8]$ (7) afforded a deactivation-resistant $[\text{Pt}_2\text{Au}_4]$ heterogeneous catalyst for hexane conversion. Highly dispersed Pt–Au NPs with diameters around 3.5 nm were obtained. The distribution of light carbon species obtained was very similar to that found for the corresponding $[\text{Pt}_2\text{Cu}_4]$ catalyst (see section 2.4.17).^{98,99}

2.5. Hydrogenation Reactions

Heterometallic complexes and clusters are good candidates for hydrogen activation, which represents a key step in hydrogenation catalysis, as reviewed recently.^{13k,100}

2.5.1. Hydrogenation of Carbon–Carbon Multiple Bonds. **2.5.1.1. V–Fe.** Cubane clusters containing a VFe_3S_4 core, such as $[\text{NEt}_4][\text{VFe}_3\text{S}_4\text{Cl}_3(\text{DMF})_3]$, were examined in the homogenous catalytic reduction of acetylene to ethylene.¹⁰¹

2.5.1.2. Ta–Rh. The methylene-bridged complex $[\text{Cp}_2\text{Ta}(\mu\text{-CH}_2)_2\text{Rh}(\text{CO})(\text{PPh}_3)]$ (8a) homogeneously catalyzed the hydrogenation of alkenes (ethylene, propylene, 1-butene, and *cis*-2-butene). In contrast, the phosphine-free analogue $[\text{Cp}_2\text{Ta}(\mu\text{-CH}_2)_2\text{Rh}(\text{CO})_2]$ (8b) formed a colloidal suspension, which was assumed to constitute the active species.⁴⁸ These bimetallic Ta–Rh complexes were better hydrogenation catalysts than the corresponding Ta–Ir complexes (see section 2.5.1.3).

2.5.1.3. Ta–Ir. The complexes $[\text{Cp}_2\text{Ta}(\mu\text{-CH}_2)_2\text{Ir}(\text{CO})(\text{PPh}_3)]$ (9a) and $[\text{Cp}_2\text{Ta}(\mu\text{-CH}_2)_2\text{Ir}(\text{CO})_2]$ (9b) are active in alkene hydrogenation (ethylene, propylene, 1-butene, and *cis*-2-butene), but at slower rates than their Ta–Rh analogues (see section 2.5.1.2).⁴⁸ Reductive elimination of one of the bridging methylene groups seems to take place during the reactions.

If the presence of tantalum appears necessary for the catalytic activity of 9b in ethylene hydrogenation,⁴⁹ the reasons remain unclear. The corresponding hydride complex $[\text{Cp}_2\text{Ta}(\mu\text{-CH}_2)_2\text{IrHCp}^*]$ partially decomposed under the reaction conditions to give a very active heterogeneous ethylene hydrogenation catalyst.¹⁰²

2.5.1.4. Cr–Pd. Selective hydrogenation of 1,5-COD to COE was performed with the planar cluster $[\text{Cr}_2\text{Pd}_2\text{Cp}_2(\text{CO})_6(\text{PEt}_3)_2]$ (10) as a homogeneous catalyst, although isomerization was the main reaction. At full conversion, the product mixture contained ca. 15% of COE with traces of COA, the remaining being isomerization products (see section 2.2.4 for more details on the product distribution).⁵¹

2.5.1.5. Mo–W–Fe, Mo–W–Co, Mo–W–Ni. The three cage-type clusters $K_8[\text{P}_2\text{Mo}_2\text{W}_{18}\text{M}_2(\text{H}_2\text{O})\text{O}_{68}]\cdot\text{MoO}_6\cdot 15\text{H}_2\text{O}$ ($M = \text{Fe}, \text{Co}, \text{Ni}$) were used as precursors for alumina-supported catalysts in cyclohexene hydrogenation reactions.¹⁰³

2.5.1.6. Mo–Fe. Acetylene reduction to ethylene was achieved with various multinuclear Mo–Fe cluster complexes. The anionic complexes $[\text{MoFeS}_4(\text{SCN})_2(\text{OMe})_2]^{2-}$ and $[\text{Mo}_2\text{FeS}_8\text{O}(\text{OMe})_2]^{3-}$ were found to have a higher activity when the percentage of Fe in the complex increased.¹⁰⁴

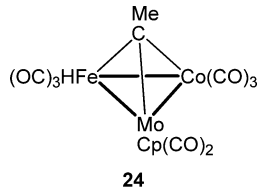
A study revealed that the clusters $[\text{Et}_4\text{N}]_3[\text{Mo}_2\text{Fe}_6\text{S}_8(\text{OMe})_3\cdot(\text{L}^1)_3(\text{L}^2)_3]$ ($\text{L}^1 = \text{L}^2 = \text{SPh}$ or Cl ; $\text{L}^1 = \text{SPh}$, $\text{L}^2 = \text{Cl}$) catalyze

the reduction of acetylene by KBH_4 , with a lower activity than $[\text{Et}_4\text{N}]_3[\text{Mo}_2\text{Fe}_4\text{Co}_2\text{S}_8(\text{SPh})_6(\text{OMe})_3]\cdot\text{MeCN}$.¹⁰⁵ The cubane cluster $[\text{Et}_4\text{N}]_2[\text{MoFe}_3\text{S}_4\text{Cl}_3(\text{Cl}_4\text{-cat})(\text{MeCN})]$ ($\text{Cl}_4\text{-cat}$ = tetrachlorocatecholate) is also active in the reduction of acetylene to ethylene in the presence of a proton source (lutidine hydrochloride) and an electron source (cobaltocene). Small amounts of ethane were also obtained.^{101b,d,106}

Hydrogenation of 1-octene to octane could be achieved with the arsenido-bridged complex $[\text{Cp}(\text{OC})_2\text{Mo}(\mu\text{-AsMe}_2)\text{Fe}(\text{CO})_4]$ as a homogeneous catalyst, although isomerization to *cis*- and *trans*-2-octene was the most favored reaction.⁵²

When adsorbed on alumina, the linear complex $[\text{Et}_4\text{N}]_2[\text{Mo}_2\text{FeS}_4\text{O}_4]$ and the cubane-type cluster $[\text{Et}_4\text{N}]_3[\text{Mo}_2\text{Fe}_6\text{S}_8(\text{SPh})_6(\text{OMe})_3]$ were used for the hydrogenation of cyclohexene.¹⁰³

2.5.1.7. Mo–Fe–Co. The heterotrimetallic cluster $[\text{HMnFeCo}(\mu_3\text{-CMe})\text{Cp}(\text{CO})_8]$ (24) catalyzed the homogeneous hydrogenation of styrene to ethylbenzene, but the yield was low (ca. 10%) and only 10% of the catalyst could be recovered.¹⁰⁷

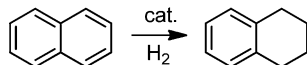


The heterotrimetallic cluster $[\text{Et}_4\text{N}]_3[\text{Mo}_2\text{Fe}_4\text{Co}_2\text{S}_8(\text{SPh})_6(\text{OMe})_3]\cdot\text{MeCN}$ was found to be more efficient for the homogeneously catalyzed reduction of acetylene than clusters containing only Fe or Mo.¹⁰⁵

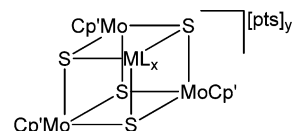
Hydrogenation of cyclohexene was performed in the presence of the two alumina-supported cubane-type clusters $[\text{Et}_4\text{N}]_3[\text{Mo}_2\text{Fe}_5\text{CoS}_8(\text{SPh})_6(\text{OMe})_3]$ and $[\text{Et}_4\text{N}]_3[\text{Mo}_2\text{Fe}_4\text{Co}_2\text{S}_8(\text{SPh})_6(\text{OMe})_3]$.¹⁰³

2.5.1.8. Mo–Ru. Hydrogenation of naphthalene to tetralin (Scheme 8) was performed simultaneously to the HDS of

Scheme 8



dibenzothiophene and the HDN of indole (see section 2.16.4) in the presence of the alumina-supported $[\text{Mo}_3\text{S}_4\text{Ru}]$ catalyst, obtained from the cubane-type cluster $[\text{Mo}_3\text{Ru}(\mu_3\text{-S})_4\text{Cp'}_3(\text{CO})_2][\text{pts}]$ (25a) sulfided *in situ* at 623 K by a 2.5% solution of dimethyldisulfide in *n*-heptane. This catalyst was compared to its Mo–M (M = Rh, Ir, Pd, Pt) analogues, and it appeared that the activities were in the order $\text{Mo}_3\text{Pd} < \text{Mo}_3\text{Pt} < \text{Mo}_3\text{Ru} < \text{Mo}_3\text{Rh} < \text{Mo}_3\text{Ir}$.¹⁰⁸



25a $\text{ML}_x = \text{Ru}(\text{CO})_2$, $y = 1$

25b $\text{ML}_x = \text{Rh}(\text{COD})$, $y = 2$

25c $\text{ML}_x = \text{IrCl}(\text{COE})$, $y = 1$

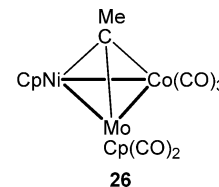
25d $\text{ML}_x = \text{Pd}(\text{PPh}_3)$, $y = 1$

25e $\text{ML}_x = \text{Pt}(\text{NBE})$, $y = 1$

2.5.1.9. Mo–Ru–Co. Hydrogenation of styrene to ethylbenzene was catalyzed by the tetrahedral cluster $[\text{MoRuCo}(\mu_3\text{-S})\text{Cp}(\text{CO})_8]$ with very low yields (ca. 5%). The complex could be recovered almost completely.¹⁰⁷

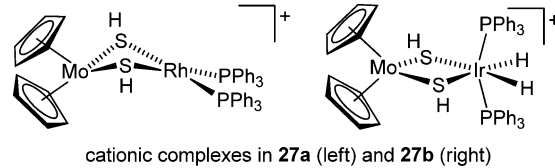
2.5.1.10. Mo–Co. Cyclohexene hydrogenation was catalyzed by the trinuclear linear complex $[\text{Et}_4\text{N}]_2[\text{Mo}_2\text{CoS}_4\text{O}_4]$ supported on alumina.¹⁰³

2.5.1.11. Mo–Co–Ni. The cluster $[\text{MoCoNi}(\mu_3\text{-CMe})\text{Cp}_2(\text{CO})_5]$ (26) catalyzes the homogeneous hydrogenation of styrene to ethylbenzene with very low yields (ca. 4%). However, the catalyst could not be recovered after the reaction.¹⁰⁷



2.5.1.12. Mo–Rh. Preliminary studies show that hydrogenation of cyclohexene to cyclohexane can be achieved with the complex $[\text{MoRhCp}(\mu\text{-CO})_2(\text{CO})(\text{PPh}_3)_2]$ in toluene at ambient temperature and atmospheric pressure of dihydrogen, but at a much slower rate than the mononuclear complex $[\text{RhCl}(\text{PPh}_3)_3]$.¹¹⁰

The dinuclear complex $[\text{Cp}_2\text{Mo}(\mu\text{-SH})_2\text{Rh}(\text{PPh}_3)_2][\text{PF}_6]$ (27a) was evaluated in the hydrogenation of 1-octyne and *t*-Bu-propiolate at room temperature and under 1 atm of H_2 , to yield 1-octene and *t*-Bu-acrylate, respectively. It was more active than its Mo–Ir, W–Rh, and W–Ir analogues, but less active than the mononuclear complex $[\text{H}_2\text{Rh}(\text{Me}_2\text{CO})(\text{EtOH})(\text{PPh}_3)_2][\text{PF}_6]$. More precisely, it quantitatively converted 1-octyne to a mixture of 1-octene (32% yield) and 2-octenes (50% combined yield) within 15 h, while the other heterobimetallic systems required 2–4 days. It also hydrogenated *t*-Bu-propiolate with 100% conversion after 5 h, affording *t*-Bu-acrylate in 99% yield. In the latter case, although the mononuclear complex $[\text{H}_2\text{Rh}(\text{Me}_2\text{CO})(\text{EtOH})(\text{PPh}_3)_2][\text{PF}_6]$ hydrogenates faster, it also hydrogenates too far and yields *t*-Bu-propionate, thus decreasing the yield of acrylate.¹¹¹



cationic complexes in 27a (left) and 27b (right)

Hydrogenation of naphthalene was achieved, simultaneously to the HDS of dibenzothiophene and the HDN of indole (see section 2.16.6), in the presence of the alumina-supported heterogeneous catalyst prepared from the sulfidation at 623 K with a 2.5% dimethyldisulfide solution of the cubane-type cluster $[\text{Mo}_3\text{Rh}(\mu_3\text{-S})_4\text{Cp'}_3(\text{COD})][\text{pts}]_2$ (25b). The main product was tetralin. This system was more active than the Ru-, Pd-, and Pt-containing analogues and almost as active as the Ir-containing one. It was suggested that the better activity of Rh- and Ir-containing systems may be ascribed to the better distribution of Rh and Ir nanoparticles on the MoS_2 phase formed on alumina during the sulfidation treatment.¹⁰⁸

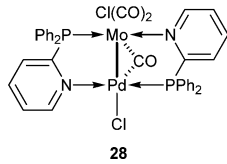
2.5.1.13. Mo–Ir. Similarly to the aforementioned Mo–Rh catalyst, the hydrosulfido-bridged complex $[\text{Cp}_2\text{Mo}(\mu\text{-SH})_2\text{IrH}_2(\text{PPh}_3)_2][\text{PF}_6]$ (27b) exhibited activity in hydro-

genation of carbon–carbon triple bonds of 1-octyne and *t*-Bu-propiolate. It was found to be a much slower and much less active catalyst than the Mo–Rh system described above. Indeed, hydrogenation of *t*-Bu-propiolate affords *t*-Bu-acrylate with 39% yield after 7 days of reaction, and at 68% conversion only.¹¹¹

The alumina-supported cubane cluster $[\text{Mo}_3\text{Ir}(\mu_3\text{-S})_4\text{Cp}'_3\text{Cl}(\text{COE})][\text{pts}]$ (**25c**) afforded a $[\text{Mo}_3\text{Ir}]$ catalyst upon sulfidation at 623 K with a 2.5% dimethyldisulfide solution. This system was active in the simultaneous HDS of dibenzothiophene, HDN of indole (see section 2.16.6), and hydrogenation of naphthalene to tetralin. It was more active than other Mo–M (M = Ru, Pd, Pt, Rh) systems, probably due to the better distribution of Ir nanoparticles on the surface of the MoS_2 /alumina surface.¹⁰⁸

2.5.1.14. Mo–Ni. The alumina-supported linear complex $[\text{Et}_4\text{N}]_2[\text{Mo}_2\text{NiS}_4\text{O}_4]$ was tested for the hydrogenation of cyclohexene.¹⁰³

2.5.1.15. Mo–Pd. The complex $[\text{Cl}(\text{OC})_2\text{Mo}(\mu\text{-CO})(\mu\text{-Ph}_2\text{Ppy})_2\text{PdCl}]$ (**28**) was used either as homogeneous or as resin-immobilized catalyst for the hydrogenation of 1,5,9-cyclododecatriene. The free complex yielded 93.2% of cyclododecene and 6.8% of cyclododecane with 92.5% conversion, while the supported catalyst afforded 84.2% cyclododecene and 15.8% cyclododecane at 89.4% conversion.¹¹²



Hydrogenation, in competition with double-bond isomerization, of 1,5-cyclooctadiene was performed with the planar clusters $[\text{Mo}_2\text{Pd}_2\text{Cp}_2(\text{CO})_6(\text{PEt}_3)_2]$ (**11a**) and $[\text{Mo}_2\text{Pd}_2\text{Cp}_2(\text{CO})_6(\text{PPh}_3)_2]$ (**11b**) with moderate activities. These clusters also catalyzed the hydrogenation of phenylacetylene to a mixture of styrene and ethylbenzene. Styrene was the major product, suggesting that these clusters might lead to efficient and selective catalysts for alkyne reduction to alkene.⁵¹

Hydrogenation of naphthalene to tetralin was tested, along with the simultaneous HDS of dibenzothiophene and the HDN of indole (see section 2.16.8), in the presence of the $[\text{Mo}_3\text{Pd}]$ catalyst obtained by impregnation of the cubane cluster $[\text{Mo}_3\text{Pd}(\mu_3\text{-S})_4\text{Cp}'_3(\text{PPh}_3)][\text{pts}]$ (**25d**) on alumina, and subsequent sulfidation at 623 K. The presence of poorly dispersed Pd aggregates on a MoS_2 phase probably accounts for the poor activity. Comparison with the related catalysts Mo–M (M = Ru, Rh, Ir, Pt) afforded the following trend of activities: $\text{Mo}_3\text{Pd} < \text{Mo}_3\text{Pt} < \text{Mo}_3\text{Ru} < \text{Mo}_3\text{Rh} < \text{Mo}_3\text{Ir}$.¹⁰⁸

2.5.1.16. Mo–Pt. The linear chain complex *trans*- $[\text{Pt}\{\text{MoCp}(\text{CO})_3\}_2(\text{CNCy})_2]$ was found to catalyze the mono- and dihydrogenation of terminal alkynes. Indeed, phenylacetylene was converted to ca. 63% styrene and 33% ethylbenzene.¹¹³

Hydrogenation reactions were achieved with the planar clusters $[\text{Mo}_2\text{Pt}_2\text{Cp}_2(\text{CO})_6(\text{PR}_3)_2]$ (R = Et, Ph) as homogeneous catalysts.⁵¹ Thus, hydrogenation of 1,5-cyclooctadiene and hydrogenation of phenylacetylene to a mixture of styrene (main product) and ethylbenzene were catalyzed by these compounds.

The MMCD catalyst derived from the chain complex *trans*- $[\text{Pt}\{\text{MoCp}(\text{CO})_3\}_2(\text{CNPh})_2]$ supported on MgO, consisting of aggregates that contain ca. 20 Pt-atoms stabilized by Mo

cations, was tested in toluene hydrogenation at 1 atm and 333 K. It was observed that coimpregnation of the monometallic complexes $[\text{PtCl}_2(\text{PhCN})_2]$ and $[\text{Mo}(\text{CO})_6]$ afforded a better catalytic system, thus exhibiting 1 order magnitude better activity, probably due to the formation of bigger segregated Pt clusters (ca. 2.4 Å). The monometallic catalyst obtained from the complex $[\text{PtCl}_2(\text{PhCN})_2]$ gave similar results, thus confirming the need in this case to have segregated Pt particles, and ruling out any possible cooperative effect.¹¹⁴

The alumina-supported cluster-derived $[\text{Mo}_3\text{Pt}]$ catalyst, obtained by sulfidation of $[\text{Mo}_3\text{Pt}(\mu_3\text{-S})_4\text{Cp}'_3(\text{NBE})][\text{pts}]$ (**25e**), showed poor activity in the simultaneous HDS of dibenzothiophene, HDN of indole (see section 2.16.8), and hydrogenation of naphthalene to yield tetralin. The presence of Pt centers close to Mo centers seems to inhibit the Mo activity, because a coimpregnated $\text{Mo}_3 + \text{Pt}$ system was found to be more active.¹⁰⁸

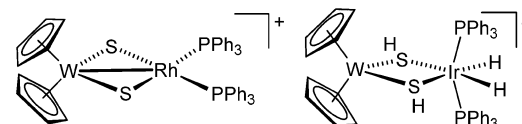
2.5.1.17. W–Fe. After deposition onto an alumina matrix, the trinuclear complex $[\text{Et}_4\text{N}]_2[\text{W}_2\text{FeS}_4\text{O}_4]$ was tested for the hydrogenation of cyclohexene.¹⁰³

2.5.1.18. W–Fe–Co. Hydrogenation of styrene to ethylbenzene did not proceed in the presence of the cluster $[\text{WFeCo}(\mu_3\text{-PMe})\text{Cp}(\text{CO})_8]$.¹⁰⁷

2.5.1.19. W–Os. The cluster $[\text{PPN}][\text{HWOs}_3(\text{CO})_{14}]$ was used in the hydrogenation of some dienes, cycloalkenes, and in particular of styrene to ethylbenzene. The activity of the catalyst was enhanced when the solvent used was an ionic liquid, instead of a common organic solvent. This was explained by the absence of deactivation of the catalysts in ionic liquids.¹¹⁵

2.5.1.20. W–Co. The hydrogenation of cyclohexene was carried out in the presence of the alumina-supported linear complex $[\text{Et}_4\text{N}]_2[\text{W}_2\text{CoS}_4\text{O}_4]$.¹⁰³

2.5.1.21. W–Rh, W–Ir. Hydrogenation of alkynes such as 1-octyne and *t*-Bu-propiolate was performed with the complexes $[\text{Cp}_2\text{W}(\mu\text{-S})_2\text{Rh}(\text{PPh}_3)_2][\text{PF}_6]$ (**29a**) and $[\text{Cp}_2\text{W}(\mu\text{-SH})_2\text{IrH}_2(\text{PPh}_3)_2][\text{PF}_6]$ (**29b**) at room temperature and under 1 atm of H_2 . They were found to be less active than the Mo–Rh analogue (see section 2.5.1.12). Indeed, *t*-Bu-propiolate was quantitatively hydrogenated to *t*-Bu-acrylate with 85% yield after 2 days in the presence of **29a**. The same substrate afforded *t*-Bu-acrylate with 30% yield after 7 days at 59% conversion only, in the presence of **29b**. For comparison, the Mo–Rh analogue **27a** required only 5 h and showed higher selectivity.¹¹¹



cationic complexes in **29a** (left) and **29b** (right)

2.5.1.22. W–Ni. The heterogenized linear complex $[\text{Et}_4\text{N}]_2[\text{W}_2\text{NiS}_4\text{O}_4]$, supported on alumina, was found to be very active for the hydrogenation of cyclohexene.¹⁰³

2.5.1.23. W–Pd. Homogeneous hydrogenation of 1,5-cyclooctadiene, in competition with isomerization, was catalyzed by the planar clusters $[\text{W}_2\text{Pd}_2\text{Cp}_2(\text{CO})_6(\text{PEt}_3)_2]$ (**12a**) and $[\text{W}_2\text{Pd}_2\text{Cp}_2(\text{CO})_6(\text{PPh}_3)_2]$ (**12b**). The main products of the hydrogenation were cyclooctene and cyclooctane. They were also active in the hydrogenation of phenylacetylene to a mixture of styrene (major) and ethylbenzene.⁵¹

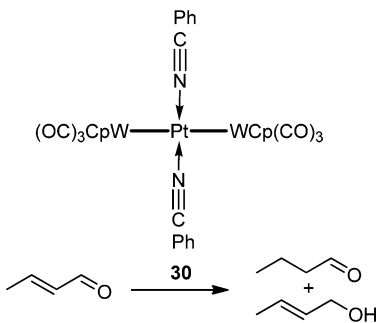
2.5.1.24. W–Pt. Just like the W–Pd clusters described previously, the planar clusters $[W_2Pt_2Cp_2(CO)_6(PEt_3)_2]$ and $[W_2Pt_2(CO)_6(PPh_3)_2]$ were used in the homogeneous hydrogenation of 1,S-cyclooctadiene and of phenylacetylene to styrene and ethylbenzene.⁵¹

Toluene hydrogenation at 1 atm and 333 K was carried out in the presence of a heterogeneous $[W_2Pt]$ catalyst prepared from *trans*- $[Pt\{WCp(CO)_3\}_2(NCPH)_2]$ (30) supported on MgO. Strong W–Pt interactions appear to lower the catalytic activity relative to catalysts containing the same metals but lacking bimetallic interactions (see also section 2.5.1.16).^{114a}

The $[W_2Pt]$ and $[W_2Pt_2]$ catalysts obtained by thermal treatment of the alumina-supported chain complex 30 and planar cluster $[Pt_2W_2Cp_2(CO)_6(PPh_3)_2]$ showed poor activity for toluene hydrogenation. The $[Pt]$ and $[W+Pt]$ catalysts prepared from the monometallic precursors $[PtCl_2(PhCN)_2]$ and $[W(CO)_6]$ were 15 times more active. The lower activity of the heterometallic species was attributed to W–Pt interactions in the homogeneous dispersion of the Pt–W particles, as opposed to the larger and more segregated Pt aggregates obtained from monometallic complexes.¹¹⁶

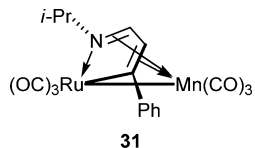
In the hydrogenation of crotonaldehyde, these $[W_2Pt]$ and $[W_2Pt_2]$ catalysts yielded mainly butyraldehyde, as a result of the hydrogenation of the C=C bond of crotonaldehyde (Scheme 9). Yet they were more selective for crotyl alcohol, although it was less than 10%, than the $[Pt]$ and $[W+Pt]$ catalysts.¹¹⁶

Scheme 9



2.5.1.25. Mn–Fe. The arsenido-bridged complex $[(OC)_4Mn(\mu\text{-AsMe}_2)Fe(CO)_4]$ was found to be a homogeneous catalyst for the hydrogenation of 1-octene to octane, although isomerization to *cis*- and *trans*-2-octene occurred to a larger extent.⁵²

2.5.1.26. Mn–Ru. Hydrogenation of styrene to ethylbenzene was catalyzed in the presence of the complex $[MnRu(CO)_6\{\mu\eta^2:\eta^4\text{-}(PhC=CH-CH=N-iPr)\}]$ (31). The reversible hapticity change of the Mn-coordinated azadienyl cycle was proposed to be the key to the binding of the styrene substrate.¹¹⁷



2.5.1.27. Re–Rh. In the presence of 1 mol % of the homogeneous catalyst precursor $[H_5(HCy_2P)Re(\mu\text{-PCy}_2)_2RhH(PCy_2H)]$ at 298 K under 1 atm of H₂, the substrates allylbenzene, 2,3-dimethylbutadiene, and 2-butyne

were readily hydrogenated to the corresponding alkanes. However, such results are typical of phosphine rhodium hydride complexes, thus ruling out in this case any synergism between the two metals.¹¹⁸

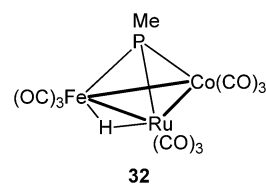
2.5.1.28. Re–Pt. The heterobimetallic complex $[HCp(CO)_2RePtH(PPh_3)_2]$ was shown to catalyze the hydrogenation of ethylene to ethane in benzene, at room temperature and 0.6 atm of H₂. After 2 days, 2.4 equiv of ethane was formed. The mechanism seems to involve the formation of the mononuclear complexes $[H_2ReCp(CO)_2]$ and $[Pt(C_2H_2)(PPh_3)_2]$ due to the binding of ethylene to the Pt center.¹¹⁹

2.5.1.29. Fe–Ru. Several Fe–Ru clusters with various Fe/Ru ratios ($[Fe_2Ru_2(CO)_{12}]$, $[Fe_2Ru(CO)_{12}]$, and $[H_2FeRu_3(CO)_{13}]$) were tested in the homogeneous hydrogenation of 1,*3-cis*- and 1,*3-trans*-pentadiene, 1- and 2-pentyne, or diphenylacetylene. The adsorption of these clusters onto alumina led to a decrease in activity for pentyne hydrogenation but to increased activity for pentadiene hydrogenation. The absence of reactivity in toluene hydrogenation suggested that the adsorbed species were not metallic nanoparticles but rather clusters or cluster fragments.⁵⁴

When supported on glc Chromosorb, the cluster $[H_2FeRu_3(CO)_{13}]$ led to a catalyst for the hydrogenation of several mono- (cyclohexene) and dienes (1,3- and 1,4-cyclohexadiene), of aromatic hydrocarbons (benzene, toluene), as well as alkynes (3-hexyne), with very high activities and excellent selectivities (>99% in almost all cases) for the fully hydrogenated products at 333 K. The supported cluster $[HRuCo_3(CO)_{12}]$ was even more selective (100% in all cases), probably due to the lower hydrogenation ability of iron as compared to cobalt (see section 2.5.1.36).¹²⁰

The cluster $[H_2FeRu_3(CO)_{13}]$ was deposited on pyrex borosilicate glass and used as catalyst without further activation for the solid–gas hydrogenation of 3-hexyne and 1,4-cyclohexadiene. A selectivity of 90% for *trans*-3-hexene was reached for the former reaction, with a conversion of 75%, while the latter gave 90% selectivity for cyclohexene with a conversion of 98%.¹²¹

2.5.1.30. Fe–Ru–Co. The trimetallic cluster $[HFeRuCo(\mu_3\text{-PMe})(CO)_9]$ (32) was used to catalyze the hydrogenation of styrene to ethylbenzene with quantitative yields. However, hydrogenation of α -methylstyrene to cumene did not proceed.¹⁰⁷



2.5.1.31. Fe–Co. The arsenido-bridged complex $[(OC)_3Co(\mu\text{-AsMe}_2)Fe(CO)_4]$ was more active in the homogeneous isomerization/hydrogenation of 1-octene to octane and *cis*- and *trans*-2-octene than the corresponding Mo–Fe and Mn–Fe complexes (see sections 2.5.1.6 and 2.5.1.25, respectively).⁵²

Hydrogenation of dienes, aromatic hydrocarbons, and alkynes was performed in the presence of highly dispersed metal particles on glc Chromosorb obtained from the cluster $[HFeCo_3(CO)_{12}]$. Almost only fully hydrogenated products were obtained.¹²²

2.5.1.32. Fe–Rh. When the cluster $[HFe_3Rh(CO)_{11}(\mu_4\text{-}\eta^2\text{-C=CHPh})]$ (13) was used for the isomerization of 1-heptene

to *cis*- and *trans*-2-heptene (see section 2.2.14), the formation of 14% heptane was also observed. This is a rare example of a mixed iron–rhodium system in which the known hydrogenation ability of rhodium is inhibited by iron, thus favoring isomerization over hydrogenation reactions. A similar observation was made above when this cluster was used in the isomerization of alkenes (see section 2.2.14).⁵⁸

2.5.1.33. Fe–Pd. Hydrogenation of 1-hexyne in the presence of 1-hexene was selectively catalyzed by the complex $[(OC)_4Fe(\mu\text{-}PPPh_2)Pd(\mu\text{-}Cl)]_2$ (**15**). At 448 K, under 100 atm of H₂, 93% of a sample of 1-hexyne in benzene was reduced to hexene and only 3% to hexane. This was unexpected because palladium is usually an excellent catalyst for the hydrogenation of olefins.⁶⁰

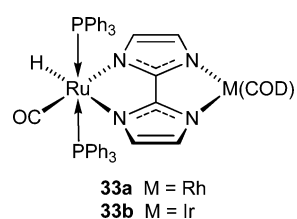
2.5.1.34. Fe–Pt. The cluster $[Fe_2Pt(CO)_9(PPPh_3)]$ was immobilized on a phosphine-functionalized poly(styrene-divinylbenzene) support to yield the species $[Fe_2Pt(CO)_8(Ph_2P\sim\text{polym})_2]$. This material was found to catalyze ethylene hydrogenation under mild conditions. Similar results were obtained with the Ru–Pt analogous system (see section 2.5.1.41), thus suggesting that the reaction goes through a similar mechanism in both cases.⁷³

2.5.1.35. Ru–Os. During ethylene hydrogenation at 340 K, the cluster $[Al]^+[HRuOs_3(CO)_{13}]^-$, obtained from the adsorption of $[H_2RuOs_3(CO)_{13}]$ on alumina, decomposed to give catalytically active metal particles.⁶²

2.5.1.36. Ru–Co. Hydrogenation of 2-pentene, styrene, and α -substituted styrenes was achieved with the clusters $[RuCo_2(\mu_3\text{-}S)(CO)_9]$, $[RuCo_2(\mu_3\text{-}PR)(CO)_9]$ (R = Me, Ph), and $[HRu_2Co(\mu_3\text{-}PMe)(CO)_9]$ as catalysts. In particular, these clusters proved to be very efficient in styrene hydrogenation. With the exception of $[RuCo_2(\mu_3\text{-}S)(CO)_9]$, all of them afforded ethylbenzene with yields in the range 98–100%. The cluster $[RuCo_2(\mu_3\text{-}S)(CO)_9]$, however, afforded ethylbenzene in 25% only, the main product being polystyrene (95% conversion).¹⁰⁷ The hydrogenation of 1-hexene was also catalyzed by $[RuCo_2(\mu_3\text{-}S)(CO)_9]$ and $[RuCo_2(\mu_3\text{-}Se)(CO)_9]$.⁶⁴

Highly dispersed metal particles on glc Chromosorb were prepared from the cluster $[HRuCo_3(CO)_{12}]$ and found to be catalytically active for the full hydrogenation of monoenes, dienes, aromatic hydrocarbons, and alkynes. The selectivity for the fully hydrogenated compounds was quantitative in all cases. The use of higher surface area supports, such as aerosil, afforded even more active catalysts.^{120,122}

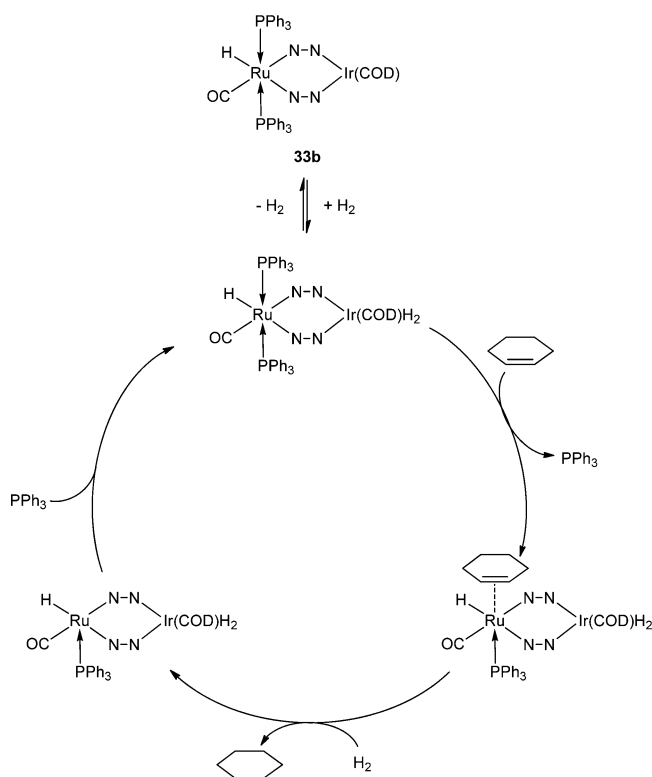
2.5.1.37. Ru–Rh. Electronic communication between the metal centers, through the bridging ligand, is believed to account for the higher catalytic activity in hydrogenation of cyclohexene of the complex $[H(OC)(PPPh_3)_2Ru(\mu\text{-bim})Rh(COD)]$ (bim = 2,2'-bi-imidazolato) (**33a**) (see section 2.5.1.38 below for more details).¹²³ This system was also found to be more active in hydrogen transfer from propan-2-ol to styrene than the corresponding Ru and Rh mononuclear complexes.^{123,124}



Hydrogenation of the C=C double bond of 2-cyclohexene was selectively catalyzed by $[H_2Ru_2Rh_2(CO)_{12}]$ with high activity (68% conversion), to afford cyclohexanone (99% of the product mixture). A solution of the homometallic complexes $[H_4Ru_4(CO)_{12}]$ and $[Rh_4(CO)_{12}]$ afforded a less active system (ca. 48% conversion), which exhibited 86% selectivity for cyclohexanone. The other observed products were 2-cyclohexenol and cyclohexanol.¹²⁵

2.5.1.38. Ru–Ir. Likewise, the bimetallic complex $[H(OC)(PPPh_3)_2Ru(\mu\text{-bim})Ir(COD)]$ (**33b**) is active in hydrogenation of cyclohexene and styrene, and the electronic communication through the bi-imidazolato ligand was considered the most likely explanation for its higher catalytic activity as compared to the corresponding mononuclear complexes. More precisely, the electron density on the ruthenium atom is significantly decreased by the replacement of the acid proton of the $[H\text{bim}]^-$ ligand in $[RuH(H\text{bim})(CO)(PPPh_3)_2]$ by the "Ir-(COD)" fragment, as evidenced by a displacement of the ν_{co} absorption toward higher frequencies. This effect is even amplified by the binding of hydrogen on the iridium center (see Scheme 10). Thus, the authors suggested a catalytic cycle for

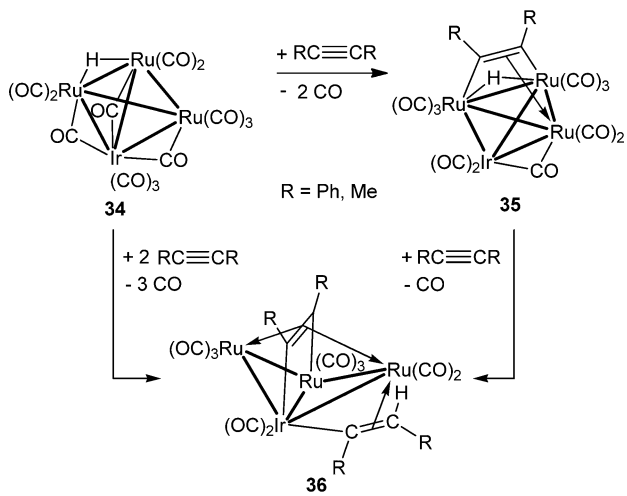
Scheme 10. Proposed Catalytic Cycle for Cyclohexene Hydrogenation by 33b¹²⁴



cyclohexene hydrogenation in the presence of **33b**, involving PPh₃ dissociation from the ruthenium atom to bind the substrate. This complex was slightly more active than the Ru–Rh analogue described above.^{123,124}

The clusters $[IrRu_3(\mu\text{-}H)(CO)_{11}(\mu_3\text{-}\eta^2\text{-}RC\equiv CR)]$ (R = Ph, Me) (**35**) and $[IrRu_3(CO)_{10}(\mu_4\text{-}\eta^2\text{-}RC\equiv CR)(\mu\text{-}\eta^2\text{-}RC\equiv CHR)]$ (R = Ph, Me) (**36**) were compared to $[HIrRu_3(CO)_{13}]$ (**34**) in the hydrogenation of diphenylacetylene to stilbene (Scheme 11). Even if these alkyne-coordinated clusters were active, the latter cluster was by far the best catalyst, with up to 98% selectivity toward *trans*-stilbene, in the absence of CO. It

Scheme 11. Synthetic Routes to Clusters 35 and 36 Starting from 34¹²⁶

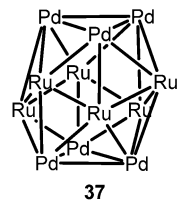


was also found that $[\text{H}_3\text{IrRu}_3(\text{CO})_{12}]$ is formed from 34 under H_2 pressure, but its activity was lower than that of the monohydride precursor.¹²⁶

2.5.1.39. Ru–Ni. The tetrahedral cluster $[\text{Ru}_3\text{Ni}(\mu\text{-H})_3\text{Cp}(\text{CO})_9]$ is a selective hydrogenation catalyst for linear dienes such as *cis*-1,3-pentadiene. The conjugated cyclic diene 1,3-cyclohexadiene is selectively hydrogenated to cyclohexene. However, its ability to hydrogenate is limited by the fast decomposition of the cluster (extensive decomposition observed after 40 min only), unlike its Os–Ni analogue.^{65,127}

The Chromosorb P-supported $[\text{Ru}_3\text{Ni}]$ catalyst derived from this Ru–Ni cluster was found to be more active in the hydrogenation of benzene or toluene, to cyclohexane or methylcyclohexane, respectively, than the $[\text{Os}_3\text{Ni}]$ catalyst prepared from the isostructural cluster $[\text{Os}_3\text{Ni}(\mu\text{-H})_3\text{Cp}(\text{CO})_9]$.⁶⁵ It is also active for the hydrogenation of dienes.¹²⁸

2.5.1.40. Ru–Pd. Heterogeneous $[\text{RuPd}]$ catalysts with a Pd/Ru ratio of 1:1 were prepared by gentle decarbonylation of the single-source precursor $[\text{Et}_4\text{N}]^+[\text{Ru}_6\text{Pd}_6(\text{CO})_{24}]$ (37) supported in MCM-41 mesoporous silica. This system was efficient for the hydrogenation of 1-hexene (68% selectivity for *n*-hexane at 99% conversion) and 1-dodecene (63% of *n*-dodecane for 88% conversion) under 20 bar of H_2 , without solvent. It was also active for the hydrogenation of naphthalene, mainly to *cis*-decalin,¹²⁹ of benzoic acid to cyclohexane carboxylic acid, of dimethyl terephthalate (DMT) to 1,4-cyclohexanediethanol (CHDM) (see section 3.14),^{129e} and of muconic acid to adipic acid.¹³⁰

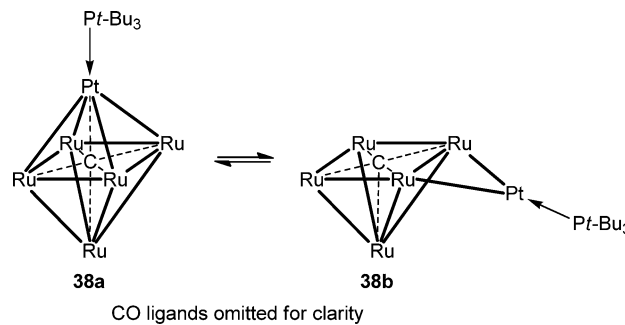


Metal core of the Pd_6Ru_6 cluster 37

2.5.1.41. Ru–Pt. Ethylene hydrogenation was achieved under mild conditions in the presence of the $[\text{RuPt}_2(\text{CO})_5(\text{PPh}_3)_3]$ cluster anchored to a phosphine-functionalized poly(styrene-divinylbenzene) support. The resulting polymer-bound cluster $[\text{RuPt}_2(\text{CO})_5(\text{Ph}_2\text{P}\sim\text{polym})_3]$

was considered to be the active species. The analogous Fe–Pt system gave similar results, suggesting a similar mechanistic pathway in both cases.⁷³

Hydrogenation of phenylacetylene was performed with the carbido cluster $[\text{Ru}_5\text{C}(\text{CO})_{15}\{\text{Pt}(\text{P}-t\text{-Bu}_3)\}]$ (38). According to the nature of the species isolated during the catalytic reactions, the platinum atom seems to play an important role in activating either hydrogen or the alkyne. This was strongly suggested to be due to its mobility, as illustrated with the equilibrium between the closo (38a) and more open, nido (38b) structures.¹³¹



CO ligands omitted for clarity

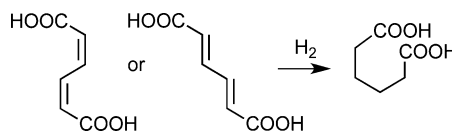
The cluster $[\text{Ru}_5\text{PtC}(\mu_3\text{-PhC}\equiv\text{CH})(\text{CO})_{13}(\text{P}-t\text{-Bu}_3)]$ was used as a precursor for the catalytic hydrogenation of $\text{PhC}\equiv\text{CH}$ to styrene and ethylbenzene. It was observed that the cluster fragments during the reactions, and that one of the species formed, the mononuclear complex $[\text{Pt}(\eta^2\text{-PhC}\equiv\text{CH})(\text{CO})(\text{P}-t\text{-Bu}_3)]$, is responsible for such a high activity.¹³²

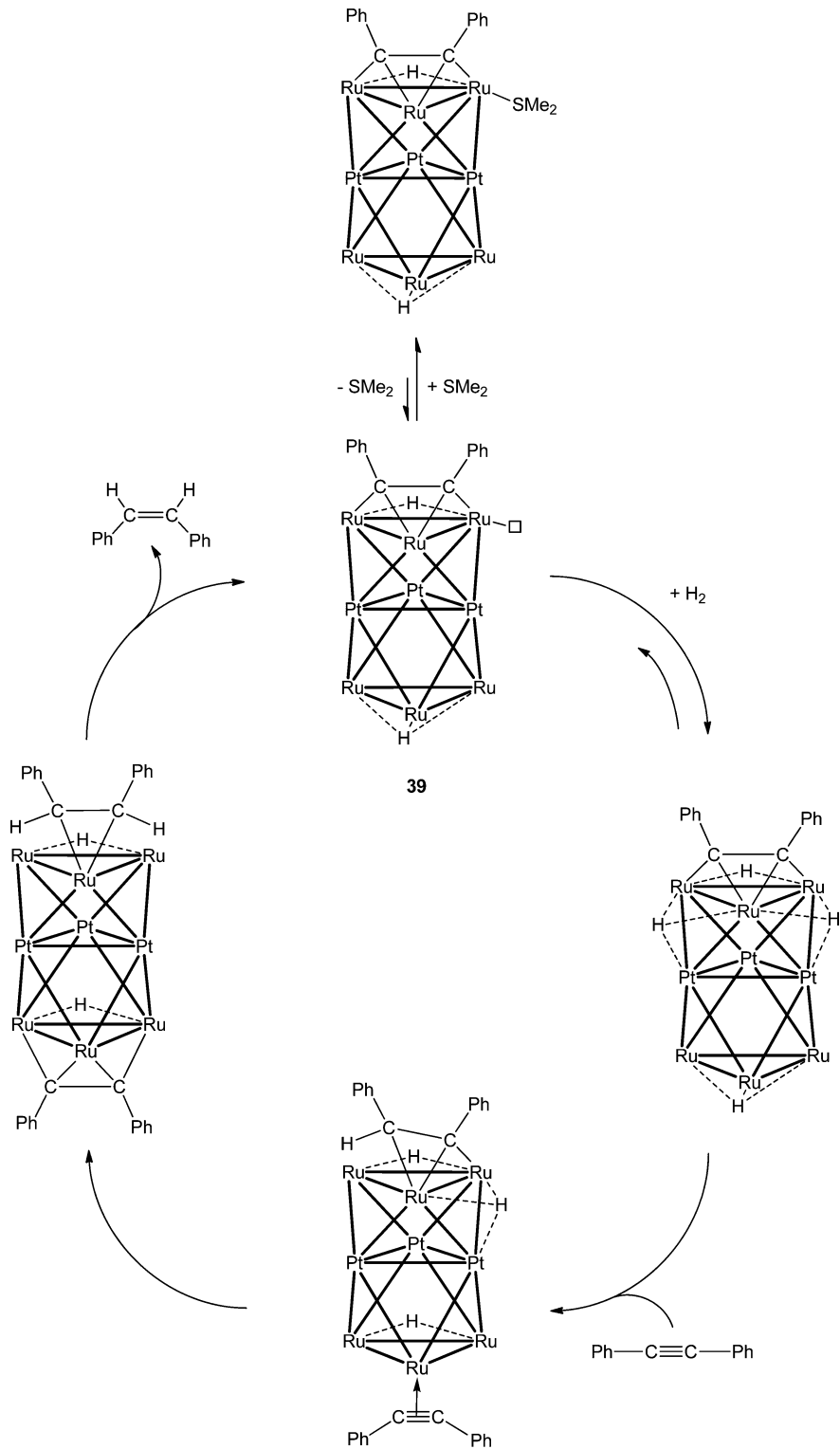
Several silica-supported decarbonylated heterometallic clusters, obtained from the clusters $[\text{Ph}_4\text{P}]_2[\text{Ru}_5\text{PtC}(\text{CO})_{15}]$, $[\text{PPN}]_2[\text{Ru}_{10}\text{Pt}_2(\text{C})_2(\text{CO})_{28}]$,^{129e} $[\text{Ru}_5\text{PtC}(\mu\text{-SnPh}_2)(\text{CO})_{15}]$, $[\text{Ru}_5\text{PtC}(\mu\text{-GePh}_2)(\text{CO})_{15}]$, and $[\text{Ru}_5\text{PtC}(\text{CO})_{16}]$,¹³³ were tested in the conversion of dimethyl terephthalate to 1,4-cyclohexanediethanol (see section 3.14). The first step consists of the hydrogenation of the $\text{C}\equiv\text{C}$ bonds of the benzene ring. The carbonyl group of the ester function then is reduced to alcohol (see section 2.5.3.6). The presence of tin seems to greatly enhance the activity and the selectivity for the desired product.

The silica-supported $[\text{Ru}_5\text{Pt}]$ and $[\text{Ru}_{10}\text{Pt}_2]$ catalysts, derived from the clusters $[\text{Ph}_4\text{P}]_2[\text{Ru}_5\text{PtC}(\text{CO})_{15}]$ and $[\text{PPN}]_2[\text{Ru}_{10}\text{Pt}_2(\text{C})_2(\text{CO})_{28}]$, were also good catalysts for the hydrogenation of naphthalene mostly to *cis*-decalin, of benzoic acid to cyclohexane carboxylic acid,^{129e} and of muconic acid to adipic acid.¹³⁰

The clusters $[\text{Ph}_4\text{P}]_2[\text{Ru}_5\text{PtC}(\text{CO})_{15}]$ and $[\text{PPN}]_2[\text{Ru}_{10}\text{Pt}_2(\text{C})_2(\text{CO})_{28}]$ were anchored inside MCM-41 channels and subjected to thermal treatment to afford NPs with compositions close to that of the precursor cluster. These catalysts showed slightly lower activities in the hydrogenation of *cis,cis*- and *trans,trans*-muconic acid to adipic acid (Scheme 12) (ca. 90% conversion) than the commercially available Pt/SiO₂ and Rh/Al₂O₃ systems (95–99% conversion), but $[\text{Ru}_{10}\text{Pt}_2]$ is more selective for the formation of adipic acid

Scheme 12



Scheme 13. Proposed Catalytic Cycle for the Hydrogenation of Diphenylacetylene to *cis*-Stilbene with the Cluster 39¹³⁷

(ca. 95%) as compared to the homometallic systems (ca. 85–90%). Furthermore, [Ru₅Pt] shows almost 80% selectivity toward succinic and glutaric acids, as a result of simultaneous hydrogenation and hydrogenolysis, but only 25% selectivity for adipic acid was observed.¹³⁰

Hydrogenation of citral was performed, in the presence of magnesia-¹³⁴ or mesoporous silica-supported¹³⁵ catalysts derived from the trimetallic cluster [Ru₅PtC(μ-SnPh₂)(CO)₁₅],

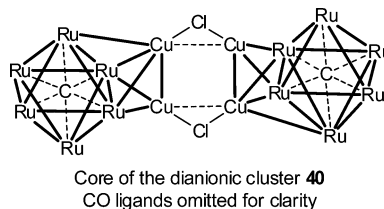
with higher conversion than using conventionally prepared Ru–Pt–Sn catalysts. It appeared that the aldehyde functions were reduced first, thus leading to geraniol and nerol (see section 2.5.3.6). Alkene bonds were subsequently partially hydrogenated to give 3,7-dimethyloctanol. At 50% conversion, up to 56% selectivity to unsaturated alcohols (geraniol/nerol = 0.88) was observed when the silica-supported catalyst was used, and only 19% for the aldehyde citronellal.¹³⁵

Hydrogenation of ethylene was performed in the presence of $[\text{Ru}_6\text{Pt}_3]$ catalysts prepared from the cluster $[\text{Ru}_6\text{Pt}_3(\mu_3\text{-H})(\mu\text{-H})_3(\text{CO})_{21}]$ (22) adsorbed onto alumina and magnesia, and then decarbonylated at 573 K under He.⁹³

Hydrogenation of $\text{PhC}\equiv\text{CPh}$ to *cis*-stilbene at 1 atm and 323 K was catalyzed in the presence of the bioctahedral cluster $[\text{Ru}_6\text{Pt}_3(\mu_3\text{-H})(\mu\text{-H})(\mu_3\text{-PhC}\equiv\text{CPh})(\text{CO})_{20}]$ (39). It was reported to exhibit a high catalytic activity and 100% selectivity. These results were significantly better than when either pure platinum or pure ruthenium clusters were used, suggesting the existence of cooperativity effects.¹³⁶ This cluster contains discrete triangular layers of pure platinum and pure ruthenium, which may synergistically interact. A proposed mechanism is given in Scheme 13.

The reaction of 39 with SMe_2 yielded the compound $[\text{Ru}_6\text{Pt}_3(\mu_3\text{-H})(\mu\text{-H})(\mu_3\text{-PhC}\equiv\text{CPh})(\text{SMe}_2)(\text{CO})_{19}]$, which was found to be much more active for the hydrogenation of $\text{PhC}\equiv\text{CPh}$ to (*Z*)-stilbene than its precursor. However, its activity rapidly decreased over time to reach that of its precursor 39, which tends to form during the catalytic reaction.¹³⁷

2.5.1.42. Ru–Cu. The carbido cluster $[\text{PPN}]_2[\text{Ru}_{12}\text{Cu}_4(\text{C})_2(\mu\text{-Cl})_2(\text{CO})_{32}]$ (40) was used as a precursor for the synthesis of supported RuCu NPs in the channels of mesoporous silica MCM-41.



Core of the dianionic cluster 40
CO ligands omitted for clarity

Activation was achieved by gentle decarbonylation under vacuum at 453 K for 2 h. The particles are located on the silica surface (Figure 1). This material was an efficient catalyst for the

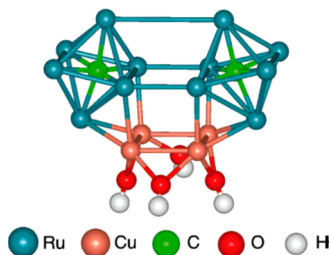
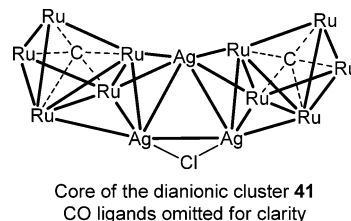


Figure 1. Proposed structure (based on EXAFS studies) of Ru–Cu particles obtained from 40, deposited onto silica surface. Reproduced with permission from ref 138. Copyright 1998 Wiley-VCH Verlag GmbH.

hydrogenation of various alkenes (1-hexene), arenes (*trans*-stilbene, *cis*-cyclooctene, *d*-limonene), and alkynes (phenyl-acetylene and diphenylacetylene).^{129c,138} In particular, hydrogenation of phenylacetylene yielded quantitatively ethylbenzene under 65 atm of H_2 , at 373 K.^{122,130}

The same $[\text{Ru}_{12}\text{Cu}_4]/\text{MCM-41}$ catalytic system could hydrogenate dimethyl terephthalate to 1,4-cyclohexanedimethanol (see section 3.14),^{129e} naphthalene to *cis*-decalin, benzoic acid to cyclohexane carboxylic acid,^{129e} and muconic acid to adipic acid.¹³⁰

2.5.1.43. Ru–Ag. Hydrogenation of 1-hexene to hexane was performed in the presence of supported nanoparticles obtained by thermal activation of the adsorbed cluster $[\text{Ph}_4\text{As}]_2[\text{Ru}_{10}\text{Ag}_3(\text{C})_2(\mu\text{-Cl})(\text{CO})_{28}]$ (41) onto the inner walls of mesoporous silica MCM-41. Preliminary results indicate a TOF of at least 6300 mol hexane per mol $[\text{Ru}_{10}\text{Ag}_3]$ per hour, which is significantly higher than previously reported homogeneous Ru monometallic complexes under similar conditions.¹³⁹



Core of the dianionic cluster 41
CO ligands omitted for clarity

2.5.1.44. Os–Rh. Anchoring of the coordinatively unsaturated cluster $[\text{H}_2\text{Os}_3\text{Rh}(\text{acac})(\text{CO})_{10}]$ on poly(styrene-divinylbenzene) led to $[\text{H}_2\text{Os}_3\text{Rh}(\text{acac})(\text{CO})_{10}(\text{Ph}_2\text{P}\sim\text{polym})]$, which is active for the hydrogenation of ethylene. Fragmentation of the cluster was found to occur upon anchoring to give catalytically active species, exhibiting conversion lower than 1%. The authors suggested the formation of rhodium aggregates smaller than 1 nm, which were responsible for the activity. The same system was also used for the isomerization of 1-butene.⁷⁰

2.5.1.45. Os–Ni. Hydrogenation of mono- and dienes has been investigated in the presence of $[\text{Os}_3\text{Ni}(\mu\text{-H})_3\text{Cp}(\text{CO})_9]$.^{65,71} Selective homogeneous hydrogenation of linear dienes such as 1,3-*cis*-pentadiene is more effective than with the ruthenium analogue.¹²⁷ The cluster displays low activity and selectivity for the hydrogenation of *t*-butyl-alkynes or *t*-butyl-alkenes,¹⁴⁰ but is more effective for the selective hydrogenation of *t*-butyl-acetylene.⁷¹ Similarly, it catalyzes the hydrogenation of 1-pentyne more readily than that of 1-pentene and affords 1-pentene. During the hydrogenation reactions of *t*-butyl-alkynes and of *t*-butyl-alkenes, the cluster $[\text{Os}_3\text{Ni}_3\text{Cp}_3(\text{CO})_9]$ decomposed to $[\text{Os}_3\text{Ni}(\mu\text{-H})_3\text{Cp}(\text{CO})_9]$, which is less active, but more stable. Indeed, it can be recovered after long reaction times.¹⁴⁰

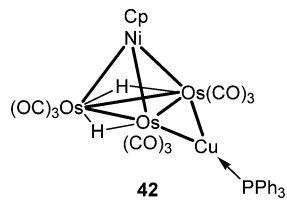
The phosphine derivatives of this cluster, $[\text{Os}_3\text{Ni}(\mu\text{-H})_3\text{Cp}(\text{CO})_8\text{L}]$ ($\text{L} = \text{PPh}_2\text{H}$ or $\text{P}(\text{C}_6\text{H}_4\text{Me}-\text{o})_3$), were also studied. They were reported to be active for the hydrogenation of dienes to monoenes, and selective for the hydrogenation of triple and double C–C bonds.⁷¹

When supported on Chromosorb P, $[\text{Os}_3\text{Ni}(\mu\text{-H})_3\text{Cp}(\text{CO})_9]$ catalyzed the hydrogenation of 1,3-*cis*- and 1,3-*trans*-pentadiene. A gas-chromatographic column was used as a catalytic reactor.¹⁴¹ Furthermore, when this cluster was supported on $\gamma\text{-Al}_2\text{O}_3$, the resulting heterogeneous catalyst $[\text{Os}_3\text{Ni}]$ was shown to be very efficient for the hydrogenation of acetylene to ethylene and ethane. Also, ethylene, propylene, and benzene were converted to ethane, propane, and cyclohexane, respectively, at room temperature.¹⁴²

Hydrogenation of acetone to propane using the $[\text{Os}_3\text{Ni}]$ heterogeneous catalyst derived from the Chromosorb P-supported cluster $[\text{Os}_3\text{Ni}(\mu\text{-H})_3\text{Cp}(\text{CO})_9]$ was assumed to involve a carbon–carbon bond hydrogenation step.¹⁴³ Indeed, hydrogenation of acetone to isopropanol (see section 2.5.3.7), then dehydration to propene (see section 2.7.2), would be followed by the hydrogenation of the C=C bond to yield propane.

Both of the γ -Al₂O₃ supported clusters [Os₃Ni(μ -H)₃Cp(CO)₉] and [Os₃Ni₃Cp₃(CO)₉] were used for the heterogeneous hydrogenation of benzene and acetylene. In particular, the former proved to be 100% selective for the full hydrogenation of benzene to cyclohexane despite a moderate activity at 375 K (conversion of ca. 1.3 mol of benzene per mole of catalyst). Increasing the temperature to 423 K improved the activity, but lowered slightly the selectivity (98%). The [Os₃Ni₃] catalyst was tested in the temperature range 346–418 K, and exhibited activities similar to those of [Os₃Ni], but with lower selectivities for cyclohexane (76–95%). In both cases, a selectivity up to 5% was observed for the hydrogenolysis product *n*-hexane. For comparison, the catalyst obtained from the alumina-supported cluster [H₂Os₃(CO)₁₀] was found to be almost 2 times more active than the mixed-metal systems, with selectivities ranging from 80% to 97% for cyclohexane.¹⁴⁴

2.5.1.46. Os–Ni–Cu. Hydrogenation of 1,3-*cis*- and 1,4-*cis*-pentadiene was achieved in the presence of Chromosorb P-supported heterogeneous catalysts derived from the trimetallic cluster [Os₃Ni(μ -CuPPh₃) $(\mu$ -H)₂Cp(CO)₉] (**42**) with good activities. In particular, at 100% conversion of 1,3-*cis*-pentadiene, the selectivity for pentane dropped from 84% to 58% when the temperature was raised from 353 to 503 K, while that for 2-pentenes increased from 16% to 36%. Cracking products and 1-pentene were detected in very small amounts. A similar profile was observed for 1,4-*cis*-pentadiene hydrogenation.^{128a}



2.5.1.47. Os–Au. No activity in ethylene hydrogenation was detected below 383 K with the silica-immobilized catalysts [HOs₃Au(CO)₁₀(Ph₂P~SIL)] and [ClOs₃Au(CO)₁₀(Ph₂P~SIL)], prepared by anchoring the PPh₃ derivatives onto phosphine-functionalized silica.⁷² The system “ClOs₃Au” was much less stable than the “HOs₃Au” system. However, when it was anchored onto a functionalized poly(styrene-divinylbenzene) support to afford [ClOs₃Au(CO)₁₀(Ph₂P~polym)], it became much more stable than its silica-supported counterpart, and it was found to be an active catalyst for ethylene hydrogenation at 1 atm and temperatures below 373 K.¹⁴⁵

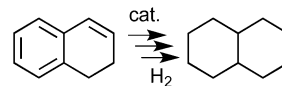
2.5.1.48. Co–Rh. Low pressure hydrogenation of styrene was tested in the presence of Co–Rh complexes with different Co/Rh ratios, which emphasized the influence of the composition of the metal core. Typically, the initial hydrogenation rate with [Co₂Rh₂(CO)₁₂] is roughly twice that of [Co₃Rh(CO)₁₂], while [Co₄(CO)₁₂] alone is inactive. Addition of trimethylphosphite resulted in enhanced rate of hydrogenation.¹⁴⁶

The cluster [Co₂Rh₂(CO)₁₂] was encapsulated in a silica sol–gel matrix for applications in alkene hydrogenation. Thus, styrene afforded ethylbenzene, and 1-chloronaphthalene yielded mainly 5-chlorotetralin, *cis*-decaline, and *trans*-decaline in the following respective amounts: first run 29%, 58%, and 8%; second run 11%, 72%, and 12%; third run 6%, 82%, and 12%. Under the reaction conditions, the entrapped clusters

turned to CoRh NPs via CO loss.⁶¹ Upon heating at 373 K for 16 h, the same silica-entrapped system afforded CoRh NPs, which proved efficient enough to fully hydrogenate styrene to ethylcyclohexane.¹⁴⁷ A pretreatment with H₂ greatly enhanced the hydrogenation rates of the catalyst. A wide scope of aromatic and unsaturated molecules such as biphenyl, diphenylacetylene could be hydrogenated.

The same research group developed an interesting system by entrapping lipase and [Co₂Rh₂(CO)₁₂] in a silica sol–gel matrix for applications in one-pot esterification and C=C hydrogenation.¹⁴⁸ Similarly, when the Co–Rh cluster was entrapped with acids such as MoO₃–SiO₂ or Me₃Si(CH₂)₃SO₃H, it was able to fully hydrogenate 1,2-hydronaphthalene (Scheme 14).¹⁴⁹

Scheme 14



2.5.1.49. Co–Pt. The linear complex *trans*-[Pt{Co(CO)₄}₂(CNCy)₂] and the triangular clusters [Co₂Pt(CO)₇(dppe)] and [Co₂Pt(CO)₇(dpae)] were used in homogeneous hydrogenation of 1-hexyne. The main products were 1-hexene (60–84% of product mixture) and 2-hexenes (14–18% of the product mixture). Hexane was also obtained in various amounts, ranging from 2% to 22%, depending on the cluster.⁵¹

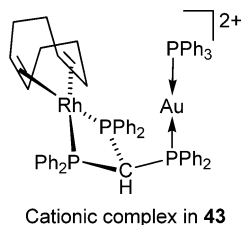
Hydrogenation of 1,3- and 1,5-octadiene was achieved in the presence of the Co–Pt cluster [Co₂Pt₂(CO)₈(PPh₃)₂] with very low activity (<7% conversion) and selectivity.¹¹³ The clusters [Co₂Pt₂(CO)₈L₂] (L = PPh₃, AsPh₃) were relatively good homogeneous catalysts for the selective hydrogenation of diphenylacetylene to *cis*-stilbene. In particular, [Co₂Pt₂(CO)₈(PPh₃)₂] afforded *cis*-stilbene with ca. 23% yield at 24% conversion. It also hydrogenated 1-octyne to 1-octene (55%) and to octane (43%) at 98% conversion. Hydrogenation of phenylacetylene was much less efficient, affording oligomerization products and exhibiting low activity (<40% conversion). Extensive transformation and rearrangement was found for this catalyst.¹¹³

The polymer-immobilized catalyst [Co₂Pt₂(CO)₈(Ph₂P~polym)₂], obtained from the butterfly cluster [Co₂Pt₂(CO)₈(PPh₃)₂]¹⁵⁰, was found to be active in olefin hydrogenation. Its slightly improved stability as compared to that of its molecular precursor under homogeneous conditions is interesting to note because in the latter case the mixed-metal cluster rapidly transformed into the homonuclear cluster [Pt₅(CO)₆(PPh₃)₄].¹¹³

2.5.1.50. Rh–Pt. Active catalysts prepared from [Et₄N]⁺[Rh₅Pt(CO)₁₅][–] on an Amberlite anion exchange resin were tested in the aromatic ring hydrogenation reactions of toluene, phenol, and anisole, with less efficiency than when the Amberlite-supported cluster [Pt₁₅(CO)₃₀]^{2–} was used. The former catalyst did not work for aniline or nitrobenzene.¹⁵¹

The [Rh₅Pt(CO)₁₅][–] cluster was adsorbed on MgO and activated under He or H₂. Its activity for toluene hydrogenation to give methylcyclohexane was compared to that of Rh/MgO obtained from [Rh₆(CO)₁₆]. It appeared that Pt slightly improved the activity, but both catalysts underwent deactivation after a few runs.¹⁵²

2.5.1.51. Rh–Au. In the presence of the dinuclear complex $[\text{RhAu}(\text{HC}(\text{PPh}_3)_3)(\text{COD})(\text{PPh}_3)](\text{BF}_4)_2$ (**43**), hydrogenation of diphenylacetylene and 1-hexene afforded *cis*-stilbene and hexane, respectively, with rather good selectivity. The Ir–Au analogue was inactive under the same reaction conditions.¹⁵³



2.5.1.52. Ir–Pt. The hydrogenation of cyclohexene to cyclohexane, 2-methylcyclohexene to 2-methylcyclohexane, 2-cyclohexenone to cyclohexanone, and crotonaldehyde to butyraldehyde was performed in the presence of $[\text{Ir}_2\text{Pt}_2(\text{CO})_7(\text{PPh}_3)_3]$ as a homogeneous catalyst. Noteworthy is that only the olefinic bond was hydrogenated in the latter two compounds, although trace amounts of the corresponding alcohols were detected.¹⁵⁴

2.5.1.53. Pt–Cu. The silica-supported cluster $[\text{Pt}_2\text{Cu}_4(\text{C}\equiv\text{C}-t\text{-Bu})_8]$ (**6**) afforded a heterogeneous $[\text{Pt}_2\text{Cu}_4]$ catalyst, which exhibited poor activity for the hydrogenation of toluene to methylcyclohexane.¹⁵⁵

2.5.1.54. Pt–Au. The silica-supported $[\text{Pt}_2\text{Au}_4]$ catalyst, obtained from the cluster $[\text{Pt}_2\text{Au}_4(\text{C}\equiv\text{C}-t\text{-Bu})_8]$ (**7**), although more active than the Pt–Cu analogue described above, was much less active in toluene hydrogenation to methylcyclohexane than the standard Pt/SiO₂ catalysts.¹⁵⁵ A complementary study was carried out with the hydrogenation of propylene in the presence of the titania-supported $[\text{Pt}_2\text{Au}_4]$ catalyst derived from cluster **7**. While Pt catalysts are very active for this reaction, it seems that the presence of Au had a “diluting effect” on the Pt atoms, thus decreasing the overall activity.¹⁵⁶

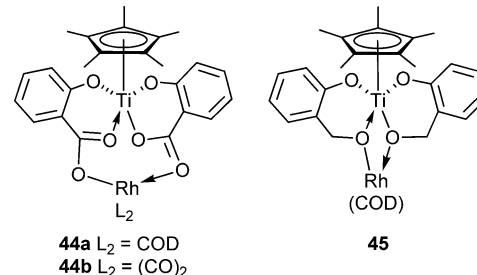
Hydrogenation of ethylene to ethane was slowly catalyzed by the 16 electron cluster $[\text{Pt}(\text{AuPPh}_3)_8](\text{NO}_3)_2$ (**5**) in the form of solid microcrystals. The intermediate formation of a hydrido cluster was suggested to occur.^{43b,46b}

The silica-supported cluster $[\text{Pt}(\text{AuPPh}_3)_6(\text{PPh}_3)](\text{NO}_3)_2$ (**3**) was found to be a slow catalyst for the hydrogenation of ethylene, exhibiting turnover frequencies of 8×10^{-4} and $5 \times 10^{-4} \text{ s}^{-1}$ with or without preliminary thermal treatment at 473 K, respectively. For comparison, the turnover frequencies for H₂–D₂ equilibration reactions in the presence of the same catalytic system were much higher and found in the range 11–29 s⁻¹.^{46a}

2.5.2. Hydrogenation of CO and CO₂. A considerable amount of work has been dedicated to the hydrogenation of CO, mainly because of the interest in Fischer–Tropsch synthesis. Efficient transformations of CO₂ are also receiving considerable attention, from both chemical and environmental viewpoints. The direct incorporation of CO₂ into organic substrates is clearly an elegant route to functionalized chemicals.¹⁵⁷ So far, only monometallic catalysts have been reported for such reactions. The hydrogenation of the carbon–oxygen multiple bonds of both CO and CO₂ will be examined together, as partial reduction of CO₂ is known to afford CO, which can be further reduced.

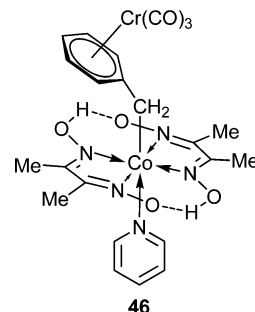
2.5.2.1. Ti–Rh. The complex $[\text{Cp}^*\text{Ti}(\mu-\eta^2:\eta^1\text{-sal})_2\text{Rh}(\text{COD})]$ (salH₂ = salicylic acid) (**44a**) was used in the

hydrogenation of CO. It exhibited not only higher activities (56% conversion) than monometallic Rh complexes (<10%), but also better selectivities toward oxygenates (56%), especially to C₂ oxygenates. The complexes $[\text{Cp}^*\text{Ti}(\mu-\eta^2:\eta^1\text{-sal})_2\text{Rh}(\text{CO})_2]$ (**44b**) and $[\text{Cp}^*\text{Ti}(\mu-\eta^2:\eta^1\text{-O}_2\text{Bn})\text{Rh}(\text{COD})]$ (**45**) (O₂Bn = 2-(oxomethyl)phenolate) also showed good selectivity for the oxygenates, but were less active.¹⁵⁸

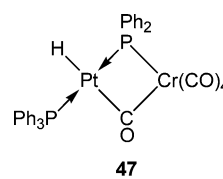


2.5.2.2. Cr–Ru. Hydrogenation of CO to hydrocarbons and oxygenates was achieved with a heterogeneous silica-supported catalyst derived from $[\text{PPN}]_2[\text{Cr}_2\text{Ru}_3\text{C}(\text{CO})_{16}]$. It was much less active and selective than $[\text{RuCo}_2]$, $[\text{RuCo}_3]$, and $[\text{Ru}_3\text{Co}_3]$ MMCD catalysts (see section 2.5.2.31), and the selectivity for oxygenates was ca. 12%.¹⁵⁹

2.5.2.3. Cr–Co. Although the separation between the metal centers is clearly nonbonding, the complex $[\text{CrCo}(\text{PhCH}_2)-(\text{DH})(\text{CO})_3(\text{py})]$ (DH⁻ = monoanion of dimethylglyoxime) (**46**) was reported to be a promising precursor for heterogeneous catalytic CO hydrogenation with good catalyst lifetime. Unfortunately, no details were provided concerning possible synergistic effects.¹⁶⁰



2.5.2.4. Cr–Pt. A [CrPt] heterogeneous catalyst prepared from $[\text{HCrPt}(\mu\text{-PPh}_2)(\mu\text{-CO})(\text{CO})_4(\text{PPh}_3)]$ (**47**, proposed structure) on SiO₂ exhibited higher activity and methanol selectivity (>50%) than conventional monometallic or bimetallic heterogeneous catalysts (12–15% selectivity) for CO₂ hydrogenation at ca. 2.2% CO₂ conversion. This system is 5.5–6.5 times more active than the monometallic system Pt/SiO₂, suggesting the occurrence of synergistic effects in the bimetallic system. However, the corresponding W–Pt analogous system was much more selective, reaching more than 90% methanol selectivity.¹⁶¹

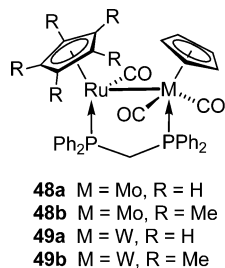


2.5.2.5. Mo–Fe. The $[\text{Mo}_2\text{Fe}_2]$ catalysts derived from the sulfido cluster $[\text{Mo}_2\text{Fe}_2\text{S}_2\text{Cp}_2(\text{CO})_8]$ and supported on MgO

showed high selectivity for C₂ products in CO hydrogenation.¹⁶² Infrared, EXAFS, and Mössbauer studies confirmed that no structural change took place upon initial adsorption of the former cluster on the support, whereas oxidation occurred upon heating.¹⁶³ These observations were consistent with the higher selectivities of the [Mo₂Fe₂] catalysts when compared to those of Mo/Al₂O₃, MoS₂, and Fe/Al₂O₃.¹⁶⁴ When adsorbed on MgO, this [Mo₂Fe₂] catalyst displayed a selectivity higher than 95 mol % C₂H₄ and C₂H₆ (ca. 1:2) against more than 95 mol % CH₄ when it was adsorbed or γ -Al₂O₃. In a similar fashion, the alumina-supported cluster [Mo₂Fe₂S₄Cp₂(CO)₆] catalyzed the hydrogenation of CO.^{164a}

2.5.2.6. Mo–Ru. Similarly to [PPN]₂[Cr₂Ru₃C(CO)₁₆] (see section 2.5.2.2), the cluster [Et₄N]₂[Mo₂Ru₃C(CO)₁₆] was used to prepare silica-supported heterogeneous catalysts for CO hydrogenation to hydrocarbons and oxygenates. However, even if the selectivities for oxygenates was 26%, the activity was lower than those of [RuCo₂], [RuCo₃], and [Ru₃Co₃] catalysts.¹⁵⁹

In the course of studies of the possible interactions between H₂ and the heterobimetallic complexes [Cp(OC)₂Mo(μ -dppm)Ru(CO)(C₅R₅)] (48a, R = H; 48b, R = Me), it was found that such systems exhibited activity, albeit very low, in the reversible hydrogenation of CO₂ to formic acid. In comparison, monometallic Ru analogues were inactive toward CO₂ hydrogenation, suggesting that both metals play a role in the reaction. It was suggested that the low activity might be due to the nonfacile reaction of the complexes with H₂ to yield dihydride species, and to the formation of a too stable Ru–H–Mo intermediate.¹⁶⁵



2.5.2.7. Mo–Os. The catalytic reduction of CO by alumina-supported catalysts derived from the tetrahedral cluster [HMnOs₃Cp(CO)₁₂] was examined. Its activity was compared to that of heterogeneous catalysts derived from [HWOs₃Cp(CO)₁₂] and [Os₃(CO)₁₂]. The fragmentation of the surface-bound clusters during thermal activation or a poisoning effect from the group 6 metal atom by carbon originating from the cyclopentadienyl ligands are thought to be responsible for the similar activities observed for all catalysts.¹⁶⁶

2.5.2.8. Mo–Co. The heterogeneous catalyst [Mo₂Co₂] derived from the sulfido cluster [Mo₂Co₂(μ ₃-S)₃Cp₂(CO)₄], supported on various inorganic matrixes, has been studied in CO methanation. It was considered that the clusters did not undergo fragmentation and reaggregation into larger crystallites.¹⁶⁴

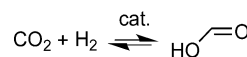
2.5.2.9. Mo–Rh. A [MoRh] catalyst derived from the bimetallic complex [MoRhCp(μ -CO)₂(CO)(PPh₃)₂] on alumina or silica catalyzed the selective hydrogenation of CO and CO₂ to oxygenates, methanol being the main product, with higher selectivities than the catalysts prepared by mixing of the homometallic precursors. The performance of this catalyst was attributed to the greater dispersion of the Rh and Mo atoms.¹⁶⁷

Similarly, the [Mo₂Rh] catalyst prepared from [Mo₂RhCp₃(CO)₅] on SiO₂ showed higher selectivity toward alcohols than the conventional catalysts. The authors explained the higher selectivity in CO hydrogenation toward alcohols than conventional catalysts by Mo-promoted CO-insertion for both [MoRh] and [Mo₂Rh] catalysts.¹⁶⁸ A comparison with the related [W₂Rh] catalyst revealed that the promotor effect of molybdenum is more significant than that of tungsten (see section 2.5.2.13). Indeed, for the [Mo₂Rh] system, at 523 K, the overall selectivity for oxygenates was superior to 54% (ca. 39% for methanol and 15% for ethanol), at conversions close to 10%.¹⁶⁹

2.5.2.10. Mo–Ni. The alumina-supported [Mo₂Ni₂] heterogeneous catalysts derived from the sulfido clusters [Mo₂Ni₂S₄Cp₄] and [Mo₂Ni₂S₄Cp₂(CO)₂] have been patented for CO methanation.^{164a}

2.5.2.11. W–Ru. The reversible hydrogenation of CO₂ to formic acid was catalyzed in the presence of the heterobimetallic complexes [Cp(OC)₂W(μ -dppm)Ru(CO)(C₅R₅)] (49a, R = H; 49b, R = Me) (Scheme 15). The yields were low, but tests with monometallic Ru analogues suggested the need of both metal centers in the reaction (see also section 2.5.2.6).¹⁶⁵

Scheme 15

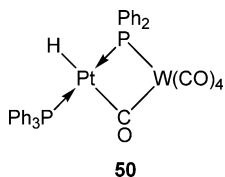


2.5.2.12. W–Os. The activity in CO reduction of alumina-supported [WOs₃] catalysts, derived from the cluster [HWOs₃Cp(CO)₁₂], has been compared to those of related heterogeneous [MoOs₃] catalysts (see section 2.5.2.7).¹⁶⁶

2.5.2.13. W–Rh. A heterogeneous [W₂Rh] catalyst prepared from the cluster [W₂RhCp₃(CO)₅] supported on SiO₂ was active in CO hydrogenation, showing rather good selectivities to oxygenate products. At 523 K, the system was able to reach almost 10% conversion and afforded gaseous hydrocarbons (mainly methane, with ca. 66% selectivity) with oxygenates such as methanol (ca. 18% selectivity) and ethanol (ca. 16% selectivity). The Mo–Rh analogous system was a better catalyst (see section 2.5.2.9), but the presence of W was necessary to improve the selectivity toward oxygenates, as compared to monometallic Rh-based catalysts.¹⁶⁹

2.5.2.14. W–Ir. Upon temperature-programmed decomposition in flowing hydrogen of the alumina-supported clusters [WIr₃Cp(CO)₁₁] (19b) and [W₂Ir₂Cp₂(CO)₁₀] (20b) and of the corresponding homometallic complexes [Ir₄(CO)₁₂] and [W₂Cp₂(CO)₆], most of the CO released was converted to CH₄. This occurred to a lesser extent when the W/Ir ratio was increased.⁸⁴

2.5.2.15. W–Pt. The [WPt] catalysts prepared from [HWPt(μ -PPh₂)(μ -CO)(CO)₄(PPh₃)₂] (50, proposed structure) on SiO₂ exhibited higher activity and methanol selectivity in CO₂ hydrogenation, as compared to conventional mono- or bimetallic catalysts (see also section 2.5.2.4). The “promotion” effect of platinum on tungsten in [WPt] resulted in a yield in MeOH 313 times higher as compared to Pt alone, and was more significant than in the case of the corresponding [CrPt] catalyst where this factor was only 148. When CO₂ conversions were in the range 2.2–4%, methanol selectivities were greater than 90%, and carbon monoxide was the only other product detected (no methane or C₂ hydrocarbons were observed).¹⁶¹



2.5.2.16. Mn–Fe. Addition of manganese to conventional iron- or cobalt-based Fischer–Tropsch catalysts generally leads to an increased formation of light olefins, whereas the catalyst activity decreases.

When supported on Al_2O_3 , SiO_2 , MgO , TiO_2 , and ZrO_2 , the carbonyl cluster $[\text{Et}_4\text{N}][\text{MnFe}_2(\text{CO})_{12}]$ was used as a precursor to $[\text{MnFe}_2]$ MMCD catalysts. Mn–Fe interactions still existed after thermal decomposition of the supported cluster, as indicated by the decreased CO methanation and increased yield of olefins and higher hydrocarbons when the $[\text{MnFe}_2]$ catalyst was compared to conventional catalysts.¹⁷⁰

The silica-supported potassium salt $\text{K}[\text{MnFe}_2(\text{CO})_{12}]$ was studied for CO/H₂ conversion. At moderate temperatures, the reaction led to aliphatic olefins in the C₁–C₅ range (no oxygenates were detected), while at elevated temperatures, the reaction led to aromatics (mainly toluene and xylenes) with a maximum of ca. 20% at 673 K.¹⁷¹

The $[\text{MnFe}_2]$ catalysts derived from $\text{K}[\text{MnFe}_2(\text{CO})_{12}]$ gave variable selectivities in CO hydrogenation, depending on the support (Al_2O_3 , MgO , or $\text{ZrO}_2 + \text{Al}_2\text{O}_3$). With magnesia and alumina, the main products were light hydrocarbons (C₁–C₄). When zirconia and alumina were used jointly, the selectivity for oxygenates increased dramatically (dimethyl ether and methanol being the main products, the latter undergoing dehydration to the former at higher temperatures), and the activity reached 20% at 473 K after 13 h and almost 60% at 553 K after 158 h.¹⁷²

Carbon-supported Mn–Fe and K–Mn–Fe catalysts with different Mn/Fe ratios were prepared from complexes $\text{K}[\text{MnFe}(\text{CO})_9]$, $[\text{Et}_4\text{N}][\text{MnFe}(\text{CO})_9]$, and the mixed-metal clusters $[\text{Mn}_2\text{Fe}(\text{CO})_{14}]$ and $[\text{Et}_4\text{N}][\text{MnFe}_2(\text{CO})_{12}]$. They were used in the selective synthesis of C₂–C₄ olefins from CO and H₂.¹⁷³ Highly dispersed Mn–Fe catalysts were obtained, which displayed selectivities to C₂–C₄ olefins as high as 85–90 wt %, with the balance being methane.^{173a}

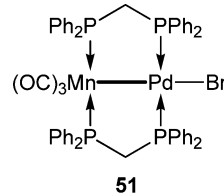
2.5.2.17. Mn–Ru. The silica-supported $[\text{MnRu}_3]$ MMCD catalyst derived from $[\text{Et}_4\text{N}][\text{MnRu}_3\text{C}(\text{CO})_{13}]$ was much less active for the hydrogenation of CO to hydrocarbons and oxygenates than $[\text{RuCo}_2]$, $[\text{RuCo}_3]$, and $[\text{Ru}_3\text{Co}_3]$ catalysts. The selectivity for oxygenates was ca. 20%, and methane was the main product.¹⁵⁹

2.5.2.18. Mn–Co. The performance for CO hydrogenation of the alumina-supported $[\text{MnCo}]$ MMCD catalyst prepared from $[\text{MnCo}(\text{CO})_9]$ was much higher than that of conventional catalysts and of catalysts prepared by successive or simultaneous impregnation of $[\text{Mn}_2(\text{CO})_{10}]$ and $[\text{Co}_2(\text{CO})_8]$ ($[\text{Mn}_2+\text{Co}_2]$). All systems gave similar selectivities, the only products being linear alkanes (especially n-hexane), but this $[\text{MnCo}]$ catalyst was much more active.¹⁷⁴

2.5.2.19. Mn–Rh. The use of $[\text{Mn}\{\text{Rh}_{12}(\text{CO})_{30}\}]$ salt was patented for the catalytic hydrogenation of CO to oxygenates such as methanol, ethylene glycol, glycerine, or 1,2-propylene glycol.¹⁷⁵

2.5.2.20. Mn–Pd. Preliminary results show that the synthesis of ethylformate from a CO₂/H₂ mixture (1:1, 12 atm) in the presence of ethanol and triethylamine at 403 K can be

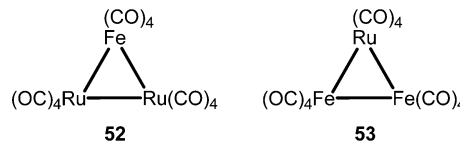
performed with the complex $[(\text{OC})_3\text{Mn}(\mu\text{-dppm})_2\text{PdBr}]$ (51), at a rate of 7 mol/mol catalyst/h.¹⁷⁶



2.5.2.21. Re–Os. CO hydrogenation to hydrocarbons (selectivity to methane >70%) was performed with a MgO-supported $[\text{ReOs}_3]$ catalyst prepared from $[\text{H}_3\text{ReOs}_3(\text{CO})_{13}]$ and compared to monometallic catalysts obtained from $[\text{Os}_3(\text{CO})_{12}]$ and $[\text{H}_3\text{Re}_3(\text{CO})_{12}]$. Although all catalysts lost activity during operation, the bimetallic particles were stable enough under catalytic conditions to make the MMCD catalyst live longer than the other. The presence of Re was found to prevent formation of the otherwise observed cluster $[\text{Os}_{10}\text{C}(\text{CO})_{24}]^{2-}$.¹⁷⁷

2.5.2.22. Re–Rh. A salt formulated as $[\text{Re}_2\{\text{Rh}_{12}(\text{CO})_{30}\}_3]$ was reported in a patent to catalyze CO hydrogenation to oxygenated products such as methanol, ethylene glycol, glycerine, and 1,2-propylene glycol.¹⁷⁸

2.5.2.23. Fe–Ru. When supported on ZrO_2 , the MMCD catalysts obtained from $[\text{FeRu}_2(\text{CO})_{12}]$ (52) and $[\text{Fe}_2\text{Ru}(\text{CO})_{12}]$ (53) were much more active than monometallic or conventional catalysts.¹⁷⁹



The $[\text{Fe}_2\text{Ru}]$ catalyst derived from $[\text{Fe}_2\text{Ru}(\text{CO})_{12}]$ (53) on $\gamma\text{-Al}_2\text{O}_3$ was ca. 50 times more active and ca. 6.2 times more selective toward C₂–C₅ hydrocarbons (ca. 74%) in CO hydrogenation than the $[\text{Fe}_3]$ catalyst derived from $[\text{Fe}_3(\text{CO})_{12}]$. In comparison, conventional Fe–Ru catalysts, prepared by impregnation of the corresponding monometallic salts $[\text{Fe}(\text{NO}_3)_3]$ and $[\text{RuCl}_3]$, produced predominantly CH₄.⁸⁹

When supported on Al_2O_3 , $\text{Al}_2\text{O}_3/\text{KOH}$, or MgO , the $[\text{FeRu}_3]$ catalysts derived from $[\text{H}_2\text{FeRu}_3(\text{CO})_{13}]$ were active for methanation and Fischer–Tropsch reactions involving CO and CO₂. Their catalytic activity and selectivity were found to strongly depend on the nature of the bimetallic couple, the activation temperature, and the nature of the support.¹²²

The activity and selectivity in CO hydrogenation of highly dispersed MMCD catalysts obtained from the silica-supported clusters $[\text{Fe}_2\text{Ru}(\text{CO})_{12}]$ (53) and $[\text{H}_2\text{FeRu}_3(\text{CO})_{13}]$ have been compared to those of catalysts prepared from a mixture of the homometallic clusters $[\text{Fe}_3(\text{CO})_{12}]$ and $[\text{Ru}_3(\text{CO})_{12}]$. Whether obtained from mono- or bimetallic precursors, the catalysts with the highest Ru content were the most active.⁸⁵

At 623 K under CO/H₂ (1:2) pressure, $[\text{FeRu}_3]$ catalysts derived from $[\text{H}_2\text{FeRu}_3(\text{CO})_{13}]$ supported on alumina, silica, or Na–Y zeolite afforded methane with yields in the range 40–43%, depending on the support. The main byproduct observed was CO₂, as a result of the water gas shift reaction (H₂O + CO → CO₂ + H₂) involving the water formed in situ (3H₂ + CO → CH₄ + H₂O).¹⁸⁰

The use of amorphous carbon black as support for $[\text{FeRu}_2(\text{CO})_{12}]$ (52), $[\text{Fe}_2\text{Ru}(\text{CO})_{12}]$ (53), or

$[\text{H}_2\text{FeRu}_3(\text{CO})_{13}]$ afforded highly dispersed Fe–Ru bimetallic crystallites. It seems that the reduction of these clusters on carbon is more facile and complete than on many oxide supports. It was found that ruthenium is more active than iron for CO hydrogenation but is less active than iron in forming CO_2 . Thus, varying the Fe/Ru ratio allowed one to tune the activity toward one substrate or another. In particular, methane formation increased with the Ru content.¹⁸¹

A sequentially impregnated $[\text{Fe}_3+\text{Ru}_3]$ catalyst produced a higher olefin:paraffin ratio than any of the bimetallic Fe–Ru clusters examined. This result is similar to the increased selectivity of silica-supported Fe–Ru catalysts prepared by sequential impregnation of Ru and Fe salts.¹⁸²

The silica-supported $[\text{Fe}_3\text{Ru}_3]$ catalyst derived from $[\text{Fe}_3\text{Ru}_3\text{C}(\text{CO})_{13}]^{2-}$ was less active in CO hydrogenation than $[\text{RuCo}_2]$, $[\text{RuCo}_3]$, and $[\text{Ru}_3\text{Co}_3]$ catalysts (see section 2.5.2.31) but displayed significant selectivity for $\text{C}_1\text{--C}_5$ oxygenates (ca. 28%).^{159,183}

2.5.2.24. Fe–Os. When physisorbed on silica, the cluster $[\text{H}_2\text{FeOs}_3(\text{CO})_{13}]$ yielded metallic particles (ca. 16 Å) under argon at temperatures higher than 523 K, but cleavage of the heteronuclear Fe–Os bonds occurred around 400 K. As a consequence, their activity in Fischer–Tropsch catalysis was found to be intermediate between those of the corresponding $[\text{Fe}_3]$ and $[\text{Os}_3]$ homometallic systems.¹⁸⁴

The MMCD $[\text{FeOs}_3]$ catalyst derived from the same cluster $[\text{H}_2\text{FeOs}_3(\text{CO})_{13}]$ on $\gamma\text{-Al}_2\text{O}_3$ was found to be 2 orders of magnitude less active at 543 K in CO hydrogenation than the $[\text{Os}_3\text{Rh}]$ catalyst obtained from $[\text{H}_2\text{RhOs}_3(\text{acac})(\text{CO})_{10}]$ (see section 2.5.2.35), but showed a high selectivity for ether formation (up to 36% after 55 h on stream), methane still being the main product. It appears that under such catalytic conditions, metal segregation occurred, which resulted in small iron oxide particles and mononuclear osmium complexes.¹⁸⁵

2.5.2.25. Fe–Co. Homogeneous proton-induced reduction of coordinated CO to CH_4 , by reaction with HSO_3CF_3 , was catalyzed by a series of mono- and bimetallic tetranuclear clusters, including Fe–Co compounds. Their efficiency was found to increase in the order: $[\text{Co}_4(\text{CO})_{12}] < [\text{PPN}][\text{FeCo}_3(\text{CO})_{12}] < [\text{PPN}][\text{Ru}_3\text{Co}(\text{CO})_{13}] < [\text{PPN}][\text{Fe}_3\text{Co}(\text{CO})_{13}] < \text{K}_2[\text{Ru}_4(\text{CO})_{13}] < [\text{PPN}]_2[\text{Fe}_4(\text{CO})_{13}]$. It appeared that higher Co contents lowered the ability to produce methane in Fe- and Ru-based clusters.¹⁸⁶

Highly active Fischer–Tropsch catalysts could be obtained by anchoring the cluster $[\text{HFeCo}_3(\text{CO})_{12}]$ on a silica gel matrix bearing amino functions and subsequent decarbonylation in a stream of hydrogen at atmospheric pressure and 473 K. At atmospheric pressure and 513 K, 20% conversion of synthesis gas was observed, and an unusually narrow product distribution showed a maximum at C_6 .¹⁸⁷

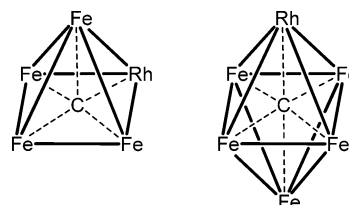
The highly active alumina-supported $[\text{FeCo}]$ catalyst derived from $[\text{FeCoCp}(\text{CO})_6]$ was used in the hydrogenation of CO at atmospheric pressure and 493–553 K. This system was highly selective toward olefins (up to 44% at 553 K) and showed conversions in the range 9–12%.¹⁸⁸

When supported on carbon, the catalysts derived from $\text{K}[\text{FeCo}(\text{CO})_8]$, $[\text{HFeCo}_3(\text{CO})_{12}]$, $\text{K}[\text{FeCo}_3(\text{CO})_{12}]$, $\text{K}[\text{Fe}_3\text{Co}(\text{CO})_{13}]$, and $[\text{Et}_4\text{N}][\text{Fe}_3\text{Co}(\text{CO})_{13}]$ were active in CO hydrogenation. Interestingly, addition of potassium markedly decreased the catalytic activity but greatly enhanced olefin selectivity.¹⁸⁹

Methanation and Fischer–Tropsch reactions involving CO and CO_2 have been catalyzed by a heterogeneous catalysts derived from $[\text{HFeCo}_3(\text{CO})_{12}]$.¹²²

2.5.2.26. Fe–Rh. Catalysts of the type $\text{C}_2[\text{Fe}_2\text{Rh}_4(\text{CO})_{16}]$ /NaY zeolite (cation $\text{C}^+ = [\text{Me}_3(\text{CH}_2\text{Ph})\text{N}]^+$, tris(4-bromophenyl)ammonium (TBPA)) were tested for CO hydrogenation, and afforded selectively a mixture of methane and $\text{C}_2\text{--C}_4$ alkenes.^{90,190} Promotion by iron in CO hydrogenation may be associated with the presence of heteronuclear adjacent Fe–Rh sites in zeolite supercages, which enhance CO migratory insertion into Rh–H and Rh–alkyl bonds.^{190b,c}

Ethanol formation from the $\text{CO} + \text{H}_2$ reaction was studied in the presence of MMCD catalysts derived from SiO_2 -supported clusters $[\text{TMBA}]_2[\text{Fe}_2\text{Rh}_4(\text{CO})_{16}]$, $[\text{Me}_4\text{N}]_2[\text{FeRh}_4(\text{CO})_{15}]$, $[\text{TMBA}][\text{FeRh}_5(\text{CO})_{16}]$, and $[\text{Fe}_3\text{Rh}_2\text{C}(\text{CO})_{14}]$. The results were better than with monometallic Fe or Rh precursors, and a selectivity for ethanol of 33% was observed in the case of $[\text{Fe}_2\text{Rh}_4]$.¹⁹¹ Formation of C_{2+} hydrocarbons was largely suppressed, possibly due to the site-blocking of the Fe–Rh ensembles.^{191b,192}

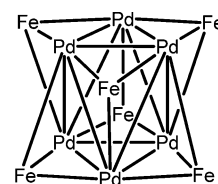


Core of the anionic carbido clusters
54 (left) and **55** (right)
(CO ligands omitted for clarity)

With the silica-supported $[\text{Fe}_4\text{Rh}]$ and $[\text{Fe}_3\text{Rh}]$ catalysts derived from $[\text{Et}_4\text{N}][\text{Fe}_4\text{RhC}(\text{CO})_{14}]$ (**54**) and $[\text{Et}_4\text{N}][\text{Fe}_3\text{RhC}(\text{CO})_{16}]$ (**55**), respectively, hydrogenation reactions were catalyzed with high activity and selectivity to oxygenates.¹⁹³

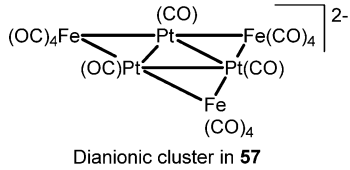
2.5.2.27. Fe–Ir. The synthesis of methanol from $\text{CO} + \text{H}_2$ was efficiently catalyzed in the presence of clusters such as $[\text{Et}_4\text{N}]_2[\text{Fe}_2\text{Ir}_2(\text{CO})_{12}]$ and $[\text{Et}_4\text{N}]_2[\text{Fe}_2\text{Ir}_4(\text{CO})_{16}]$ on MgO .¹⁹⁴ The same reaction was also performed in the presence of the MMCD silica-supported $[\text{FeIr}_4]$ catalyst, prepared from $[\text{TMBA}]_2[\text{FeIr}_4(\text{CO})_{15}]$. This catalyst was found to be much more selective for methanol formation than Fe–Rh MMCD catalysts and was also more active than a catalyst prepared by mixing homometallic iron and iridium clusters.^{97,195}

2.5.2.28. Fe–Pd. A silica-supported catalyst $[\text{Fe}_4\text{Pd}]$, prepared from $[\text{TMBA}]_2[\text{Fe}_4\text{Pd}(\text{CO})_{16}]$, was active in MeOH synthesis by CO reduction, and it gave mostly methane and C_{2+} hydrocarbons. Furthermore, a supported $[\text{Fe}_6\text{Pd}_6]$ catalyst, obtained from $[\text{TMBA}]_3[\text{HFe}_6\text{Pd}_6(\text{CO})_{24}]$ (**56**), was less active, but more selective (79%) in MeOH formation, a behavior reminiscent of a palladium-only catalyst.^{191,195}



Core of the tricationic cluster in **56**
(CO and H ligands omitted for clarity)

2.5.2.29. Fe–Pt. A silica-supported $[Fe_3Pt_3]$ heterogeneous catalyst prepared from the planar, raft-type cluster $[TMBA]_2[Fe_3Pt_3(CO)_{15}]$ (**57**) was very selective in CO hydrogenation and yielded mainly methanol like a Pt catalyst prepared from $[Et_4N]_2[Pt_{12}(CO)_{24}]$, whereas the $[TMBA]_2[Fe_4Pt(CO)_{16}]$ -derived $[Fe_4Pt]$ catalyst was more active but yielded predominantly methane.^{97,191}

Dianionic cluster in **57**

2.5.2.30. Ru–Os. A heterogeneous alumina-supported $[RuOs_3]$ catalyst prepared from $[H_2RuOs_3(CO)_{13}]$ was slightly active in the formation of hydrocarbons and dimethyl ether from CO + H₂.¹⁹⁶

2.5.2.31. Ru–Co. Together with some Fe–Co analogues, the cluster $[PPN][Ru_3Co(CO)_{13}]$ was investigated for the proton-induced homogeneous reduction of coordinated CO to CH₄ (proton source: HSO₃CF₃).¹⁸⁶

The bimetallic MMCD catalysts obtained from $[RuCo_2(CO)_{11}]$, $[HRuCo_3(CO)_{12}]$, and $[H_3Ru_3Co(CO)_{12}]$ on silica showed low activity in CO hydrogenation but higher selectivity for oxygenated products than the corresponding monometallic systems.¹⁹⁷

Xiao et al. have found that $[RuCo_2]$, $[RuCo_3]$, and $[Ru_3Co_3]$ catalysts on silica derived from the clusters $[RuCo_2(CO)_{11}]$, $[HRuCo_3(CO)_{12}]$, and $[Ru_3Co_3C(CO)_{14}]$ were more active for the production of both hydrocarbons and oxygenates than $[Fe_3Ru_3]$ catalyst derived from $[Fe_3Ru_3C(CO)_{13}]^{2-}$. Selectivities for oxygenates could reach 38% at 458 K.^{159,183}

Methanation and Fischer–Tropsch reactions involving CO or CO₂ took place with a catalyst derived from $[HRuCo_3(CO)_{12}]$ on γ -Al₂O₃, γ -Al₂O₃/KOH, and MgO.¹²²

For CO hydrogenation, a comparative study of MMCD catalysts prepared from $[HRuCo_3(CO)_{12}]$, $[Ru_2Co_2(CO)_{13}]$, $[H_2Ru_2Co_2(CO)_{12}]$, and $[H_3Ru_3Co(CO)_{12}]$ on silica showed that those with a 1:1 ratio of Ru/Co had the lowest activity, while the corresponding monometallic $[Ru_4]$ and $[Co_4]$, obtained from $[H_4Ru_4(CO)_{12}]$ and $[Co_4(CO)_{12}]$, respectively, were the most active.¹⁹⁸ Those materials were also studied in Fischer–Tropsch synthesis.^{198,199}

Hydrogenation of CO with a $[RuCo_3]$ catalyst was suggested to involve a carbene mechanism.²⁰⁰

Methanation of CO was achieved with γ -alumina-, silica-, and Na–Y zeolite-supported catalysts derived from $[PPN][Ru_3Co(CO)_{13}]^{180}$ and $[HRuCo_3(CO)_{12}]$.²⁰¹ The formation of CO₂ suggested the occurrence of the WGSR and the possibility, at low CO/H₂ ratio (1:4), to observe some CO₂ methanation. The alumina-supported catalysts yielded the best results under these conditions.

The clusters $[HRuCo_3(CO)_{12}]$ and $[HRu_3Co(CO)_{13}]$ were synthesized inside the cages of NaY zeolites by ion exchange, and subsequently activated under reducing atmosphere. The resulting $[RuCo_3]$ and $[Ru_3Co]$ materials were more active in CO hydrogenation than the corresponding $[Ru]$ and $[Co]$ catalysts prepared from monometallic precursors. Thus, $[Ru_3Co]$ exhibited 36.6% selectivity toward oxygenates for 2.8% CO conversion, while $[RuCo_3]$ showed 48.8% selectivity for a conversion of 6.7%, suggesting a positive effect of a higher Co/Ru ratio on both conversion and selectivity.²⁰²

2.5.2.32. Ru–Rh. The Ru(acac)₃–Rh(acac)₃ systems, dispersed in a low-melting point quaternary phosphonium salt (such as Bu₄PBr or C₇H₁₅Ph₃PBr), from which the cluster $[RuRh_2(CO)_{12}]$ was isolated, was active in the conversion of synthesis gas to ethylene glycol and its monoalkyl ether derivatives. Methanol and ethanol were the major byproducts detected.²⁰³

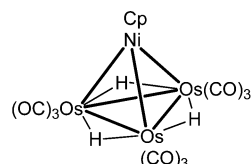
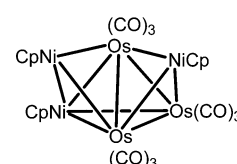
The silica-supported $[Ru_3Rh_3]$ catalyst prepared from $[Et_4N][Ru_3Rh_3C(CO)_{15}]$ catalyzed CO hydrogenation to methane and oxygenates, and proved to be the least selective catalyst for oxygenates (12%) as compared to Ru–Mo, Ru–Mn, Ru–Fe, and Ru–Ni analogues.¹⁵⁹

2.5.2.33. Ru–Ni. Similarly, when supported on silica, the cluster $[Et_4N]_2[Ru_3Ni_3C(CO)_{13}]$ exhibited poor activity and selectivity toward C₁–C₅ oxygenates (16%) in CO hydrogenation albeit with lower activity and selectivity toward oxygenates (12%) than the corresponding Ru–Mo, Ru–Mn, or Ru–Fe clusters.¹⁵⁹

2.5.2.34. Ru–Cu, Ru–Ag, Ru–Au. A homogeneous process for the synthesis of methanol from CO and H₂ (CO/H₂ ratio = 1:1, THF, 548 K, 1200 atm) has been investigated in the presence of the heterometallic carbide clusters $[Ru_6(ML)_2C(CO)_{16}]$ (M = Cu, Ag, Au; L = organonitrile). Although the presence of ruthenium is known to catalyze the formation of hydrocarbons from synthesis gas, none was observed in these cases.²⁰⁴

2.5.2.35. Os–Rh. The cluster $[H_2Os_3Rh(acac)(CO)_{10}]$ was physisorbed on γ -Al₂O₃ and tested in CO + H₂ reactions. Under the conditions used, fragmentation of the cluster seemed to occur to give mononuclear rhodium complexes and triosmium clusters. In comparison, the corresponding Fe–Rh cluster-derived catalyst was 2 orders of magnitude more active at 543 K. The major product observed was methane, and hydrocarbons were formed in approximately a Schulz–Flory–Anderson distribution. The heterogeneous $[Os_3Rh]$ catalyst was 2 orders of magnitude more active at 543 K than the corresponding $[FeOs_3]$ catalyst, but showed a lower selectivity for ether formation.¹⁸⁵

2.5.2.36. Os–Ni. Hydrogenation of CO and CO₂ was carried out in the presence of the γ -Al₂O₃ supported clusters $[Os_3Ni(\mu-H)_3Cp(CO)_9]$ (**58**) and $[Os_3Ni_3Cp_3(CO)_9]$ (**59**) as heterogeneous catalysts.¹⁴⁴ These $[Os_3Ni]$ catalysts were more efficient in CO methanation than the $[Ni_2]$ and $[Os_3]$ catalysts derived from $[Ni_2Cp_2(CO)_2]$, $[H_2Os_3(CO)_{10}]$, and $[Os_3(CO)_{12}]$, respectively. Good conversions (0.83 mol of CO converted per g·atom of metals) and high selectivity in CH₄ (96–100%) were observed at temperatures above 523 K, with small amounts of CO₂ and C₂ hydrocarbons as byproducts.¹⁴² The catalysts $[Os_3Ni]$ were found to give yields superior to 90% for CO₂ methanation at temperatures between 523 and 623 K. It led to better conversion and selectivity than the $[H_2Os_3]$, $[Os_3]$, or $[Ni_2]$ catalysts.^{142,144}

**58****59**

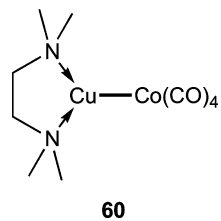
2.5.2.37. Co–Rh. The synthesis of oxygenated compounds such as methanol, ethylene glycol, glycerine, or 1,2-propylene glycol from CO and H₂ was achieved in the presence of the

complex $[\text{Co}\{\text{Rh}_{12}(\text{CO})_{30}\}]^{175}$ and salts of the dianion $[\text{Co}_3\text{Rh}_9(\text{CO})_{30}]^{2-205}$.

Hydrogenation of CO was tested with $[\text{Co}_2\text{Rh}_2]$ and $[\text{Co}_3\text{Rh}]$ catalysts derived, respectively, from $[\text{Co}_2\text{Rh}_2(\text{CO})_{12}]$ and $[\text{Co}_3\text{Rh}(\text{CO})_{12}]$ on silica¹⁹⁸ or on ZrO_2 ,²⁰⁶ and higher selectivity for oxygenates was observed as compared to monometallic systems.

Amine-functionalized resins to which Co–Rh clusters such as $[\text{Co}_{4-x}\text{Rh}_x(\text{CO})_{12}]$ ($x = 0-2$) were tethered have been used in a two-step process for the production of isobutene from propylene and synthesis gas. The alcohol mixture obtained in the first step was dehydrated on aluminum oxide.²⁰⁷

2.5.2.38. Co–Cu. The dinuclear complex $[(\text{OC})_4\text{CoCu}(\text{TMED})]$ (**60**) was impregnated onto a crystalline silica wafer, then reduced in CO and H_2 atmospheres at 473 K. The resulting heterogeneous $[\text{CoCu}]$ catalyst was assumed to consist of dispersed Co small NPs among Cu aggregates. This system catalyzed CO hydrogenation to a mixture of C_1 , C_2 , and MeOH, with conversions ranging from 1.5% to 2.5% between 433 and 473 K.^{27g}



2.5.2.39. Rh–Ir. Hydrogenation of CO was performed with salts formulated as $[\text{Ir}_2\{\text{Rh}_{12}(\text{CO})_{30}\}]^{208}$ and $[\text{Ir}_2\{\text{Rh}_{12}(\text{CO})_{30}\}_3]^{178}$ and with Al, Ga, Ir, Se, Y, or Re salts of anions such as $[\text{Rh}_6\text{Ir}_6(\text{CO})_{30}]^{2-}$ or $[\text{Rh}_9\text{Ir}_3(\text{CO})_{30}]^{2-}$. Oxygenated compounds, such as methanol, ethylene glycol, glycerol, and 1,2-propylene glycol, were produced.²⁰⁵

2.5.2.40. Rh–Pt. Ethylene glycol and methanol were the favored products resulting from hydrogenation of CO catalyzed by $[\text{PPN}][\text{Rh}_3\text{Pt}(\text{CO})_{15}]$.²⁰⁹ In contrast, the catalytic properties of $[\text{PPN}]_2[\text{Rh}_4\text{Pt}(\text{CO})_{12}]$ are greatly reduced. This low activity was correlated with the enhanced amount of $[\text{PPN}]^+$ present rather than with the increased Pt/Rh ratio. Because platinum-only catalysis yields methanol and not ethylene glycol,²¹⁰ the authors suggested that mixed molecular clusters of unknown nature were probably involved in the catalysis.²⁰⁹

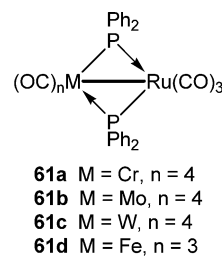
The synthesis of organic compounds such as methanol, ethylene glycol, glycerol, and 1,2-propylene glycol from CO and H_2 was achieved with a metal salt formulated as $[\text{Pt}\{\text{Rh}_{12}(\text{CO})_{30}\}]^{175}$.

2.5.2.41. Rh–Cu, Rh–Ag, Rh–Au, Rh–Zn. The transformation of CO and H_2 to oxygenates such as methanol, ethylene glycol, glycerol, and 1,2-propylene glycol was achieved with the salts formulated as $[\text{M}_2\{\text{Rh}_{12}(\text{CO})_{30}\}]$ ($\text{M} = \text{Cu, Ag, Au}$),²⁰⁸ and $[\text{Zn}\{\text{Rh}_{12}(\text{CO})_{30}\}]^{175}$. The clusters were recovered from the filtrate by recrystallization.

2.5.3. Hydrogenation of Aldehydes and Ketones

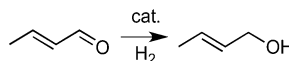
2.5.3.1. Cr–Ru, Mo–Ru. Hydrogenation of cyclohexanone, at 413 K and under 40 bar of H_2 , was performed with the dinuclear metal–metal bonded complex $[(\text{OC})_4\text{Cr}(\mu\text{-PPh}_2)_2\text{Ru}(\text{CO})_3]$ (**61a**) as a homogeneous catalyst. Cyclohexanol was obtained in rather low yields (21%). This system was more active than the W–Ru and Fe–Ru analogues, but less active than the Mo–Ru one. Indeed, the complex $[(\text{OC})_4\text{Mo}(\mu\text{-PPh}_2)_2\text{Ru}(\text{CO})_3]$ (**61b**) afforded cyclohexanol with 56%

yield. Only the homometallic Ru–Ru analogue gave similar results, with 41% yield for cyclohexanol.²¹¹



2.5.3.2. Mo–Co. Selective hydrogenation of crotonaldehyde to crotyl alcohol (Scheme 16) was catalyzed by a heteroge-

Scheme 16



neous catalyst obtained by pyrolysis of the mixed carboxylates $[\text{Mo}_2\{\text{Co}_3(\text{CO})_9\text{CCO}_2\}_4]$, in contrast to conventional catalysts that are selective for the hydrogenation of the C=C double bond. In particular, selectivities for crotyl alcohol up to 36% were observed, at 6.5% conversion. A catalyst obtained from the homometallic cluster $[\text{Co}_2\{\text{Co}_3(\text{CO})_9\text{CCO}_2\}_4]$ was able to reach 100% selectivity, albeit at 3.5% conversion only.²¹²

2.5.3.3. Mo–Rh. A $[\text{Mo}_2\text{Rh}]$ catalyst derived from $[\text{Mo}_2\text{RhCp}_3(\text{CO})_5]$ on silica was used for the hydrogenation of acetaldehyde. The presence of molybdenum significantly suppresses the C–C bond splitting reaction whereas hydrogenation to ethanol is promoted by more than 1 order of magnitude. Thus, selectivities for ethanol reached 95–98%. A catalyst prepared from impregnation of the salts RhCl_3 and MoCl_5 gave similar results.²¹³

2.5.3.4. W–Ru, Fe–Ru. Similarly to the Cr–Ru (**61a**) and Mo–Ru (**61b**) systems described above, the complexes $[(\text{OC})_4\text{W}(\mu\text{-PPh}_2)_2\text{Ru}(\text{CO})_3]$ (**61c**) and $[(\text{OC})_3\text{Fe}(\mu\text{-PPh}_2)_2\text{Ru}(\text{CO})_3]$ (**61d**) catalyzed the hydrogenation of cyclohexanone to cyclohexanol. They were both much less active than **61a** and **61b**, giving yields of 6% and 10%, respectively. In all cases, byproducts included butane, 1-butanal, and 1-butanol.²¹¹

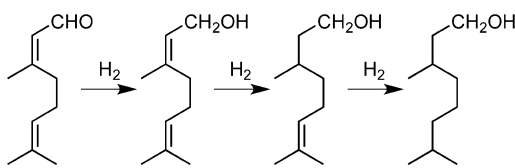
2.5.3.5. Ru–Rh, Ru–Ir. The complexes $[\text{H}(\text{OC})(\text{PPh}_3)_2\text{Ru}(\mu\text{-bim})\text{Rh}(\text{COD})]$ (bim = 2,2'-bi-imidazolato) (**33a**) and $[\text{H}(\text{OC})(\text{PPh}_3)_2\text{Ru}(\mu\text{-bim})\text{Ir}(\text{COD})]$ (**33b**) were more active in hydrogen transfer from propan-2-ol to cyclohexanone (to afford cyclohexanol), or benzylideneacetophenone than the corresponding mononuclear complexes. The electronic communication through the bi-imidazolato ligand was considered key to the higher catalytic activity observed in comparison to the corresponding mononuclear complexes (see section 2.5.1.38 for more details).^{123,124}

Reduction of cyclohexanone to cyclohexanol by hydrogen transfer from propan-2-ol was more efficiently catalyzed with the complexes $[\text{H}(\text{OC})(\text{PPh}_3)_2\text{Ru}(\mu\text{-Cl})(\mu\text{-pz})\text{M}(\text{diolefin})]$ ($\text{M} = \text{Rh or Ir; pz = pyrazolate; diolefin = COD or TFB (TFB = tetrafluorobenzobarrelene)}$) than with the corresponding mononuclear rhodium and iridium complexes. The authors also suggested that the diolefin ligand TFB stabilizes the bridged $(\mu\text{-Cl})(\mu\text{-pz})$ heterometallic species, thus preventing cleavage of the complexes and keeping the two metal centers in close proximity.²¹⁴

2.5.3.6. Ru–Pt. The single-step hydrogenation of dimethyl terephthalate to 1,4-cyclohexanediethanol (see section 3.14) was achieved with several silica-supported decarbonylated heterometallic carbido clusters: $[\text{Ph}_4\text{P}]_2[\text{Ru}_5\text{PtC}(\text{CO})_{15}]$,^{129e} $[\text{PPN}]_2[\text{Ru}_{10}\text{Pt}_2(\text{C})_2(\text{CO})_{28}]$,^{129e} $[\text{Ru}_5\text{PtC}(\mu\text{-SnPh}_2)(\text{CO})_{15}]$,¹³³ $[\text{Ru}_5\text{PtC}(\mu\text{-GePh}_2)(\text{CO})_{15}]$,¹³³ and $[\text{Ru}_5\text{PtC}(\text{CO})_{16}]$.¹³³ The first step, as mentioned in section 2.5.1.41, consists of the hydrogenation of the $\text{C}=\text{C}$ bonds of the benzene ring. The second step involves the reduction of the $\text{C}=\text{O}$ bond of the ester functions to yield alcohol groups.

Magnesia-supported¹³⁴ and mesoporous silica-supported¹³⁵ $[\text{Ru}_5\text{Pt}]$ composites derived from the trimetallic cluster $[\text{Ru}_5\text{PtC}(\mu\text{-SnPh}_2)(\text{CO})_{15}]$ were efficient catalysts for the hydrogenation of citral. They were very selective (90%) toward the formation of α,β -unsaturated alcohols (geraniol and nerol) at 100% conversion after 6 h of reaction.¹³⁴ Partial subsequent hydrogenation of the carbon–carbon double bonds led to 3,7-dimethyloctanol (see section 2.5.1.41) (Scheme 17).

Scheme 17



2.5.3.7. Os–Ni. Thermal treatment under H_2 of the ChromoP-supported cluster $[\text{Os}_3\text{Ni}(\mu\text{-H})_3\text{Cp}(\text{CO})_9]$ (**58**) afforded a $[\text{Os}_3\text{Ni}]$ heterogeneous catalyst active in the hydrogenation of acetone to propane. A multistep reaction pattern was proposed, which involved first hydrogenation of acetone to isopropanol, dehydration of the latter on the support with formation of propylene (see section 2.7.2), followed by hydrogenation of the latter to propane (see section 2.5.1.45).¹⁴³

2.5.3.8. Co–Cu, Co–Zn. Selective hydrogenation of crotonaldehyde to crotol alcohol was tested in the presence of high surface area catalysts prepared by controlled pyrolysis of the clusters $[\text{Cu}_2\{\text{Co}_3(\text{CO})_9\text{CCO}_2\}_4]$ and $[\text{Zn}_4\text{O}\{\text{Co}_3(\text{CO})_9\text{CCO}_2\}_6]$. Both systems could reach 60–65% selectivity at 2–3% conversion.²¹²

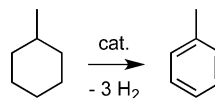
2.5.4. Hydrogenation of Oxygen. **2.5.4.1. Pt–Au.** Hydrogenation of oxygen to water at 303 K and 1 atm was achieved with a microcrystalline powder of the cluster $[\text{Pt}(\text{AuPPh}_3)_8](\text{NO}_3)_2$ (**5**). The reaction $2\text{D}_2 + \text{O}_2 \rightarrow 2\text{D}_2\text{O}$ was monitored by mass spectrometry. The rate of this reaction is similar to that observed for $\text{H}_2\text{–D}_2$ equilibration.^{43b}

2.6. Dehydrogenation of Alkanes (to Alkenes) and Alcohols (to Aldehydes)

2.6.1. Mo–Pt. Highly active $[\text{Mo}_6\text{Pt}]$ catalysts for the dehydrogenation of butane, isobutane, and propane were prepared by impregnation of the inorganic cluster $[\text{NH}_4]_4[\text{H}_4\text{PtMo}_6\text{O}_{24}]$ on MgO . They were more active and more resistant to deactivation than the conventionally prepared bimetallic Mo–Pt/ MgO or monometallic Pt/ MgO and Mo/ MgO catalysts. The selectivity to the corresponding alkene was typically above 97%.²¹⁵

2.6.2. Re–Pt. The linear complex $[\text{Re}_2\text{Pt}(\text{CO})_{12}]$ supported on Al_2O_3 yielded a MMCD catalyst, which was more resistant to deactivation during catalytic dehydrogenation of methylcyclohexane to toluene than conventional catalysts (Scheme 18). This could be explained by the role of Re in stabilizing the

Scheme 18



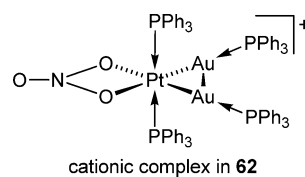
Pt dispersion. All catalysts examined for comparison showed high initial conversions (>90%) and good selectivities for toluene (ca. 90% yield after 20 h on stream). However, after 40 h on stream, the MMCD catalyst remained active, while the activity of the conventional Pt-based catalysts dramatically decreased.²¹⁶

2.6.3. Fe–Ru. The glc Chromosorb-supported $[\text{FeRu}_3]$ MMCD catalyst derived from $[\text{H}_2\text{FeRu}_3(\text{CO})_{13}]$ catalyzed dehydrogenation/disproportionation reactions at temperatures in the range 373–503 K. A broad range of substrates, including cyclic mono- and dienes (cyclohexane, cyclohexene, cyclohexadienes, methylcyclohexane), was studied. In all cases, the main reaction was dehydrogenation, but some disproportionation products were also observed. For instance, at 423 K, cyclohexene gave a mixture of benzene (97.5%) and cyclohexane (2.5%).¹²⁰

2.6.4. Ru–Ni, Os–Ni, Os–Ni–Cu. The Chromosorb P-supported $[\text{Ru}_3\text{Ni}]$ and $[\text{Os}_3\text{Ni}]$ catalysts derived from the clusters $[\text{Ru}_3\text{Ni}(\mu\text{-H})_3\text{Cp}(\text{CO})_9]$ and $[\text{Os}_3\text{Ni}(\mu\text{-H})_3\text{Cp}(\text{CO})_9]$ (**58**), respectively, catalyzed the hydrogenation–dehydrogenation of alcohols. Both catalysts afforded almost quantitatively dimethyl ether as a result of dehydration of methanol ($2\text{MeOH} \rightarrow \text{Me}_2\text{O} + \text{H}_2\text{O}$). Similarly, ethanol yielded diethyl ether with 70% or 25–35% selectivity when $[\text{Ru}_3\text{Ni}]$ and $[\text{Ru}_3\text{Os}]$ were used, respectively. The latter system afforded $\text{C}_1\text{–C}_2$ alkanes with even higher selectivity.¹²⁸

The $[\text{Os}_3\text{NiCu}]$ MMCD catalyst derived from $[\text{Os}_3\text{Ni}(\mu\text{-CuPPh}_3)(\mu\text{-H})_2\text{Cp}(\text{CO})_9]$ (**42**) on Chromosorb P exhibited a significantly different behavior toward dehydrogenation of alcohols as compared to the catalysts obtained from $[\text{Ru}_3\text{Ni}(\mu\text{-H})_3\text{Cp}(\text{CO})_9]$ and $[\text{Os}_3\text{Ni}(\mu\text{-H})_3\text{Cp}(\text{CO})_9]$. Formaldehyde and acetaldehyde were obtained from methanol and ethanol, respectively, with more than 80% selectivity when no H_2 was used, either by direct dehydrogenation, or by hydration of the in situ formed ethylene. Also, acetone could be obtained from *i*-propanol.¹²⁸

2.6.5. Pt–Au. The clusters $[\text{Pt}(\text{AuPPh}_3)_8](\text{NO}_3)_2$ (**5**) and $[\text{Pt}(\text{NO}_3)(\text{AuPPh}_3)_2(\text{PPh}_3)_2](\text{NO}_3)$ (**62**) were supported on commercial SiO_2 and activated under O_2 at 573 K, then under H_2 at 473 K. Elemental analyses evidenced that most of the phosphorus from the cluster precursors remained after thermal activation, which resulted in enhanced stability of the resulting catalysts. These $[\text{PtAu}_8]$ and $[\text{PtAu}_2]$ catalysts were tested in hexane and propane conversion. In the former case, a maximum of 10% conversion was achieved, with selectivities for hexenes around 90%, mainly due to the presence of P in the samples. The results for propane conversion were quite similar, mainly yielding propene with 90% selectivity at 35% conversion.²¹⁷

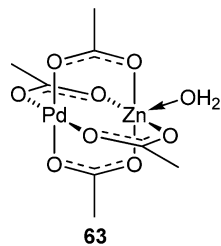


2.7. Dehydration of Alcohols

2.7.1. Mo–Pd. The octanuclear cluster $\text{Na}_2[\text{Pd}_4\{\text{MoCp}(\text{CO})_3\}_4]$ was used for the dehydration of MeOH , EtOH , and Me_2CHOH , which occurred via C–O bond cleavage and H transfer to give carbene ligands. In the case of PhCH_2OH , *trans*-stilbene was formed.²¹⁸

2.7.2. Os–Ni. Hydrogenation of acetone with the Chromosorb P-supported $[\text{Os}_3\text{Ni}]$ catalyst obtained from $[\text{Os}_3\text{Ni}(\mu\text{-H})_3\text{Cp}(\text{CO})_9]$ was assumed to involve a dehydration step. Thus, hydrogenation of acetone would lead to the formation of isopropanol (see section 2.5.3.7), which could afford propene upon dehydration. Subsequent hydrogenation of the carbon–carbon double bond would yield propane (see section 2.5.1.45).¹⁴³

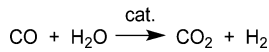
2.7.3. Pd–Zn. When supported on alumina, the acetato-bridged complex $[\text{Pd}(\mu\text{-O}_2\text{CMe})_4\text{Zn}(\text{OH}_2)]$ (63) calcined under Ar and activated with H_2 afforded a $[\text{PdZn}]$ heterogeneous catalyst. It was compared to the corresponding monometallic $[\text{Zn}]$ and $[\text{Pd}]$ catalysts in the dehydration of alcohols. In particular, ethanol conversion afforded $\text{C}_1\text{--C}_{11}$ alkanes and olefins, oxygenates, CO , and CO_2 . The $[\text{Pd}]$ catalyst was more selective toward alkanes and CO , whereas $[\text{Zn}]$ and $[\text{PdZn}]$ yielded more olefins in the range of $\text{C}_3\text{--C}_{10}$. Moreover, the $[\text{Zn}]$ catalyst did not afford any CO or CO_2 . Addition of glycerol to any of these systems enhanced the selectivity for aliphatic $\text{C}_4\text{--C}_{10+}$ hydrocarbons. The surface of the catalyst was probed by EXAFS and XRD, which suggested the presence of $\text{Pd}(0)$, Pd hydride, $\text{Pd}\text{--Zn}$ alloy, and mixed zinc–alumina spinel.²¹⁹



2.8. Water Gas Shift Reaction

2.8.1. Fe–Ru. The clusters $[\text{FeRu}_2(\text{CO})_{12}]$ (52), $[\text{Fe}_2\text{Ru}(\text{CO})_{12}]$ (53), their phosphine and phosphite derivatives $[\text{FeRu}_2(\text{CO})_{11}(\text{PR}_3)]$, $[\text{FeRu}_2(\text{CO})_{10}(\text{PR}_3)_2]$ ($\text{R} = \text{Ph}, \text{OMe}$), $[\text{FeRu}_2(\text{CO})_{10}(\text{dppe})]$, $[\text{Fe}_2\text{Ru}(\text{CO})_{11}(\text{PR}_3)]$, $[\text{Fe}_2\text{Ru}(\text{CO})_{10}(\text{PR}_3)_2]$ ($\text{R} = \text{Ph}, \text{OMe}$), and $[\text{Fe}_2\text{Ru}(\text{CO})_{10}(\text{dppe})]$, as well as $[\text{H}_2\text{FeRu}_3(\text{CO})_{13}]$ were more active WGSR catalyst precursors than the monometallic precursors $[\text{Fe}_3(\text{CO})_{12}]$ and $[\text{Ru}_3(\text{CO})_{12}]$, at 373 K and 0.40–0.60 atm CO .²²⁰ The results showed a clear decrease in turnover frequency as the iron content of the cluster decreased. If monosubstitution by phosphine or phosphite enhances the activity of the clusters with a high iron content by stabilizing the parent cluster, it seems that disubstitution of $[\text{Fe}_2\text{Ru}(\text{CO})_{12}]$ rather diminishes the stability of the cluster under basic WGSR conditions (Scheme 19).^{220d} Interestingly, under the same conditions, the clusters $[\text{H}_2\text{FeOs}_3(\text{CO})_{13}]$ and $[\text{FeOs}_2(\text{CO})_{12}]$ were found inactive.

Scheme 19



2.8.2. Fe–Ir. Moderate activity was observed with $\text{Na}_2[\text{FeIr}_4(\text{CO})_{15}]$ as homogeneous catalyst precursor for the WGSR, indicating a weak synergistic effect between the two metals, although it was more active than the monometallic precursor $[\text{Ir}_4(\text{CO})_{12}]$ alone. The hydrido cluster $[\text{HFeCo}_3(\text{CO})_{12}]$, however, was inactive under the same conditions, and a mixture of $[\text{Fe}(\text{CO})_5]$ and $[\text{Rh}_4(\text{CO})_{12}]$ ^{220d} did not reveal any synergistic effect between the two metals.

2.8.3. Ru–Co. Water gas shift reactions were investigated with Ru–Co clusters as homogeneous catalysts. Only $[\text{H}_3\text{Ru}_3\text{Co}(\text{CO})_{12}]$ was observed to initiate a catalytic system. Under basic conditions, $[\text{RuCo}_2(\text{CO})_{11}]$ and $[\text{HRuCo}_3(\text{CO})_{12}]$ were practically inactive. The cluster $[\text{H}_3\text{Ru}_3\text{Co}(\text{CO})_{12}]$ decomposes easily under a CO atmosphere to yield $[\text{Ru}_3(\text{CO})_{12}]$, which appears responsible for the catalytic activity of the system, thus ruling out any synergism between the two metals.^{220d,221}

2.8.4. Ru–Rh. Pyridine solutions of the mixed-metal clusters $[\text{PPN}][\text{RuRh}_5(\text{CO})_{16}]$, $[\text{H}_2\text{Ru}_2\text{Rh}_2(\text{CO})_{12}]$ were less active for the catalytic WGSR than the homometallic complex $[\text{Rh}_2(\text{CO})_4\text{Cl}_2]$, suggesting that no synergistic effect takes place.^{220d}

2.8.5. Co–Rh. The clusters $[\text{Co}_2\text{Rh}_2(\text{CO})_{12}]$ and $[\text{Co}_3\text{Rh}(\text{CO})_{12}]$ produced a highly active catalytic system under basic WGSR conditions. The cobalt carbonyls are totally inactive, but rhodium complexes were as active as the bimetallic species, indicating the lack of synergistic effect between the two metals.^{220d}

2.8.6. Co–Ir. The cluster $[\text{Co}_2\text{Ir}_2(\text{CO})_{12}]$ was only a poor catalyst precursor under basic WGSR conditions, and no synergistic effect was observed between the two metals, because iridium complexes were more active than the bimetallic species.^{220d}

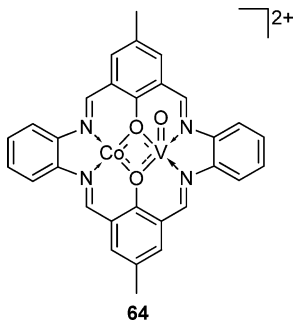
From a comparison between the systems described above, it appears that the most active monometallic catalysts were based on Ru and Rh complexes, the latter being ca. 2 orders of magnitude more active than the former. Only two metal couples were found to exhibit synergism under the reaction conditions (373 K, 0.40–0.60 atm of CO): Fe–Ru and Co–Rh. In particular, Fe–Ru clusters proved to be 2 orders of magnitude more active than monometallic Fe or Ru species, while Co–Rh compounds were almost 3 times more active than the Fe–Ru systems.

2.9. Oxidation Reactions

2.9.1. Oxidation of Alkanes and Alkenes. As shown below, the oxidation of alkanes and alkenes under mild conditions with O_2 usually leads to ketones (and aldehydes to some extent). However, when $\text{H}_2\text{O}_2/\text{O}_2$ was used, the selectivity toward alcohols was enhanced, as a result of the reduction of the carboxylic acids obtained during the reaction.

2.9.1.1. V–Co. Air-oxidation of cyclohexane to yield cyclohexanone was catalyzed in the presence of the complex $[\text{VCoOL}]^{2+}$ ($\text{L} =$ the macrocyclic ligand $\{-\text{NCHC}_6\text{H}_2\text{MeOCHNC}_6\text{H}_4-\}_2$) (64) covalently linked to carbamate-modified alumina. Some unidentified products, along with cyclohexanol, were observed, and the selectivity toward cyclohexanone was higher than 75%.²²²

2.9.1.2. V–Rh. The SiO_2 -grafted rhodium vanadate cubane-type clusters $[\text{Bu}_4\text{N}]_2[(\eta^3\text{-C}_4\text{H}_7)_2\text{Rh}](\text{V}_4\text{O}_{12})_2$ and $[(\text{Cp}^*\text{Rh})_4\text{V}_6\text{O}_{19}]$ catalyzed the selective oxidation of propene to acetone with higher TOFs than monometallic Rh- and V-based species. The selectivity for acetone was of 41% for



$[\text{Bu}_4\text{N}]_2[\{\eta^3-\text{C}_4\text{H}_7\}_2\text{Rh}\}_2(\text{V}_4\text{O}_{12})_2$ and of 85% for $[(\text{Cp}^*\text{Rh})_4\text{V}_6\text{O}_{19}]$, the latter being much more selective than the monometallic species (<55%).^{80,223}

2.9.1.3. Cr–Mn, Cr–Co, Mn–Co. Oxidation of cyclohexene to cyclohexenone was catalyzed by silica-supported Cr–Mn, Cr–Co, and Mn–Co complexes. Only the first two systems were found to involve synergistic effects between the different metal atoms.²²⁴

2.9.1.4. Fe–Co. The heterobimetallic Schiff base complex $[\text{Fe}_2\text{Co}_4\text{OSae}_8] \cdot 4\text{DMF}\cdot\text{H}_2\text{O}$ (H_2Sae = salicylidene-2-ethanolamine) (65) (Figure 2) was used for alkane oxidation by

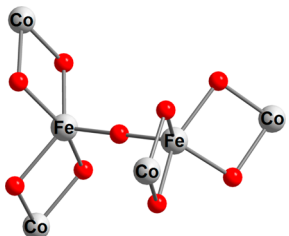


Figure 2. Core of the FeCo Schiff base cluster 65. Adapted from ref 225.

hydrogen peroxide under mild conditions, in the presence of nitric acid, which afforded the corresponding ketones (along with some aldehydes) and alcohols. Kinetic studies led to the assumptions that hydroxyl radicals were involved and attack the C–H bonds of the alkanes. Electrospray ionization mass spectrometry (ESI–MS) experiments suggested that $[\text{Co}_2\text{Fe}(\text{Sae})_4]^+$, formed during the oxidation reactions, could be the active catalyst.²²⁵

2.9.1.5. Fe–Co–Cu. The heterotrimetallic complex $[\text{FeCoCu}(\text{L})_3(\text{NCS})_2(\text{MeOH})]_2 \cdot 3.2\text{H}_2\text{O}$ (H_2L = diethanolamine) (66) (Figure 3) is a highly active and selective catalyst for the oxidation of cycloalkanes (namely cyclopentane and

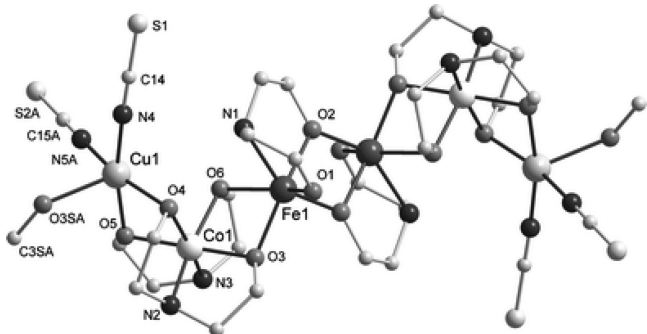
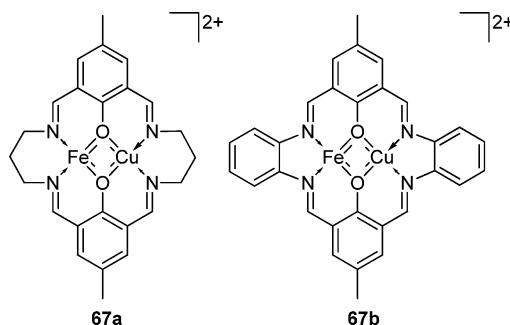


Figure 3. Structure of the FeCoCu complex 66. Reproduced with permission from ref 226. Copyright 2006 Royal Society of Chemistry.

cyclohexane) by hydrogen peroxide to the corresponding ketones and alcohols under ambient conditions. Such a high activity when compared to monometallic Fe, Cu, or Co catalysts suggests the occurrence of strong synergistic effects. More precisely, selectivities were close to 100%, and yields of alcohols were in the range 25–40%, depending on the reaction time and the H_2O_2 to catalyst molar ratio, while the yields of ketones were in the range 2–7%.²²⁶

2.9.1.6. Fe–Cu. Cyclohexane oxidation by O_2 was performed in the presence of the intercalated complex $[\text{FeCuL}^1](\text{NO}_3)_2 \cdot 4\text{H}_2\text{O}$ [L^1 = the macrocyclic ligand $\{-\text{NCHC}_6\text{H}_2\text{MeOCHN}-(\text{CH}_2)_3-\}_2$] (67a) in Zr-pillared montmorillonite clay. A selectivity of 87% toward cyclohexanone was reached for a conversion of 14% at 463 K. The formation of an unidentified species was observed in the catalysis reaction mixture.²²⁷



A Fe–Cu complex formulated as $[\text{FeCuL}^2](\text{NO}_3)_2$ where L^2 = the macrocyclic ligand $\{-\text{NCHC}_6\text{H}_2\text{MeOCHNC}_6\text{H}_4-\}_2$ (67b) was covalently anchored to carbamate-functionalized alumina for performing cyclohexane oxidation. EDX analysis indicated a Cu/Fe ratio of ca. 5.7 in the catalytic material, which suggests that most of the species are Cu–Cu complexes. The only obtained product was cyclohexanone.²²⁸

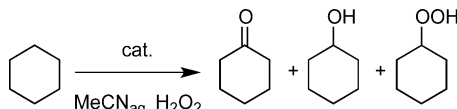
2.9.1.7. Fe–Au. Total oxidation of toluene and chlorobenzene was tested in the presence of heterogeneous $[\text{Fe}_4\text{Au}_4]$ and $[\text{Fe}_4\text{Au}]$ catalysts, obtained by thermal treatment of $[\text{Et}_4\text{N}]_4[\text{Fe}_4\text{Au}_4(\text{CO})_{16}]$ and $[\text{Et}_4\text{N}][\text{Fe}_4\text{Au}(\text{CO})_{16}]$, respectively. The $[\text{Fe}_4\text{Au}_4]$ cluster converts to the $[\text{Fe}_4\text{Au}]$ cluster upon oxidation. Thus, when adsorbed on TiO_2 , it oxidizes, and the resulting species are $[\text{Fe}_8\text{Au}_{13}(\text{CO})_{32}]^{n-}$, $[\text{Fe}_4\text{Au}(\text{CO})_{16}]^-$, along with $[\text{HFe}(\text{CO})_4]^-$ and $[\text{HFe}_3(\text{CO})_{11}]^-$ fragments. The cluster $[\text{Et}_4\text{N}][\text{Fe}_4\text{Au}(\text{CO})_{16}]$ remained intact upon adsorption on the support. A subsequent thermal treatment led to segregated Au/ $\text{FeO}_x/\text{TiO}_2$ material in both cases. Under N_2 or H_2 , dispersed Au NPs with sizes in the range of 3–7 nm were obtained, whereas agglomeration occurred under oxygen and afforded NPs of 20–25 nm. The FeO_x layer is responsible for the good dispersion of the gold species. These catalysts were not stable in the presence of dichlorobenzene, but gave 100% conversion in toluene combustion, CO_2 being the only product formed.²²⁹ A complementary study revealed that the presence of Au was necessary to achieve 100% selectivity for CO_2 , because $\text{FeO}_x/\text{TiO}_2$ materials yielded a mixture of CO_2 , CO, and H_2O as products.²³⁰

The same cluster precursor $[\text{Et}_4\text{N}][\text{Fe}_4\text{Au}(\text{CO})_{16}]$ was also deposited on ceria, to perform catalytic toluene combustion. However, ceria alone was found to be a better catalyst than either $\text{FeO}_x/\text{CeO}_2$ or $\text{Au}/\text{FeO}_x/\text{CeO}_2$.²³¹

2.9.1.8. Co–Cu. The complex $[\text{Co}_3\text{CuCl}_3(\text{MeDea})_3(\text{solv.})]$ (where H_2Dea = diethanolamine and solv. = $(\text{MeOH})_{0.55}(\text{H}_2\text{O})_{0.45}$) was studied for its magnetic and

catalytic properties. It was reported to be active in oxidation of cyclohexane by hydrogen peroxide to cyclohexanol and cyclohexanone under ambient conditions with yields up to 23% (Scheme 20). The addition of PPh_3 to the reaction mixture was necessary for the reduction of Ph-O-OH to Ph-OH , thus enhancing the selectivity toward cyclohexanol.²³²

Scheme 20



2.9.1.9. Co–Cu–Zn. The heterotrimetallic complexes $[\text{CoCuZn}_2\text{Cl}_3(\text{MeDea})_3(\text{solv.})]$ (H_2Dea = diethanolamine; solv. = $(\text{MeOH})_{0.74}(\text{H}_2\text{O})_{0.26}$ or DMF) were tested in cyclohexane oxidation by hydrogen peroxide. Their activities were much lower than those of the corresponding Co–Cu compound described earlier (see section 2.9.1.8), with yields up to 4%. The main product was cyclohexanone, along with a small amount of cyclohexanol. These results suggested either a strong synergistic effect of Co–Cu moieties or an inhibitory effect of the Zn atoms.²³²

2.9.1.10. Pd–Cu. The oxidation of 1-decene to 2-decanone by O_2 was tested in the presence of the μ_4 -oxo cluster $[\text{Pd}_6\text{Cu}_4\text{Cl}_{12}\text{O}_4(\text{HMPA})_4]$. The reaction also proceeded under argon atmosphere, with the oxygen atoms from the cluster being able to oxidize the substrate, albeit with lower yields.²³³

The polymeric complex $[\text{CuL}_4\text{Cl}(\mu\text{-Cl})\text{PdCl}_2\cdot\text{PdCl}_2]_n$ (L = pyrrolidin-2-one) catalyzed the oxidation of cyclohexene to a mixture of cyclohexanone and cyclohexenone (88:12) with a 36% yield.²³⁴

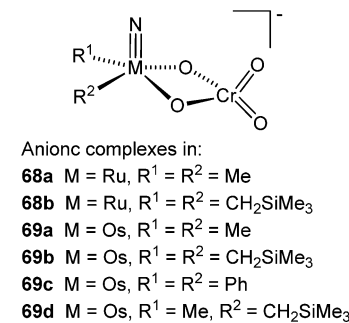
2.9.1.11. Pt–Au. Oxidation of propylene in the absence of NO (otherwise used for selective catalytic reduction of NO by hydrocarbons) was evaluated with the silica-supported $[\text{Pt}_2\text{Au}_4]$ catalyst, derived from $[\text{Pt}_2\text{Au}_4(\text{C}\equiv\text{C}-t\text{-Bu})_8]$ (7). Similarly to the reduction of NO by the same catalytic system (see section 2.15.1.3), activity was detected only at temperatures higher than 623 K, whereas catalysts prepared by coimpregnation of monometallic complexes were active at 473 K.⁴⁷

2.9.2. Oxidation of Alcohols. **2.9.2.1. Ta–Re.** The alkoxide complex $[\text{Ta}_4(\text{ReO}_4)_2\text{O}_2(\text{OEt})_{14}]$ was used as a precursor to titania-supported $\text{ReO}_x/\text{Ta}_2\text{O}_5/\text{TiO}_2$ catalysts with different loadings (1 and 10 wt %). Those systems were used in oxidation of methanol to selectively afford dimethoxymethane, as opposed to $\text{ReO}_x/\text{TiO}_2$ catalysts, which instead exhibited high selectivity to formaldehyde.²³⁵

2.9.2.2. Cr–Ru, Cr–Os. The complexes $\text{C}[\text{RuNR}_2(\mu\text{-O})_2\text{CrO}_2]$ (68a, cation $\text{C}^+ = \text{Ph}_4\text{P}^+$, $\text{R} = \text{Me}$; 68b, cation $\text{C}^+ = \text{Bu}_4\text{N}^+$, $\text{R} = \text{CH}_2\text{SiMe}_3$) were active in air-oxidation of various alcohols, to yield the corresponding aldehydes.²³⁶

Similarly, selective air oxidation of alcohols was possible in the presence of various oxo-bridged complexes: $[\text{Ph}_4\text{P}][\text{Os}(\text{N})\text{Me}_2(\mu\text{-O})_2\text{CrO}_2]$ (69a), $\text{C}[\text{Os}(\text{N})(\text{CH}_2\text{SiMe}_3)_2(\mu\text{-O})_2\text{CrO}_2]$ (cation $\text{C}^+ = (\text{n-Bu})_4\text{N}^+$, Ph_4P^+) (69b), $[(\text{n-Bu})_4\text{N}][\text{Os}(\text{N})\text{Ph}_2(\mu\text{-O})_2\text{CrO}_2]$ (69c), and $[\text{Ph}_4\text{P}][\text{Os}(\text{N})\text{Me}(\text{CH}_2\text{SiMe}_3)(\mu\text{-O})_2\text{CrO}_2]$ (69d). Benzylic primary and secondary alcohols could thus be transformed into the corresponding aldehydes and ketones, respectively.^{236,237}

A mechanism was suggested, which involved coordination of the alcohol to the ruthenium or osmium center, followed by

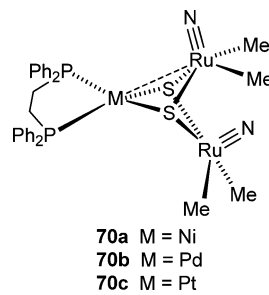


proton transfer from the alcohol to an oxo-bridge, and β -hydrogen elimination.

2.9.2.3. Fe–Au. The ceria-supported $[\text{Fe}_4\text{Au}]$ material, obtained from $[\text{Et}_4\text{N}][\text{Fe}_4\text{Au}(\text{CO})_{16}]$, was tested in the catalytic combustion of methanol. The catalyst had the same composition as the aformentioned $\text{Au}/\text{FeO}_x/\text{TiO}_2$ supported catalysts (see section 2.9.1.7). $\text{FeO}_x/\text{CeO}_2$ exhibited the same activity as bare ceria, but the presence of gold greatly enhanced the total oxidation of methanol.²³¹

The same reaction was evaluated in the presence of the mesoporous silica SBA-15-supported cluster-derived $\text{Au}/\text{FeO}_x/\text{SiO}_2$ catalyst obtained from $[\text{Et}_4\text{N}][\text{Fe}_4\text{Au}(\text{CO})_{16}]$. The Au NPs were located mostly outside the pores, with sizes around 13 nm. The presence of gold significantly improved the activity and selectivity for CO_2 , as compared to the gold-free $\text{FeO}_x/\text{SiO}_2$ catalysts. Moreover, the close proximity of Au and Fe, favoring synergistic effects, was responsible for the higher activity of this catalyst as compared to $\text{Au}/\text{FeO}_x/\text{SiO}_2$ catalysts prepared by deposition–precipitation methods.²³⁸

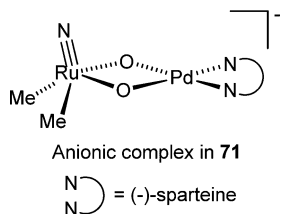
2.9.2.4. Ru–Ni, Ru–Pd, Ru–Pt. The heterotrinuclear complexes $[(\text{dppe})\text{M}(\mu_3\text{-S})_2\{\text{Ru}(\text{N})\text{Me}_2\}_2]$ ($\text{M} = \text{Ni}, \text{Pd}, \text{Pt}$; 70a–c) were tested in the oxidation of benzyl alcohol to benzaldehyde in toluene and in supercritical CO_2 . The Ru–Ni complex was slightly more active than the corresponding Ru–Pd and Ru–Pt complexes, but all systems gave similar product distributions.²³⁹



The complex $[\text{PPh}_4][\text{Ru}(\text{N})\text{Me}_2(\mu\text{-O})_2\text{Pd}((\text{--})\text{-sparteine})]$ (71) is an efficient catalyst for the aerobic oxidation of aryl and allyl alcohols. In particular, in the presence of O_2 , it catalyzed the conversion of allyl alcohol to propionaldehyde and acrolein in a 1:2 ratio, and the oxidation of benzyl alcohol to benzaldehyde. The addition of molecular sieves to trap the water during the reactions greatly improved the yields.²⁴⁰

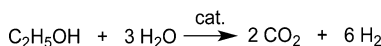
The cluster $[\text{Ru}_4\text{Pt}_2(\text{CO})_{18}]$ was used to prepared carbon-supported RuPt/C NPs for the electrocatalytic oxidation of methanol (to CO_2 most likely). It was more active than commercial catalysts, probably due to the high dispersion of very small NPs.²⁴¹

Alumina-supported RuPt NPs were prepared by decarbonylation of the cluster precursor $[\text{Ph}_4\text{P}]_2[\text{Ru}_5\text{PtC}(\text{CO})_{15}]$ at 468



K under reduced pressure. This system was tested in the production of H₂ from steam reforming of ethanol (Scheme 21). It gave better results than commercial Ru/Al₂O₃ and the

Scheme 21



salt-impregnated corresponding catalysts, in terms of selectivity and ethanol conversion, probably due to the NPs size (<2 nm on average) and high dispersion. Also, the presence of Pt in the catalysts seemed to help reduce the coking process during the reaction.²⁴²

2.9.2.5. Co–Ni. The cubane-type cluster [Co₂Ni₂(μ₃-OMe)₄(acac)₄(OAc)₂] was used to prepare NaY-supported CoNi oxide heterogeneous catalysts. This CoNiO₂/NaY system was used in the oxidation of methanol with conversions >80% and selectivity toward CO₂ > 98%. The monometallic analogues CoO/NaY and NiO/NaY exhibited slightly better and worse activities, respectively, than the bimetallic materials.²⁴³

2.9.3. Oxidation of CO. The preferential oxidation of CO (PROX) in the presence of H₂-rich gas stream is of essential importance for applications in proton-exchange membrane fuel cells (PEMFC), as it allows for its removal. In PEMFCs, H₂ is produced from the reaction (fuel + O₂ + H₂O ⇌ CO_x + H₂), followed by the WGSR (CO + H₂O ⇌ CO₂ + H₂). The composition of the gas after the WGSR contains up to 1% of CO in H₂, which can poison the anode of the PEMFC, hence the need to avoid it as much as possible. Among the known methods to remove the CO formed, preferential oxidation (PROX) appeared most promising. The PROX method involves two reactions in competition: the oxidation of CO to CO₂ and the oxidation of H₂ to H₂O, hence the need for selective catalysts. Typically, catalysts containing Ru, Rh, Ir, Pt or Cu, Ag, Au metals were used on inorganic oxides such as ceria or maghemite. In particular, the Fe–Pt couple, arising from the adsorption of Pt catalysts onto Fe₂O₃ supports, seems the most promising system, although Au-based, and more generally precious metal-based, catalysts are widely studied.²⁴⁴

2.9.3.1. Fe–Pt. Oxidation of CO in air, or in the presence of H₂ (PROX), was performed with the silica-supported [Fe₂Pt] and [Fe₂Pt₅] catalysts derived from the heterobimetallic clusters [Fe₂Pt(COD)(CO)₈]²⁴⁵ and [Fe₂Pt₅(COD)₂(CO)₁₂]^{245a,246} respectively, after decarbonylation at 623 K under H₂ or He. These catalysts were mostly constituted of small FePt NPs of 1–2 nm, homogeneously dispersed on the matrix, as opposed to samples prepared from homometallic salt precursors. The cluster-derived catalysts were more active than the latter, suggesting that Fe has a positive effect on the activity, but underwent deactivation (slower in PROX than in air) under catalytic conditions.

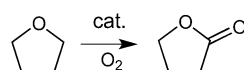
2.9.3.2. Fe–Au. Preferential oxidation of CO in the presence of H₂ (PROX) (see introduction to this section) was tested with [Fe₄Au] obtained from the titania- or ceria-supported

cluster [Et₄N][Fe₄Au(CO)₁₆]. These catalysts were less active than the usual catalysts described in the literature.²⁴⁷

2.9.3.3. Pt–Au. Oxidation of CO was achieved with the intact silica-supported cluster [Pt(AuPPh₃)₆(PPh₃)](NO₃)₂ (3).^{46a} Oxidation of CO was also evaluated in the presence of TiO₂- or SiO₂-supported [Pt₂Au₄] catalysts, derived from [Pt₂Au₄(C≡C-t-Bu)₈] (7). When silica was used as a support, the Pt–Au catalysts were slightly less effective than the catalysts prepared from metallic salts, but when titania was used as a support, the system became active at much lower temperatures than the coimpregnated salt-derived catalysts, due to the high dispersion of Au and of the nature of the support.²⁴⁸

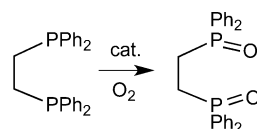
2.9.4. Oxidation of THF. **2.9.4.1. Mo–Ru.** The dinuclear complexes [R(CO)₃MoRu(CO)₂Cp] (R = η⁵-indenyl, η⁵-cyclopentadienyl) were found to be active catalysts for the aerobic oxidation of THF under ambient conditions, the main product being γ-butyrolactone (Scheme 22). However, [Ru(CO)₂Cp]₂ was much more active and selective (up to 70%) than these heterobimetallic species.²⁴⁹

Scheme 22



2.9.5. Oxidation of Phosphines. **2.9.5.1. Cr–Os.** The complex C[Os(N)(CH₂SiMe₃)₂(μ-O)₂CrO₂] (cation C⁺ = Bu₄N⁺, Ph₄P⁺) (69b) was reacted with Ph₂PCH₂CH₂PPh₂ (dppe) to yield the air-sensitive compound C[(dppe)Os(N)-(CH₂SiMe₃)₂(μ-O)₂CrO₂], which was observed to slowly decompose to afford 69b and Ph₂P(O)CH₂CH₂P(O)Ph₂. With high amounts of dppe, the reaction proceeds catalytically (Scheme 23). The authors believe that the chromate ligand helps in stabilizing the complex, thus allowing for multiple uses.^{236,250}

Scheme 23



2.9.5.2. Ru–Pd. The complex [PPh₄][Ru(N)Me₂(μ-O)₂Pd((-)-sparteine)] (71) catalyzed the oxidation of PPh₃. It could be recovered after the reaction, even if a small amount of the phosphine remained coordinated to the metal center. Full conversion was observed after 24 h reaction time.²⁴⁰

2.10. Carbon–Carbon Bond Formation

Because cyclization reactions have already been mentioned in the section dealing with hydrogenolysis reactions (see section 2.4), we shall not deal with them in this section.

2.10.1. Homologation Reactions. With the exception of a Ru–Co catalyst, which catalyzed methyl acetate homologation, this section exclusively deals with methanol homologation reactions.

2.10.1.1. Mn–Pd. Homologation of methanol was tested with the iodo complex [(OC)₃Mn(μ-dppm)₂PdI]. In the presence of aqueous HI, methanol reacted with CO/H₂ (1:1, 14 atm) at 403 K to afford Me₂O, AcOH, AcOMe, and MeCH(OMe)₂ (55% molar selectivity for the latter).¹⁷⁶

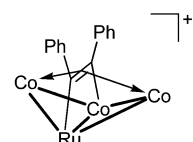
2.10.1.2. Fe–Co. Methanol homologation was catalyzed by the Fe–Co salts $C[FeCo_3(CO)_{12}]$ (cation $C^+ = Et_4N^+$ or Bu_4N^+)²⁵¹ or $[Et_4N][Fe_3Co(CO)_{13}]^{251b,c}$ when promoted with methyl iodide and carried out at relatively high pressures and moderate temperatures. It was possible to obtain acetaldehyde in 80% selectivity at methanol conversions of 75%. Optimal ethanol selectivity required long reaction times at high temperature.^{251a} In particular, a higher selectivity for ethanol at lower conversion of methanol was obtained with $[Et_4N][Fe_3Co(CO)_{13}]$ at 40 atm CO, 80 atm H₂, and 453 K.^{251b}

2.10.1.3. Ru–Co. Methyl acetate homologation was achieved in the presence of syn-gas, with the clusters $[Et_4N][RuCo_3(CO)_{12}]$ and $[Et_4N][Ru_3Co(CO)_{13}]$ as homogeneous catalyst precursors. The presence of the two metals improved considerably the yield of ethyl acetate. Conversions ranging from 50% to 70% were achieved, with selectivities for ethyl acetate up to 33%. Other observed products include acetic acid, ethanol, and ethers. Mechanistic insights included hydrolysis of methyl acetate to methanol (and acetic acid), which is further homologated to ethanol. Subsequent condensation of ethanol and acetic acid affords ethyl acetate.²⁵²

Methanol homologation with catalysts containing ruthenium in addition to cobalt are preferred for ethanol production, presumably due to their ability to readily hydrogenate acetaldehyde, thereby eliminating undesired byproducts. Thus, high ethanol selectivity at high methanol conversion was observed with $[CpRu(PPh_3)_2Co(CO)_4]$. However, a mixture of $[CpRu(PPh_3)_2Cl]$ and $[Co_2(CO)_8]$ provided the same activity.²⁵³

When promoted by methyl iodide, the clusters $[HRuCo_3(CO)_{12}]$ and $C[RuCo_3(CO)_{12}]$ (cation $C^+ = Na^+, Cs^+, Et_4N^+, Ph_4P^+, PPN^+$) exhibited improved catalytic activities in methanol homologation, as compared to the homometallic complexes $[Co_2(CO)_8]$ and $[Ru_3(CO)_{12}]$ alone.^{251c,254} The anionic cluster $[Ru_3Co(CO)_{13}]^-$ gave a lower yield of ethanol under the same conditions.^{251c,254b}

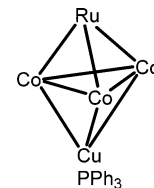
Although consistent with consecutive transformations, the synergy resulting from a mixed-metal system has been identified in the case of Ru–Co carbonyl clusters. High activity and good selectivity for ethanol were observed in methanol homologation with $[Et_4N][RuCo_3(\mu_2-\eta^2-PhC_2Ph)(CO)_{10}]$ (72). In this case, up to 54% selectivity for ethanol was achieved, at 46% methanol conversion. This system was slightly more active than both the Ru–Co–Cu and the Ru–Co–Au clusters described below, with similar selectivity. Other reaction products include methyl acetate, ethyl acetate, diethyl ether, and traces of acetaldehyde.²⁵⁵



Cationic cluster in 72
(CO ligands omitted for clarity)

2.10.1.4. Ru–Co–Cu, Ru–Co–Au. Under the same reaction conditions as for the aforementioned cluster 72, methanol homologation was catalyzed with high activity and good selectivity by the trimetalllic clusters $[RuCo_3(\mu_3-CuPPh_3)-(CO)_{12}]$ (73) and $[Au(PPh_3)_2][RuCo_3(CO)_{12}]$ as homogeneous catalysts. The Ru–Co–Au cluster was more active (41% conversion) and selective for ethanol (ca. 60%) than the Ru–

Co–Cu one (ca. 52% selectivity at 35% methanol conversion).²⁵⁵



Metal core of 73
(CO ligands omitted for clarity)

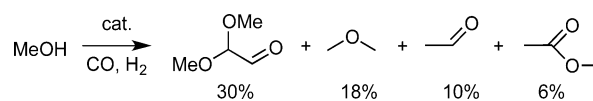
2.10.1.5. Ru–Rh. When ruthenium and rhodium salts were used in the same system, a synergistic effect for methanol homologation was observed at 100 atm synthesis gas pressure, whereas ruthenium or rhodium chloride alone were inactive for ethanol synthesis.²²¹ No enhancement of ethanol production was observed with the mixed-metal compounds $[HRuRh_3(CO)_{12}]$, $[HRuRh_3(CO)_{10}(PPh_3)_2]$, $[H_2Ru_2Rh_2(CO)_{12}]$, and $[PPN][RuRh_5(CO)_{16}]$ as catalyst precursors, which is consistent with the decomposition of the clusters found to occur in all of the experiments.²⁵⁶

2.10.1.6. Os–Co. Methanol homologation was catalyzed in the presence of the cluster $[Et_4N][OsCo_3(CO)_{12}]$, which exhibited high activity, although the selectivity in ethanol was much lower than that observed with Ru–Co systems.^{251b}

2.10.1.7. Co–Rh. Methanol homologation was also catalyzed by the tetranuclear precursors $[Co_2Rh_2(CO)_{12}]$ and $[Co_3Rh-(CO)_{12}]$. High activities (more than 50% conversion) were observed, but selectivities for ethanol were always very low (less than 2%). The selectivities were highest for dimethyl acetal, methyl acetate, and dimethyl ether.^{251b,c,253c,254b}

2.10.1.8. Co–Pd, Co–Pt. In the methanol homologation reaction, ethanol was obtained with less than 1% yield when $[Co_2Pd(CO)_7(dppe)]$ was used as a homogeneous catalyst (ca. 61% methanol conversion). The main products were acetaldehyde dimethylacetal, dimethylether, acetaldehyde, and methyl acetate (Scheme 24).^{251b,254b}

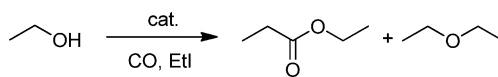
Scheme 24



Similar results were observed when the triangular cluster $[Co_2Pt(CO)_7(dppe)]$ was used under the same reaction conditions, except that the selectivity for ethanol was ca. twice that of the Co–Pd catalyst (3.3% vs 1.3%) and the conversion was lower (ca. 49%).^{251b,254b}

2.10.2. Carbonylation Reactions. **2.10.2.1. Carbonylation of Alcohols.** **2.10.2.1.1. Mo–Fe, Fe–Rh, Fe–Ni, Fe–Cu, Fe–Hg.** Homogeneous carbonylation of ethanol in the presence of ethyl iodide to ethylpropionate and diethyl ether (Scheme 25) was catalyzed by a series of Fe-containing heterobimetallic complexes: $[MoFe(\mu-Ph_2Ppy)_2(CO)_6]$ (I), $[FeRh(\mu-Ph_2Ppy)_2(\mu-CO)(CO)_3Cl]$ (II), $[FeNi(\mu-Ph_2Ppy)_2(\mu-CO)(CO)_3Cl]$ (III).

Scheme 25



$(CO)_3(NCS)_2$] (**III**), $[FeCu(\mu-Ph_2Ppy)_2(CO)_3Cl]$ (**IV**), and $[FeHg(\mu-Ph_2Ppy)_2(CO)_3(SCN)_2]$ (**V**). They were compared to the mononuclear complex $[RhCl(PPh_3)_3]$.²⁵⁷

The results are compiled in Table 2. All catalysts led to high conversions (from 88.5% to 99.5%). Most complexes are more

Table 2. Catalytic Carbonylation of Ethanol at 493 K^a

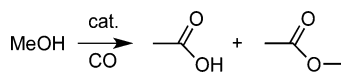
entry	complex	ethanol conversion (%)	selectivity (%)	
			diethyl ether	ethyl propionate
1	I	88.5	81.3	18.7
2	II	99.5	1.4	98.6
3	III	95.2	52.3	47.7
4	IV	91.4	76	24
5	V	94.4	73.2	26.8
6	$RhCl(PPh_3)_3$	96.4	32.3	67.7

^aEntries 2 and 6 were performed at 473 K.

selective for diethyl ether (entries 1, 3, 4, and 5), but the Rh-based complexes are very selective for ethyl propionate (entries 2 and 6). In particular, the Fe–Rh complex **II** yields almost quantitatively ethyl propionate.

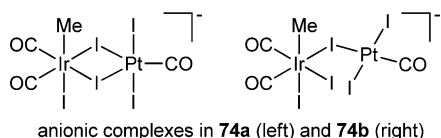
2.10.2.1.2. Os–Ir. The cluster $[PPN][Os_3Ir(CO)_{13}]$ was used in the carbonylation of methanol with MeI or HI as cocatalysts. The two products obtained were acetic acid and methyl acetate (Scheme 26). The former undergoes

Scheme 26



esterification due to the excess of MeOH in the system, thus leading to a higher amount of methyl acetate. It was found that no intact Os_3Ir cluster remained after catalysis, but rather a mixture of $[PPN][Os_3(CO)_3I_3]$ and $[Ir_4(CO)_{12}]$ was formed.²⁵⁸

2.10.2.1.3. Ir–Pt. Carbonylation of methanol to acetic acid was achieved in the presence of the Ir and Pt iodo-complexes $[PPN][IrI_3Me(CO)_2]$ and $[Pt(\mu-I)I(CO)]_2$. During the catalytic reactions, the iodo-bridged heterometallic complex $[PPN][IrPtMeI_5(CO)_3]$ (74), most likely responsible for the activity of such a system, could be isolated. This short-lived intermediate undergoes decomposition to $[PPN][PtI_3(CO)]$ and $[IrMeI_2(CO)_3]$ under CO pressure.^{10,259} The authors considered two different isomers, **74a** and **74b**, for the complex $[PPN][IrPtMeI_5(CO)_3]$, from FAB-MS and ^{13}C NMR studies.²⁶⁰



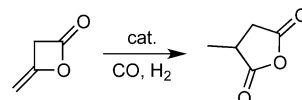
anionic complexes in **74a** (left) and **74b** (right)

2.10.2.2. Hydrocarbylation Reactions. **2.10.2.2.1. Ru–Co.** Carbon-supported MMCD catalysts obtained from $[HRuCo_3(CO)_{12}]$, $[Ru_2Co_2(CO)_{13}]$ and $[HRu_3Co(CO)_{13}]$, respectively, were used to investigate the role of ruthenium as promoter in the cobalt-catalyzed hydrocarbylation of MeOH. A close proximity of the promoter metal and the cobalt centers seems to be a condition for cooperative carbonylation and hydrogenation to occur. The observed primary reactions under

the catalytic conditions were hydrocarbylation, affording acetaldehyde and its dimethylacetal, carbonylation, leading to methyl acetate, and methane formation. The reduction steps are facilitated by the presence of ruthenium.²⁶¹

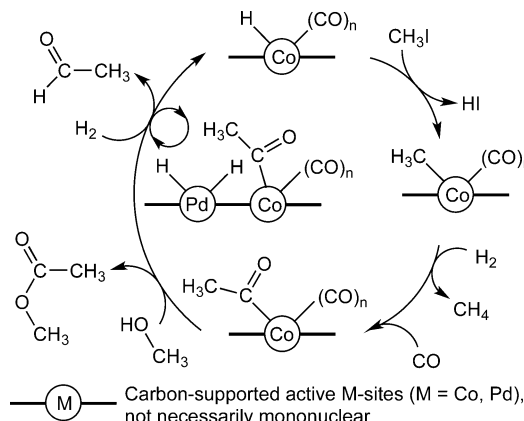
2.10.2.2.2. Co–Rh. A mixed-metal species formulated as $[CoRh(CO)_7]$, formed *in situ* when $[Co_2(CO)_8]$ and $[Rh_4(CO)_{12}]$ were reacted under CO/H₂ pressure, has been postulated as an active catalyst in the hydrocarbylation of diketene. In particular, diketene and substituted diketene gave 3-substituted succinic anhydrides under such conditions (Scheme 27).²⁶²

Scheme 27



2.10.2.2.3. Co–Pd. The carbon-supported $[Co_2Pd]$ catalyst derived from the triangular cluster $[Co_2Pd(CO)_7(dppe)]$ was tested in the hydrocarbylation of MeOH. The close proximity between the promoter metal (palladium) and cobalt centers appears critical for the occurrence of cooperative carbonylation and hydrogenation (Scheme 28). The primary

Scheme 28. Catalytic Cycle for Methanol Hydrocarbylation^a



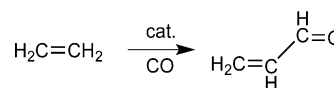
^aAdapted from ref 261.

reactions were hydrocarbylation, affording acetaldehyde and its dimethylacetal, carbonylation, leading to methyl acetate, and methane formation. The reduction steps were facilitated by the presence of palladium.²⁶¹

The existence and importance of heterometallic centers was deduced from the comparison of activities and selectivities with those of mechanical mixtures of monometallic catalysts and of catalysts prepared by coimpregnation.

2.10.2.3. Carbonylation of Olefins. **2.10.2.3.1. Zr–Rh.** The early late bimetallic complex $[Ph_4As][Cp^*_2Zr(\mu-S)_2Rh(CO)_2]$ was reported to initiate the carbonylation of ethylene to acrolein in the presence of PPh_3 (Scheme 29). It yielded 2

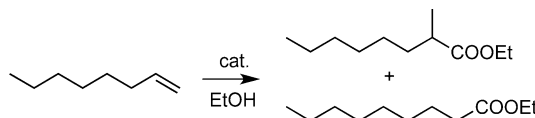
Scheme 29



times more acrolein than the complex $[\text{Cp}^*_2\text{Zr}(\text{SH})_2]$. Under the same conditions, rhodium complexes were inactive. Moreover, addition of triethyl orthoformate allowed for the reaction to be catalytic.²⁶³

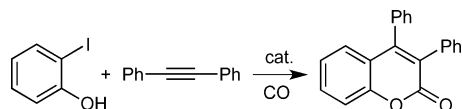
2.10.2.3.2. Fe–Pd. The phosphanido-bridged complex $[(\text{OC})_4\text{Fe}(\mu\text{-PPH}_2)\text{Pd}(\mu\text{-Cl})_2]$ (**15**) was found to be active in the carbonylation of 1-octene and 1,5-cyclooctadiene in the presence of ethanol to afford the corresponding esters under mild conditions (348 K, 50 atm). In the case of 1-octene, the total yield of esters was 10 times greater than when $[\text{PdCl}_2(\text{PPh}_3)_2]$ was used as a catalyst (Scheme 30). In both cases, the isomer distribution was ca. 1:1.⁶⁰

Scheme 30



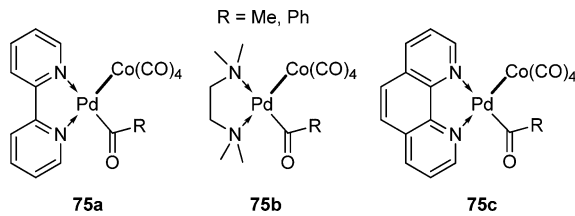
2.10.2.4. Other Carbonylation Reactions. **2.10.2.4.1. Co–Rh.** The synthesis of coumarins by cyclocarbonylation of alkynes with 2-iodophenol in the presence of CO and pyridine could be performed with the reusable $[\text{Co}_2\text{Rh}_2]$ catalyst obtained from the cluster $[\text{Co}_2\text{Rh}_2(\text{CO})_{12}]$ in yields higher than 80% (Scheme 31). Various substituents were tested on the internal alkyne, such as Me, Et, Pr, or Ph. Coumarins were also obtained from the reaction between phenols and propylic esters.²⁶⁴

Scheme 31



Heterobimetallic $[\text{Co}_2\text{Rh}_2]$ NPs exhibit good activity and selectivity in the cyclohydrocarbonylation of alkynes. In particular, diphenylacetylene was reacted with CO (30 atm) and water in the presence of NEt_3 , and afforded furanone in 85–88% yields even after five uses. Alkynes with various substituents were also tested with good yields. The tandem CO insertion-cyclohydrocarbonylation of a broad range of α -keto alkynes yielded substituted furanones with very good regioselectivity.²⁶⁵

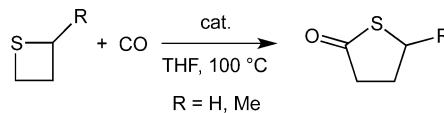
2.10.2.4.2. Co–Pd. Copolymerization of unsubstituted and C- or N-substituted aziridines with CO was investigated under mild conditions in the presence of the complex $[(\text{bpy})\text{AcPdCo}(\text{CO})_4]$. In particular, aziridine afforded the corresponding copolymer with 89% yield, 2-methylaziridine with 69% yield, and N-ethylaziridine with 81% yield. Mo–Pd analogous complexes were found to be inactive, indicating the importance of the bimetallic couple employed.²⁶⁶



Further investigations on this reaction showed that complexes such as $[\text{L}\{\text{RC(O)}\}\text{Pd–Co}(\text{CO})_4]$ (**75a**, L = bpy; **75b**, L = TMEDA; **75c**, L = phen; R = Me, Ph) were also highly active.²⁶⁷

2.10.2.4.3. Co–Pt. The complex $[\text{Me}(\text{dppe})\text{PtCo}(\text{CO})_4]$ was reported to promote the catalytic carbonylation of thietanes to γ -thiobutyrolactones (Scheme 32). Comparing

Scheme 32

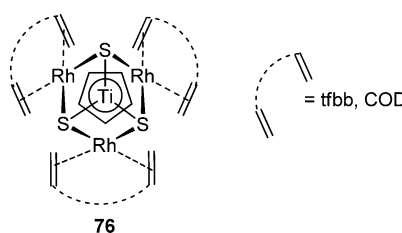


the activities of monometallic and Pt–Mn, Pt–Fe, or Pt–Mo materials revealed that the presence of both Pt and Co is necessary for the process to occur. Furthermore, the activity of this cluster was even higher than that of the usual $[\text{Co}_2(\text{CO})_8]/[\text{Ru}_3(\text{CO})_{12}]$ catalytic system. The authors suggested a mechanism involving Co–Pt bond cleavage, allowing the thietane to bind to the platinum, followed by C–S bond cleavage, CO insertion, and a ring-closing step to release the desired product.²⁶⁸

2.10.3. Hydroformylation Reactions. **2.10.3.1. Hydroformylation of Olefins.** It should be noted that because hydroformylation is performed in the presence of CO/H_2 mixtures, subsequent hydrogenation of the aldehyde first obtained often leads to the formation of alcohols. Thus, under appropriate conditions and in the presence of a specific catalyst, selectivity toward alcohols can be enhanced. It is noteworthy that only one example was reported for the hydroformylation of alkynes (see section 2.10.3.1.8).

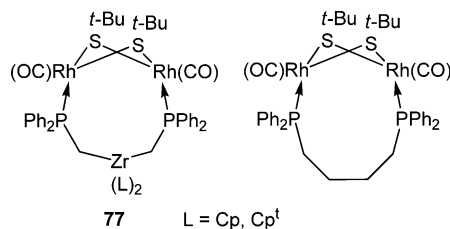
In homogeneous olefin hydroformylation reactions, strong synergistic effects involving mononuclear precursors are sometimes observed, even though no heterometallic species, and thus no metal–metal bond, are evidenced. In particular, catalytic binuclear elimination appears to be the origin of the good results obtained for rhodium-based systems.²⁶⁹

2.10.3.1.1. Ti–Rh. Under mild temperature and pressure, the complexes $[\text{CpTi}(\mu_3\text{-S})_3\{\text{Rh}(\text{L})\}_3]$ (L = tetrafluorobenzobarrelene [tfbb], COD) (**76**) were used in the catalytic hydroformylation of 1-hexene and styrene in the presence of CO and P-donor ligands. The P/Rh ratio was found to rule the activity and selectivity of the catalysts. No hydrogenation or isomerization was observed. In the case of 1-hexene hydroformylation, the best results were obtained with PPh_3 , when L = tfbb and P/Rh = 2 or 4. Thus, at 96% aldehyde conversion, 77–78% regioselectivity for the linear aldehyde was observed. Note-worthy is that the presence of phosphite ligands resulted in inactive systems, whereas with L = tfbb, better conversions were achieved with phosphites. The use of chiral diphosphine ligands allowed even better conversions (up to 99% with (–)-BDPP) and selectivities such as 95% (with (–)-BDPP too) (BDPP = 2,4-bis(diphenylphosphino)pentane).²⁷⁰

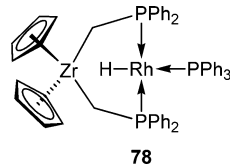


Although not as active as the mononuclear compound $[\text{Rh}(\text{COD})(\text{PPh}_3)_2][\text{BPh}_4]$, the bimetallic complex $[\text{Cp}_2\text{Ti}(\mu\text{-CH}_2\text{PPh}_2)_2\text{Rh}(\text{COD})][\text{BPh}_4]$ can be used for the hydroformylation of 1-hexene and 1,5-cyclooctadiene.²⁷¹

2.10.3.1.2. Zr–Rh. Hydroformylation of 1-hexene was achieved with the phosphanido-bridged complex $[\text{Cp}_2\text{Zr}(\mu\text{-PPh}_2)_2\text{RhH}(\text{CO})(\text{PPh}_3)]$ as a homogeneous catalyst. It afforded *n*-heptanal with ca. 80% yield. The complex $[\text{HRh}(\text{CO})(\text{PPh}_3)_3]$ was more active, but the overall *n*-heptanal yield was lower because the selectivity was lower. The main byproduct was 2-methylhexanal.²⁷² The same reaction was catalyzed by the complexes $[\text{L}_2\text{Zr}(\mu\text{-CH}_2\text{PPh}_2)_2\text{Rh}_2(\text{CO})_2(\mu\text{-S-}t\text{-Bu})_2]$ ($\text{L} = \text{Cp}, \text{Cp}^\ddagger$) (77) at 353 K and 5 atm ($\text{CO} + \text{H}_2$). Almost quantitative conversion occurred within 2 h, and the *n*-heptanal to methylhexanal ratio was ca. 2. The authors explained this enhanced activity as compared to the related monometallic complex $[(\mu\text{-PPh}_2(\text{CH}_2)_4\text{PPh}_2)\text{Rh}_2(\text{CO})_2(\mu\text{-S-}t\text{-Bu})_2]$ by an increased electron density on rhodium atoms from the Zr.²⁷³



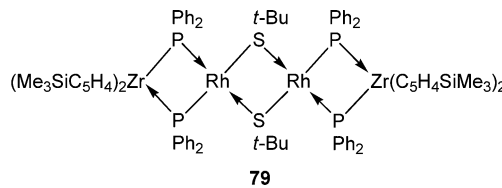
Hydroformylation of 1-hexene was achieved with 100% conversion, under mild conditions, and with very short induction time, in the presence of the bridged complex $[\text{Cp}_2\text{Zr}(\mu\text{-CH}_2\text{PPh}_2)_2\text{RhH}(\text{PPh}_3)]$ (78). Addition of PPh_3 in a 1:3 ratio slightly enhanced the selectivity toward *n*-heptanal.²⁷⁴ This bimetallic system is more active than monometallic Zr or Rh species. Similar results were obtained with $[\text{Cp}_2\text{Zr}(\mu\text{-CH}_2\text{PPh}_2)_2\text{RhH}(\text{CO})(\text{PPh}_3)]$.²⁷⁵



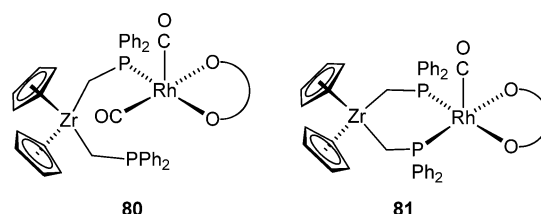
The complex $[\text{Cp}_2\text{Zr}(\mu\text{-CH}_2\text{PPh}_2)_2\text{Rh}(\text{COD})][\text{BPh}_4]$ ^{271,276} and its Cp-substituted analogue $[\text{Cp}^\ddagger\text{Zr}(\mu\text{-CH}_2\text{PPh}_2)_2\text{Rh}(\text{COD})][\text{BPh}_4]$ ²⁷⁶ are active catalysts in hydroformylation of 1-hexene and 1,5-cyclooctadiene, reaching 100% conversion, but after longer induction times than the complex $[(\text{PPh}_3)_2\text{Rh}(\text{COD})][\text{BPh}_4]$. The complexes $[\text{Cp}_2\text{Zr}(\mu\text{-CH}_2\text{PPh}_2)_2\text{Rh}_2(\mu\text{-S-}t\text{-Bu})_2(\text{CO})_2]$ and $[\text{Cp}^\ddagger\text{Zr}(\mu\text{-CH}_2\text{PPh}_2)_2\text{Rh}_2(\mu\text{-S-}t\text{-Bu})_2(\text{CO})_2]$ gave very similar results, except for the slightly shorter induction times.²⁷⁶ Noteworthy is that all of the Zr–Rh complexes tested in 1-hexene hydroformylation gave a linear to branched aldehyde ratio of approximately 2.

The tetranuclear complex $[(\text{C}_5\text{H}_4\text{SiMe}_3)_2\text{Zr}(\mu\text{-PPh}_2)_2\text{Rh}(\mu\text{-S-}t\text{-Bu})_2]_2$ (79) was also tested in 1-hexene hydroformylation at 353 K, under 20 bar of H_2/CO (1:1). It appeared to be a poor catalyst, as compared to the aforementioned Zr–Rh complexes, probably because of the lack of coordination sites to anchor H and CO during the reaction.²⁷⁷

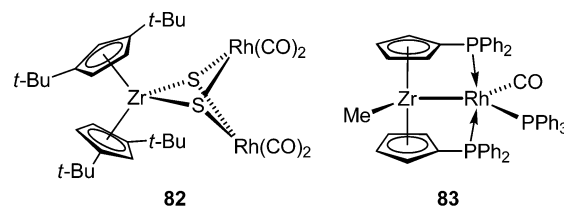
The catalytic systems $\{[\text{Rh}(\text{acac})(\text{CO})_2] + [\text{Cp}_2\text{Zr}(\text{CH}_2\text{PPh}_2)_2]\}$ and $\{[\text{Rh}(\text{acac})(\text{CO})_2] + [\text{Cp}_2\text{ZrH}(\text{CH}_2\text{PPh}_2)_2]\}$ were tested in the hydroformylation of 1-



hexene. Their good activities were attributed to the *in situ* formation of the heterobimetallic species $[\text{Cp}_2(\text{CH}_2\text{PPh}_2)\text{Zr}(\mu\text{-CH}_2\text{PPh}_2)\text{Rh}(\text{acac})(\text{CO})_2]$ (80) and $[\text{Cp}_2\text{Zr}(\mu\text{-CH}_2\text{PPh}_2)_2\text{Rh}(\text{acac})(\text{CO})]$ (81), respectively, because the Zr complexes alone are inactive, and $[\text{Rh}(\text{acac})(\text{CO})_2]$ is much less active than these bimetallic systems. The same systems were also tested in hydroformylation of 1,5-hexadiene and 1,7-octadiene, but with much lower activities.²⁷⁸



Hydroformylation of 1-octene was performed with the precatalyst $[\text{Cp}^\ddagger\text{Zr}(\mu_3\text{S})_2\{\text{Rh}(\text{CO})_2\}_2]$ ($\text{Cp}^\ddagger = \eta^5\text{-1,3-ditert-butylcyclopentadienyl}$) (82) in the presence of the P-donor ligands $\text{P}(\text{OMe})_3$, $\text{P}(\text{OPh})_3$, and PPh_3 and under mild conditions.²⁷⁹ No synergistic effect was observed, and the complex could not be completely recovered after the reaction, most likely due to the formation of monometallic Rh complexes. The only products of the reaction were 1-nonalan and 2-methyloctanal, while only traces of octane were detected. Varying the P/Rh ratio did not seem to impact the activity, but the nature of the phosphine cocatalyst did. The highest conversion was achieved with $\text{P}(\text{OPh})_3$, but the amount of isomerization product was much higher; thus only 70% selectivity for the aldehyde was obtained. The best results were found with $\text{P}(\text{OMe})_3$: the selectivity for the aldehyde product reached 95–98% for conversions higher than 80%; while with PPh_3 , the selectivity was >90%, but the conversion was only 25–30%.

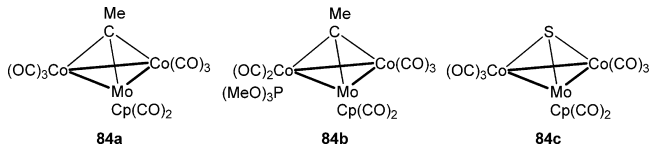


Although details were not provided, the zirconocene-bridged complex $[\text{MeZr}\{\mu\text{-}\eta^5\text{-}(\text{C}_5\text{H}_4\text{PPh}_2)\}_2\text{Rh}(\text{CO})(\text{PPh}_3)]$ (83) catalyzed the hydroformylation of 1-hexene to heptanals with very good activity at 353 K.²⁸⁰

2.10.3.1.3. Mo–Fe–Co. The dppe ligand bridging the Fe–Co bond in the cluster $[\text{MoFeCoCp}'(\mu_3\text{-S})(\mu\text{-dppe})(\text{CO})_6]$ is believed to render the Fe and Co sites more active for the binding of the substrates during olefin hydroformylation.²⁸¹

2.10.3.1.4. Mo–Co. The hydroformylation of 1-pentene was studied with the mixed-metal clusters $[\text{MoCo}_2(\mu_3\text{-CMe})\text{Cp}(\text{CO})_8]$ (84a), $[\text{MoCo}_2(\mu_3\text{-CMe})\text{Cp}(\text{CO})_7\{\text{P}(\text{OMe})_3\}]$ (84b), and $[\text{MoCo}_2(\mu_3\text{-S})\text{Cp}(\text{CO})_8]$ (84c) as homogeneous catalysts.¹⁰⁹ However, it should be noted that isomerization of

1-pentene competes with hydroformylation to hexanal and 2-methylpentanal. Thus, aldehyde yields of 13.5%, 25.5%, and 2.4% were obtained for **84a**, **84b**, and **84c**, respectively. The first two catalysts exhibited a linear to branched ratio of 2.4 and 2.9, while the third was 100% selective for the linear isomer. The clusters could be recovered almost entirely (>90%) after catalysis. Moreover, the cluster **84b** was also active in styrene hydroformylation, affording aldehydes with ca. 41% yield, with high selectivity for 2-phenylpropionaldehyde.^{109a}



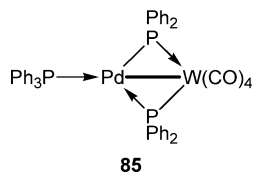
2.10.3.1.5. Mo–Co–Ni. Hydroformylation of alkenes to linear and branched aldehydes was catalyzed by the cluster $[\text{MoCoNi}(\mu_3\text{-CMe})\text{Cp}_2(\text{CO})_5]$ (**26**) with low activities. In particular, ca. 8% and 6% aldehyde yields were obtained in 1-pentene and styrene hydroformylation, respectively. Isomerization of 1-pentene competed strongly under the reaction conditions.¹⁰⁹

2.10.3.1.6. Mo–Rh. The silica-supported $[\text{Mo}_2\text{Rh}]$ catalyst, derived from $[\text{Mo}_2\text{Rh}\text{Cp}_3(\text{CO})_5]$, was used as a heterogeneous catalyst for the hydroformylation of ethylene and propene. Molybdenum appears to increase the rate of both hydrogenation and hydroformylation of olefins. Propanal, the primary product of the hydroformylation, was suggested to be hydrogenated to propanol on active bimetallic centers.^{168a,213}

2.10.3.1.7. W–Ru. The complex $[(\text{OC})_4\text{W}(\mu\text{-PPH}_2)_2\text{Ru}(\text{CO})_3]$ (**61c**) was studied as a homogeneous catalyst for the hydroformylation of styrene. The reaction occurred with 10% yield and ca. 70% selectivity for the branched aldehyde, while the corresponding Cr–Ru and Mo–Ru catalysts gave yields lower than 2%. Under the same conditions, only the W–Pd and Fe–Ru analogues were more active.²¹¹

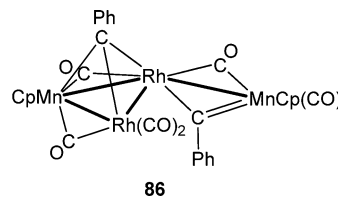
2.10.3.1.8. W–Rh. The phosphanido-bridged complex $[(\text{OC})_4\text{W}(\mu\text{-PPH}_2)\text{RhH}(\text{CO})(\text{PPH}_3)]$ was found to be a homogeneous catalyst for hydroformylation of alkenes and alkynes. In the reaction with styrene, the conversion was complete after 20 h, and almost 100% selectivity was observed for the branched chain aldehyde.²⁸²

2.10.3.1.9. W–Pd. Hydroformylation of styrene to aldehydes was performed in the presence of the dinuclear complex $[(\text{OC})_4\text{W}(\mu\text{-PPH}_2)_2\text{Pd}(\text{PPH}_3)]$ (**85**) with 15% yield. The corresponding Cr–Pd and Mo–Pd complexes showed yields lower than 2%, while the Mo–Pt and W–Pt complexes were even less active. Only the Fe–Ru analogous catalyst was more active.²¹¹



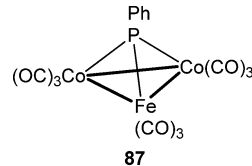
2.10.3.1.10. Mn–Rh. The cluster $[\text{Mn}_2\text{Rh}_2(\mu_3\text{-CPh})(\mu\text{-CPh})\text{Cp}_2(\mu\text{-CO})_3(\text{CO})_3]$ (**86**) was used as a homogeneous catalyst precursor for the hydroformylation of styrene at 333 K and 2 MPa CO/H₂. The conversion was complete after 4 h, and selectivity for the branched isomer 2-phenylpropionaldehyde was in the range 92–94%. The product recovered after

reaction could not be fully characterized, but it was assumed to be a Rh–Mn carbonyl compound, responsible for the catalytic activity.²⁸³



2.10.3.1.11. Fe–Ru. The homogeneous hydroformylation of styrene (393 K, 20 atm, CO/H₂ = 1) was performed in the presence of the bimetallic complex $[(\text{OC})_3\text{Fe}(\mu\text{-PPH}_2)_2\text{Ru}(\text{CO})_3]$ (**61d**). It proved to be the most active system of a series of M–Ru, M–Pd (M = Cr, Mo, W), and M–Pt (M = Mo, W) catalysts, leading to a yield of 42%. Its activity was explained by synergistic effects between the two metals, because Fe–Fe and Ru–Ru analogous complexes gave only 9% and 3% yields, respectively. The complex was recovered intact at the end of the reaction, unlike in the case of M–Pd and M–Pt systems.²¹¹

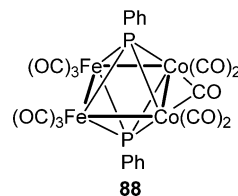
2.10.3.1.12. Fe–Co. The trinuclear cluster $[\text{FeCo}_2(\mu_3\text{-PPH})(\text{CO})_9]$ (**87**) has been used as a homogeneous catalyst in hydroformylation of 1-pentene. The aldehyde yield was of ca. 90%, and the selectivity was rather poor (linear to branched ratio of 1.4).¹⁰⁹



Hydroformylation of cyclohexene to yield cyclohexanecarbaldehyde was catalyzed by the cluster $[\text{Et}_4\text{N}][\text{FeCo}_3(\text{CO})_{12}]$, and synergistic effects were involved. Thus, 27% yield could be obtained after 4 h. However, the cluster $[\text{Et}_4\text{N}][\text{Fe}_3\text{Co}(\text{CO})_{13}]$ exhibited little activity. A mixture of $[\text{Co}_2(\text{CO})_8] + [\text{Ru}_3(\text{CO})_{12}]$ with a Ru:Co ratio of 9.9 afforded the desired product almost quantitatively after 4 h.²⁸⁴

Hydroformylation of terminal, internal, and cyclic olefins was achieved in the presence of the cluster $[(\text{PhCH}_2)\text{Me}_3\text{N}][\text{FeCo}_3(\text{CO})_{12}]$, which showed good catalytic activity and a selectivity close to 100%.²⁸⁵

The cluster $[\text{Fe}_2\text{Co}_2(\mu_4\text{-PPH})_2(\text{CO})_{11}]$ (**88**) was shown to persist during hydroformylation of terminal olefins at 403 K.²⁸⁶



2.10.3.1.13. Fe–Rh. The complex $[\text{FeRh}(\mu\text{-P}(t\text{-Bu})_2)(\mu\text{-dppm})(\mu\text{-CO})(\text{CO})_3]$ was used for the catalytic hydroformylation of ethylene with 100% selectivity for propionaldehyde. The complex apparently decomposed during the process, to afford mononuclear complexes, most likely responsible for the activity of the system.²⁸⁷

The cluster $[\text{HFe}_3\text{Rh}(\text{CO})_{11}(\mu_4\text{-}\eta^2\text{-C=CHPh})]$ (**13**) showed the same activity as $[\text{Rh}_4(\text{CO})_{12}]$ in the hydro-

formylation of 1-pentene. Typically, after 6 h reaction time, 70% conversion was achieved, and the selectivity was higher for hexanal than for 2-methylpentanal (linear to branched ratio of 2).⁵⁸

Hydroformylation of 1-pentene was performed in the presence of the nitrido clusters $[\text{Ph}_4\text{P}][\text{Fe}_4\text{Rh}_2\text{N}(\text{CO})_{15}]$ and $[\text{Ph}_4\text{P}]_2[\text{Fe}_5\text{RhN}(\text{CO})_{15}]$ as homogeneous catalysts with a selectivity of 35–65% in *n*-hexanal.²⁸⁸

The carbide cluster $[\text{Ph}_4\text{P}][\text{Fe}_5\text{RhC}(\text{CO})_{16}]$ (**55**) was also used as catalyst precursor for the hydroformylation of 1-pentene. Under catalytic conditions (60 atm CO + H₂ at 373 K), it transformed into $[\text{Fe}_4\text{Rh}_2\text{C}(\text{CO})_{16}]$ and $[\text{Ph}_4\text{P}][\text{Fe}_4\text{RhC}(\text{CO})_{14}]$ (**54**). The $\text{Fe}_4\text{Rh}_2\text{C}$ cluster was found to be more active precursor than **55**. The Fe_4RhC cluster transformed further into $[\text{Ph}_4\text{P}][\text{Fe}_3\text{Rh}_3\text{C}(\text{CO})_{15}]$ during catalysis, which showed an activity similar to that of **55**. The latter exhibited activity similar to that of $[\text{Fe}_4\text{Rh}_2\text{C}(\text{CO})_{16}]$ in hydroformylation of 1-pentene.²⁸⁹

Propene hydroformylation reactions could be catalyzed with high activity and selectivity when the $[\text{Fe}_4\text{Rh}]$ and $[\text{Fe}_5\text{Rh}]$ catalysts obtained from $[\text{Et}_4\text{N}][\text{Fe}_4\text{RhC}(\text{CO})_{14}]$ and $[\text{Et}_4\text{N}][\text{Fe}_5\text{RhC}(\text{CO})_{16}]$, respectively, were supported on silica. The $[\text{Fe}_3\text{Rh}_3]$ catalyst derived from the cluster $[\text{Et}_4\text{N}][\text{Fe}_3\text{Rh}_3\text{C}(\text{CO})_{15}]$ was comparatively less active.¹⁹³

The clusters $[\text{Me}_4\text{N}]_2[\text{FeRh}_4(\text{CO})_{15}]$, $[\text{TMBA}][\text{FeRh}_5(\text{CO})_{16}]$, $[\text{TMBA}]_2[\text{Fe}_2\text{Rh}_4(\text{CO})_{16}]$, and $[\text{Fe}_3\text{Rh}_2\text{C}(\text{CO})_{14}]$ have also been used in olefin hydroformylation when supported on silica and proved to be much more active than $[\text{Rh}_4(\text{CO})_{12}]$ -derived catalysts. Moreover, good selectivities for butanol were observed in propylene hydroformylation (in the range 42–63%).^{97,191,290}

2.10.3.1.14. Fe–Ir. Ethylene hydroformylation was performed in the presence of the heterogeneous silica-supported catalyst derived from $[\text{TMBA}]_2[\text{FeIr}_4(\text{CO})_{15}]$, which exhibited enhanced alcohol selectivity as compared to $[\text{Ir}_4]$ on SiO₂.^{191a,195}

2.10.3.1.15. Fe–Pd. The heterogeneous $[\text{Fe}_6\text{Pd}_6]$ catalysts prepared from $[\text{TMBA}]_3[\text{HFe}_6\text{Pd}_6(\text{CO})_{24}]$ (**56**) on SiO₂ showed enhanced alcohol selectivity in ethylene hydroformylation as compared to $[\text{PdCl}_2]$.¹⁹⁵ Ethylene hydroformylation with the silica-supported $[\text{Fe}_4\text{Pd}]$ catalyst obtained from $[\text{TMBA}]_2[\text{Fe}_4\text{Pd}(\text{CO})_{16}]$ led to higher selectivity in alcohol, because of its higher Fe content.^{191a} Propylene hydroformylation was also catalyzed by these bimetallic systems with high selectivities for alcohols.

2.10.3.1.16. Fe–Pt. The silica-supported $[\text{Fe}_3\text{Pt}_3]$ and $[\text{Fe}_4\text{Pt}]$ heterogeneous catalysts prepared from $[\text{TMBA}]_2[\text{Fe}_3\text{Pt}_3(\text{CO})_{15}]$ (**57**) and $[\text{TMBA}]_2[\text{Fe}_4\text{Pt}(\text{CO})_{16}]$, respectively, were less active in propylene hydroformylation than the corresponding iron–palladium systems (see section 2.10.3.1.15).^{191a}

2.10.3.1.17. Ru–Os. The polymer-supported cluster $[\text{polym}\sim\text{NR}_3][\text{H}_3\text{RuOs}_3(\text{CO})_{12}]$, obtained from cation exchange with the cluster $[\text{Ph}_4\text{As}][\text{H}_3\text{RuOs}_3(\text{CO})_{12}]$, was active in the hydroformylation of 1-hexene. It was found to be more active and selective toward *n*-heptanal than the corresponding Ru and Os tetranuclear homometallic clusters, thus suggesting synergistic effects. In particular, the selectivity for *n*-heptanal was ca. 72% under the reaction conditions. Noteworthy is the formation of small amounts of 2-hexene as a result of simultaneous isomerization.⁶³

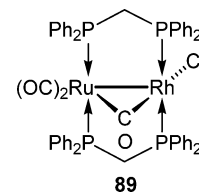
2.10.3.1.18. Ru–Co. Hydroformylation of cyclohexene to cyclohexanecarbaldehyde, in the presence of triphenylphos-

phine and tris(diphenylphosphino)methane, was tested with the cluster $[\text{HRuCo}_3(\text{CO})_{12}]$ as a homogeneous catalyst. The desired product was obtained in 37% yield. A mixture of the complexes $[\text{Co}_2(\text{CO})_8] + [\text{Ru}_3(\text{CO})_{12}]$ in a Ru to Co ratio of 9.9 gave 100% yield.^{254a,284}

Polymer-supported Co–Ru clusters anchored via N, P, or S coordinating atoms were tested in hydroformylation of cyclohexene. It was found that the surface Co/Ru ratio played a more important role than the total Co/Ru ratio.²⁹¹

Ethylene and propylene hydroformylation was catalyzed by carbon-supported heterogeneous catalysts derived from the clusters $[\text{HRuCo}_3(\text{CO})_{12}]$, $[\text{H}_3\text{Ru}_3\text{Co}(\text{CO})_{12}]$, or $[\text{Et}_4\text{N}][\text{Ru}_3\text{Co}(\text{CO})_{13}]$. Higher rates and selectivities to *n*-alcohol production were observed with the cobalt-rich MMCD catalysts.²⁹²

2.10.3.1.19. Ru–Rh. The complex $[\text{RuRh}(\mu\text{-dppm})_2\text{Cl}(\text{CO})_3]$ (**89**) was tested in the homogeneous hydroformylation of pentene under mild conditions.²⁹³



When the cluster $[\text{PPN}][\text{RuRh}_5(\text{CO})_{16}]$ was used in the hydroformylation of 1-hexene, some hydrogenation was also noted, but aldehydes were obtained in 98% yields. Moreover, the linear to branched ratio was of 0.7, and no alcohol formation was noted.²⁹⁴

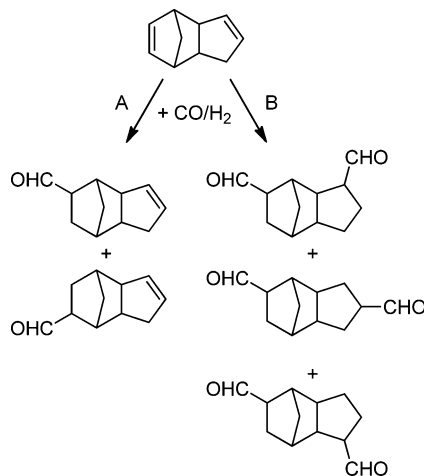
2.10.3.1.20. Co–Rh. The coordinatively unsaturated bimetallic compound $[\text{CoRh}(\text{CO})_7]$ seems to be involved as an active species in hydroformylation reactions.²⁹⁵ Indeed, a synergistic effect was evidenced in the hydroformylation of pentafluorostyrene.²⁹⁶ Excellent regioselectivities were reported for the hydroformylation step of the hydroformylation-amidocarbonylation of trifluoropropene using a $[\text{Co}_2(\text{CO})_8]/[\text{Rh}_6(\text{CO})_{12}]$ system in which $[\text{CoRh}(\text{CO})_7]$ could have been generated.

The dinuclear complexes $[(\text{OC})\text{LCo}(\mu\text{-H})\{\mu\text{-P}(t\text{-Bu})_2\}\text{Rh}(\text{CO})\{\text{HP}(t\text{-Bu})_2\}]$ ($\text{L} = \text{CO}, \text{HP}(t\text{-Bu})_2$) were reported to homogeneously catalyze the hydroformylation of terminal olefins such as ethylene, propylene, and 1-octene with better selectivities for the linear isomers.²⁹⁷

A cobalt–rhodium system, promoted by triphenylphosphine, enables a selective hydroformylation of dicyclopentadiene (DCPD) under relatively mild conditions. The main products obtained were those of paths A and B (Scheme 33), depending on the initial $\text{PPh}_3/\text{metal}$ ratio and the CO/H₂ pressure. Typically, path A was favored at 1 atm, while path B was preferred when the pressure was raised to 40 atm. Under pressure, the complexes $[\text{CoRh}(\text{CO})_6(\text{PPh}_3)]$ and $[\text{CoRh}(\text{CO})_5(\text{PPh}_3)_2]$ seem to be the active species, and they could be recovered after the experiments. Moreover, synergistic effects were observed. At ambient temperature, however, the fragmentation of the clusters to monometallic complexes causes a loss of activity.²⁹⁸

The cluster $[\text{Co}_2\text{Rh}_2(\text{CO})_{12}]$ was reported to catalyze the hydroformylation of 1-hexene and 3,3-dimethylbut-1-ene, whereas $[\text{Co}_3\text{Rh}(\text{CO})_{12}]$ catalyzed only that of 1-hexene.^{295b,299} The cluster $[\text{Co}_2\text{Rh}_2(\text{CO})_{12}]$ was more active in the hydroformylation of cyclohexene, under mild conditions

Scheme 33



(323 K, 1 atm CO + H₂), than [Rh₄(CO)₁₂], and addition of P(OPh)₃ enhanced its activity.³⁰⁰

Hydroformylation of 1-hexene was achieved with [Co₂Rh₂(CO)₁₂] supported on alumina, silica, or magnesium silicate to form C₇-aldehydes with good yields. The best results for the production of C₇-alcohols (yields >90%) were obtained with alumina as a support in the presence of NEt₃ at 50 bar (CO:H₂ = 1) and 373 K.²⁹⁹

When the cluster [Co₂Rh₂(CO)₁₂] was entrapped in silica with polystyrene sulfonic acid, it allowed styrene hydroformylation with moderate yields (ca. 10%).¹⁴⁹

Olefin hydroformylation was tested in the presence of amine-functionalized resins to which Co–Rh clusters, such as [Co_{4-x}Rh_x(CO)₁₂] ($x = 0\text{--}2$), were tethered. In particular, [Co₂Rh₂(CO)₁₂] catalyzed the hydroformylation of acrolein dimethyl acetal in the presence of PhMe to give HOCH₂CHMeCH(OMe)₂ and HO(CH₂)₃CH(OMe)₂, in 50.4% and 12.1% yield, respectively, at 100% conversion.³⁰¹

The silica-anchored cluster [Co₃Rh(CO)₁₀(Ph₂P~SIL)₂] was used for 1-hexene hydroformylation, leading to 94.2% conversion and 97.7% selectivity to aldehydes (linear to branched ratio = 2.1).³⁰²

The SiO₂-supported [Co₂Rh₂(CO)₁₂] and [Co₃Rh(CO)₁₂]-derived catalysts [Co₂Rh₂] and [Co₃Rh], respectively, showed excellent activities for the formation of oxygenates (alcohols + aldehydes) in atmospheric hydroformylation of ethylene and propylene.³⁰³ For ethylene hydroformylation, the activity of the [Co₃Rh] catalyst was reported to be about 20 times that of a [Rh₄(CO)₁₂]/SiO₂-derived monometallic catalyst.³⁰⁴ The activities and selectivities of those two catalysts deposited on ZnO were studied as a function of the composition of the clusters in the vapor-phase hydroformylation of ethylene and propene.³⁰⁵ Performances decreased in the order: [Rh₄] > [Co₂Rh₂] > [Co₃Rh] > [Co₄]. Precursors with higher cobalt contents produced more linear aldehyde. When supported on carbon, the same catalysts [Co₂Rh₂] and [Co₃Rh] were also tested in the gas-phase hydroformylation of ethylene and propene. They were found to be active catalysts.³⁰⁵ The [Co₂Rh₂] catalyst on various supports, such as alumina, silica, magnesium oxide, and NaY zeolite, was studied for hexene hydroformylation and found to give 97% yield of the C₇ alcohol.^{301c,306}

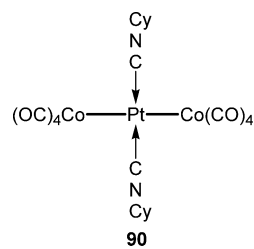
Charcoal-supported heterobimetallic NPs with sizes ranging from 1 to 3 nm were obtained from the cluster

[Co₂Rh₂(CO)₁₂]. Hydroformylation of 1-dodecene and other aliphatic and aromatic olefins was tested, and afforded linear and branched aldehydes. This system could be reused up to five times without noticeable loss of activity, and the selectivity was better (close to 100% at 100% conversion) when aromatic olefins were used as substrates. Synergistic effects seem to be at the origin of such results when compared to monometallic [Co] and [Rh] catalysts obtained from the corresponding homometallic carbonyl clusters.³⁰⁷

2.10.3.1.21. Co–Ni. Homogeneous hydroformylation of 1-pentene to hexanal and 2-methylpentanal has been catalyzed by the cluster [Co₂Ni(μ_3 -CMe)Cp(CO)₆]. After 24 h, the aldehyde yield was 87.5%. While most analogous Mo–Co, Mo–Co–Ni, and Fe–Co systems were selective for the linear aldehyde hexanal, the selectivity of this system was higher for 2-methylpentanal (linear to branched ratio of 0.6). Hydroformylation of styrene was achieved under mild conditions in 89% aldehyde yield and with moderate to high branched to normal selectivity (ratio of 7.6). The cluster could be recovered in high yield (>90%) after catalysis.^{109a}

2.10.3.1.22. Co–Pd. An anchored heteronuclear cobalt–palladium complex, obtained by the reaction of an anchored cobalt complex [SIL-(CH₂–CH₂–CH₂PCy₂)₃Co₃(CO)₇] with a benzene solution of [PdL₄] [$L = (\text{PhCH=CH})_2\text{C=O}$], was tested in the catalytic hydroformylation of propylene under mild conditions (313–373 K, 1 atm of CO). This system exhibited greater activity than the individual homometallic cobalt and palladium complexes, under similar conditions, and was even active at 313 and 333 K, when the homometallic complexes were inactive. Moreover, selectivities for the linear aldehyde were in the range 84–87% at temperatures between 353 and 373 K.³⁰⁸ A possible reason for the synergistic effect observed when using cobalt–palladium complexes could be the simultaneous formation of reactive Pd–H and Co–C bonds.³⁰⁹

2.10.3.1.23. Co–Pt. The linear complex *trans*-[Pt{Co(CO)₄}₂(CNCy)₂] (90), the triangular cluster [Co₂Pt(CO)₇(dppe)], and the butterfly cluster [Co₂Pt₂(CO)₈(PPh₃)₂] are quite active catalysts in hydroformylation of 1-pentene within the 353–373 K range but not at 333–338 K. At 373 K, the tetranuclear cluster afforded hexanal with 63.5% selectivity at 85.4% conversion. Interestingly, the dppe analogue of [Co₂Pt(CO)₇(dppe)] is not active at 353 K, even though the chelating ligand is not bonded to the active cobalt atoms.⁵¹

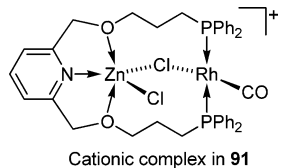


Hydroformylation of 1-hexene and 1,3-butadiene was catalyzed by the butterfly cluster [Co₂Pt₂(CO)₈(PPh₃)₂] with higher activity than the corresponding mononuclear Co–P and Pt–P complexes.³¹⁰ This was related to the electron distribution within the mixed-metal cluster.⁷⁵

2.10.3.1.24. Co–Cu. A silica-supported [CoCu] catalyst derived from the bimetallic cluster [(CO)₄CoCu(TMED)] (60), consisting of discrete Co NPs with Cu aggregates, was tested in hydroformylation of ethylene. More than 70%

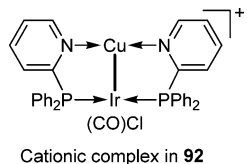
selectivity toward propanal was achieved at 453 K, for a conversion of 4.3%. Two other products were formed: 3-pentanone (23%) and propanol (<3%).^{27g}

2.10.3.1.25. Rh–Zn. Hydroformylation of functionalized terminal olefins, such as 1-hexene, 5-hexen-1-ol, propene, and 2-propen-1-ol, was achieved in the presence of the Rh–Zn complex $[\text{ZnRhCl}_2(\text{CO})(\text{NOP})][\text{BF}_4^-]$ (**91**) (NOP is the heterobinucleating ligand 2,6-bis[(3-(diphenylphosphino)-prooxy)methyl]pyridine). No induction period was observed, unlike in the case of the mononuclear complex $[\text{RhCl}(\text{CO})(\text{PPh}_3)_2]$, which required 2–3 h. Metal ion cooperativity was thus observed.



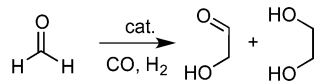
It is possible that Zn(II) functions as an internal acceptor, which abstracts the chloride ion from the Rh(I) center during formation of the active species.³¹¹

2.10.3.1.26. Ir–Cu. The complex $[\text{Cl}(\text{CO})\text{Ir}(\mu-\text{Ph}_2\text{Ppy})_2\text{Cu}][\text{BF}_4^-]$ (**92**) was used as a homogeneous catalyst for the hydroformylation of styrene at 353 K, 80 atm of CO/H_2 (1:1). Conversions ranging from 50% to 70% were achieved, and selectivities for branched aldehydes were the highest. The other main product was ethylbenzene, as a result of sole hydrogenation.³¹²



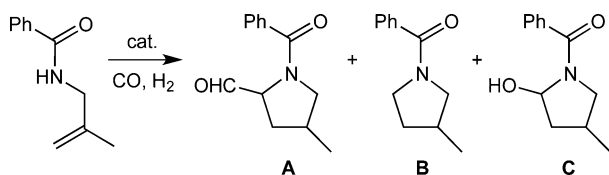
2.10.3.2. Other Hydroformylation Reactions. **2.10.3.2.1. Co–Rh.** In the homogeneous hydroformylation of formaldehyde, $[\text{Co}_2\text{Rh}_2(\text{CO})_{12}]$ afforded unexpectedly both glycolaldehyde and ethylene glycol with an overall molar selectivity of ca. 50% (Scheme 34).³¹³

Scheme 34



Using $[\text{Co}_2\text{Rh}_2(\text{CO})_{12}]$ as a homogeneous catalyst, hydroformylation of *N*-allylacetamide afforded pyrrolidine **B** with ≥98% selectivity (Scheme 35). With rhodium catalysts, 2-formylpyrrolidine **A** was the major product. (The hemiaminal **C** was shown to be the precursor of **A** and **B**.) Such a selectivity

Scheme 35



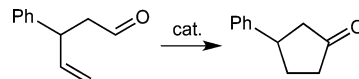
was explained by synergistic effects of the mixed-metal system.³¹⁴

2.10.4. Intramolecular Hydroacylation Reactions.

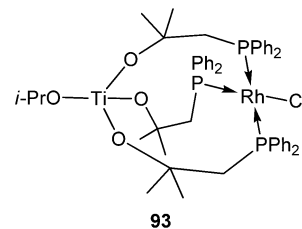
Hydroacylation is a convenient route for the formation of ketones starting from aldehydes and alkenes/alkynes. In particular, as the intramolecular reaction is generally favored, the products are usually cyclic ketones. Some heterometallic complexes were used to catalyze such reactions.

2.10.4.1. Ti–Rh. Intramolecular hydroacylation of 3-substituted pentenals, such as 3-phenyl-4-pentenal and styrene 2-carboxaldehyde, could be achieved in the presence of the O–P bridged complex $[\text{O}i\text{PrTi}(\mu-\eta^1:\eta^1-\text{OCMe}_2\text{CH}_2\text{PPh}_2)_3\text{RhCl}]$ (**93**). In the case of 3-phenyl-4-pentenal, only 3-phenylpentanone was obtained, in 98% yield (Scheme 36).³¹⁵

Scheme 36



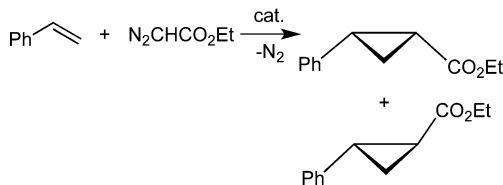
Similarly, the hydroacylation of styrene 2-carboxaldehyde led to the cyclization product only, with 40% yield. The authors suggested a cooperative effect between the metal centers where Ti(IV) would activate Rh(I) through +/+ charge repulsion.³¹⁵



2.10.5. Cyclopropanation of Styrene. 2.10.5.1. Ti–Ru.

The bridged complexes $[\text{CpCl}_2\text{Ti}(\mu-\eta^5:\eta^1-\text{C}_5\text{H}_4(\text{CH}_2)_n\text{PR}_2)-\text{RuCl}_2(p\text{-cymene})]$ ($\text{R} = \text{Ph}, n = 0, 2; \text{R} = \text{Cy}, n = 2$), similar to **18**, were active in the addition of ethyldiazoacetate to styrene (Scheme 37). They showed slightly higher activities than the

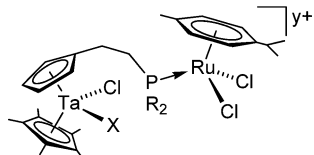
Scheme 37



corresponding half-sandwich complexes $[\text{X}_3\text{Ti}(\mu-\eta^5:\eta^1-\text{C}_5\text{H}_4(\text{CH}_2)_n\text{PR}_2)\text{RuCl}_2(p\text{-cymene})]$ ($\text{R} = \text{Ph}, n = 0, \text{X} = \text{Cl}; \text{R} = \text{Ph}, n = 2, \text{X} = \text{O}-i\text{-Pr}; \text{R} = \text{Cy}, n = 2, \text{X} = \text{O}-i\text{-Pr}$). In all cases, only the cyclopropanation products were obtained, and no metathesis product could be identified.³¹⁶

2.10.5.2. Ta–Ru. Cyclopropanation of styrene with diazoacetate $\text{N}_2\text{CHCO}_2\text{Et}$ was performed with a set of tantalocene heterometallic complexes as precatalysts. Thus, $[\text{Cp}^*\text{Cl}_2\text{Ta}(\mu-\eta^5:\eta^1-\text{C}_5\text{H}_4(\text{CH}_2)_2\text{PR}_2)\text{RuCl}_2(p\text{-cymene})]$ ($\text{R} = \text{Ph}, \text{Cy}$) (**94a**), their hydroxo analogues $[\text{Cp}^*\text{Cl}(\text{HO})\text{Ta}(\mu-\eta^5:\eta^1-\text{C}_5\text{H}_4(\text{CH}_2)_2\text{PR}_2)\text{RuCl}_2(p\text{-cymene})]\text{Cl}$ (**94b**), and the oxo versions $[\text{Cp}^*\text{Cl}(\text{O})\text{Ta}(\mu-\eta^5:\eta^1-\text{C}_5\text{H}_4(\text{CH}_2)_2\text{PR}_2)\text{RuCl}_2(p\text{-cymene})]$ (**94c**) were all active, with conversions ranging from 33% to 61% (achieved with $[\text{Cp}^*\text{Cl}(\text{HO})\text{Ta}(\mu-\eta^5:\eta^1-$

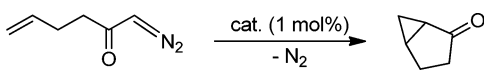
$C_5H_4(CH_2)_2PCy_2RuCl_2(p\text{-cymene})]Cl$), and *trans/cis* ratios of the cyclopropane products around 62/38. Moreover, almost no metathesis reaction was observed, as opposed to the Ru complexes $[(PR_3)RuCl_2(p\text{-cymene})]$, which suggests that the Ta center contributes to the selectivity of the cyclopropanation.³¹⁷



94a X = Cl; R = Ph, Cy; y = 0
94b X = OH; R = Ph, Cy; y = 1
94c X = O; R = Ph, Cy; y = 0

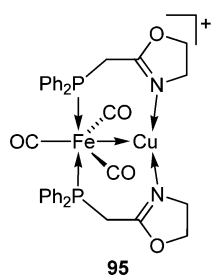
2.10.5.3. Mo–Cu. Cyclopropanation of styrene with ethyl diazoacetate (Scheme 37) in the presence of a racemic solution of $[Mo_3CuS_4(dmpe)_3Cl_4]^+$ afforded the two isomers with 80% yields. When the enantiopure cluster $[Mo_3CuS_4\{(R,R)\text{-Me-BPE}\}_3Cl_4]^+$ where $\{(R,R)\text{-Me-BPE}\} = (+)\text{-}1,2\text{-bis}[(2R,5R)\text{-}2,5\text{-}(dimethylphospholan-1-yl)]\text{ethane}$ was used instead, asymmetric induction was observed, with 88% yield of product and 20–21% ee for each isomer. Intramolecular cyclopropanation of 1-diazo-5-hexen-2-one (Scheme 38) was catalyzed by the racemic

Scheme 38



mixture in refluxing CH_2Cl_2 , affording 95% yield of bicyclo[3.1.0]hexan-2-one, whereas the enantiopure cluster gave 84% yield with 25% ee. In all cases, the clusters were recovered intact after the reaction.³¹⁸ Mechanistic studies, substituting S by Se and/or Cl by Br in the chiral cluster, suggested that the reaction proceeds through Cu–chalcogenide bond cleavage.³¹⁹

2.10.5.4. Fe–Cu. The heterobimetallic complex *trans*- $[(OC)_3Fe(\mu\text{-L}^{P,N})_2Cu][BF_4]$ ($L^{P,N} = (2\text{-oxazoline-2-ylmethyl})\text{-diphenylphosphine}$) (95) was used in styrene cyclopropanation by ethyl diazoacetate. The *trans*- and *cis*-ethyl 2-phenyl-1-cyclopropanecarboxylates were obtained, in 91% isolated yield and in a 70:30 ratio. The complex 95 could be recovered after complete conversion of ethyl diazoacetate.³²⁰

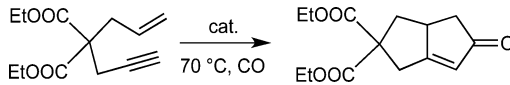


2.10.6. Pauson–Khand Reactions. The Pauson–Khand reaction (PKR), which consists of the coupling of an alkyne, an alkene, and CO, represents a convenient procedure to access cyclopentenones with high regio- and stereoselectivities.³²¹

2.10.6.1. Fe–Co. The tetrahedral cluster $[HFeCo_3(CO)_{11}(PPh_3)]$ was used as a precatalyst for the intramolecular Pauson–Khand reaction of diethyl(allylpropargyl)-malonate to afford the corresponding cyclopentenone, under 8

bar of CO at 343 K (Scheme 39). The yield was 65% at almost quantitative conversion.³²²

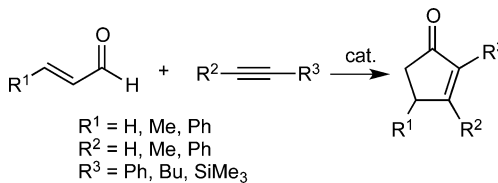
Scheme 39



2.10.6.2. Ru–Co. The clusters $C[RuCo_3(CO)_{12}]$ (cation $C^+ = H^+, Et_4N^+, bmim^+$) were used in the intramolecular Pauson–Khand reaction of diethyl(allylpropargyl)malonate to afford cyclopentenone, as described above. For conversions of 100%, the yields were superior to 90% in most cases, with 2 mol % catalyst loading.³²²

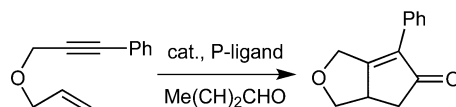
2.10.6.3. Co–Rh. Charcoal-supported $[Co_2Rh_2]$ and $[Co_3Rh]$ NPs with sizes around 2 nm were prepared from $[Co_2Rh_2(CO)_{12}]$ and $[Co_3Rh(CO)_{12}]$, respectively. They were tested in the Pauson–Khand-type reaction between α,β -unsaturated aldehydes and alkynes to yield 2-substituted pentenones,³²³ and more widely in reactions involving aldehydes as CO source for the reaction (Scheme 40).^{323,324} They were much more active than [Co] and [Rh] catalysts, suggesting some synergy between the metal centers.

Scheme 40



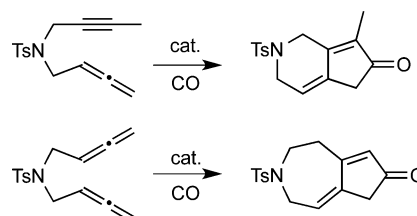
These catalytic systems were also used for the asymmetric intramolecular Pauson–Khand-type reactions with an alkyne, in the presence of crotonaldehyde as CO source, and a chiral phosphine ligand to enhance the selectivity (Scheme 41). The best results were obtained when (2*S*,4*S*)-(−)-2,4-bis(diphenylphosphino)pentane was used.³²⁴

Scheme 41

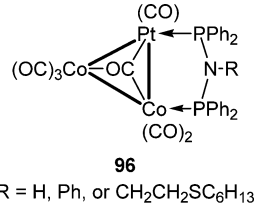


In a similar manner, the supported $[Co_2Rh_2]$ material mentioned above catalyzed the intramolecular Pauson–Khand reaction of allenynes³²⁵ and the Pauson–Khand-like carbonylative cycloaddition of bisallenenes³²⁶ with yields up to 85% and 70%, respectively (Scheme 42).

Scheme 42

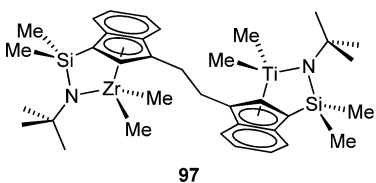


2.10.6.4. Co–Pt. The intramolecular Pauson–Khand reaction of diethyl(allylpropargyl)malonate was performed in the presence of the trinuclear clusters $[(\text{PNP})\text{PtCo}_2(\text{CO})_7]$ ($\text{PNP} = \text{dppa}$, $\text{PhN}(\text{PPh}_2)_2$, $\text{C}_6\text{H}_{13}\text{S}(\text{CH}_2)_2\text{N}(\text{PPh}_2)_2$) (96). A minimum of 5% loading was required to obtain yields in the range 85–93%.³²²



2.10.7. Transformations of Ethylene. Strong cooperative effects in olefin polymerization catalysis may be observed when secondary interactions occur between weakly basic monomer substituents and a second metal center, whether the system is homo- or heterometallic. In particular, substantial cooperative effects may result from well-designed interactions between the active sites. Even in the absence of direct metal–metal interaction in the precursor complex, heterometallic complexes have often been found to achieve high activities, cooperative effects being enhanced by a closer proximity between the metal centers.^{14a,24,327} However, some examples are shown below for bimetallic couples otherwise not or under-represented, and we hope that the lack of studies on corresponding metal–metal bonded heterometallic precursor complexes could encourage further research in the field.

2.10.7.1. Ti–Zr. The dinuclear complex $(\mu\text{-CH}_2\text{CH}_2\text{-3,3'})\{(\eta^5\text{-indenyl})[1\text{-Me}_2\text{Si}(t\text{-BuN})](\text{TiMe}_2)\}\{(\eta^5\text{-indenyl})[1\text{-Me}_2\text{Si}(t\text{-BuN})](\text{ZrMe}_2)\}$ (97) was tested in the homopolymerization of ethylene, in the presence of the cocatalyst $(\text{Ph}_3\text{C})^+[\text{B}(\text{C}_6\text{F}_5)_4]^-$. Mainly branched long-chain polyethylene products ($>\text{C}_6$) were obtained in high yields. For comparison, a mixture of monometallic Ti and Zr complexes bearing the same ligands afforded almost exclusively nonbranched products. Thus, the branching process would suggest a mechanism involving both metal centers.³²⁸

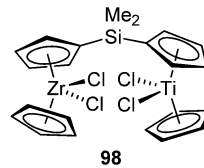


The oxo-bridged complex $[\text{Cp}^*_2\text{MeZr}(\mu\text{-O})\text{TiMe}_2\text{Cp}^*]$, when activated with MAO, efficiently catalyzed the polymerization of ethylene at room temperature in toluene. The products are linear low-density polyethylene species. The presence of the oxo bridge could be responsible for the enhanced acidity at the metal centers.³²⁹

The related compound $[\text{Cp}^*_2\text{MeZr}(\mu\text{-O})\text{Ti}(\text{NMe}_2)_3]$, after MAO activation, was also tested as a catalyst for the polymerization of ethylene and styrene. DFT calculations supported the hypothesis that the Zr center is mostly responsible for the formation of polyethylenes, while polystyrene seems to be formed mainly at the Ti center, which is sterically more accessible, although less energetically favorable.³³⁰

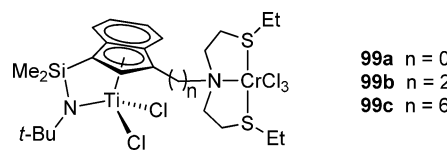
Ethylene polymerization was catalyzed by the MAO-activated complex $[\text{CpCl}_2\text{Zr}\{\mu\text{-}(\eta^5\text{-}\eta^5\text{-C}_5\text{H}_4\text{SiMe}_2\text{C}_5\text{H}_4)\}\text{TiCl}_2\text{Cp}]$ (98),

with a broad molecular weight distribution for the products, with M_w/M_n ratios up to 5.42. Also, it was less active than the corresponding homometallic Zr–Zr complex.³³¹



Similarly, in the presence of MAO, the Ti–Zr complex $[\text{CpCl}_2\text{Zr}\{\mu\text{-}(\eta^5\text{-}\eta^5\text{-C}_5\text{H}_4\text{C}(\text{CH}_2)_4\text{C}_5\text{H}_4)\}\text{TiCl}_3]$ catalyzed the polymerization of ethylene with a much lower activity than $[\text{ZrCp}_2\text{Cl}_2]$ and the homometallic Zr–Zr analogue.³³²

2.10.7.2. Ti–Cr. Strong synergism was observed in ethylene polymerization in the presence of a series of Ti–Cr bimetallic complexes with different metal–metal distances and MAO as cocatalyst. Indeed, complexes $\{(\eta^5\text{-indenyl})[1\text{-Me}_2\text{Si}(t\text{-BuN})]\text{-}(\text{TiCl}_2)\}(\text{CH}_2)_n\{\text{N}[(\text{CH}_2)_2(\text{SEt})_2](\text{CrCl}_3)\}$ (99a–c) exhibited very good selectivity for *n*-butyl-branched polymers, as opposed to mononuclear Ti or Cr analogous complexes, as well as mixtures of both, which yielded linear polymers only. In particular, increasing M_n values and increasing activities were observed in the order 99a > 99b > 99c. From a mechanistic point of view, it was suggested that oligomerization to 1-hexene occurs at the Cr center, while subsequent polymerization occurs at the Ti center. More precisely, the covalent bonding of the two metal centers, and thus their close proximity, induces a confinement that seems beneficial for the integrity and the efficiency of the transfer of the oligomers from the Cr center to the Ti center, resulting in better results with 99a than 99b and 99c.³²⁷

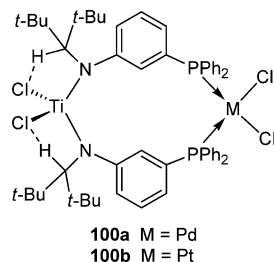


2.10.7.3. Ti–W. The dinuclear complex $[\text{Cp}^*\text{Cl}_2\text{Ti}(\mu\text{-N}_2)\text{WCl}(\text{depe})_2]$ exhibited higher activity in the polymerization of ethylene than the constrained geometry catalyst complex $[(t\text{-BuNSiMe}_2\text{C}_5\text{Me}_4)\text{TiCl}_2]$, with both modified MAO and $\text{Al}(i\text{-Bu})_3/[\text{Ph}_3\text{C}]^+[\text{B}(\text{C}_6\text{F}_5)_4]^-$ as cocatalysts.³³³

2.10.7.4. Ti–Pd. Ethylene polymerization was tested with the MAO-activated complex $[\text{TiCl}_2\{\mu\text{-}(t\text{-Bu}_2\text{CH})\text{N}(\text{C}_6\text{H}_4)\text{-PPh}_2\}_2\text{PdCl}_2]$ (100a). It was 3 times less active than the corresponding mononuclear Ti complex, and the polydispersity of the products obtained was larger, evidencing an inhibiting effect of Pd on the activity. The Ti–Ni analogue yielded no polymer at all under these conditions. Whether the poor catalytic performances are related to the absence of metal–metal interaction in the precursor complexes was not established.³³⁴

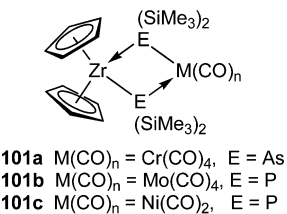
2.10.7.5. Ti–Pt. The complex $[\text{TiCl}_2\{\mu\text{-}(t\text{-Bu}_2\text{CH})\text{N}(\text{C}_6\text{H}_4)\text{-PPh}_2\}_2\text{PtCl}_2]$ (100b), when activated with MAO, was evaluated in ethylene polymerization, but it was found to be even less active than its Ti–Pd counterpart (see section 2.10.7.4).³³⁴

2.10.7.6. Zr–Hf. The metallocene derivative complex $[\text{CpCl}_2\text{Zr}\{\mu\text{-}(\eta^5\text{-}\eta^5\text{-C}_5\text{H}_4\text{C}(\text{CH}_2)_5(\eta^5\text{-C}_9\text{H}_6)\}\text{HfCl}_2\text{Cp}]$ is a poor catalyst for ethylene polymerization in the presence of MAO.³³⁵



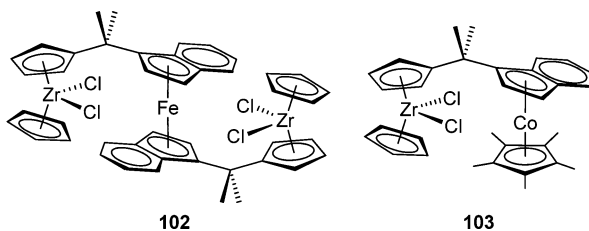
Also, $[\text{CpCl}_2\text{Zr}\{\mu-(\eta^5:\eta^5-\text{C}_5\text{H}_4\text{C}(\text{CH}_2)_4\text{C}_5\text{H}_4)\}\text{HfCl}_2\text{Cp}]$ is less active than its Zr–Zr analogue and than $[\text{ZrCp}_2\text{Cl}_2]$ in ethylene polymerization in the presence of MAO.³³²

2.10.7.7. Zr–Cr. The arsenido-bridged heterobimetallic complex $[\text{Cp}_2\text{Zr}\{\mu\text{-As}(\text{SiMe}_3)_2\}_2\text{Cr}(\text{CO})_4]$ (**101a**) is a good precatalyst for the polymerization of ethylene, after activation with MAO, under mild conditions. However, the phosphanido-bridged Zr–Mo analogue $[\text{Cp}_2\text{Zr}\{\mu\text{-P}(\text{SiMe}_3)_2\}_2\text{Mo}(\text{CO})_4]$ is more active. The authors assumed a mechanism involving the formation of Zr cations and P-bridged Cr-MAO anionic species, the latter being mostly responsible for the activity.³³⁶



2.10.7.8. Zr–Mo. Similarly, ethylene polymerization was achieved in the presence of the complex $[\text{Cp}_2\text{Zr}\{\mu\text{-P}(\text{SiMe}_3)_2\}_2\text{Mo}(\text{CO})_4]$ (**101b**) as precatalyst and MAO as cocatalyst. It exhibited a better activity as compared to its arsenido-bridged Zr–Cr and phosphanido-bridged Zr–Ni counterparts.³³⁶

2.10.7.9. Zr–Fe. In the presence of MAO, the metallocene derivative $[\text{Fe}\{\mu-(\eta^5\text{-C}_9\text{H}_6)\text{CMe}_2(\eta^5\text{-C}_5\text{H}_4)\text{Zr}(\eta^5\text{-C}_5\text{H}_5)\text{Cl}_2\}_2]$ (**102**) exhibited activity in ethylene polymerization similar to that of the model catalyst $[\text{ZrCp}_2\text{Cl}_2]$.³³⁵



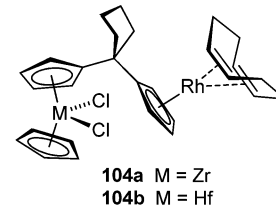
2.10.7.10. Zr–Co. In the presence of MAO, the complex $[\text{Cp}^*\text{Co}\{\mu-(\eta^5\text{-C}_9\text{H}_6)\text{CMe}_2(\eta^5\text{-C}_5\text{H}_4)\text{Zr}(\eta^5\text{-C}_5\text{H}_5)\text{Cl}_2\}]$ (**103**) showed activities in ethylene polymerization similar to that of the Zr–Fe complex $[\text{Fe}\{\mu-(\eta^5\text{-C}_9\text{H}_6)\text{CMe}_2(\eta^5\text{-C}_5\text{H}_4)\text{Zr}(\eta^5\text{-C}_5\text{H}_5)\text{Cl}_2\}_2]$.³³⁵

Ethylene polymerization was successfully initiated with the dinuclear complex $[\text{Cl}_2\text{Zr}(\eta^5\text{-C}_5\text{Me}_4)\text{SiMe}_2(\eta^5\text{-C}_5\text{H}_3)\text{CH}_2(\text{CH}_2)\text{CO}_2\text{CH}_2(\text{C}_5\text{H}_3\text{N})\text{CHN}(\text{dipp})\text{CoCl}_2]$ (**105a**) (see section 2.10.7.12) in the presence of modified MAO. Ethyl-branched polymers were thus obtained, suggesting dimerization of ethylene at the cobalt center and copolymerization of 1-butene and ethylene at the zirconium center.³³⁷

2.10.7.11. Zr–Rh. The complexes $[\text{LRh}(\eta^2\text{-CH}_2=\text{CH})_2\text{Si}(\eta^5\text{-C}_5\text{H}_2\text{-}2,4\text{-Me}_2)_2\text{ZrCl}_2]$ ($\text{L} = \eta^5\text{-C}_9\text{H}_7$, $\eta^5\text{-C}_5\text{H}_5$, $\eta^5\text{-C}_5\text{Me}_5$)³³⁸ and $[(\eta^5\text{-C}_9\text{H}_7)\text{Rh}(\eta^2\text{-CH}_2=\text{CH})_2\text{Si}(\eta^5\text{-C}_5\text{H}_2\text{-}2,4\text{-Me}_2)_2\text{ZrCl}_2]$ ³³⁹ were tested in the polymerization of ethylene with MAO as cocatalyst. These complexes yielded isotactic polymers (>95% selectivity) with higher molecular weight than zirconocene complexes.³³⁸

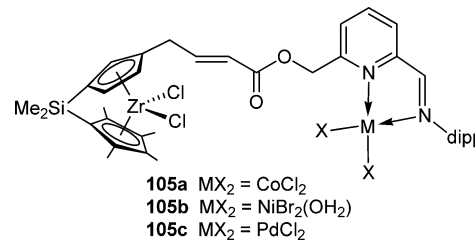
$[\text{C}_5\text{Me}_4)_2\text{ZrCl}_2]$ ³³⁹ were tested in the polymerization of ethylene with MAO as cocatalyst. These complexes yielded isotactic polymers (>95% selectivity) with higher molecular weight than zirconocene complexes.³³⁸

Ethylene polymerization was performed in the presence of the MAO-activated complex $[\text{CpCl}_2\text{Zr}\{\mu-(\eta^5:\eta^5\text{-C}_5\text{H}_4\text{C}(\text{CH}_2)_4\text{C}_5\text{H}_4)\}\text{Rh}(\text{COD})]$ (**104a**). The Zr–Zr analogue was more active and yielded polymers with a narrower molecular weight distribution, probably due to the difference between the two metal centers.³³²



2.10.7.12. Zr–Ni. When activated with MAO, the phosphanido-bridged compound $[\text{Cp}_2\text{Zr}\{\mu\text{-P}(\text{SiMe}_3)_2\}_2\text{Ni}(\text{CO})_2]$ (**101c**) catalyzed the polymerization of ethylene at temperatures between 298 and 338 K. It proved to be more active than the Zr–Cr analogous complex, but less than the Zr–Mo one.^{336,340}

The complex $[\text{Cl}_2\text{Zr}(\eta^5\text{-C}_5\text{Me}_4)\text{SiMe}_2(\eta^5\text{-C}_5\text{H}_3)\text{-CH}_2(\text{CH}_2)\text{CO}_2\text{CH}_2(\text{C}_5\text{H}_3\text{N})\text{CHN}(\text{dipp})\text{NiBr}_2(\text{H}_2\text{O})]$ (**105b**) afforded a mixture of methyl- and ethyl-branched polymers in the catalytic polymerization of ethylene, with MAO as a cocatalyst.³³⁷



2.10.7.13. Zr–Pd. The complex $[\text{Cl}_2\text{Zr}(\eta^5\text{-C}_5\text{Me}_4)\text{SiMe}_2(\eta^5\text{-C}_5\text{H}_3)\text{-CH}_2(\text{CH}_2)\text{CO}_2\text{CH}_2(\text{C}_5\text{H}_3\text{N})\text{CHN}(\text{dipp})\text{PdCl}_2]$ (**105c**) catalyzed the polymerization of ethylene to yield linear polyethylene, in contrast to its Co and Ni counterparts.³³⁷

2.10.7.14. Hf–Rh. In the presence of MAO as cocatalyst, the complex $[\text{CpCl}_2\text{Hf}\{\mu-(\eta^5:\eta^5\text{-C}_5\text{H}_4\text{C}(\text{CH}_2)_4\text{C}_5\text{H}_4)\}\text{Rh}(\text{COD})]$ (**104b**) was found to be less active than its Zr–Rh counterpart **104a** in ethylene polymerization.³³²

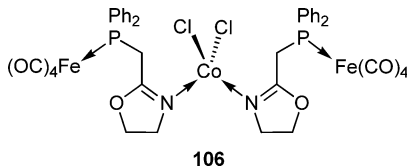
2.10.7.15. V–Cr. Ethylene polymerization was achieved with a [VCr] catalyst prepared from $[\text{VCrCp}_3(\text{CO})_3]$ on SiO_2 . Polymers with a broad weight distribution were obtained.³⁴¹

2.10.7.16. Cr–Mo. The complex $[\text{CrMo}(\text{OAc})_4\cdot 2\text{H}_2\text{O}]$ supported on silica catalyzed the polymerization of ethylene at 358 K. Comparisons were made with the corresponding homometallic precatalysts $[\text{Cr}_2(\text{OAc})_4\cdot 2\text{H}_2\text{O}]$ and $[\text{Mo}_2(\text{OAc})_4\cdot 2\text{H}_2\text{O}]$. Lewis acid cocatalysts (aluminum or tin alkyls) favor the formation of isomers and oligomers. The corresponding $[\text{CrMo}]$ and $[\text{Cr}_2] + [\text{Mo}_2]$ heterogeneous catalysts revealed a cooperative effect of the two centers.³⁴²

2.10.7.17. Fe–Ru. Ethylene self-homologation was catalyzed by silica-supported $[\text{Fe}_{3-x}\text{Ru}_x]$ ($x = 0\text{--}3$) catalysts, among which $[\text{Fe}_2\text{Ru}]$, prepared from $[\text{Fe}_2\text{Ru}(\text{CO})_{12}]$, showed the maximum activity. Increased selectivity toward propene/butene ($\text{C}_3:\text{C}_4$ ratio) was observed when increasing the Fe content in

the MMCD catalysts, in contrast to the conventional catalysts.⁸⁹

2.10.7.18. Fe–Co. A phosphinooxazoline ligand was used to prepare the bimetallic, trinuclear complex *trans*-[{(OC)₄Fe(μ-PPh₂CH₂-oxazoline)}₂CoCl₂] (**106**). This compound is active in ethylene oligomerization and gave linear α-olefins in the range C₄–C₂₆, with a maximum of the Schulz–Flory distribution around C₆.³⁴³



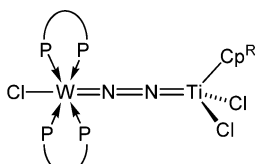
2.10.8. Transformations of Other Linear Olefins.

2.10.8.1. Ti–Zr. The oxo-bridged complex [Cp*₂MeZr(μ-O)Ti(NMe₂)₃] was tested as a catalyst for the polymerization of styrene, after activation with MAO. Mechanistic studies revealed the important role of the Ti center in forming polystyrenes, as supported by DFT calculations.³³⁰

Ethylene-propylene copolymerization was achieved in the presence of the MAO-activated complex [CpCl₂Zr{μ-(η⁵:η⁵-C₅H₄SiMe₂C₅H₄)}TiCl₂Cp]. The product showed a broad molecular weight distribution.³³¹

The Ti–Zr complex [CpCl₂Zr{μ-(η⁵:η⁵-C₅H₄C(CH₂)₄C₅H₄)}TiCl₃] was tested in the polymerization of propylene with MAO as cocatalyst. Its activity was much lower than that of [ZrCp₂Cl₂] and of the homometallic Zr–Zr analogue. The polymers obtained had higher molecular weight and broader mass distributions, due to the presence of two different metal centers.³³²

2.10.8.2. Ti–W. Copolymerization of ethylene and 1-hexene was efficiently catalyzed by the bimetallic complexes [Cp^RCl₂Ti(μ-N₂)WCl(dppe)₂] (Cp^R = Cp, Cp') (**107a**), [Cp^RCl₂Ti(μ-N₂)WCl(depe)₂] (Cp^R = Cp, Cp', Cp*, Ind) (**107b**), or [CpCl₂Ti(μ-N₂)WCl(PMe₂Ph)₄] (**107c**). The former exhibited very high activity, while the latter was much less active, probably due to the lability of the PMe₂Ph ligand.³³³



107a P–P = dppe, Cp^R = Cp, Cp'

107b P–P = depe, Cp^R = Cp, Cp', Cp*, Ind

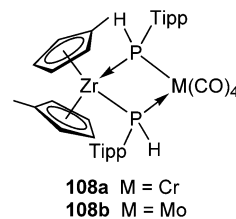
107c P–P = 2 PMe₂Ph, Cp^R = Cp

2.10.8.3. Zr–Hf. The complex [CpCl₂Zr{μ-(η⁵:η⁵-C₅H₄C(CH₂)₄C₅H₄)}HfCl₂Cp] is not as active as its Zr–Zr analogue or as [ZrCp₂Cl₂] for propene polymerization in the presence of MAO.³³²

2.10.8.4. Zr–Cr. The polymerization of propylene was performed with the complexes [Cp₂Zr{μ-As(SiMe₃)₂}₂Cr(CO)₄] (**101a**) and [Cp'₂Zr(μ-PHTipp)₂Cr(CO)₄] (Tipp = 2,4,6-*i*-Pr₃C₆H₂) (**108a**) as catalysts and with MAO as a cocatalyst. The best activities were observed between 298 and 338 K, but the phosphanido-bridged Zr–Mo analogues were more active.³⁴⁰

2.10.8.5. Zr–Mo. The phosphanido-bridged complexes [Cp₂Zr{μ-P(SiMe₃)₂}₂Mo(CO)₄] (**101b**) and [Cp'₂Zr(μ-PHTipp)₂Mo(CO)₄] (Tipp = 2,4,6-*i*-Pr₃C₆H₂) (**108b**) cata-

lyzed the polymerization of propylene in the presence of MAO. They showed better activities than their arsenido-bridged Zr–Cr and phosphanido-bridged Zr–Ni counterparts.³⁴⁰



2.10.8.6. Zr–Fe. Dinuclear and trinuclear ferrocenyl derivatives of the type [CpFe(μ-C₅H₄SiMe₂C₅H₄R¹R²)-ZrCpCl₂] (R¹ = R² = H; R¹ = Me, R² = H; R¹ = R² = Me; R¹ = Ph, R² = H) are very active olefin polymerization catalysts. In particular, [{CpFe(μ-C₅H₄SiMe₂C₅H₄)}ZrCpCl₂] allows copolymerization of ethylene and propylene and terpolymerization of ethylene, propylene, and diene.³⁴⁴

The metallocene derivative [Fe{μ-(η⁵-C₉H₆)CMe₂(η⁵-C₅H₄)Zr(η⁵-C₅H₅)Cl₂}]**102** has been tested as a cocatalyst for propylene polymerization in the presence of MAO. It exhibited activities close to that of the model system [ZrCp₂Cl₂]-MAO.³³⁵

2.10.8.7. Zr–Co. The activity in propylene polymerization of the complex [Cp*Co{μ-(η⁵-C₉H₆)CMe₂(η⁵-C₅H₄)Zr(η⁵-C₅H₅)Cl₂}]**103**, when activated with MAO, is close to that of [Fe{μ-(η⁵-C₉H₆)CMe₂(η⁵-C₅H₄)Zr(η⁵-C₅H₅)Cl₂}]**102**.³³⁵

2.10.8.8. Zr–Rh. The polymerization of α-olefins was carried out in the presence of the complexes [Cp^RRh(η²-CH=CH)₂Si(η⁵-C₅H₂-2,4-Me₂)₂ZrCl₂] (Cp^R = Cp, Cp*, Ind)³³⁸ and [(η⁵-C₉H₇)Rh(η²-CH=CH)₂Si(η⁵-C₅Me₄)₂ZrCl₂]³³⁹ with MAO as cocatalyst. These complexes yielded isotactic polymers (>95% selectivity) with higher molecular weight than when zirconocene complexes were used in polymerization of 1-hexene or propylene. A mixture of mononuclear Zr and Rh complexes showed lower activities and selectivities, suggesting synergistic effects in the case of the bimetallic precursors, even though the metal centers are separated by more than 6 Å.³³⁸

The MAO-activated complex [CpCl₂Zr{μ-(η⁵:η⁵-C₅H₄C(CH₂)₄C₅H₄)}Rh(COD)]**104a** catalyzed the polymerization of propylene with lower activity than Ti–Zr, Zr–Zr, and Zr–Hf analogous complexes. However, it was more efficient than the Hf–Hf and Hf–Rh precursors.³³²

2.10.8.9. Zr–Ni. The phosphanido-bridged complex [Cp₂Zr{μ-P(SiMe₃)₂}₂Ni(CO)₂]**101c**, when activated with MAO, catalyzes the polymerization of propylene under mild temperature conditions.³⁴⁰

2.10.8.10. Hf–Rh. Propylene polymerization was performed in the presence of [CpCl₂Hf{μ-(η⁵:η⁵-C₅H₄C(CH₂)₄C₅H₄)}-Rh(COD)]**104b** and of MAO as cocatalyst, but this complex was less active than its Zr–Rh counterpart.³³²

2.10.8.11. Cr–Mo. The silica-supported complex [CrMo(OAc)₄·2H₂O] catalyzed the polymerization of 1-octene at 296 K. Oligomers and isomers were obtained in higher yields in the presence of Lewis acid cocatalysts, such as aluminum or tin alkyls. The cluster-derived catalysts [CrMo] and [Cr₂] + [Mo₂] exhibited a cooperative effect of the two centers.³⁴²

2.10.8.12. Mo–Pd, W–Pd. Butadiene oligomerization was performed in the presence of the clusters [M₂Pd₂Cp₂(CO)₆(PEt₃)₂] (M = Mo, **11a**, or W, **12a**) and [M₂Pd₂Cp₂(CO)₆(PPh₃)₂] (M = Mo, **11b**, or W, **12b**) to give

low molecular weight polymers, as well as a mixture of 4-vinylcyclohexene, 1,5-cyclooctadiene, and cyclododecatriene.⁵¹

2.10.8.13. Co–Pt. The catalytic cyclo-oligomerization of 1,3-butadiene by the butterfly cluster $[\text{Co}_2\text{Pt}_2(\text{CO})_8(\text{PPh}_3)_2]$ was studied.⁷⁵

2.10.9. Transformations of Norbornadiene.

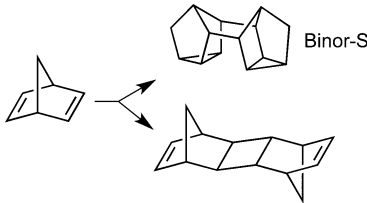
2.10.9.1. Mo–Pt, W–Pt. Preliminary studies with the trinuclear chain complexes *trans*- $[\text{Pt}\{\text{MoCp}(\text{CO})_3\}_2(\text{CNCy})_2]$ and *trans*- $[\text{Pt}\{\text{WCp}(\text{CO})_3\}_2(\text{CNR})_2]$ ($\text{R} = \text{Cy}, t\text{-Bu}$) as homogeneous catalysts revealed that no dimerization occurred during polymerization of norbornadiene, even after full conversion.³⁴⁵

2.10.9.2. Fe–Co. The tetrahedral cluster $[\text{Me}_4\text{N}]^+[\text{FeCo}_3(\text{CO})_{12}]$ was more active for the stereospecific dimerization of norbornadiene to “Binor-S” (Scheme 39) than $[\text{HFeCo}_3(\text{CO})_{12}]$ or $[\text{Co}_4(\text{CO})_{12}]$.³⁴⁶

The cluster $[\text{Et}_4\text{N}]^+[\text{FeCo}_3(\text{CO})_{12}]$ was entrapped in a silica sol–gel matrix. It remained intact upon adsorption onto silica, and was tested in the dimerization of norbonadiene to “Binor-S”. Quantitative yields were obtained for the first two runs, but the activity slightly decreased for the third and fourth runs due to partial pore clogging.⁶¹

2.10.9.3. Fe–Pt, Co–Pt. The chain complexes *trans*- $[\text{Pt}\{\text{Fe}(\text{CO})_3\text{NO}\}_2(\text{CNR})_2]$ ($\text{R} = \text{Cy}, t\text{-Bu}$), *trans*- $[\text{Pt}\{\text{Co}(\text{CO})_4\}_2(\text{CNR})_2]$ ($\text{R} = \text{Cy}, t\text{-Bu}$), the butterfly clusters $[\text{Co}_2\text{Pt}_2(\text{CO})_8\text{L}_2]$ ($\text{L} = \text{PET}_3, \text{PPh}_3, \text{AsPh}_3$), and the trigonal bipyramidal cluster $[\text{Co}_2\text{Pt}_3(\text{CO})_9\text{L}_3]$ ($\text{L} = \text{PET}_3, \text{PPh}_3$) exhibited high catalytic activity (100% conversion) with stereospecific dimerization of NBD to the “head-to-head” dimer “Binor-S” when a Lewis acid was present. However, in its absence, the “exo-trans-exo” isomer was obtained selectively (Scheme 43). Related Mo–Pt–Mo and W–Pt–W complexes resulted in polymerization of norbornadiene.³⁴⁵

Scheme 43



2.10.9.4. Co–Zn. Dimerization of norbornadiene yielded quantitatively “Binor-S” in the presence of the bimetallic transition metal catalyst $[\text{Zn}\{\text{Co}(\text{CO})_4\}_2]$, with or without a Lewis acid cocatalyst. A possible transition state was suggested in which two substrate molecules could come sufficiently close for bond formation, giving rise to “Binor-S”.³⁴⁷

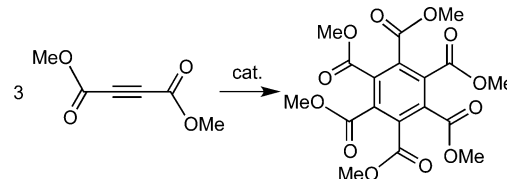
In a similar fashion, stereospecific dimerization of norbornadiene was catalyzed by the complex $[\text{Co}_2\{\mu\text{-ZnCo}(\text{CO})_4\}_2(\text{CO})_7]$. The induction period was much shorter than that with $[\text{Zn}\{\text{Co}(\text{CO})_4\}_2]$. Yields in the range 70–80% were obtained after 2 h reaction time.³⁴⁸

2.10.9.5. Co–Cd, Co–Hg. The trinuclear complex $[\text{Cd}\{\text{Co}(\text{CO})_4\}_2]$ catalyzed the dimerization of norbornadiene to a mixture of dimers, including “Binor-S”, and thus behaves differently from its mercury analogue $[\text{Hg}\{\text{Co}(\text{CO})_4\}_2]$. Indeed, with the latter complex, a mixture of four dimers was obtained, but no “Binor-S” was formed. In the presence of Lewis acids, however, $[\text{Hg}\{\text{Co}(\text{CO})_4\}_2]$ afforded “Binor-S” exclusively.³⁴⁹

2.10.10. Trimerization of Alkynes. 2.10.10.1. Cr–Rh.

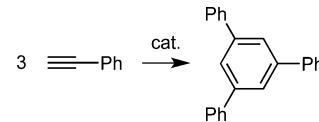
The complex $[(\text{OC})_3\text{Cr}(\mu\text{-}\eta^6\text{-}\eta^5\text{-Ind}^*)\text{Rh}(\text{CO})_2]$ ($\text{Ind}^* = \text{heptamethylindenyl}$) efficiently catalyzed the cyclotrimerization of DMAD (dimethyl acetylenedicarboxylate) to yield hexacarbomethoxybenzene (Scheme 44). The authors point to the formation of the complex $[(\text{OC})_3\text{Cr}(\mu\text{-}\eta^6\text{-}\eta^5\text{-Ind}^*)\text{Rh}(\text{DMAD})_2]$ as the slow step of the reaction, during the induction time.³⁵⁰

Scheme 44

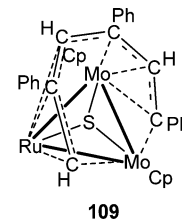


2.10.10.2. Mo–Ru. A head-to-tail coupling around the mixed-metal cluster $[\text{Mo}_2\text{Ru}(\mu_3\text{-S})\text{Cp}_2(\text{CO})_7]$, thus affording the cluster 109, allowed for the trimerization of phenylacetylene at 371 K (Scheme 45). It is believed that the

Scheme 45



dimolybdenum unit serves as the alkyne oligomerization site, but the chemistry overall is dependent on the entire cluster functioning as a unit. It was possible to induce the elimination of 1,3,5-triphenylbenzene from 109 by treatment with CO.³⁵¹



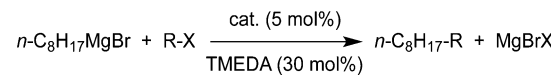
CO ligands omitted for clarity

2.10.11. Coupling Reactions. 2.10.11.1. Ti–Pd.

Suzuki–Miyaura coupling between phenylboronic acid and 3,5-dimethoxybromobenzene in dioxane at 353 K in the presence of Cs_2CO_3 yielded 90% of the expected biaryl compound, along with 10% of biphenyl, in the presence of the complex $[\text{TiCl}_2\{\mu\text{-}(t\text{-Bu}_2\text{CH})\text{N}(\text{C}_6\text{H}_4)\text{PPh}_2\}_2\text{PdCl}_2]$ (100a). Under the same conditions, the coupling of 4-nitrobromobenzene with phenyl boronic acid gave similar results: 85% of the desired biaryl product and 10% of biphenyl.³³⁴

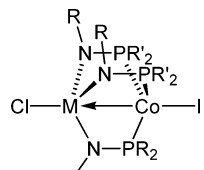
2.10.11.2. Zr–Co. The Kumada coupling of unactivated alkyl halides with alkyl Grignard reagents such as *n*-octylmagnesium bromide (Scheme 46) was achieved in the presence of the complexes $[\text{ClZr}(i\text{-PrNPPh}_2)_3\text{CoI}]$ (110a), $[\text{ClZr}(\text{MesNP-}i\text{-Pr})_3\text{CoI}]$ (110b), and $[\text{ClZr}(\text{MesNP-}i\text{-Pr})_2\text{CoI}]$ (110c).

Scheme 46



$\text{Pr}_2)_3\text{CoI}$] (**110b**), and $[\text{ClZr}(i\text{-PrNP-}i\text{-Pr}_2)_3\text{CoI}]$ (**110c**) as catalysts. Typically, the coupling of 4-bromobutane with $n\text{-C}_8\text{H}_{17}\text{MgBr}$ in the presence of these complexes gave yields of 62.9%, 81.9%, and 83.3% for **110a**, **110b**, and **110c**, respectively. Overall, **110a** was found to be slightly less active than the other two catalysts.

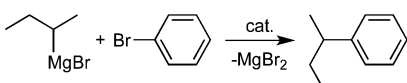
Adding 30 mol % of TMEDA greatly improved the yields. The fact that homometallic Co complexes were inert toward such substrates indicated that the presence of Zr is necessary for catalytic activity.³⁵²



110a M = Zr, R = *i*-Pr, R' = Ph
110b M = Zr, R = Mes, R' = *i*-Pr
110c M = Zr, R = R' = *i*-Pr
111 M = Hf, R = Mes, R' = *i*-Pr

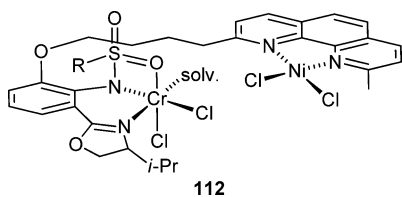
2.10.11.3. Zr–Pd. The cross-coupling reaction between *sec*-butylmagnesium bromide and bromobenzene yielded almost exclusively *sec*-butylbenzene in the presence of $[\text{Cl}_2\text{Zr}\{\mu\text{-}\eta^5\text{:}\eta^1\text{-}(\text{C}_5\text{H}_4\text{PPh}_2)_2\}\text{PdCl}_2]$ as catalyst (Scheme 47). This complex is a much better catalyst than the known (P–P)-chelated Pd complexes.²⁸⁰

Scheme 47



2.10.11.4. Hf–Co. The Hf–Co analogue of the aforementioned Zr–Co complex, $[\text{ClHf}(\text{MesNP-}i\text{-Pr}_2)_3\text{CoI}]$ (**111**), was tested in the same Kumada coupling reaction, but exhibited much lower activity than its Zr–Co counterpart.³⁵³

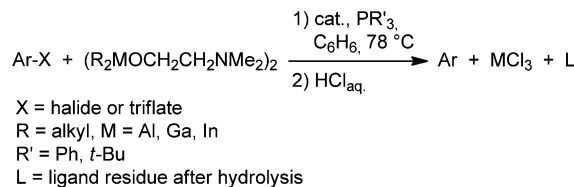
2.10.11.5. Cr–Ni. Coupling reactions between 3-phenylpropanal and 2-iodohex-1-ene were performed in the presence of the complexes $[\text{Cl}_2\text{Cr}(i\text{-Pr-oxazo-Ph}(\text{NSO}_2\text{R})\text{O}(\text{CH}_2)_4\text{-phenMe})\text{NiCl}_2]$ (R = Me, 3,5-chlorophenyl) (**112**), Mn, $[\text{ZrCl}_2\text{Cp}_2]$, LiCl, in MeCN at room temperature. Full conversion was reached after several hours and afforded more than 95% cross-coupling product (the byproducts resulted from the homocoupling of iodohexene) with good enantiomeric ratios (>10:1 in most cases). This system outperformed a mixture of the corresponding monometallic Cr and Ni fragments in terms of selectivity. Various other aldehydes were tested, with similar results.³⁵⁴



112

2.10.11.6. Mo–Pd, W–Pd. The clusters $[\text{Mo}_2\text{Pd}_2\text{Cp}_2(\text{CO})_6(\text{PPh}_3)_2]$ (**11b**) and $[\text{W}_2\text{Pd}_2\text{Cp}_2(\text{CO})_6(\text{PPh}_3)_2]$ (**12b**) were found to be active in the cross-coupling of aryl halides and triflates with Al-, Ga-, or In-alkylating agents, in the presence of a phosphine (Scheme 48). No hydrogenolysis or homocoupling

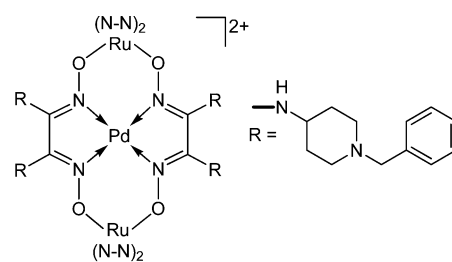
Scheme 48



of the aryl halides was observed. As the monometallic precursors are inactive in these reactions, it appears that synergistic effects take place between the different metal nuclei of the catalysts. These catalysts are more stable and more selective than the Ni and Pd catalysts commonly used, because with several substrates, almost quantitative yields could be obtained.³⁵⁵

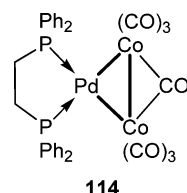
2.10.11.7. Fe–Pd. The linear tetranuclear complex $[(\text{OC})_4\text{Fe}(\mu\text{-PPh}_2)\text{Pd}(\mu\text{-Cl})]_2$ (**15**) was found to be a highly active homogeneous catalyst for the cross-coupling of aryl halides or naphthyl halides and triflates with group 13-metal alkylating agents in the presence of a tertiary phosphine. Almost no homocoupling or hydrodehalogenation took place during the reactions. The monometallic precursors were catalytically inactive, which suggested the occurrence of strong synergistic effects between the different metal centers.³⁵⁶

2.10.11.8. Ru–Pd. Suzuki coupling of phenylboronic acid with arylhalides was catalyzed by Ru(II)–Pd(II) trinuclear complexes $[\text{PdL}_2\text{Ru}_2(\text{bpy})_4](\text{ClO}_4)_2$ (**113a**) and $[\text{PdL}_2\text{Ru}_2(\text{phen})_4](\text{ClO}_4)_2$ (**113b**) (L = *N,N'*-(4-amino-1-benzyl piperidine)-glyoxime, see scheme). The Ru(bpy)₂ cluster was the most active. Indeed, for the coupling between 1-(4-bromophenyl)ethanone and phenylboronic acid, yields up to 97% and 94% for **113a** and **113b**, respectively, were observed after 2 h. Using the corresponding aryl chloride caused a dramatic drop in the activities, with yields of 42% and 30%, respectively, after 2 h.³⁵⁷



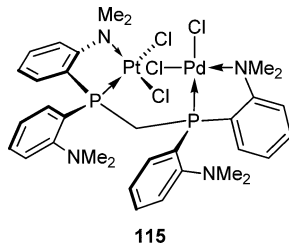
Dicationic complex in
113a (N-N) = bpy
113b (N-N) = phen

2.10.11.9. Co–Pd. The cross-coupling of aryl halides or naphthyl halides with triflates in the presence of Al-, Ga-, In-alkylating agents and a phosphine was catalyzed by the cluster $[\text{Co}_2\text{Pd}(\text{CO})_7(\text{dppe})]$ (**114**) with a good activity, exhibiting yields close to 100% for several substrates. However, it was generally less active than the Fe–Pd complex **15** described above.³⁵⁶



114

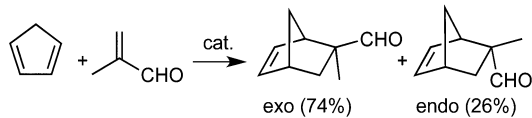
2.10.11.10. Pd–Pt. The heterobimetallic complex $[\text{PdPtCl}_4(\text{dmampm})]$ ($\text{dmampm} = 1,1\text{-bis}[\text{di}(o\text{-N,N-dimethylanilinyl})\text{phosphino}]\text{methane}$) (**115**) was compared to the monometallic analogue $[\text{Pd}_2\text{Cl}_4(\text{dmampm})]$ in the aerobic Heck coupling of iodobenzene with styrene in $\text{DMF}/\text{H}_2\text{O}$ at 373 K, with K_2CO_3 as a base. The former was more active than the latter, suggesting some degree of intermetallic cooperativity. During the catalytic reactions, slow oxidation at the phosphorus centers occurred, which led to a decrease in the activity of the compounds.³⁵⁸



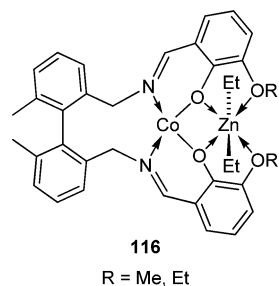
2.10.12. Other Carbon–Carbon Bond Formation Reactions.

2.10.12.1. Fe–Cu. The heterobimetallic complex $\text{trans}-[(\text{OC})_3\text{Fe}(\mu\text{-L}^{\text{P},\text{N}})_2\text{Cu}][\text{BF}_4^-]$ ($\text{L}^{\text{P},\text{N}} = (2\text{-oxazoline-2-ylmethyl)diphenylphosphine}$) (**95**) was tested in the Diels–Alder reaction between cyclopentadiene and methacrolein, and yielded the two diastereoisomers exo and endo, with a total yield of 76% (Scheme 49).³²⁰

Scheme 49

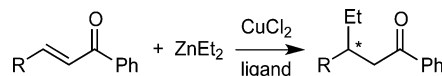


2.10.12.2. Co–Zn. The asymmetric reductive alkylation of benzaldehyde was performed in the presence of ZnEt_2 and Co(II) complexes bearing various salen ligands. In the case of the ligands $(\text{ROC}_6\text{H}_3(\text{OH})\text{CHNCH}_2\text{C}_6\text{H}_3\text{Me})_2$ ($\text{R} = \text{Me, Et}$), the authors identified and proposed a structure for what they believe to be the active species, the axially chiral bimetallic complex $[\text{CoZnEt}_2(\text{ROC}_6\text{H}_3\text{OCH}=\text{NCH}_2\text{C}_6\text{H}_3\text{Me})_2]$ (**116**) formed in situ. These catalytic systems afforded (*S*)-1-phenylpropan-2-ol with 78% and 90% ee when $\text{R} = \text{Me}$ and Et , respectively.³⁵⁹

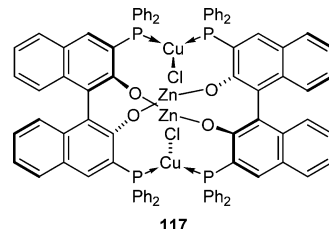


2.10.12.3. Cu–Zn. The asymmetric addition of ZnEt_2 to enones (such as $\text{RCH}=\text{CH}_2\text{C}(\text{O})\text{Ph}$) was investigated in the presence of CuCl_2 and various binol-derived ligands (Scheme 50). It was found that the active species were heterometallic complexes formed in situ. Thus, the polynuclear complex $[\text{ClCuZn}\{\text{Ph}_2\text{PC}_{10}\text{H}_5(\text{O})\}_2]_2$ (**117**) exhibited very good

Scheme 50



activity (>95%) and excellent selectivity (up to 91% ee for the (*S*) isomer).³⁶⁰



2.11. Carbon–Nitrogen Bond Formation

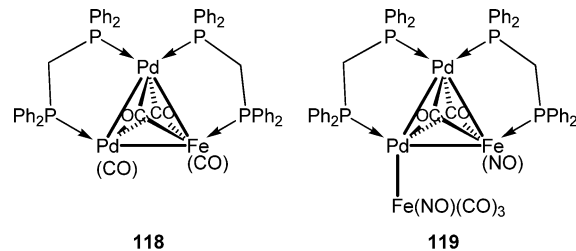
Carbonylation of organic nitro compounds specifically leads to the important class of organic isocyanates, or carbamates if alcohol is added. Carbon–nitrogen bond formation can also be achieved in the presence of heterometallic catalysts to afford several kinds of substituted amines.

2.11.1. Carbonylation of Organic Nitro Derivatives.

2.11.1.1. Mo–Pd. Carbonylation of organic nitro derivatives into isocyanates was performed in the presence of the $[\text{Mo}_2\text{Pd}_2]$ catalyst, derived from $[\text{Mo}_2\text{Pd}_2\text{Cp}_2(\text{CO})_6(\text{PPh}_3)_2]$ (**11b**).³⁶¹ It gave rise to higher selectivity in phenylisocyanate (71–80%) than conventional catalysts prepared by mixing the individual components (62–67%). Both systems allowed for complete conversion of the substrate. Incidentally, this reaction provided the first example of the use of mixed-metal clusters for the preparation of heterogeneous catalysts. More recently, it was found that when solutions of such bimetallic clusters of composition $[\text{Mo}_2\text{Pd}_2\text{Cp}_2(\text{CO})_6(\text{PR}_3)_2]$ ($\text{R} = \text{Et or Ph}$) were impregnated into amorphous xerogels or ordered SBA-15, their subsequent thermal decomposition under a reducing atmosphere afforded nanoparticles of a new bimetallic phosphide of composition $\text{Pd}_x\text{Mo}_y\text{P}$, isostructural with Mo_3P .^{18d} This emphasizes the care with which the assignment of catalytically active species/phases should be made because thermal treatments may be associated with unexpected transformations.

2.11.1.2. Fe–Rh. The cluster $[\text{PPN}]_2[\text{FeRh}_4(\text{CO})_{15}]$ catalyzed the carbonylation of nitrobenzene to methyl phenylcarbamate in the presence of methanol and bipyridine. At a $\text{PhNO}_2/\text{catalyst}$ ratio of 1500, conversions and selectivities up to ca. 44.2% and 42.2%, respectively, were obtained. The analogous Ru–Rh and Os–Rh gave slightly better results under similar conditions.³⁶²

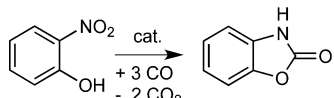
2.11.1.3. Fe–Pd. The transformation of *o*-nitrophenol to benzoxazol-2-one was catalyzed by the silica-supported MMCD



prepared from the clusters $[\text{FePd}_2(\text{CO})_4(\mu\text{-dppm})_2]$ (**118**) and $[\text{Fe}_2\text{Pd}_2(\text{CO})_5(\text{NO})_2(\mu\text{-dppm})_2]$ (**119**), respectively (Scheme

51). Both clusters showed almost complete conversions (>98%) and very high selectivities (95–96%).^{18b,c}

Scheme 51

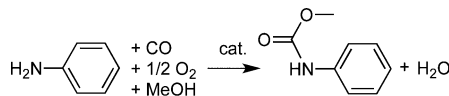


The results clearly indicate that both MMCD catalysts have significantly improved properties over the corresponding conventional catalysts under comparable conditions. Using silica instead of alumina as a support gave much better results with these Fe/Pd catalysts. It was found that the initially formed bimetallic particles eventually undergo metal segregation.^{18c}

2.11.1.4. Ru–Rh, Os–Rh. The clusters $[PPN]_2[RuRh_4(CO)_{15}]$ and $[PPN]_2[OsRh_4(CO)_{15}]$ catalyzed the carbonylation of nitrobenzene to phenylcarbamate in the presence of methanol and bipyridine, which enhanced the activity of the system. In particular, the activity and selectivity of those catalysts were quite similar, and slightly higher than in the case of the Fe–Rh analogue: 45.5% and 56.6%, respectively, for the Ru–Rh system, and 45.8% and 49.1%, respectively, for the Os–Rh one. However, at a lower $\text{PhNO}_2/\text{catalyst}$ ratio, 400 instead of 1500, the conversions could reach 98.5% and 100% for the Ru–Rh and Os–Rh catalysts, respectively, and the selectivities for the carbamate were 87.9% and 89.0% for the Ru–Rh and Os–Rh systems, respectively. The only byproduct detected was aniline. Noteworthy is that the Ru–Rh system was also tested in the carbonylation of nitrobenzene in the absence of methanol, thus yielding the corresponding isocyanate, but the activity was low (20.6% conversion) and the selectivity was only 27.5%.³⁶²

2.11.1.5. Os–Au. The hydrido-bridged cluster $[\text{Os}_4\text{Au}(\mu-\text{H})_3(\text{CO})_{12}(\text{PPh}_3)]$ catalyzed the oxidative carbonylation of aniline in the presence of MeOH to give methyl phenylcarbamate with good conversion and selectivity (Scheme 52) at

Scheme 52



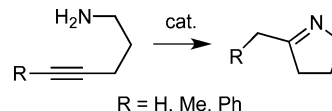
453 K. Quantitative conversions were observed in all cases, but the selectivity toward the carbamate product was found to dramatically decrease upon increasing quantities of methanol in the reaction mixture, thus favoring the formation of quinazoline or azobenzene. Nevertheless, this system was much more active than monometallic Os-containing cluster-derived systems.³⁶³

At 428 K, the influence of the Os/Au atomic ratio was studied with the clusters $[\text{Os}_4\text{Au}(\mu-\text{H})_3(\text{CO})_{12}(\text{PPh}_3)]$ and $[\text{Os}_4\text{Au}_4(\mu-\text{H})_2(\text{CO})_{11}(\text{PPh}_3)_4]$ in the same reaction. They were both active (at high methanol content and with addition of PPh_3 as promoter), with conversions between 60% and 90%, and selectivity toward methyl phenylcarbamate between 41% and 65%.³⁶⁴

2.11.2. Other Carbon–Nitrogen Bond Formation Reactions. **2.11.2.1. Mo–Pd.** The intramolecular hydroamination of aminoalkynes in the presence of the cubane-type complexes $[\text{Cp}^*_3\text{Mo}_3(\mu_3-\text{S})_4\text{PdL}][\text{PF}_6]$ ($\text{L} = \text{dba}$, maleic

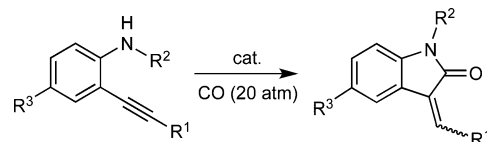
anhydride) afforded the corresponding cyclic imines with yields >95% after less than 1 h (Scheme 53).³⁶⁵

Scheme 53



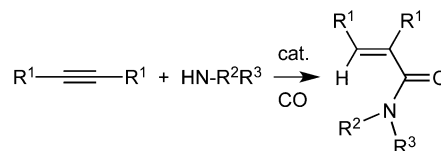
2.11.2.2. Co–Rh. The preparation of oxindoles from 2-alkynylanilines was performed in the presence of the $[\text{Co}_2\text{Rh}_2]$ catalyst derived from $[\text{Co}_2\text{Rh}_2(\text{CO})_{12}]$. A broad range of alkynyl substituents was tested, and the corresponding oxindoles were obtained with yields ranging from 52% to 93% (Scheme 54).³⁶⁶

Scheme 54



The reaction between internal alkynes, amines, and CO (5 atm) to afford α,β -unsaturated amides (Scheme 55) was

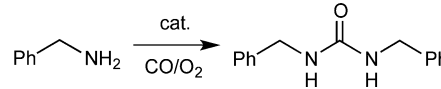
Scheme 55



catalyzed by NPs derived from $[\text{Co}_2\text{Rh}_2(\text{CO})_{12}]$. The yields were moderate to high (42–79% for the reaction between diphenylacetylene and butylamine), depending on the temperature and the CO pressure. In comparison, aminocarbonylation reactions in the presence of the monometallic catalysts $[\text{Co}_4]$ and $[\text{Rh}_4]$ were much less effective.³⁶⁷

Carbon-supported Co_2Rh_2 NPs derived from $[\text{Co}_2\text{Rh}_2(\text{CO})_{12}]$ were used as catalysts for the oxidative carbonylation of aliphatic and aromatic primary amines to ureas (Scheme 56). The system could be used several times before a

Scheme 56



significant loss of activity could be noticed. A broad range of substituents were tried, and yields in the range 12–89% were obtained depending on the substrate.³⁶⁸

2.11.2.3. Co–Pd. The catalytic intramolecular C–H amination and aziridination of various sulfamate esters has been carried out in the presence of the bimetallic complex $[\text{CoPd}(\text{OAc})_4]$ and the oxidant $\text{Phi}(\text{OAc})_2$. Yields in the range 50–99% were observed in most cases. This system gave better results than when $[\text{Co}(\text{OAc})_2]$ or $[\text{Pd}(\text{OAc})_2]$ were used, thus suggesting cooperative effects.³⁶⁹

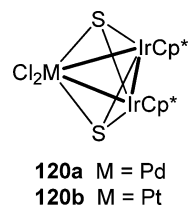
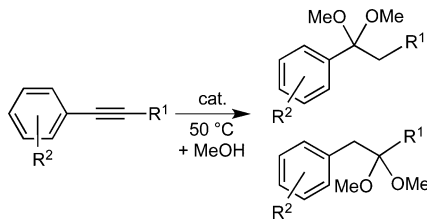
2.11.2.4. Pd–Ag. The catalytic ortho-amination of *N*-arylbenzamide by $[\text{Pd}(\text{OAc})_2]$ in the presence of $[\text{Ag}(\text{OAc})]$ and CsF was studied by DFT calculations. The authors assume that the active species can be formulated as a bimetallic acetate-bridged complex $[\text{Pd}(\mu\text{-OAc})_3\text{Ag}]$, and that its activity is superior to that of the monometallic acetate complexes.³⁷⁰

2.12. Carbon–Oxygen Bond Formation

2.12.1. Addition of Alcohols to Alkynes. The addition of alcohols to alkynes affords ketals as main products. The use of Ir–Pd and Ir–Pt heterometallic cluster-derived catalysts in such reactions is described below.

2.12.1.1. Ir–Pd, Ir–Pt. The triangular clusters $[(\text{Cp}^*\text{Ir})_2(\mu_3\text{-S})_2\text{PdCl}_2]$ (**120a**) and $[(\text{Cp}^*\text{Ir})_2(\mu_3\text{-S})_2\text{PtCl}_2]$ (**120b**) were found to catalyze the addition of alcohols to alkynes. In particular, 1-aryl-1-alkynes were converted almost quantitatively upon addition of MeOH to the corresponding 2,2-dialkoxy-1-arylalkanes (Scheme 57). The cluster **120a** proved to be the most selective catalyst (>90% in most cases), while **120b** gave slightly higher total yields of products.³⁷¹

Scheme 57

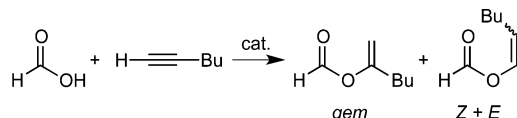


2.12.2. Addition of Carboxylic Acids to Alkynes. The addition of carboxylic acids to alkynes generally leads to the formation of esters (see section 3.8). However, enol lactones can be obtained by intramolecular cyclization of alkynoic acids (Scheme 58) with (gem)/(Z+E) ratios ranging from 60/40 to 82/18.

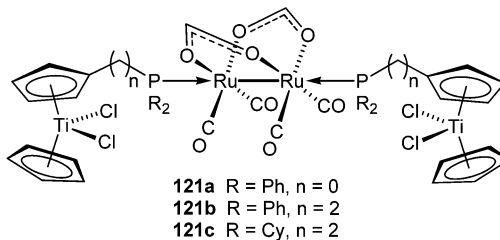
2.12.2.1. Ti–Ru. Although they do not contain metal–metal bonds, the complexes $[\text{CpCl}_2\text{Ti}(\mu\text{-}\eta^5\text{:}\eta^1\text{-C}_5\text{H}_4(\text{CH}_2)_n\text{PR}_2)\text{-RuCl}_2(p\text{-cymene})]$ (R = Ph, n = 0, 2; R = Cy, n = 2) catalyze the addition of formic acid to 1-hexyne and to phenylacetylene and yield the corresponding enol formates (Scheme 58) with (gem)/(Z+E) ratios ranging from 60/40 to 82/18.

Only $[\text{CpCl}_2\text{Ti}(\mu\text{-}\eta^5\text{:}\eta^1\text{-C}_5\text{H}_4\text{PPPh}_2)\text{RuCl}_2(p\text{-cymene})]$ was able to compete with monometallic complexes in terms of activity and selectivity. The tetranuclear complexes $[\text{CpCl}_2\text{Ti}(\mu\text{-}\eta^5\text{:}\eta^1\text{-C}_5\text{H}_4(\text{CH}_2)_n\text{PR}_2)\text{Ru}(\text{CO})_2(\mu\text{-O}_2\text{CH})]_2$ (**121a**, R = Ph, n = 0; **121b**, R = Ph, n = 2; **121c**, R = Cy, n = 2) were

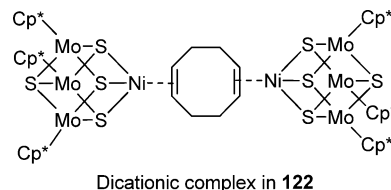
Scheme 58



also tested under the same conditions, and showed even better results, but still not as good as the homometallic complex $[\text{Ru}_2(\mu\text{-O}_2\text{CH})(\text{CO})_4(\text{PPh}_3)_2]$.³⁷²

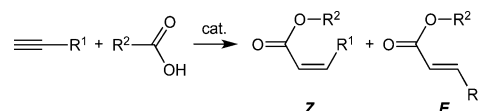


2.12.2.2. Mo–Ni. The cubane-type cluster $[\{\text{Cp}^*\text{Mo}_3\text{Ni}(\mu_3\text{-S})_4\}_2(\mu\text{-}\eta^2\text{:}\eta^2\text{-COD})][\text{PF}_6]_2$ (**122**) was used in the intramolecular cyclization of alkynoic acids to enol lactones. After 1 h reaction in the presence of this cluster and NEt₃ at room temperature, 4-pentynoic acid afforded the corresponding enol lactone in 96% yield. For the same reaction, the cluster $[\text{Cp}^*\text{Mo}_3\text{Ni}(\mu_3\text{-S})_4(\eta^2\text{-dmad})][\text{PF}_6]$ (dmad = dimethyl acetylenedicarboxylate) gave the desired product in 95% yield after 3 h.³⁷³



2.12.2.3. Mo–Pd. Stereoselective addition of carboxylic acids to electron-deficient (terminal) alkynes (Scheme 59) was

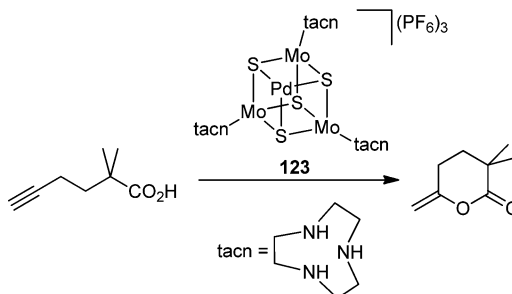
Scheme 59



efficiently catalyzed by the cuboidal cluster $[\text{Mo}_3\text{PdS}_4(\text{tacn})_3\text{Cl}][\text{PF}_6]_3$ (tacn = 1,4,7-triazacyclononane) (**123**). Typically, at full conversions, the selectivity for the Z-isomers was higher than 97% with yields ranging from 50% to 85%.³⁷⁴

The intramolecular cyclization of a series of alkynoic acids to the corresponding enol lactones, in the presence of NEt₃, was catalyzed by the same cluster **123** (see Scheme 60), in yields greater than 80% for most substrates, after short times (a few minutes in some cases). For instance, 2,2-dimethyl-5-hexynoic

Scheme 60



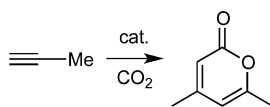
acid yielded 3,3-dimethyl-6-methylene-2-pyrone with 98% yield after 3 h (Scheme 60).³⁷⁵

2.12.2.4. Re–Ru. The complexes $[\text{Cp}^*\text{Ru}(\mu\text{-dppm})(\mu\text{-CO})_2\text{Re}(\text{CO})_3]$, $[\text{Cp}(\text{CO})\text{Ru}(\mu\text{-dppm})\text{Re}(\text{CO})_4]$, and $[\text{Cp}(\text{CO})_2\text{RuRe}(\text{CO})_5]$ were tested in the addition of carboxylic acids to terminal alkynes. They showed good regioselectivity (>90% for most substrates) toward the anti-Markovnikov products (*Z*+*E*).³⁷⁶

2.12.3. Cycloaddition of CO_2 and Alkynes.

2.12.3.1. Fe–Rh. Cycloaddition of CO_2 and propyne to afford 4,6-dimethyl-2-pyrone (Scheme 61) was achieved with a mildly

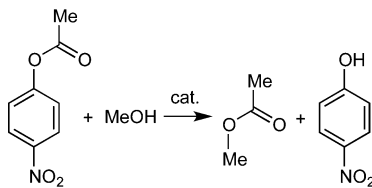
Scheme 61



oxidized $[\text{Fe}_2\text{Rh}_4]$ catalyst derived from $[\text{TMBA}]_2[\text{Fe}_2\text{Rh}_4(\text{CO})_{16}]$ supported on silica. Other observed products include the trimerization products 1,3,5- and 1,2,4-trimethylbenzene, as well as other oligomers, all of them being formed even in the absence of CO_2 . Such a system was much more selective toward the desired lactone than $[\text{Rh}_4(\text{CO})_{12}]$ -derived catalysts, probably due to the stabilizing effect of iron on rhodium ions, thus providing basic O^{2-} sites favoring the cycloaddition of CO_2 , as suggested by $^{13}\text{CO}_2$ labeling and FTIR studies.³⁷⁷

2.12.4. Transesterification. **2.12.4.1. Co–Zn, Co–Cd, Zn–Cd.** The polymeric complex $[\text{CoZn}_2(\text{O}_2\text{CPh})_6]_n(\text{bpa})_n$ ($\text{bpa} = 1,2\text{-bis}(4\text{-pyridyl})\text{ethane}$) was used as a catalyst in transesterification of esters by methanol at 323 K (Scheme 62).

Scheme 62

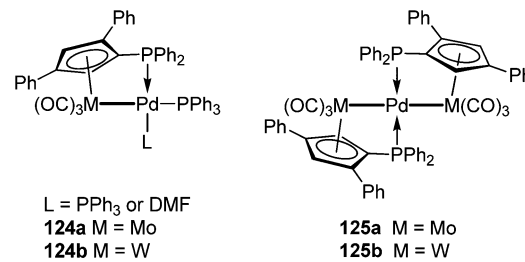


A broad range of substrates was tested, and all of the reactions afforded quantitatively the corresponding methyl acetate or benzoate within 0.17–1.29 or 1.67–4 days, respectively. The complex $[\text{Zn}_2\text{Cd}(\text{O}_2\text{CPh})_6]_n(\text{bpa})_n$ was more active (much shorter induction times), because it needed less than 1 day or 1–4 days to afford quantitatively the desired methyl acetates or benzoates, respectively, while the complex $[\text{Co}_2\text{Cd}(\text{O}_2\text{CPh})_6]_n(\text{bpa})_n$ was a much slower catalyst under the same conditions, as it required more than 1 week to achieve quantitative yields in most cases.³⁷⁸

2.13. Metal–Carbon Bond Formation

2.13.1. Mo–Pd, W–Pd. The dinuclear complexes $[(\text{CO})_3\text{M}(\mu\text{-}\eta^5\text{-}\text{C}_5\text{H}_2\text{Ph}_2(\text{PPh}_2))\text{Pd}(\text{PPh}_3)\text{L}]$ ($\text{M} = \text{Mo}$, 124a or W, 124b; L = PPh₃, DMF) and the trinuclear chain complexes $[\text{Pd}\{\text{M}(\text{CO})_3(\mu\text{-}\eta^5\text{-}\text{C}_5\text{H}_2\text{Ph}_2(\text{PPh}_2))\}_2]$ ($\text{M} = \text{Mo}$, 125a or W, 125b) were isolated and are relevant to the metal–carbon bond formation between $[\text{Bu}_3\text{SnC}\equiv\text{CPh}]$ and the iodide complexes $[\text{M}(\text{CO})_3\text{I}(\eta^5\text{-}\text{C}_5\text{H}_2\text{Ph}_2(\text{PPh}_2))]$ ($\text{M} = \text{Mo}$ or W) catalyzed by Pd^0/PPh_3 . The main steps of this Pd-catalyzed M–C bond formation process are closely related to

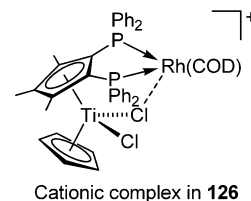
the sequence of oxidative addition/transmetalation/trans-to-cis isomerization/reductive elimination steps, which occur in the Stille reaction, that is, the palladium-catalyzed coupling of organic electrophiles and organostannanes.³⁷⁹



2.14. Silylation Reactions

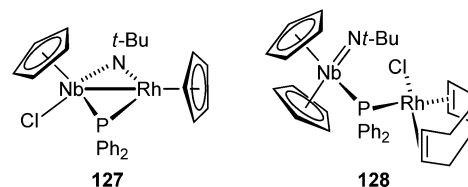
2.14.1. Hydrosilylation of Olefins and Alkynes.

2.14.1.1. Ti–Rh. The dinuclear complex $[\text{CpCl}_2\text{Ti}\{\mu\text{-}\eta^5\text{-}\text{C}_5\text{Me}_3(\text{PPh}_2)_2\}\text{Rh}(\text{COD})][\text{OTf}]$ (126) was evaluated in the catalytic hydrosilylation of acetophenone with Ph_2SiH_2 . It afforded 1-phenylethanol in 62% yield, which is better than the Rh complex $[(o\text{-dppbe})\text{Rh}(\text{COD})][\text{OTf}]$ (dppbe = 1,2-bis(diphenylphosphino)benzene).³⁸⁰



Cationic complex in 126

2.14.1.2. Nb–Rh. The heterobimetallic compounds $[\text{CpClNb}(\mu\text{-N-t-Bu})(\mu\text{-PPh}_2)\text{RhCp}]$ (127) and $[\text{Cp}_2\text{Nb}(\text{N-t-Bu})(\mu\text{-PPh}_2)\text{RhCl}(\text{COD})]$ (128) were used as homogeneous catalyst precursors for the hydrosilylation of benzaldehyde and acetophenone.³⁸¹



2.14.1.3. Ta–Rh. Good activity in hydrosilylation of acetophenone with PhMeSiH_2 was achieved in the presence of the complex $[\text{Cp}_2\text{Ta}(\mu\text{-PEt}_2)_2\text{Rh}(\eta^2\text{-C}_2\text{H}_4)]$, but the reactions were slower than with the Nb–Rh complexes mentioned before (see section 2.14.1.2). Also, the phosphine-free Rh complex $[\text{Rh}(\mu\text{-Cl})(\text{COD})]_2$ was still more active.³⁸²

2.14.1.4. Ta–Ir. The hydrosilylation of ethylene by Me_3SiH , Et_3SiH , or Ph_3SiH was achieved with the complex $[\text{Cp}_2\text{Ta}(\mu\text{-CH}_2)_2\text{Ir}(\text{CO})_2]$ (9b); heavier alkenes were isomerized instead. The role of tantalum is still not fully understood, because the substrates seem to bind to the iridium center.⁴⁹

2.14.1.5. Mo–Fe–Co, Mo–Co, Mo–Co–Ni. The optically active sulfido-bridged cluster $[\text{CpMoFeCo}(\mu_3\text{-S})(\text{CO})_8]$ was tested in the asymmetric photoinitiated hydrosilylation of acetophenone, but, unfortunately, photoracemization proceeds faster than the hydrosilylation reaction.³⁸³

The clusters $[\text{CpMoCo}_2(\mu_3\text{-CMe})(\text{CO})_8]$, $[\text{CpMoCo}_2(\mu_3\text{-CMe})(\text{CO})_7(\text{P}(\text{OMe})_3)]$, $[\text{CpMoCo}_2(\mu_3\text{-S})(\text{CO})_8]$, and $[\text{MoCoNi}(\mu_3\text{-CMe})\text{Cp}_2(\text{CO})_5]$ (26) were active too, but afforded $\text{PhC}(\text{OSiEt}_3)\text{CH}_2$ with 100% selectivity.³⁸³

2.14.1.6. Mo–Pd, Mo–Pt. The photocatalyzed hydrosilylation of 1-pentene was tentatively catalyzed by the clusters $[Mo_2Pd_2Cp_2(CO)_6(PEt_3)_2]$ (**11a**) and $[Mo_2Pd_2Cp_2(CO)_6(PPh_3)_2]$ (**11b**). However, only isomerization and hydrogenation products could be detected. Under the same conditions, the clusters $[Mo_2Pt_2Cp_2(CO)_6(PEt_3)_2]$ and $[Mo_2Pt_2Cp_2(CO)_6(PPh_3)_2]$ catalyzed the hydrosilylation of 1-pentene, albeit with little activity, to $C_5H_{11}SiEt_3$ with 4% and 3% yield, respectively. The predominant reaction was olefin isomerization to *trans*-2-pentene.³⁸¹

2.14.1.7. W–Co. Photoinitiated hydrosilylation of acetophenone with triethylsilane occurred in the presence of the complex $[WCo_2(\mu_3\text{-CH})Cp(CO)_8]$ and afforded $\text{PhC}(OSiEt_3)CH_2$ as the only product.³⁸³

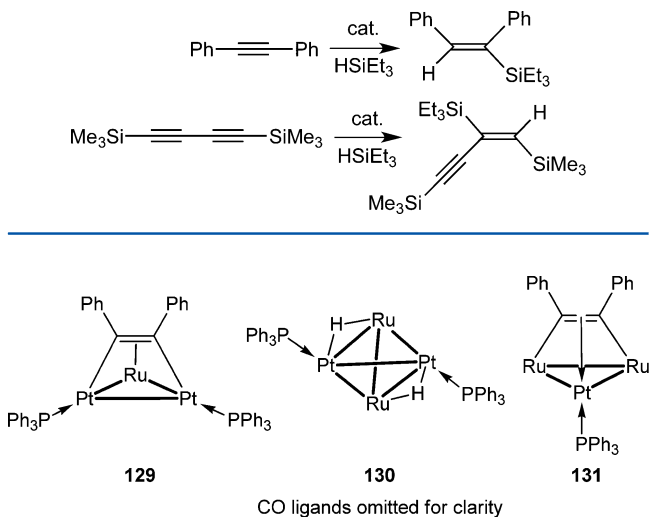
2.14.1.8. W–Pd. The planar clusters $[W_2Pd_2Cp_2(CO)_6(PEt_3)_2]$ (**12a**) and $[W_2Pd_2Cp_2(CO)_6(PPh_3)_2]$ (**12b**) were tested in the photocatalyzed hydrosilylation of 1-pentene but afforded only hydrogenation and isomerization products, such as pentane and 2-pentenes.³⁸¹

2.14.1.9. Fe–Co. Homogeneous photoinitiated hydrosilylation of acetophenone to $\text{PhC}(OSiEt_3)CH_2$ could be catalyzed in the presence of the cluster $[FeCo_2(\mu_3\text{-PPh})(CO)_9]$.³⁸³

2.14.1.10. Fe–Rh. Hydrosilylation of phenylacetylene was catalyzed by $[Me_4N][Fe_5RhC(CO)]_{16}$, and the activity was assigned to the Rh atom.³⁸⁴

2.14.1.11. Fe–Pt, Ru–Pt, Os–Pt. The clusters $[FePt_2(\text{PhC}\equiv\text{CPh})(CO)_5(PPh_3)_2]$, $[RuPt_2(\text{PhC}\equiv\text{CPh})(CO)_5(PPh_3)_2]$ (**129**), $[Ru_2Pt_2(\mu\text{-H})_2(CO)_8(PPh_3)_2]$ (**130**), $[Ru_2Pt(\text{PhC}\equiv\text{CPh})(CO)_7(PPh_3)]$ (**131**), and $[OsPt_2(\text{PhC}\equiv\text{CPh})(CO)_5(PPh_3)_2]$ were tested in the catalytic hydrosilylation of diphenylacetylene and 1,4-bis(trimethylsilyl)butadiyne with triethylsilane (Scheme 63).

Scheme 63



Good conversions were reached, but the monometallic Pt complex $[Pt(PPh_3)(\text{PhC}\equiv\text{CPh})]$ was a much better catalyst. The authors suggest that, in all cases, the active species are Pt fragments of the initial catalyst, which are responsible for the observed activity.³⁸⁵

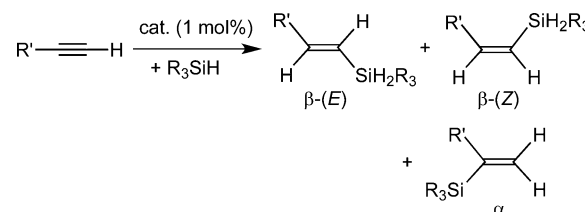
The layer-segregated cluster $[Pt_3Ru_6(\mu_3\text{-RC}\equiv\text{CR})(\mu_3\text{-H})(\mu\text{-H})(CO)_{20}]$ ($R = \text{Ph, Tol}$) was a good precursor to the catalytic hydrosilylation of diphenylacetylene by HSiEt₃ to afford $(E)\text{-}[(1,2\text{-diphenyl})\text{ethenyl}]$ triethylsilane. Very high activity and

selectivity could be achieved, although small quantities of *cis*-stilbene were also observed. Mercury poisoning tests evidenced that the active species are not Pt colloids. The active species were assumed to be the decarbonylated intact metal core of the cluster and not fragments. The cluster $[Bu_4N][Pt_3Ru_6(\mu_3\text{-PhC}\equiv\text{CPh})(\mu\text{-H})(CO)_{20}]$, obtained by deprotonation of the former cluster, gave similar results, although it appears that heterogeneous species might be responsible, at least in part, for the activity. The cluster $[PtRu_2(\mu_3\text{-PhC}\equiv\text{CPh})(CO)_8(\text{dppe})]$ exhibited poor activity for the reaction.³⁸⁶

2.14.1.12. Co–Ni. The cluster $[Co_2Ni(\mu_3\text{-CMe})Cp(CO)_6]$ was found to catalyze the photoinitiated hydrosilylation of acetophenone to $\text{PhC}(OSiEt_3)CH_2$ as the only product.³⁸³

2.14.1.13. Ir–Pt. The complexes $[(PPh_3)_2Pt(\mu\text{-SRS})\text{-IrClCp}^*][SbF_6]$ ($R = cis\text{-C}_8H_{14}, trans\text{-C}_8H_{14}$) were used in the catalytic hydrosilylation of terminal alkynes $R'\text{C}\equiv\text{CH}$ ($R' = \text{Ph, Bu, COOMe}$) with Et₃SiH or Ph₃SiH to afford $\beta\text{-}(Z)$ -vinylsilanes (Scheme 64) in high yields (71–97%). Noteworthy is that 100% selectivity for the $\beta\text{-}(Z)$ product was achieved when Ph₃SiH was used, while it was in the range 74–96% when Et₃SiH was used.³⁸⁷

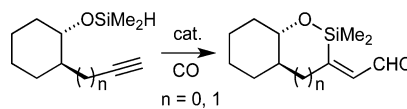
Scheme 64



2.14.2. Hydrosilylation of Ketones. **2.14.2.1. Zr–Co.** The dinuclear complex $[(\text{THF})Zr\{\mu\text{-(MesNP-}i\text{-Pr}_2\}\}_3Co(N_2)]$ exhibited enhanced activity in ketone hydrosilylation as compared to monometallic Zr or Co complexes. A broad range of substrates was probed, with yields higher than 95% in most cases. The authors evidenced a mechanism involving radical coupled intermediates such as $[(R_2CO)Zr(\text{MesNP-}i\text{-Pr}_2)_3Co(N_2)]_2$, unlike the typical Chalk–Harrod-type hydrosilylation pathway.³⁸⁸

2.14.3. Silylformylation Reactions. **2.14.3.1. Co–Rh.** The tetrahedral clusters $[Co_2Rh_2(CO)]_{12}$ and $[Co_3Rh(CO)]_{12}$ catalyze the regioselective inter- or intramolecular silylformylation of alkynes (Scheme 65) and 1-alkynals and the silylcyclization of enynes, diynes, and alkynals. These synthetically important reactions have been reviewed.³⁸⁹

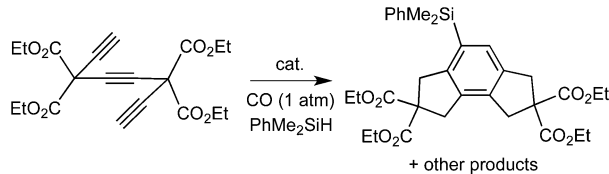
Scheme 65



Silylformylation of the C–C triple bond of $C_4H_9C\equiv CH$ was achieved in the presence of the cluster $[Co_2Rh_2(CO)]_{12}$. Synergism between the metal centers was elucidated by DFT calculations. The theoretical studies suggest that the role of the Co atoms is to bind the substrate to the catalyst, thus preventing hydrosilylation to occur, and subsequently to provide electrons during the process. The reaction itself takes place at the Rh centers.³⁹⁰

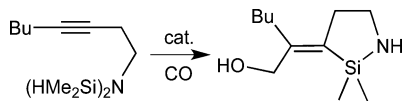
The cluster $[\text{Co}_2\text{Rh}_2(\text{CO})_{12}]$ was used in a wide range of catalytic reactions, including the silylcarbocyclization of triynes. At 295 K, the conversion was total, and the major product (Scheme 66) was obtained with 86% selectivity.³⁹¹

Scheme 66



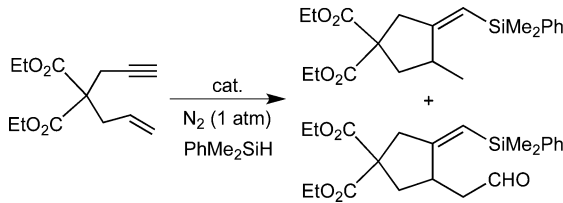
The complexes $[\text{Co}_2\text{Rh}_2(\text{CO})_{12}]$ and $[(t\text{-BuNC})\text{RhCo}(\text{CO})_4]$ were found to be efficient catalysts for the intramolecular silylformylation of some bis(silyl)aminoalkynes with yields ranging from 75% to 87% (Scheme 67).³⁹²

Scheme 67



These two complexes also catalyzed the silylcarbocyclization of enynes. The former was more active, with conversions close to 100% under very mild conditions, and without using CO atmosphere, and a selectivity of 100% toward the methyl compound could be achieved. The complex $[(t\text{-BuNC})\text{RhCo}(\text{CO})_4]$, however, yielded a mixture of the methyl and the aldehyde products (Scheme 68).³⁹³

Scheme 68



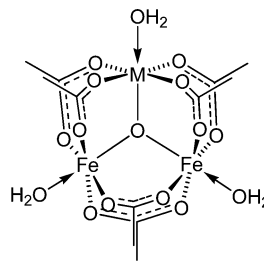
Bimetallic NPs derived from the cluster $[\text{Co}_2\text{Rh}_2(\text{CO})_{12}]$ appeared to be active in the silylcarbocyclization of enynes. It was found that in the presence of a CO atmosphere, carbonylative cyclization occurred, yielding only the aldehyde product, while in the absence of CO, the methyl product was formed alone. A wide scope of substrates was tested, and good conversions were achieved in most cases. This catalyst was reusable several times without loss of activity.³⁹⁴

2.15. Reduction of Nitrogenated Compounds

2.15.1. Reduction of NO. **2.15.1.1. Mo–Pd.** Selective catalytic reduction of NO, in the presence of CO and O₂, has been achieved with the alumina-supported $[\text{Mo}_2\text{Pd}_2]$ catalysts derived from $[\text{Mo}_2\text{Pd}_2\text{Cp}_2(\text{CO})_6(\text{PPh}_3)_2]$ (11b). This system was more selective than a catalyst prepared from the corresponding metal salts [Mo+Pd], but it rapidly decomposed under the reaction conditions, thus undergoing deactivation.³⁹⁵

2.15.1.2. Mn–Fe, Fe–Co, Fe–Ni. When treated at 673 K, the trinuclear oxoacetate-bridged cluster $[\text{Fe}_2\text{Mn}(\mu_3\text{-O})(\mu\text{-OOCMe})_6(\text{H}_2\text{O})_3]\cdot 2\text{H}_2\text{O}$ (132a) afforded Fe_2MnO_4 ferrite NPs. Those were tested in NO reduction by a propane/butane

mixture, to yield N₂. They proved to be almost inactive, reaching 11% conversion only, at 673 K. Comparatively, the CoFe_2O_4 and NiFe_2O_4 spinel nanocrystals, obtained from the clusters $[\text{Fe}_2\text{Co}(\mu_3\text{-O})(\mu\text{-OOCMe})_6(\text{H}_2\text{O})_3]\cdot 2\text{H}_2\text{O}$ (132b) and $[\text{Fe}_2\text{Ni}(\mu_3\text{-O})(\mu\text{-OOCMe})_6(\text{H}_2\text{O})_3]\cdot 2\text{H}_2\text{O}$ (132c), respectively, were more active. Thus, with the $[\text{Fe}_2\text{Co}]$ catalyst, a maximum conversion of 24% was observed at 703 K, while with the $[\text{Fe}_2\text{Ni}]$ catalyst, conversions ranging from 37% at 523 K to 70% at 753 K could be achieved.³⁹⁶



132a M = Mn
132b M = Co
132c M = Ni

2.15.1.3. Pt–Au. The silica-supported $[\text{Pt}_2\text{Au}_4]$ catalyst, obtained by thermal activation of the cluster $[\text{Pt}_2\text{Au}_4(\text{C}\equiv\text{C}^{\text{t-Bu}})_8]$ (7) in O₂/He at 573 K, then in H₂ at 473 K, was used for the catalytic reduction of NO to N₂ by propylene. This catalyst was active at higher temperature than the monometallic and heterometallic catalysts prepared from impregnation or coimpregnation of metallic salts, but it was much more selective for the formation of N₂ (82% selectivity at 641 K).^{47,397}

2.15.2. Reduction of Nitrates and Nitrites.

2.15.2.1. Mo–Fe. The cubane cluster $[\text{Et}_4\text{N}]_2[(\text{Cl}_4\text{-cat})\text{-}(\text{MeCN})\text{MoFe}_3\text{S}_4\text{Cl}_3]$, when supported on glassy carbon electrode, was studied in the electrocatalytic reduction of nitrates and nitrites.³⁹⁸

2.15.3. Reduction of Nitrobenzene to Aniline.

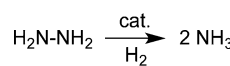
2.15.3.1. Ru–Pt. Heterogeneous catalysts supported on silica were prepared from various clusters. Thus, $[\text{Ru}_5\text{PtC}(\text{CO})_{16}]$, $[\text{Ru}_5\text{PtC}(\text{CO})_{15}(\text{SnPh}_2)]$, and $[\text{H}_2\text{Ru}_2\text{Pt}_2(\text{Sn}-t\text{-Bu}_3)_2(\text{CO})_9]$ were decarbonylated under vacuum at 473 K. These systems were used for the hydrogenation of nitrobenzene to aniline. All three catalysts reached 100% selectivity, achieving conversions in the range 80–100%.³⁹⁹

2.15.3.2. Co–Rh. The silica-entrapped $[\text{Co}_2\text{Rh}_2(\text{CO})_{12}]$ cluster was used in nitrobenzene hydrogenation. The first four runs, for a duration of 22 h, gave a mixture of aniline and aminocyclohexane with the following ratios: (1) 96/4, (2) 64/36, (3) 16/84, and (4) 2/98. This progressive change of selectivity can be explained by the fact that the cluster precursor remained intact after encapsulation, but lost its carbonyl ligands during the catalytic reactions, thus affording NPs with a diameter of 2–3 nm.⁶¹

2.15.4. Reduction of Hydrazines to Amines.

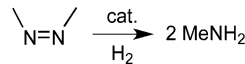
2.15.4.1. V–Fe. The reduction of hydrazine to yield ammonia (Scheme 69) was achieved with conversions above 80% after 2 h, by using the cubane-type cluster $[\text{NEt}_4][\text{VFe}_3\text{S}_4\text{Cl}_3(\text{DMF})_3]$ as a homogeneous catalyst.^{101b}

Scheme 69



2.15.4.2. Mo–Fe. The cubane cluster $[\text{Et}_4\text{N}]_2[(\text{Cl}_4\text{-cat})(\text{MeCN})\text{MoFe}_3\text{S}_4\text{Cl}_3]$ was tested, as a model for Mo–Fe nitrogenase, in the reduction of hydrazine to ammonia and of *cis*-dimethyldiazene to methylamine (Scheme 70). In the latter

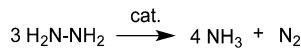
Scheme 70



case, methylamine was the only observable product, unlike in the case of the nitrogenase cofactor, which yields methylamine, ammonia, and methane, as a result of the reduction of the C–N bond. Cobaltocene was used as a source of electron, while lutidine hydrochloride was used as a source of proton.⁴⁰⁰ Such clusters are intensively studied due to their structural relationship with the nitrogenase cofactor.^{101,401}

2.15.4.3. Mo–Ru. The cubane cluster $[\text{Cp}^*\text{}_3\text{Mo}_3(\mu_3\text{-S})_4\text{RuH}_2(\text{PPh}_3)][\text{PF}_6]$ catalyzes the disproportionation of hydrazine to ammonia and dinitrogen, but $[\text{Cp}^*\text{}_3\text{Mo}_3(\mu_3\text{-S})_4\text{RuH}_2(\text{PCy}_3)][\text{PF}_6]$ is more active (Scheme 71). In

Scheme 71



particular, at 333 K, up to 20 mol of NH_3 (and thus ca. 5 mol of N_2) per mol of catalyst could be obtained in the latter case, while only 6.6 mol of ammonia (ca. 1.6 mol of dinitrogen) per mol of catalyst were converted in the former. The authors did not investigate why replacing PPh_3 with PCy_3 had so much impact on the yields. Also, these heterobimetallic clusters were less active than mononuclear Mo- and dinuclear Ru-thiolate complexes.⁴⁰²

2.15.4.4. Mo–Rh, Mo–Ir. The reduction of the hydrazine derivative $\text{H}_2\text{N–NMePh}$ to NHMePh was catalyzed in the presence of lutidine/HCl (H source), cobaltocene (electron source), and the heterobimetallic cubane-type clusters $[\{\text{Mo}(=\text{O})\text{Cl}_2\}\{\text{MoCl}_2(\text{DMF})\}\{\text{Cp}^*\text{M}_2(\mu_3\text{-S})_2(\mu_3\text{-L})_2\}]$ ($\text{M} = \text{Rh}$ or Ir , $\text{L} = \text{S}$ or Se) with good activity and selectivity. In particular, the Ir-based clusters were more active than the Rh-based ones, and the Se-containing were more active than the S-containing ones. The yields of NHMePh increased depending on the catalyst in the order: MoRhS (31%) < MoRhSe (56%) < MoIrS (64%) < MoIrSe (70%).⁴⁰³

2.15.5. Hydrogenation of N_2 . **2.15.5.1. Ru–Ni, Os–Ni.** When supported on γ -alumina (modified with 30 wt % K as KOH), the $[\text{Ru}_3\text{Ni}]$ catalyst obtained from $[\text{Ru}_3\text{Ni}(\mu\text{-H})_3\text{Cp}^*(\text{CO})_9]$ showed activity in ammonia synthesis from a H_2/N_2 mixture.⁴⁰⁴ Even if it was more effective than the $[\text{Os}_3\text{Ni}]$ catalyst prepared from the analogous $[\text{Os}_3\text{Ni}(\mu\text{-H})_3\text{Cp}(\text{CO})_9]$, the monometallic ruthenium catalyst derived from $[\text{Ru}_3(\text{CO})_{12}]$ was still the most active.⁴⁰⁵

2.16. Hydrodesulfurization and Hydrodenitrogenation

Environmental problems have emphasized the role of catalysts capable of removing sulfur, and hydrodesulfurization (HDS) has become an increasingly important reaction in both coal and petroleum refining.^{163a} The availability of new molecular sulfido bimetallic clusters provides molecular models relevant to HDS catalysis by generating a better insight into processes such as substrate coordination and mobility, C–S bond cleavage, and C–H bond formation, which may occur on the surface of

heterogeneous catalysts.⁴⁰⁶ They also allow the properties of the corresponding MMCD catalysts to be compared to those of the classical MoS_2 -promoted catalysts.

2.16.1. Mo–W–Fe, Mo–W–Co, Mo–W–Ni. The cage-type clusters $\text{K}_8[\text{P}_2\text{Mo}_2\text{W}_{18}\text{M}_2(\text{H}_2\text{O})\text{O}_{68}]\cdot\text{MoO}_6\cdot15\text{H}_2\text{O}$ ($\text{M} = \text{Fe}$, Co , Ni) were adsorbed onto an alumina matrix for applications in thiophene HDS.¹⁰³

2.16.2. Mo–Fe. The alumina-supported linear complex $[\text{Et}_4\text{N}]_2[\text{Mo}_2\text{FeS}_4\text{O}_4]$ and the cubane-type cluster $[\text{Et}_4\text{N}]_3[\text{Mo}_2\text{Fe}_6\text{S}_8(\text{SPh})_6(\text{OMe})_3]$ were used for the HDS of thiophene.¹⁰³

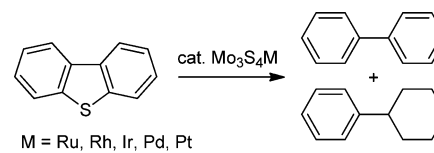
The $[\text{Mo}_2\text{Fe}_2]$ catalyst, derived from $[\text{Mo}_2\text{Fe}_2\text{S}_2\text{Cp}_2(\text{CO})_8]$, and supported on $\gamma\text{-Al}_2\text{O}_3$, SiO_2 , TiO_2 , and MgO , exhibited activities for S-removal from thiophene comparable to those of commercial HDS catalysts while showing decreased H_2 consumption (less butane formation).^{162,164b,406c}

2.16.3. Mo–Fe–Co. The two cubane-type clusters $[\text{Et}_4\text{N}]_3[\text{Mo}_2\text{Fe}_5\text{CoS}_8(\text{SPh})_6(\text{OMe})_3]$ and $[\text{Et}_4\text{N}]_3[\text{Mo}_2\text{Fe}_4\text{Co}_2\text{S}_8(\text{SPh})_6(\text{OMe})_3]$ were active in the HDS of thiophene.¹⁰³

2.16.4. Mo–Ru. The bimetallic complex $[\text{Cp}(\text{CO})_3\text{MoRu}(\text{CO})_2\text{Cp}]$ was impregnated on alumina and activated at 673 K for application in HDS catalysis. It was more active than the $[\text{Mo}]$, $[\text{Ru}]$, and $[\text{Mo}+\text{Ru}]$ catalysts, prepared by impregnation of homometallic carbonyl complexes or by gas-phase deposition. It reached 98% conversion of thiophene at 623 K, for a selectivity toward *n*-butane higher than 96%.⁴⁰⁷

The cubane-type cluster $[\text{Mo}_3\text{Ru}(\mu_3\text{-S})_4\text{Cp}'_3(\text{CO})_2][\text{pts}]$ (25a) was impregnated on alumina and sulfidated at 623 K, thus affording a $\text{Mo}_3\text{S}_4\text{Ru}$ phase. The system was tested in the simultaneous HDS of dibenzothiophene (DBT), HDN of indole, and hydrogenation of naphthalene (see section 2.5.1.8), with better results than the corresponding Mo_3Pd and Mo_3Pt materials, but not as good as the Mo_3Rh and Mo_3Ir ones. The activity of this Mo_3Ru catalyst was higher than the sum of the activities of Mo_3 + Ru materials, suggesting some degree of synergism. Under the reaction conditions, the products of the HDS of DBT were biphenyl and small amounts of cyclohexylbenzene (Scheme 72).¹⁰⁸

Scheme 72



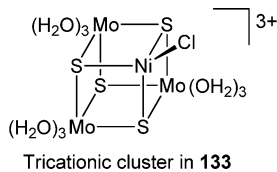
2.16.5. Mo–Co. When supported on alumina, the linear complex $[\text{Et}_4\text{N}]_2[\text{Mo}_2\text{CoS}_4\text{O}_4]$ was found to catalyze the HDS of thiophene.¹⁰³ Hydrodesulfurization (HDS) has been very much studied with this metal couple.^{163a,164b,406b,c,408}

The catalytic activity of the cluster $[\text{Mo}_2\text{Co}_2(\mu_3\text{-S})_3\text{Cp}'_2(\text{CO})_4]$ supported on alumina in HDS of thiophene and thiophenol was similar to that found for heterogeneous $\text{Mo}/\text{Co}/\text{S}$ catalysts.¹⁶² The $[\text{Mo}_2\text{Co}_2]$ catalysts derived from $[\text{Mo}_2\text{Co}_2\text{S}_3\text{Cp}_2(\text{CO})_4]$ and supported on $\gamma\text{-Al}_2\text{O}_3$, SiO_2 , TiO_2 , and MgO have been extensively studied for HDS.^{408,409} It was found to be as efficient as commercial HDS catalysts for S-removal from thiophene, while showing decreased H_2 consumption (less butane formation).^{162,164b} The cubane cluster $[\text{Mo}_2\text{Co}_2\text{S}_4(\text{C}_5\text{Me}_4\text{Et})_2(\text{CO})_2]$ reacts with PhSH under CO pressure to give PhSSPh and PhSC(O)Ph , indicating also catalytic HDS activity.⁴¹⁰

2.16.6. Mo–Rh, Mo–Ir. Alumina-supported heterogeneous catalysts were prepared from the sulfidation at 623 K of the cubane-type clusters $[\text{Mo}_3\text{Rh}(\mu_3\text{-S})_4\text{Cp}'_3(\text{COD})][\text{pts}]_2$ (**25b**) and $[\text{Mo}_3\text{Ir}(\mu_3\text{-S})_4\text{Cp}'_3\text{Cl}(\text{COE})][\text{pts}]$ (**25c**), thus affording $\text{Mo}_3\text{S}_4\text{Rh}$ and $\text{Mo}_3\text{S}_4\text{Ir}$ phases. These materials are good catalysts for the simultaneous HDS of dibenzothiophene, HDN of indole, and hydrogenation of naphthalene (see sections 2.5.1.12 and 2.5.1.13), exhibiting much better results than the corresponding Mo_3Pd , Mo_3Pt , and Mo_3Ru catalysts, Mo_3Ir being slightly more active. However, they were still one-half as active as a model Mo_3Ni catalyst. Observations by TEM suggest a good dispersion of small Rh or Ir clusters on a MoS_2 phase, accounting for the enhanced activity, as compared to $[\text{Mo}_3+\text{Rh}]$ or $[\text{Mo}_3+\text{Ir}]$ systems.¹⁰⁸

2.16.7. Mo–Ni. The linear complex $[\text{Et}_4\text{N}]_2[\text{Mo}_2\text{NiS}_4\text{O}_4]$ was used as a precursor for alumina-supported catalysis in the HDS of thiophene.¹⁰³

Incorporating the cubane-type cluster $[\text{Mo}_3\text{NiS}_4\text{Cl}(\text{H}_2\text{O})_9]^{3+}$ (**133**) into various zeolites by ion-exchange afforded a catalytically active material in HDS of benzothiophene.⁴¹¹ In particular, 97% selectivity for ethylbenzene could be achieved with $\text{Mo}_3\text{NiS}_4/\text{KL}$, at 94% conversion, which is better than $\text{Mo}_3\text{S}_4/\text{KL}$. Also, EXAFS studies showed that the Mo_3NiS_4 cluster partially decomposes to $\text{Mo}_3\text{S}_4^{2-}$ and Ni^{2+} moieties after ion-exchange.⁴¹²



2.16.8. Mo–Pd, Mo–Pt. The impregnation of the cubane cluster $[\text{Mo}_3\text{Pd}(\mu_3\text{-S})_4\text{Cp}'_3(\text{PPh}_3)][\text{pts}]$ (**25d**) and $[\text{Mo}_3\text{Pt}(\mu_3\text{-S})_4\text{Cp}'_3(\text{NBE})][\text{pts}]$ (**25e**) on alumina, and subsequent sulfidation at 623 K, afforded heterogeneous materials consisting of large Pd or Pt aggregates poorly dispersed on a MoS_2 phase. The poor dispersion of these aggregates might be responsible for the low catalytic activity of the system in the simultaneous HDS of dibenzothiophene, HDN of indole, and hydrogenation of naphthalene (see sections 2.5.1.15 and 2.5.1.16). The coimpregnated $[\text{Mo}_3+\text{Pd}]$ and $[\text{Mo}_3+\text{Pt}]$ systems were more active.¹⁰⁸

2.16.9. W–Fe, W–Co. Thiophene HDS was performed in the presence of the alumina-supported complexes $[\text{Et}_4\text{N}]_2[\text{W}_2\text{FeS}_4\text{O}_4]$ and $[\text{Et}_4\text{N}]_2[\text{W}_2\text{CoS}_4\text{O}_4]$.¹⁰³

2.16.10. W–Rh. The dinuclear complex $[(\text{triphos})\text{Rh}(\eta^3\text{-CO})_5\text{WS}(\text{C}_6\text{H}_4)\text{CH}=\text{CH}_2]$ (triphos = $\text{MeC}(\text{CH}_2\text{PPh}_2)_3$) was used as a model catalyst for HDS of benzothiophene. The isolation of the intermediate complex $[(\text{triphos})\text{RhH}(\mu\text{-H})\{\mu\text{-o-S}(\text{C}_6\text{H}_4)\text{C}_2\text{H}_5\}\text{W}(\text{CO})_4]$ suggests a pathway involving hydrogenation of the C–C double bond of the heterocycle, followed by hydrogenolysis to 2-ethylthiophenolate and desulfurization to ethylbenzene + S products such as H_2S .⁴¹³

2.16.11. W–Ni. The linear trinuclear complex $[\text{Et}_4\text{N}]_2[\text{W}_2\text{NiS}_4\text{O}_4]$ was found to be very active in thiophene HDS reactions, with nickel having a promotion role.¹⁰³

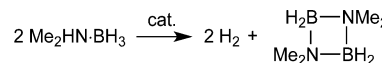
2.16.12. Ru–Co. The carbon- and γ -alumina-supported $[\text{RuCo}_2]$ and $[\text{Ru}_2\text{Co}]$ heterogeneous catalysts derived from $[\text{RuCo}_2(\mu_3\text{-S})(\text{CO})_9]$ and $[\text{HRu}_2\text{Co}(\mu_3\text{-S})(\text{CO})_9]$, respectively, were tested in thiophene desulfurization. Their activities were lower at 673 K than those of catalysts containing only Ru or Co, due to a lack of stability at such high temperatures. At

423 K, however, this trend was reversed, and mixed-metal catalysts showed higher initial conversions, although the reaction progressively stopped with time.⁴¹⁴

2.17. Dehydrogenation of Amine-boranes

2.17.1. Zr–Fe. Dehydrogenation of amine-boranes, as potential candidates for hydrogen storage, was investigated in the presence of heterobimetallic precursors. Thus, the dehydrogenation of $\text{Me}_2\text{NH}\cdot\text{BH}_3$ was performed in the presence of the complex $[\text{MeZr}(\mu\text{-}\eta^5\text{:}\eta^1\text{-C}_5\text{H}_4\text{PEt}_2)_2\text{FeCp}^*]$ at 323 K in toluene, affording H_2 with 75% of yield, along with cyclic $[\text{Me}_2\text{N}\cdot\text{BH}_2]_2$ (Scheme 73).⁴¹⁵

Scheme 73



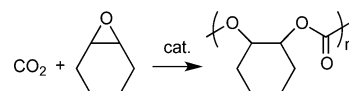
2.17.2. Zr–Ru. The dehydrogenation of $\text{Me}_2\text{NH}\cdot\text{BH}_3$ was catalyzed in toluene at 323 K by several Zr–Ru complexes. Yields of 85–98% were obtained with $[\text{MeZr}(\mu\text{-}\eta^5\text{:}\eta^1\text{-C}_5\text{H}_4\text{PEt}_2)_2\text{RuCp}^*]$, $[(\text{Me}_2\text{N})\text{Zr}(\mu\text{-}\eta^5\text{:}\eta^1\text{-C}_5\text{H}_4\text{PEt}_2)_2\text{RuCp}^*]$, and $[\{\text{Zr}(\mu\text{-}\eta^5\text{:}\eta^1\text{-C}_5\text{H}_4\text{PEt}_2)(\mu_3\text{-}\eta^5\text{:}\eta^1\text{-C}_5\text{H}_3\text{PEt}_2)(\mu\text{-H})\text{-RuCp}^*\}]$ for total conversions. The complexes $[\text{Cl}_2\text{Zr}(\mu\text{-}\eta^5\text{:}\eta^1\text{-C}_5\text{H}_4\text{PEt}_2)_2\text{RuClCp}^*]$, $[\text{Cl}\text{Zr}(\mu\text{-}\eta^5\text{:}\eta^1\text{-C}_5\text{H}_4\text{PEt}_2)_2\text{RuCp}^*]$, and $[(\text{BH}_4)\text{Zr}(\mu\text{-}\eta^5\text{:}\eta^1\text{-C}_5\text{H}_4\text{PEt}_2)_2\text{RuCp}^*]$ were poor catalysts under the same conditions, with H_2 yields below 10%. A mechanistic study with $[\text{MeZr}(\mu\text{-}\eta^5\text{:}\eta^1\text{-C}_5\text{H}_4\text{PEt}_2)_2\text{RuCp}^*]$ suggested the formation of hydrido clusters as intermediates, as well as the participation of both metallic centers in the activity.⁴¹⁵

2.17.3. Hf–Ru. The complex $[\text{MeHf}(\mu\text{-}\eta^5\text{:}\eta^1\text{-C}_5\text{H}_4\text{PEt}_2)_2\text{RuCp}^*]$ is a poor catalyst for the dehydrogenation of amine-boranes such as $\text{Me}_2\text{NH}\cdot\text{BH}_3$.⁴¹⁵

2.18. Miscellaneous

2.18.1. Ti–Zn. The copolymerization of CO_2 and cyclohexene oxide, catalyzed by $[\text{Cp}_2\text{Ti}(\text{OCH}_2\text{CH}_2\text{OZnEt})_2]$ under ambient conditions, afforded the corresponding poly(cyclohexene carbonate) (Scheme 74). After 100 h of reaction, 3.6 g of polymer per g of catalyst were obtained.⁴¹⁶

Scheme 74



2.18.2. Mo–Co. Liquefaction of a sub-bituminous and a bituminous coal was performed with a series of dispersed $[\text{Mo}_2\text{Co}_2]$ catalysts, among which the most active was that derived from the thiocubane cluster $[\text{Mo}_2\text{Co}_2\text{S}_4\text{Cp}_2(\text{CO})_2]$.⁴¹⁷

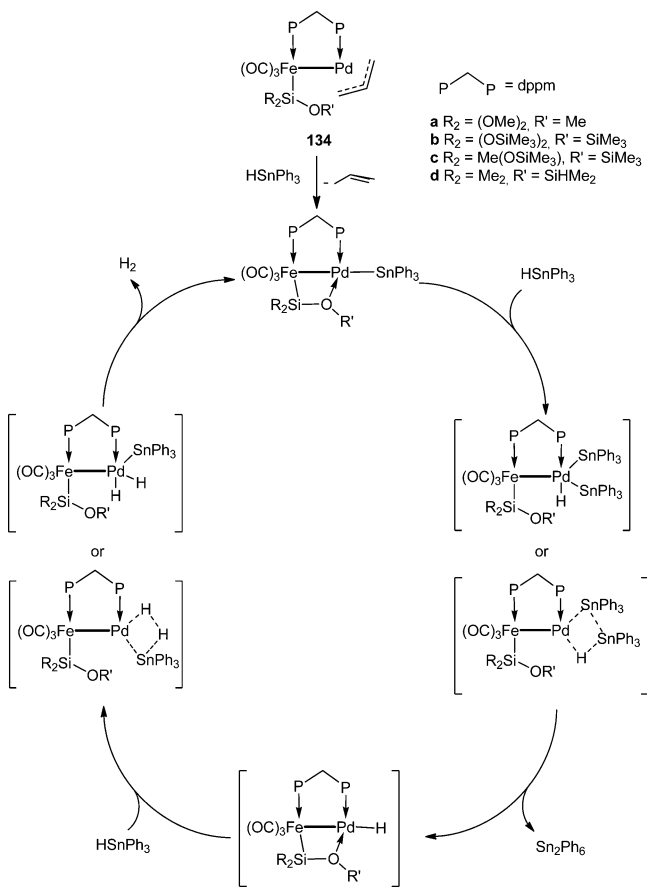
2.18.3. Mn–Zn. Catalytic water oxidation to O_2 , as a mimic reaction to natural photosynthesis, has recently emerged as a strategy toward green and renewable fuels. For this reason, many catalytic systems have been developed. While most organometallic-derived catalysts are obtained from mono- or dinuclear Mn-, Ru-, Ir-, or Pt-complexes,⁴¹⁸ heterometallic systems often consist of heterogeneous Co-based oxides.⁴¹⁹ However, Agapie and co-workers have synthesized a series of Mn-based clusters, relevant to the oxygen-evolving complex (OEC),⁴²⁰ the latter possessing a CaMn_4O_5 core involved in photosystem II (membrane protein). Some of them contain a zinc center: $[\text{LMn}_3\text{ZnO}_2(\text{OAc})_2(\text{MeCN})][\text{Otf}]_3$ ⁴²¹ and

$[LMn_3ZnO_4(OAc)_3]$ ⁴²² (L = a hexapyridyl trisalkoxido 1,3,5-triarylbenzene ligand). They were compared to Na-, Ca-, Sr-, Sc-, or Y-Mn systems, and electrochemical studies on those clusters provided useful information on the role of the redox-inactive center (early group heteroatom) in the OEC.

2.18.4. Re-Pt. Potential alumina-supported catalysts derived from $RePt_3$ molecular clusters such as $[Pt_3\{Re(CO)_3\}(\mu-dppm)_3][PF_6]$, $[Pt_3\{Re(CO)_3\}(\mu_3-O)(\mu-dppm)_3][PF_6]$, $[Pt_3\{Re(CO)_3\}(\mu_3-O)_2(\mu-dppm)_3][PF_6]$, and $[Pt_3(ReO_3)(\mu-dppm)_3][PF_6]$ were studied for petroleum refining. Their sulfidation by propylene sulfide has been investigated as a model for reactivity of metal surfaces and sulfidation of bimetallic Re-Pt/ Al_2O_3 catalysts.⁴²³

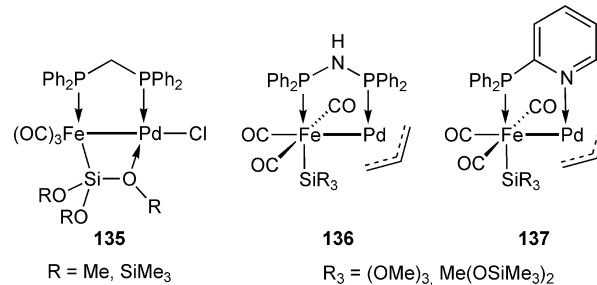
2.18.5. Fe-Pd. The heterobimetallic complexes $[(OC)_3\{R_2(R'O)Si\}Fe(\mu-dppm)Pd(\eta^3\text{-allyl})]$ (see 134, Scheme 75) and $[(OC)_3Fe\{\mu\text{-Si}(OR)_3\}(\mu-dppm)PdCl]$ ($R =$

Scheme 75

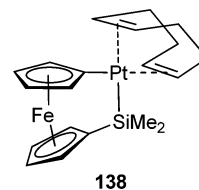


$Me, SiMe_3$) (135) are effective catalyst precursors for the dehydrogenative coupling of triorganotin hydrides $HSnR'3$ ($R' = Ph, n\text{-Bu}$) to $Sn_2R'6$.⁴²⁴ It is assumed that the bimetallic structure of the catalysts is retained throughout the reactions, and that the Sn moieties react with the catalyst to form a Fe-Pd-Sn intermediate (Scheme 75).⁴²⁵

The influence of the bridging phosphine ligand was also studied, by testing the activity of the complexes $[(OC)_3(R_3Si)Fe(\mu-L)Pd(\eta^3\text{-allyl})]$ ($R = OMe, Me(OSiMe_3)_2$; 134, $L = dppm$; 136, $L = dppa$; 137, $L = Ph_2Ppy$). It was found that the complex with a Ph_2Ppy -bridge was more active than that with a dppa bridge. The dppm-bridged complex was the least active of the three.⁴²⁶



2.18.6. Fe-Pt. The $[2]\text{-platinasilaferrrocenophane}$ $[(C_5H_4)_2Fe(SiMe_2)Pt(COD)]$ (138) was found to be a precatalyst for the ring-opening polymerization of the silicon-bridged complex $[Fe(C_5H_4)_2SiMe_2]$ to yield the poly(ferrrocenylsilane) $\{[Fe(C_5H_4)_2SiMe_2]\}_n$. A key step for the reaction is believed to involve dissociation of the COD ligand.⁴²⁷



2.18.7. Co-Rh. The cluster $[Co_2Rh_2(CO)_{12}]$ was entrapped in an alumina sol-gel matrix for applications in catalytic disproportionation of dihydroarenes. The products were a mixture of fully aromatic and tetrahydrogenated compounds. For instance, 1,3-cyclohexadiene afforded a mixture of cyclohexane (47.5% yield) and benzene (50% yield). When supported on a silica sol-gel matrix, the same cluster was totally inactive, suggesting an important role of the support. This can be explained by the change of nature of the cluster when set in contact with the support: on silica, alloying occurs, while on alumina, no NPs are observed in the reaction conditions.⁷⁴

3. SYNTHESIS OF SPECIFIC CHEMICAL FUNCTIONS IN THE PRESENCE OF HETEROMETALLIC CATALYSTS

This section presents the metal couples used for the synthesis of a given chemical function. Trends and results are provided, based on the description given in section 2. A list of the different metal couples used for the synthesis of various chemical functions is given in Table 3.

3.1. Synthesis of Alkanes

Among all of the reactions that were mentioned in section 2, several can lead to the formation of alkanes. Indeed, hydrocarbon skeletal rearrangements (see section 2.4) can afford lighter alkanes via hydrogenolysis. Similarly, hydrogenation of alkenes or alkynes can lead to alkanes (see section 2.5.1), and so does hydrogenation of CO (see section 2.5.2).

Thus, Re-Ir, Fe-Ru, Fe-Rh, and Rh-Ir bimetallic complexes were found to yield active catalysts in ethane hydrogenolysis, affording methane as the main product.

Butane hydrogenolysis can yield C_1 to C_3 products. It was observed that Mo-Ir and W-Ir clusters were very selective for ethane, and a high Ir content in the catalyst precursor increases the activity. Similarly, Rh-Ir complexes favor central C-C bond scission of butane. In this case, however, increasing the Ir content seemed to lower the activity. On the other hand, Fe-Rh clusters supported on NaY zeolites were found to be more

Table 3. Utilization of Molecular Mixed-Metal Clusters for the Synthesis of Chemical Functions

catalyzed reaction	homogeneous catalysts	immobilized catalysts	heterogeneous catalysts
Synthesis of Alkanes by hydrocarbon skeletal rearrangements			Cr–Pd, Mo–Ir, W–Ir, W–Pd Re–Os, Re–Ir, Re–Pt Fe–Ru, Fe–Rh, Fe–Pt, Ru–Ni, Ru–Pt Co–Rh, Co–Pt, Rh–Ir, Ir–Pt, Pt–Cu, Pt–Au
by hydrogenation of C–C multiple bonds	Ta–Rh, Ta–Ir Mo–Fe, Mo–Fe–Co, Mo–Ru–Co Mo–Co, Mo–Co–Ni, Mo–Rh Mo–Pd, Mo–Pt W–Fe–Co, W–Os W–Ni, W–Pd, W–Pt Mn–Fe, Re–Rh, Re–Pt Fe–Ru–Co, Fe–Rh Ru–Co, Ru–Rh, Ru–Ir, Ru–Ni, Os–Ni Co–Pt, Rh–Au, Ir–Pt	Mo–Pd, Fe–Pt Ru–Os, Ru–Pt Os–Rh, Os–Au Co–Pt, Rh–Pt	Ta–Rh, Ta–Ir Mo–W–Fe, Mo–W–Co, Mo–W–Ni Mo–Fe, Mo–Fe–Co, Mo–Co, Mo–Ni W–Fe, W–Co, W–Ni, W–Pt Fe–Ru, Fe–Co Ru–Os, Ru–Co, Ru–Ni, Ru–Pd, Ru–Pt Ru–Cu, Ru–Ag, Os–Ni Co–Rh, Rh–Pt Pt–Cu, Pt–Au
by hydrogenation of CO or CO ₂	Fe–Co, Ru–Co	Fe–Co	Cr–Ru, Mo–Fe, Mo–Ru, Mo–Co, Mo–Ni, W–Ir Mn–Fe, Mn–Ru, Re–Os Fe–Ru, Fe–Co, Fe–Rh, Fe–Pd, Fe–Pt Ru–Os, Ru–Co, Os–Rh, Os–Ni Co–Cu
Synthesis of Alkenes by isomerization of olefins	Ta–Rh, Ta–Ir, Cr–Fe, Cr–Pd Mo–Fe, Mo–Ru–Co, Mo–Co–Ni, Mo–Pd W–Fe, W–Ru–Co, W–Pd Mn–Fe, Fe–Ru, Fe–Co, Fe–Rh, Fe–Pd Ru–Co, Ru–Ni, Ru–Cu, Ru–Au Os–Rh, Os–Ni, Co–Pt	Ru–Os Os–Rh Os–Au	Fe–Pd, Ru–Os, Co–Rh
by olefin metathesis	Ti–Ru	Cr–Mo, Cr–W	Mo–Rh
by hydrogenation of C–C multiple bonds	V–Fe, Cr–Pd Mo–Fe, Mo–Fe–Co, Mo–Co–Ni Mo–Rh, Mo–Ir, Mo–Pd, Mo–Pt W–Fe–Co, W–Os, W–Rh, W–Ir, W–Pd, W–Pt Mn–Ru, Re–Rh Fe–Ru, Fe–Ru–Co, Fe–Pd Ru–Rh, Ru–Ir, Ru–Ni, Ru–Pt Os–Ni Co–Rh, Co–Pt, Rh–Au	Mo–Pd Fe–Ru	Mo–Ru, Mo–Rh, Mo–Ir, Mo–Pd, Mo–Pt Fe–Ru, Ru–Co, Ru–Pd, Ru–Pt, Ru–Cu Os–Ni, Os–Ni–Cu Co–Rh
by hydrogenation of CO or CO ₂			Mo–Fe, Mn–Fe, Fe–Co, Fe–Rh
by dehydrogenation of alkanes			Mo–Pt, Re–Pt, Pt–Au
by dehydration of alcohols	Mo–Pd		Os–Ni, Pd–Zn
Synthesis of Alcohols			
by hydrogenation of CO or CO ₂	Ti–Rh	Co–Rh	Cr–Ru, Cr–Pt, Mo–Ru, Mo–Rh, W–Rh, W–Pt
	Ru–Cu, Ru–Ag, Ru–Au Co–Rh, Rh–Ir, Rh–Pt Rh–Cu, Rh–Ag, Rh–Au		Mn–Fe, Mn–Ru Fe–Ru, Fe–Rh, Fe–Ir, Fe–Pd, Fe–Pt Ru–Co, Ru–Ni, Co–Rh, Co–Cu
by hydrogenation of aldehydes and ketones	Cr–Ru, Mo–Ru, W–Ru Fe–Ru, Ru–Rh, Ru–Ir		Mo–Co, Mo–Rh Ru–Pt, Os–Ni Co–Cu, Co–Zn
by homologation of methanol	Fe–Co Ru–Co, Ru–Co–Au, Ru–Rh Os–Co, Co–Rh, Co–Pd		
by oxidation of alkanes and alkenes	Fe–Co, Fe–Co–Cu Co–Cu, Co–Cu–Zn	V–Co	
by hydroformylation of olefins			Mo–Rh Fe–Ir, Fe–Pd, Fe–Pt, Ru–Co

Table 3. continued

catalyzed reaction	homogeneous catalysts	immobilized catalysts	heterogeneous catalysts
Synthesis of Alcohols			Co–Rh
by reductive alkylation of aldehydes	Co–Zn		
Synthesis of Ethers			
by hydrogenation of CO or CO ₂	Ti–Rh, Ru–Rh		Cr–Ru, Mo–Ru, Mo–Rh, W–Rh Mn–Fe, Mn–Ru, Fe–Ru, Fe–Os, Fe–Rh Ru–Os, Ru–Co, Ru–Ni Os–Rh, Co–Rh
by homologation of methanol	Mn–Pd, Co–Pd, Co–Pt		
by carbonylation of alcohols	Mo–Fe, Fe–Ni, Fe–Cu, Fe–Hg		
Synthesis of Aldehydes			Ru–Ni, Os–Ni, Os–Ni–Cu
by dehydrogenation of alcohols	Cr–Ru, Cr–Os		
by oxidation of alcohols	Ru–Ni, Ru–Pd, Ru–Pt		
by homologation of methanol	Fe–Co, Co–Pd, Co–Pt		Ru–Co, Co–Pd
by hydrocarbonylation of methanol	Zr–Rh		
by carbonylation of olefins	Ti–Rh, Zr–Rh	Ru–Co	Mo–Rh, Fe–Rh, Fe–Ir, Fe–Pd, Fe–Pt
by hydroformylation of olefins	Cr–Ru, Cr–Pd	Co–Rh	Co–Rh, Co–Cu
	Mo–Fe–Co, Mo–Ru, Mo–Co, Mo–Co–Ni	Co–Pd	
	W–Ru, W–Rh, W–Pd, Mn–Rh		
	Fe–Ru, Fe–Co, Fe–Rh, Ru–Co, Ru–Rh		
	Co–Rh, Co–Ni, Co–Pt		
	Rh–Zn, Ir–Cu		
Synthesis of Ketones			
by oxidation of alkanes and alkenes	Fe–Co, Fe–Co–Cu, Fe–Cu	V–Co, V–Rh	Cr–Mn, Cr–Co, Mn–Co
	Co–Cu, Co–Cu–Zn	Fe–Cu	Pt–Au
	Pd–Cu, Pt–Au		
by oxidation of alcohols	Cr–Os		
by intramolecular hydroacylation	Ti–Rh		
by Pauson–Khand reactions	Fe–Co, Ru–Co, Co–Pt		Co–Rh
Synthesis of Carboxylic Acids			
by hydrogenation of CO or CO ₂	Mo–Ru, W–Ru		
by carbonylation of alcohols	Os–Ir, Ir–Pt		
Synthesis of Esters			
by hydrogenation of CO or CO ₂	Mn–Pd		
by homologation of methanol and methyl acetate	Mn–Pd, Ru–Co		
by carbonylation of alcohols	Co–Pd, Co–Pt		
by carbonylation of olefins	Mo–Fe, Fe–Rh, Fe–Ni, Fe–Cu, Fe–Hg		
by addition of carboxylic acids to alkynes	Os–Ir, Ir–Pt		
by transesterification	Fe–Pd		
	Ti–Ru, Mo–Pd, Re–Ru		
	Co–Zn, Co–Cd, Zn–Cd		
Synthesis of Lactones			
by oxidation of THF	Mo–Ru		
by cyclization of alkynoic acids	Mo–Ni, Mo–Pd		Fe–Rh, Co–Rh
Synthesis of Acetals			
by oxidation of alcohols			Ta–Re
by homologation of methanol	Mn–Pd, Co–Pd, Co–Pt		
by hydrocarbonylation of methanol			Ru–Co, Co–Pd

Table 3. continued

catalyzed reaction	homogeneous catalysts	immobilized catalysts	heterogeneous catalysts
Synthesis of Ketals by addition of alcohols to alkynes	Ir–Pd, Ir–Pt		
Synthesis of Isocyanates and Carbamates by carbonylation of organic nitro derivatives	Fe–Rh, Ru–Rh, Os–Rh Os–Au		Mo–Pd, Fe–Pd
Synthesis of Ammonia by hydrogenation of N ₂ by N–N bond cleavage	V–Fe, Mo–Fe, Mo–Ru		Ru–Ni, Os–Ni
Hydrogen Storage by WGSR	Fe–Ru, Fe–Co, Fe–Ir Ru–Co, Ru–Rh Co–Rh, Co–Ir		
by dehydrogenation of amine-boranes	Zr–Fe, Zr–Ru, Hf–Ru		

selective toward C₁+C₃ products, and a Ru–Pt cluster gave good selectivities for methane or ethane, depending on the support used.

Cyclopentane could be hydrogenolyzed to methane and C₂₊ alkanes with a Re–Pt cluster.

Hexane hydrogenolysis was achieved with Pt–Cu and Pt–Au clusters, with a rather good selectivity for ethane (almost 50%).

Hydrogenolysis of methylcyclopentane was achieved with several heterometallic catalysts. In particular, demethylation of methylpentane has been performed with Pt containing catalysts, as it is known to be an excellent catalyst for this reaction. Thus, Fe–Pt and Co–Pt clusters were found to catalyze that reaction with results close to monometallic [Pt]. In a similar fashion, a Ru–Ni heterogeneous catalyst allowed for methylcyclohexane demethylation during the reduction of toluene to cyclohexane. Conversely, a Co–Rh cluster catalyzed the C–C bond scission of methycyclopentane to afford the acyclic C₆ isomers (hexane, 2-methylpentane, and 3-methylpentane) with good selectivity. Also, Cr–Pd and W–Pd clusters were found to be active catalysts precursors for the isomerization of 2-methylpentane. However, they exhibited very different selectivities: the former favors methylcyclopentane, while the latter yields mainly 2-methylpentane.

Another way to obtain alkanes is to fully hydrogenate the corresponding alkenes or alkynes. Although isomerization of C=C bonds usually occurs during the reaction, various substrates can be hydrogenated with heterometallic clusters as catalyst precursors. In this manner, aliphatic alkenes (linear C₂–C₁₂, cyclohexene) were hydrogenated to the corresponding alkanes. In particular, Co-containing trimetallic (Mo–Fe–Co, Mo–Ru–Co, Mo–Co–Ni, W–Fe–Co, Fe–Ru–Co) precursors were used to hydrogenate 2-pentene to pentane. Aromatic alkenes, such as benzene or toluene, were very efficiently hydrogenated to cyclohexane and methylcyclohexane with Fe–Ru, Fe–Co, Ru–Co, and Ru–Ni catalysts. Moreover, a Co–Rh heterogeneous catalyst was found to allow full hydrogenation of styrene and 1,2-hydronaphthalene to ethyl cyclohexane and decalin, respectively. Also, RuCu NPs, derived from the carbido cluster [PPN]₂[Ru₁₂Cu₄(C)₂(μ-Cl)₂(CO)₃₂], allowed for the quantitative and 100% selective hydrogenation of phenyl-acetylene to ethylbenzene. However, Cu and Au were found to

lower the activity of Pt catalysts in toluene and benzene hydrogenation.

The Fischer–Tropsch process, involving reactions between CO and H₂, often leads to a range of products, including alkanes, alcohols, and sometimes alkenes or other oxygenates. Some catalysts seem to favor the formation of methane (CO methanation). Among all of the clusters used as catalysts precursors here, most of them afford methane as the main product, along with C₂₊ alkanes. In particular, Os–Ni catalysts showed excellent selectivity for methane (close to 100%). In general, group VIII containing bimetallic catalysts are very active in CO methanation. Also, Fe–Pd and Fe–Pt catalysts were found to be more selective toward methane when the Fe/Pd or Fe/Pt ratios were superior to 1, while they yielded mainly methanol when the ratio was 1. Mn was found to enhance the selectivity of iron-based catalysts toward C₂–C₄ olefins, rather than toward methane. At higher temperatures, aromatic compounds were obtained.

3.2. Synthesis of Alkenes

Alkenes can be obtained by a range of reactions that were mentioned in the previous paragraphs. Olefin isomerization (see section 2.2) and hydrogenation (see section 2.5.1) are often competing reactions because they take place under H₂ pressure and they are usually used to obtain branched or internal alkenes starting from α-olefins. Olefin metathesis (see section 2.3) represents a greener route than common alkene syntheses, and usually leads to less byproducts and waste. The Fischer–Tropsch process can be a route to alkenes, but the selectivities and activities still remain low and not many efficient heterometallic catalysts have been described yet (see section 2.5.2). Routes like dehydrogenation of alkanes (see section 2.6) or dehydration of alcohols (see section 2.7) are still to be explored further, even if some results are already available.

Isomerization of olefins with heterobimetallic catalysts was mainly achieved with linear α-olefins (C₄–C₈) as substrates. Catalysts containing group VIII metals were the most studied, and they were generally combined with group VI or VIII metals to give the best results. Some M–Au (M = Ru, Os) catalysts were found to be less active than monometallic group VIII catalysts. A Fe–Rh catalyst was observed to be more selective toward isomerization than hydrogenation products, which is

rather unusual. Other substrates, such as 1,5-COD and linear dienes, were isomerized by M–Pd (M = Cr, Mo, W) and M–Ni (M = Ru, Os) catalysts, respectively. Allylbenzene and *cis*-stilbene could also be isomerized, mainly by group VII + group VIII catalysts.

Olefin metathesis has not been studied with many heteronuclear cluster-derived catalysts. Indeed, only four metal couples have been used so far. The ring-closing metathesis of *N,N*-diallyltosylamide was catalyzed by a Ti–Ru allenylidene complex to yield 3-tosylamide cyclopentene. Also, reduced Phillips-type catalysts from immobilized Cr–Mo and Cr–W carbene or carbyne complexes were successfully used in olefin metathesis, and Mo–Rh cubane-derived heterogeneous catalysts were found to catalyze propene metathesis.

Hydrogenation of alkynes usually affords mixtures of alkanes and alkenes, as mentioned above. Thus, acetylene could be selectively hydrogenated to ethylene by V–Fe, Mo–Fe, Mo–Fe–Co, and Os–Ni catalysts. Similarly, pentynes and hexynes could be reduced to the corresponding alkenes mainly by Fe–Ru catalysts, although Fe–Rh, Os–Ni, or Co–Pt catalysts were also used. Oct-1-yne and *t*-Bu-propiolate could be hydrogenated selectively to oct-1-ene and *t*-Bu-acrylate, respectively, by Mo–Rh, Mo–Ir, W–Rh, and W–Ir catalysts. The Mo–Rh catalyst was found to be the most active. Phenylacetylene can be hydrogenated to a mixture of styrene and ethylbenzene. Mo–Pd, Mo–Pt, W–Pd, and W–Pt catalysts were found to be highly selective for the formation of styrene. Ru–Pt and Os–Ni species were also selective for styrene. Diphenylacetylene reduction was studied with Fe–Ru, Ru–Ir, Co–Pt, or Rh–Au bimetallic species, but the most active heterometallic catalyst found was the cluster $[Ru_6Pt_3(\mu_3\text{-H})(\mu\text{-H})(\mu_3\text{-PhC}\equiv\text{CPh})\text{-}(\text{CO})_{20}]$, which exhibits 100% selectivity to *cis*-stilbene at almost full conversion.

The reduction of CO through the Fischer–Tropsch process often affords alkenes as byproducts. In some cases, it has been possible to tune the selectivity of the catalysts to enhance the formation of olefins. Thus, using heterometallic cluster-derived catalysts, it appeared that adding Mn to Fe-based catalysts enhanced that selectivity. Moreover, the use of potassium in Fe–Co systems was found to improve the selectivity toward olefins, despite the apparent loss of activity. Also, Fe–Rh systems were able to catalyze CO hydrogenation to a mixture of methane and C₂–C₄ alkenes.

Dehydrogenation of alkanes can lead to the corresponding alkenes. Not many cluster-derived heterometallic catalysts were used for such reactions, and it appears that all of them contain platinum and are supported on inorganic supports. Indeed, Mo–Pt catalysts for butane, isobutane, and propane dehydrogenation showed very high selectivity for the corresponding alkenes, with better stability and activity than conventional Mo–Pt catalysts. Also, methylcyclohexane could be dehydrogenated to toluene in the presence of a Re–Pt catalyst, which proved to be more resistant to deactivation than common catalysts. Finally, Pt–Au systems containing significant amounts of phosphorus were successfully used for the conversion of hexane and propane to the corresponding alkenes. Although the activity was rather low (10–35%), the selectivity was higher than 90% with both substrates, most likely due to the presence of phosphorus in the catalyst.

The dehydration of alcohols constitutes another way to obtain alkenes. However, it has not been explored significantly with cluster-derived heterometallic catalysts. Thus, a Mo–Pd catalyst was found to dehydrate PhCH₂OH to *trans*-stilbene,

while a Pd–Zn system afforded a mixture of C₃–C₁₀ olefins in the dehydration of EtOH.

3.3. Synthesis of Alcohols

Various methods are available to obtain alcohols. If the Fischer–Tropsch process can lead to oxygenates (see 2.5.2), the main issue lies in the selectivity. The same applies to the hydrogenation of aldehydes and ketones (see section 2.5.3) because breaking of C–C bonds can occur under high H₂ pressure. Methanol homologation is an efficient way to produce ethanol (see section 2.10.1) even if other oxygenates may be formed in rather large amounts (aldehydes, esters, carboxylic acids, acetals, etc.). Hydroformylation, although it affords mainly aldehydes, often yields alcohols as well (see section 2.10.3.1). The reduction of aldehydes affords alcohols (see section 2.10.12) in a straightforward manner.

As mentioned in sections 3.1 and 3.2, some cluster-derived heterometallic catalysts were found to favor the formation of methane and alkanes, or even alkenes in CO hydrogenation. Yet other systems afford oxygenates, and in particular alcohols, as major products. Thus, it appears that Rh-containing catalysts enhance the selectivity toward oxygenates and Ti–Rh catalysts exhibit more than 50% selectivity for oxygenates. Mo–Rh and W–Rh systems appeared to favor the formation of methanol and oxygenates, whereas Fe–Rh catalysts were highly active and selective for oxygenates, even though the Rh–Ir analogues were more selective for methanol. Co–Rh, Rh–Ir, Rh–Pt, or Rh–M (M = Cu, Ag, Au) MMCDs gave mixtures of oxygenates such as methanol, glycerol, and ethylene glycol. Ruthenium is known to be selective for the formation of methanol; thus some Ru-based systems showed good selectivities for methanol synthesis in CO hydrogenation. In particular, Cr–Ru and Mo–Ru systems allowed for selectivities in the range of 12–20% for oxygenates. Mn–Ru catalysts showed even better selectivities, although lower than Ru–Co, the selectivity of which is higher than 50%. Ru–M (M = Cu, Ag, Au) systems gave oxygenates as major products, and no hydrocarbon product could be detected. Other active catalytic systems were obtained from Fe–Pd and Fe–Pt compounds, especially for methanol synthesis. Also, Cr–Pt and W–Pt clusters offered very selective systems for the synthesis of methanol through CO₂ reduction (>90%).

Hydrogenation of aldehydes and ketones is an efficient route to obtain alcohols, provided the selectivity can be controlled and C–C bond scission avoided. Cluster-derived heterometallic catalysts were used to hydrogenate various aldehydes and ketones. Acetaldehyde could be hydrogenated to ethanol with rather good selectivity in the presence of a Mo–Rh catalyst. Also, Co-based (Mo–Co, Co–Cu, Co–Zn) catalysts were successfully used in the selective hydrogenation of crotonaldehyde to crotyl alcohol, thus favoring the reduction of the C=O bond over the C=C bond. Cyclohexanone has been used as a standard substrate during hydrogenation reactions, in the presence of M–Ru (M = Cr, Mo, W, Fe) catalysts. Mo–Ru exhibited the highest activity, while W–Ru was the least active system. Fe–Ru only showed moderate activity. Similarly, Ru–Rh and Ru–Ir complexes were used as catalysts in the proton transfer from propan-2-ol to cyclohexanone (to afford cyclohexanol) or to benzylideneacetophenone. They proved to be more active than monometallic complexes. Finally, a Os–Ni system was found to hydrogenate acetone to isopropanol, whose dehydration yielded propylene, which was subsequently hydrogenated to propane.

Alkane or alkene oxidation by hydrogen peroxide is a way to obtain alcohols. While oxidation with O_2 usually only leads to ketones (and aldehydes), the use of H_2O_2/O_2 allows for a milder oxidation and thus for the formation of alcohols. Mostly, Co-based heterometallic systems were used for such reactions. Thus, oxidation of cyclohexane in air with a V–Co catalyst afforded a mixture of cyclohexanone (up to 75% selectivity) and cyclohexanol. Oxidation of cyclohexane with H_2O_2 in the presence of Fe–Co, Fe–Co–Cu, or Fe–Cu catalysts afforded mainly cyclohexanone, with some smaller amounts of cyclohexanol. The same reactions were tested with Co–Cu and Co–Cu–Zn systems. They afforded a mixture of $C_6H_{10}O$, CyOH, and CyOOH. It was observed that the addition of Zn in the system lowered much the activity. The addition of PPh_3 to the reaction mixture appeared to enhance the selectivity toward cyclohexanol through reduction of hydroperoxycyclohexane.

Some Fe-based heterometallic catalysts were used in hydroformylation of olefins to afford alcohols. Typically, Fe–Ir, Fe–Pd, and Fe–Pt catalysts were used in ethylene hydroformylation and exhibited enhanced selectivities toward alcohols. Ru–Co systems showed increasing selectivity for *n*-alcohols with increasing the Co content in hydroformylation of various olefins. Similarly, Co–Rh catalysts, in the presence of NEt_3 , afforded very high yields of *C*₇-alcohols in 1-hexene hydroformylation.

Methanol homologation has been catalyzed in the presence of iodine-based promoters and various heterometallic clusters with metals from groups 8 and 11. In particular, Fe–Co systems were highly selective for ethanol when long reaction times and high reaction temperatures were used, despite lower conversions than at lower temperatures. Also, Ru-based systems such as Ru–Co, Ru–Co–Au, or Ru–Rh showed good activities and improved selectivities for ethanol because they favor hydrogenation of acetaldehydes during the process. In the case of the Ru–Rh system, synergistic effects are believed to operate, because it is more active than mixtures of the monometallic species. Os–Co and Co–Rh clusters showed high activities, but were less selective for ethanol than Ru–Co catalysts. In contrast, Co–Pd and Co–Pt compounds yielded almost no ethanol.

The reduction of aldehydes is a straightforward method to afford alcohols. In particular, using an axially chiral Co–Zn complex, it has been possible to perform the reductive alkylation of benzaldehyde to (*S*)-1-phenylpropan-2-ol.

3.4. Synthesis of Ethers

Among the numerous ways available to synthesize ethers, the Fischer–Tropsch process is a possibility, because oxygenates, including ethers, are among the main products (see section 2.5.2). Methanol homologation can lead to ethers too, among other oxygenates such as esters and aldehydes (see section 2.10.1). Carbonylation of alcohols in the presence of alkyl iodides may lead to the formation of ethers (see section 2.10.2.1).

If Ti–Rh, M–Ru (M = Cr, Mo, Mn, Co), W–Rh, and Mn–Fe systems can afford oxygenated compounds with rather good selectivities during the Fischer–Tropsch process, the main products are mixtures of oxygenates. However, Fe–Os and Os–Rh MMCD catalysts supported on alumina were found to afford ethers in rather good yields. In particular, Fe–Os is more selective, but less active than its Os–Rh counterpart. Also, Ru–Os MMCD/alumina species are slightly active, and yield mainly hydrocarbons with some dimethyl ether. Ru–Rh catalysts were

found to yield ethylene glycol as major product, with some monoalkyl ether derivatives.

Homologation of methanol in the presence of heterometallic cluster-derived catalysts is not very efficient for the synthesis of ethers, and only small amounts of Me_2O could be obtained. Moreover, only group 10-based (i.e., Pd and Pt) catalysts afforded ethers, as they tend to favor hydrogenation of carbonylated intermediates during the process. A Mn–Pd iodo-complex in the presence of aqueous HI yielded mainly 1,1-dimethoxyethane, along with some dimethyl ether. Co–Pd and Co–Pt systems showed up to 30% selectivity for acetaldehyde dimethylacetal, while the selectivity for Me_2O was less than 20%.

During methanol carbonylation reactions in the presence of EtI, diethyl ether was obtained as the main product, depending on the catalyst used, and only small amounts of the corresponding ester were detected. Indeed, with a series of Fe-based systems, Et_2O was the main product (with 70–80% selectivity) when Mo–Fe, Fe–Cu, or Fe–Hg catalysts were used. Conversions were typically above 85–90%. However, when a Fe–Rh complex was used, the activity and selectivity for ethyl propionate drastically improved (almost quantitative).

3.5. Synthesis of Aldehydes

Among the available routes to synthesize aldehydes, dehydrogenation of alcohols is rather efficient, because it yields only a few byproducts (see section 2.6). Oxidation of alcohols also affords aldehydes with rather good selectivity (see section 2.9.2). Homologation of methanol produces acetaldehyde, which often undergoes further hydrogenation to ethanol, but under appropriate conditions, and using adapted catalytic systems, it is possible to limit hydrogenation (see section 2.10.1). Hydrocarbylation of methanol affords aldehydes (see section 2.10.2.2), and carbonylation of olefins can lead to unsaturated aldehydes (see section 2.10.2.3). Hydroformylation of olefins is widely used in industry to produce aldehydes. However, under CO/H_2 pressure, subsequent hydrogenation often takes place to yield alcohols (see section 2.10.3.1).

Dehydrogenation of methanol and ethanol to the corresponding aldehydes could be achieved with Ni-based supported MMCD catalysts (Ru–Ni, Os–Ni, and Os–Ni–Cu). Interestingly, the Cu-containing system afforded ethylene during dehydrogenation of ethanol, which was further carbonylated to acetaldehyde.

Oxidation of a broad range of alcohols with molecular O_2 and in the presence of Cr–Ru and Cr–Os complexes afforded the corresponding aldehydes with rather good activities and selectivities. Similarly, Ru–M (M = Ni, Pd, Pt) catalysts performed the oxidation of benzyl alcohol to benzaldehyde with good selectivity. The most active system was Ru–Ni, while Ru–Pd and Ru–Pt exhibited similar activities.

For the hydroformylation of olefins, Rh-based catalysts offer good results overall, as do monometallic Rh catalysts. Thus, Mn–Rh, Fe–Rh, Co–Rh, and Rh–Zn systems were used for the hydroformylation of substrates such as ethylene, propene, 1-pentene, or styrene. Also, “early late” transition metal complexes appeared to give very good results. In particular, a Ti–Rh catalyst showed very high activity in hydroformylation of 1-hexene, and the already high selectivity toward *n*-heptanal (vs branched heptanals) could be greatly enhanced by the addition of chiral phosphines. Similarly, the addition of PPh_3 to a Zr–Rh catalyst already able to convert 100% of olefins resulted in highly selective hydroformylation of 1-hexene.

These systems were also used for the hydroformylation of styrene and 1,5-COD. Bimetallic M–Ru ($M = Cr, Mo, W, Fe$) and M’–Pd ($M' = Cr, Mo, W$) catalysts were used for styrene hydroformylation. Among them, the Fe–Ru system was found to be the most active (>40%), even though its selectivity for heptanal was rather low (<60%). All Cr- and Mo-based systems were almost inactive (<2% yield), while W-based ones had activities in the range of 10–15%. Other systems, such as Mo–Fe–Co, Mo–Co, or Mo–Co–Ni, were used in olefin hydroformylation. The latter two led to concomitant isomerization, thus affording hexanal and 2-methylpentanal in 1-pentene hydroformylation. A Fe–Co catalyst showed good hydroformylation activity for terminal, internal, and cyclic olefins with very high selectivity (close to 100%). Cobalt-based systems, such as Co–M ($M = Ni, Pd, Pt$), were used with substrates like propylene, 1-pentene, 1-hexene, 1,3-butadiene, or styrene. A Co–Cu catalyst offered very low activity, but rather good selectivity for propanal in ethylene hydroformylation. Interestingly, Fe–Pd and Fe–Pt catalysts were more selective for alcohols by favoring the hydrogenation step of the first formed aldehydes.

Homologation of methanol in the presence of a Fe–Co catalyst afforded acetaldehyde with rather high selectivity (80%) at high conversions (75%). In contrast, Co–Pd and Co–Pt systems gave low yields of acetaldehyde (<10%). However, the main product was acetaldehyde dimethylacetal, which was obtained with ca. 30% yield.

Hydrocarbonylation of methanol, which is performed under CO/H_2 pressure, usually affords aldehydes, and using Ru–Co and Co–Pd heterogeneous catalysts, it was possible to form acetaldehyde and the corresponding acetal: $MeCH(OMe)_2$. Other products were methyl acetate, originating from carbonylation, as well as methane, due to CO hydrogenation.

Homogeneous carbonylation of ethylene to acrolein could be initiated in the presence of PPh_3 and a Zr–Rh complex.

3.6. Synthesis of Ketones

Oxidation of alkanes and alkenes (see section 2.9.1) or alcohols (see section 2.9.2) can lead to the formation of ketones. Cyclic enones may be obtained through intramolecular hydroacylation (see section 2.10.4) or Pauson–Khand reactions (see section 2.10.6).

A V–Co catalyst was used in oxidation of cyclohexane to cyclohexanone with more than 75% selectivity. Similarly, a V–Rh compound catalyzed oxidation of propene to acetone. Three metal couples were tested in oxidation of cyclohexene to cyclohexenone: Cr–Mn, Cr–Co, and Mn–Co. Immobilized Fe–Co, Fe–Co–Cu, Co–Cu, and Co–Cu–Zn catalysts were found to yield ketones and alcohols by oxidation of cyclic alkanes using hydrogen peroxide. However, Zn appeared to lower the activity of the system. A Fe–Cu immobilized complex gave high selectivity (up to 87%) at 14% conversion under similar conditions. Also, a Pd–Cu compound was used as a catalyst for the oxidation of alkenes to ketones.

While the oxidation of primary alcohols affords aldehydes, that of secondary alcohols leads to ketones. A Cr–Os complex was used as an efficient catalyst for the synthesis of ketones starting from secondary alcohols.

Intramolecular hydroacylation of alkene-aldehydes affords cyclic alkenones. A Ti–Rh complex was used with excellent selectivity for the targeted cyclic ketones with yields close to 100% in the intramolecular hydroacylation of 3-phenyl-4-pentenal. Other 3-substituted pentenals, such as styrene 2-

carboxaldehyde, were converted to the corresponding cyclic ketones with ca. 40% yields.

PKR reactions offer an efficient route toward cyclic enones with good regioselectivity. Indeed, Co-based clusters (Fe–Co, Ru–Co, and Co–Pt) were used as homogeneous catalysts for the intramolecular PKR reaction of diethyl (allylpropargyl)-malonate to afford the corresponding enone. The conversion was almost quantitative in all cases, but the selectivities were different. While the Fe–Co system gave ca. 65% yield, the Co–Pt cluster led to yields in the range of 85–93% and the Ru–Co one to more than 90% selectivity. Heterogeneous Co–Rh catalysts were used in a broad range of reactions involving aldehydes as CO source and alkynes to afford substituted cyclic enones. The same systems were also used in the intramolecular PKR-like reaction between CO and allenynes or CO and bisallenenes to afford the corresponding cyclic enones.

3.7. Synthesis of Carboxylic Acids

Several routes are available for the synthesis of carboxylic acids. Among them, hydrogenation of carbon dioxide is a way to obtain formic acid (see section 2.5.2). Carbonylation of methanol (see section 2.10.2.1) also affords carboxylic acids.

Low activity was observed in CO_2 hydrogenation in the presence of Mo–Ru and W–Ru catalysts. However, monometallic Ru catalysts were not active at all.

Carbonylation of methanol in the presence of Os–Ir or Ir–Pt complexes and of MeI or HI as cocatalyst afforded acetic acid and methyl acetate. Because of the excess of methanol in the reaction mixture, ester formation is favored, thus decreasing the yield of acetic acid.

3.8. Synthesis of Esters

Among the numerous routes available to synthesize esters, hydrogenation of CO and CO_2 is a possibility (see section 2.5.2). Homologation reactions are efficient routes for the production of esters (see section 2.10.1). Carbonylation of alcohols (see section 2.10.2.1) or olefins (see section 2.10.2.3) is suitable for the production of esters, in the presence of an appropriate coreagent. Addition of carboxylic acids to alkynes (see section 2.12.2) or transesterification (see section 2.12.4) represent other available methods for the synthesis of esters.

Although several heterometallic catalysts exhibit enhanced selectivity toward oxygenates in CO_2 hydrogenation reactions (see sections 3.4 and 3.5), only a Mn–Pd system showed specific selectivity for esters. In particular, the reaction between CO_2 and H_2 in the presence of EtOH and NEt_3 afforded ethyl formate.

Homologation of methanol in the presence of Mn–Pd, Co–Pd, and Co–Pt heterometallic clusters afforded small amounts of methyl acetate (ca. 5% yield). However, homologation of methyl formate in the presence of a Ru–Co system afforded ethyl acetate with good activity and selectivity.

Carbonylation of ethanol in the presence of EtI efficiently afforded ethyl propionate when Fe-based heterometallic clusters were used as catalysts. In particular, Mo–Fe, Fe–Cu, and Fe–Hg showed activity in the range 85–95% and selectivities between 15% and 25% for the ester at 493 K. At this temperature, a Fe–Ni complex gave a ca. 50/50 mixture of ether and ester. The most active and selective system was a Fe–Rh complex, which gave almost quantitatively ethyl propionate at 473 K. Os–Ir and Ir–Pt clusters showed enhanced selectivity for methyl acetate in the methanol carbonylation because the excess of methanol in the reaction mixture tends to favor the formation of esters.

Carbonylation of 1-octene in the presence of EtOH with a Fe–Pd homogeneous catalyst gave the corresponding branched and linear esters (ethyl 2-methyloctanoate and ethyl nonoate) in 10 times better yields than when monometallic Pd complexes were used.

The addition of carboxylic acids to electron-deficient alkynes (e.g., terminal alkynes) to afford esters was catalyzed by Mo–Pd and Re–Ru catalysts with rather good regioselectivity for the Z and Z+E isomers, respectively. A series of Ti–Ru complexes proved to be almost as efficient as monometallic catalysts in the addition of formic acid to 1-hexyne or phenylacetylene to form the corresponding enol formates. These systems exhibited rather good regioselectivities.

Transesterification of esters by methanol to the corresponding methyl acetates and benzoates was efficiently performed in the presence of polymeric clusters containing Co, Zn, or Cd. Among the three systems, Co–Cd showed the worst results, because depending on the substrate, induction time of more than a week was required to reach full conversion. The Co–Zn catalyst gave better results, with full conversion time ranging from hours to 4 days. Finally, the best system was the Zn–Cd one, because a few hours proved to be sufficient to reach full conversion in most cases (see section 2.12.4).

3.9. Synthesis of Lactones

Lactones can generally be obtained by the methods used in ester synthesis. Moreover, using heterometallic cluster-derived catalysts, oxidation of THF (see section 2.9.4), cyclo(hydro)-carbonylation of alkynes (see section 2.10.2.4), cyclization of alkynoic acids (see section 2.12.2), or cycloaddition of CO₂ and alkynes (see section 2.12.3) appear as alternative options.

A dinuclear Mo–Ru complex was used as a homogeneous catalyst for the oxidation of THF to γ -butyrolactone, but it was observed that the corresponding monometallic dinuclear Ru complex was much more active and selective under similar reaction conditions.

Two Mo–Ni cubane-type clusters were used for the catalytic intramolecular cyclization of various alkynoic acids to the corresponding enol lactones. They proved to be very efficient, because full conversions and almost 100% selectivities were reached within 1–3 h for most substrates. Similarly, a Mo–Pd cubane cluster proved to be very efficient for the intramolecular cyclization of alkynoic acids to enol lactones, exhibiting yields up to 98% after sometimes very short times (several minutes).

A heterogeneous Fe–Rh catalyst was used for the cycloaddition of CO₂ and propyne to afford 4,6-dimethyl-2-pyrone. The selectivity for the desired product was higher than when monometallic analogous Rh catalysts were used, but trimerization products, obtainable even in the absence of CO₂, were still observed in large amounts.

Substituted furanones could be obtained from the cyclohydrocarbonylation of internal alkynes when catalyzed by a heterogeneous Co–Rh system. Yields above 80% were obtained for such reactions, even after several uses of the same catalyst. Similarly, a Co–Rh heterogeneous catalyst was used for the synthesis of coumarins from the reaction of substituted alkynes with CO and 2-iodophenol, with yields higher than 80%.

3.10. Synthesis of Acetals

Acetals are often used as protective groups in organic chemistry. They can be synthesized by several methods, including oxidation of alcohols (see section 2.9.2), homo-

logation of methanol (see section 2.10.1), or hydrocarbonylation of methanol (see section 2.10.2.2).

Oxidation of methanol in the presence of a heterogeneous Ta–Re catalyst selectively afforded dimethoxymethane, whereas the corresponding monometallic Re system yielded formaldehyde instead.

During methanol homologation reactions, a Mn–Pd homogeneous catalyst showed 55% selectivity for MeCH(OMe)₂. Other oxygenates such as alcohols and aldehydes were also observed. Other bimetallic couples, Co–Pd and Co–Pt, favored the formation of acetaldehyde dimethylacetal in ca. 30% yield as a major product.

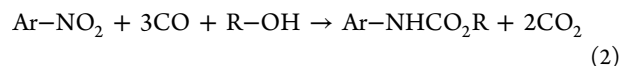
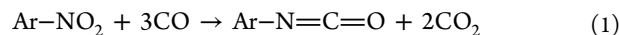
Hydrocarbonylation of methanol leads to aldehydes and the corresponding acetals, as with Ru–Co and Co–Pd heterogeneous catalysts. These systems afforded acetaldehyde and 1,1-dimethoxyethane. Other reactions include carbonylation to methyl acetate and hydrogenation of CO to methane.

3.11. Synthesis of Ketals (by Addition of Alcohols to Alkynes)

Addition of alcohols to alkynes to afford the corresponding ketals using heterometallic cluster-derived catalysts was only performed in the presence of Ir–M (M = Pd, Pt) trinuclear clusters (see section 2.12.1). More precisely, a Ir–Pd complex was more selective than the Ir–Pt one in the catalyzed addition of methanol to 2,2-dialkoxy-1-arylalkanes. In both cases, the yields were greater than 80%, and the conversions were almost quantitative.

3.12. Synthesis of Isocyanates and Carbamates (by Carbonylation of Organic Nitro Derivatives)

The preparation of aromatic isocyanates and carbamates by carbonylation of the corresponding organic nitro derivatives, as shown in eqs 1 and 2, has been investigated using MMCD catalysts (see section 2.11.1).



There is a considerable academic and industrial interest for these reactions, which grant access to aromatic isocyanates and carbamates while avoiding the use of phosgene,⁴²⁸ classically used to convert amino derivatives into this important class of chemicals.

Isocyanates were synthesized by carbonylation of organic nitro derivatives, in the presence of a heterogeneous Mo–Pd and a homogeneous Ru–Rh catalyst. While the former system proved effective, affording complete conversions and high selectivities (71–80%), and thus better performances than the corresponding monometallic systems or their mixtures, the latter showed rather poor activity (20.6% conversion) and selectivity (27.5%).

A series of M–Rh (M = Fe, Ru, Os) clusters were used as catalysts for the carbonylation of nitro derivatives in the presence of methanol. The addition of bipyridine was found to greatly improve the activity of the systems. At high substrate to catalyst ratios (see section 2.11.1), the Fe–Rh system was the least effective of all, while the Ru–Rh was the most selective, and the Os–Rh the most active. However, in the case of Ru and Os, a lower substrate to catalyst ratio proved to greatly increase the conversion (up to 98–100%) and the selectivity for the carbamates (87–89%).

Two Fe–Pd clusters were deposited on silica and alumina to prepare heterogeneous catalysts for the conversion of *o*-nitrophenol to benzoxazol-2-one. Alumina was found to be a better support, thus affording systems with very high activities and selectivities. Indeed, almost quantitative yields were observed. The use of impregnated metallic salts to prepare related catalysts resulted in only moderate activity (ca. 40%) and 90% selectivity.

Two Os–Au clusters with different Os to Au ratios were used to catalyze the oxidative carbonylation of aniline in the presence of methanol and PPh_3 as promoter, to afford phenylcarbamate with conversions ranging from 60% to 90% and selectivities as high as 65%. Moreover, in the absence of PPh_3 , it was observed that increasing the amount of methanol in the reaction mixture dramatically decreased the selectivity toward the carbamate, thus favoring the formation of quinazoline and azobenzene.

3.13. Synthesis of Ammonia

Industrially, ammonia is mainly synthesized by the Haber–Bosch process, using modified iron-based catalysts.⁴²⁹ Although organometallic compounds, including multinuclear complexes and hydride compounds,⁴³⁰ constitute an emerging tool for this reaction, heterometallic complexes and clusters have not been used much for that purpose (see section 2.15.5). It was also observed that reduction of hydrazine was another possible route (see section 2.15.4).

Hydrogenation of nitrogen was thus performed in the presence of Ru–Ni and Os–Ni heterogeneous catalysts adsorbed on K-modified alumina. The Ru-based system was more active than the Os-containing one, but it was still much less active than a monometallic Ru catalyst, pointing to a possible inhibiting effect of the Ni center.

Reduction of hydrazine to ammonia was performed in the presence of V–Fe–S and Mo–Fe–S cubane-type clusters as models for nitrogenase cofactor. These systems gave very promising results, but rather for partial reduction, such as the selective reduction of *cis*-dimethylidiazene to methylamine instead of ammonia. Also, the disproportionation of hydrazine to yield ammonia and dinitrogen was performed in the presence of Mo–Ru–S cubane-type clusters bearing a phosphine ligand. Although the authors did not investigate why, the catalyst bearing the phosphine PCy_3 proved to be more active than the one containing a PPh_3 ligand.

3.14. Miscellaneous

Hydrogenation of dimethylterephthalate (DMT) to 1,4-cyclohexanedimethanol (CHDM), which is of industrial interest, involves two reduction steps (Scheme 76). First, hydrogenation of the C=C bonds of the cyclohexene cycle leads to dimethyl hexahydroterephthalate (DMHT), and then hydrogenation of the ester groups affords CHDM. This reaction has been catalyzed by a series of silica-supported Ru-based heterometallic decarbonylated clusters. After 4 h reaction time, the $[\text{Ru}_6\text{Pd}_6]$ system shows moderate activity and 32.9% selectivity for

DMHT. Byproducts formed included 4-methyloxymethylhydroxymethylcyclohexane, bis(4-hydroxymethylcyclohexyl) ether, and CHDM. Under these conditions, the $[\text{Ru}_{12}\text{Cu}_4]$ system is inactive. However, after 8 h reaction time, the activity of the latter increased, and both catalysts resulted in a similar selectivity of ca. 22% for DMHT. The $[\text{Ru}_5\text{Pt}]$ and $[\text{Ru}_{10}\text{Pt}_2]$ catalysts were more active and selective for DMHT and CHDM than the $[\text{Ru}_6\text{Pd}_6]$ catalyst.

4. CONCLUSION

We have attempted here to emphasize the achievements in homogeneous, supported, and heterogeneous catalysis that result from the use of molecular, mixed-metal cluster compounds as precursors. An impressive number of bimetallic (and occasionally trimetallic) systems have been examined and found applications in an increasing number of catalytic reactions over the last decades (see Tables 1 and 3). A given bimetallic complex can be used in more than one type of reaction, whether in homogeneous, supported, or heterogeneous phase (see Table 4), and this illustrates the considerable scope of this approach and the potential for future developments. For a given bimetallic couple, much can be learned from qualitative comparisons as a function of the ratio between the heterometals and the type of catalysis applied for a given reaction, even though it is generally very difficult to draw more quantitative conclusions because meaningful comparisons can only be made for systems studied under strictly analogous conditions. This turns out to be only rarely possible, not only because of the considerable diversity of precursors and types of catalytic reactions studied, but also in view of the increasing number and diversity of research groups engaged in this field. In many instances, a comparison between the catalytic performances of the heterometallic and the corresponding monometallic precursors revealed synergistic and/or cooperativity effects.

The presence in a molecule of more than one metal center may confer a reactivity that is unique when compared to that of the corresponding mononuclear species. This may result, for example, from the stabilization by metal–metal bonding of unusual oxidation states. Such examples are known, even in homometallic systems, where reactions such as halide exchange with aryl iodide and C–C coupling, or C–H bond activation of aromatic compounds, were catalyzed in the presence of Pd(I)–Pd(I), or Pd(III)–Pd(III) dinuclear complexes, respectively.⁴³¹ Similarly, aldehyde olefination could be performed in the presence of a Ru(I)–Ru(I) complex.^{431,432} However, more information is needed, even for stoichiometric transformations, about the specific role of each metal in a heterometallic system. Studies with heterometallic Ni–Mo complexes have thus shown that they were able to induce stoichiometric tail-to-tail dimerization and C–H activation of methyl acrylate. Under similar conditions, the corresponding Ni–Ni or Mo–Mo complexes were found totally inactive.⁴³³ In other cases, the adjacent heterometal can be viewed as a “ligand”, enhancing the reactivity of its neighbor.⁴³⁴ We have also encountered situations where the heterometallic nature of the precursor complex was not a sufficient condition for efficient catalysis. Much remains to be learned about the stoichiometric and catalytic reactivity of mixed-metal cluster compounds and particularly about the site selectivity induced by the presence of different metal.⁴³⁵

The study of heterogenized catalysts, obtained by immobilization of molecular mixed-metal clusters on solid supports,

Scheme 76

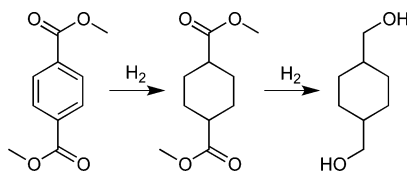


Table 4. Listing of Molecular Mixed-Metal Clusters Used in Catalysis, with the Corresponding References for the Synthesis and the Catalysis

Metallic Couple ^a	Precursor Cluster	Ref.	Support	Notation of the MMCD catalyst ^b	Catalyzed Reactions	Ref.
		Synth.				Catal.
Ti-Zr	[TiZr(CH ₂ C ₉ H ₅ SiMe ₂ N-t-Bu) ₂ Me ₄]	328	-	-	Polymerization of ethylene	328
	[TiZrOMe ₃ Cp* ₃]	329	-	-	Polymerization of ethylene	329
	[TiZrOMeCp* ₂ (NMe ₂) ₃]	330	-	-	Polymerization of alkenes	330
	[TiZr(C ₅ H ₄ SiMe ₂ C ₅ H ₄)Cp ₂ Cl ₄]	331	-	-	Polymerization of olefins	331
	[TiZr(C ₅ H ₄ C(CH ₂) ₄ C ₅ H ₄)CpCl ₅]	332	-	-	Polymerization of olefins	332
Ti-Cr	[(η ⁵ -indenyl)[1-Me ₂ Si(t-BuN)][TiCl ₂]}(CH ₂) _n {N[(CH ₂) ₂ (SEt)] ₂ (CrCl ₃)}]					
	n = 0, 2, 6	327	-	-	Polymerization of ethylene	327
Ti-W	[TiW(N ₂)Cp ^R Cl ₃ (dppe) ₂]	333a	-	-	Polymerization of olefins	333
	(Cp ^R = Cp, Cp')					
	[TiW(N ₂)Cp ^R Cl ₃ (depe) ₂]	333a	-	-	Polymerization of olefins	333
	(Cp ^R = Cp, Cp', Cp*, Ind)					
	[TiW(N ₂)CpCl ₃ (PMe ₂ Ph) ₄]	333a	-	-	Polymerization of olefins	333
Ti-Ru	[TiRuCl ₃ Cp(C ₅ H ₄ (CH ₂) ₂ PCy ₂) (=C=C=CPh ₂)(p-cymene)][OTf]					
		76	-	-	Ring-Closing Metathesis	76
	[TiRuLCl ₄ Cp(p-cymene)]	76	-	-	Cyclopropanation of styrene	316
	(L = C ₅ H ₄ (CH ₂) ₂ PR ₂)		-	-	Addition of RCOOH to alkynes	372
	(R = Ph, n = 0, 2; R = Cy, n = 2)					
	[TiRuCl ₃ LCl ₂ (p-cymene)]	316	-	-	Cyclopropanation of styrene	316
	L = C ₅ H ₄ PPPh ₂					
	[TiRu(O-i-Pr) ₃ LCl ₂ (p-cymene)]	316	-	-	Cyclopropanation of styrene	316
	L = C ₅ H ₄ (CH ₂) ₂ PR ₂ (R = Ph, Cy)					
	[TiRuCpCl ₂ L(CO) ₂ (O ₂ CH)] ₂	372	-	-	Addition of RCOOH to alkynes	372
	L = C ₅ H ₄ (CH ₂) _n PR ₂ (R = Ph, n = 0, 2; R = Cy, n = 2)					
Ti-Rh	[TiRhO-i-Pr(OCMe ₂ CH ₂ PPPh ₂) ₃ Cl]	315	-	-	Hydroacylation reactions	315
	[TiRhLCpCl ₂ (COD)][OTf]	380	-	-	Hydrosilylation of acetophenone	380
	(L = C ₅ Me ₃ (PPh ₂) ₂)					
	[TiRh(O ₂ Bn)Cp*(COD)]	438	-	-	CO Hydrogenation	158
	[TiRh(sal) ₂ Cp*(COD)]	158	-	-	CO Hydrogenation	158
	[TiRh(sal) ₂ Cp*(CO) ₂]	158	-	-	CO Hydrogenation	158
	(salH ₂ = salicylic acid)					
Ti-Pd	[TiRh(CH ₂ PPPh ₂) ₂ Cp ₂ (COD)][BPh ₄]	271	-	-	Hydroformylation of alkenes	271
	[TiRh ₃ CpS ₃ L ₃]	439	-	-	Hydroformylation of alkenes	270
	(L = tfbb, COD)					
	[TiPd{(t-Bu ₂ CH)N(C ₆ H ₄)PPh ₂) ₂ Cl ₄]	334	-	-	Polymerization of ethylene	334
			-	-	Suzuki-Miyaura cross-coupling	334

Table 4. continued

Metallic Couple ^a	Precursor Cluster	Ref.	Support	Notation of the MMCD catalyst ^b	Catalyzed Reactions	Ref.
		Synth.				Catal.
Ti-Pt	[TiPt{(<i>t</i> -Bu ₂ CH)N(C ₆ H ₄)PPh ₂ } ₂ Cl ₄]	³³⁴	-	-	Polymerization of ethylene	³³⁴
Ti-Zn	[TiZn ₂ Et ₂ (OCH ₂ CH ₂ O) ₂ Cp ₂]	⁴¹⁶	-	-	Copolymerization of CO ₂ + C ₆ H ₁₀ O	⁴¹⁶
Zr-Hf	[ZrHf{(C ₅ H ₅)C(CH ₂) ₅ (C ₆ H ₆)}Cp ₂ Cl ₄]	³³⁵	-	-	Polymerization of ethylene	³³⁵
	[ZrHf{(C ₅ H ₅)C(CH ₂) ₄ (C ₆ H ₄)}Cp ₂ Cl ₄]	³³²	-	-	Polymerization of olefins	³³²
Zr-Cr	[ZrCr{As(SiMe ₃) ₂ } ₂ Cp ₂ (CO) ₄]	⁴⁴⁰	-	-	Polymerization of ethylene	^{336,340}
			-	-	Polymerization of propylene	³⁴⁰
	[ZrCr(PHTipp) ₂ Cp' ₂ (CO) ₄]	⁴⁴¹	-	-	Polymerization of propylene	³⁴⁰
	(Tipp = 2,4,6- <i>i</i> -Pr ₃ C ₆ H ₂)					
Zr-Mo	[ZrMo{P(SiMe ₃) ₂ } ₂ Cp ₂ (CO) ₄]	⁴⁴⁰	-	-	Polymerization of ethylene	^{336,340}
			-	-	Polymerization of propylene	³⁴⁰
	[ZrMo(PHTipp) ₂ Cp' ₂ (CO) ₄]	⁴⁴¹	-	-	Polymerization of propylene	³⁴⁰
	(Tipp = 2,4,6- <i>i</i> -Pr ₃ C ₆ H ₂)					
Zr-Fe	[ZrFe(C ₅ H ₄ SiMe ₂ C ₅ H ₄)Cp ₂ Cl ₂]	³⁴⁴	-	-	Polymerization of olefins	³⁴⁴
	[ZrFe(C ₅ H ₄ PEt ₂) ₂ MeCp*]	⁴¹⁵	-	-	Dehydrogenation of amine-boranes	⁴¹⁵
	[Zr ₂ Fe{(C ₆ H ₆)CMe ₂ (C ₅ H ₄) ₂ }Cp ₂ Cl ₄]	³³⁵	-	-	Polymerization of olefins	³³⁵
Zr-Ru	[ZrRu(C ₅ H ₄ PEt ₂) ₂ MeCp*]	⁴¹⁵	-	-	Dehydrogenation of amine-boranes	⁴¹⁵
	[ZrRu(C ₅ H ₄ PEt ₂) ₂ Cp*(Me ₂ N)]	⁴¹⁵	-	-	Dehydrogenation of amine-boranes	⁴¹⁵
	[ZrRu(C ₅ H ₄ PEt ₂) ₂ Cl ₃ Cp*]	⁴¹⁵	-	-	Dehydrogenation of amine-boranes	⁴¹⁵
	[ZrRu(C ₅ H ₄ PEt ₂) ₂ ClCp*]	⁴¹⁵	-	-	Dehydrogenation of amine-boranes	⁴¹⁵
	[ZrRu(C ₅ H ₄ PEt ₂) ₂ Cp*(BH ₄)]	⁴¹⁵	-	-	Dehydrogenation of amine-boranes	⁴¹⁵
	[HZrRu(C ₅ H ₃ PEt ₂)(C ₅ H ₄ PEt ₂)Cp*]	⁴¹⁵	-	-	Dehydrogenation of amine-boranes	⁴¹⁵
Zr-Co	[ZrCo{(C ₆ H ₆)CMe ₂ (C ₅ H ₄) ₂ }CpCp*Cl ₂]	³³⁵	-	-	Polymerization of olefins	³³⁵
	[ZrCo{(C ₅ Me ₄)SiMe ₂ (C ₅ H ₃)CH ₂ (CH) ₂ CO ₂ CH ₂ (C ₅ H ₃ N)CHN(dipp)}Cl ₄]					
		³³⁷	-	-	Polymerization of ethylene	³³⁷
	[ZrCo(<i>i</i> -PrNPPPh ₂) ₃]Cl]	⁴⁴²	-	-	Kumada coupling	³⁵²
	[ZrCo(MesNP- <i>i</i> -Pr ₂) ₃]Cl]	⁴⁴²	-	-	Kumada coupling	³⁵²
	[ZrCo(<i>i</i> -PrNP- <i>i</i> -Pr ₂) ₃]Cl]	⁴⁴²	-	-	Kumada coupling	³⁵²
	[ZrCo(MesNP- <i>i</i> -Pr ₂) ₃ (N ₂)(THF)]	⁴⁴³	-	-	Hydrosilylation of ketones	³⁸⁸
Zr-Rh	[Ph ₄ As][ZrRhS ₂ Cp' ₂ (CO) ₂]	²⁶³	-	-	Carbonylation of ethylene	²⁶³
	[HZrRh(PPh ₂) ₂ Cp ₂ (CO)(PPh ₃)]	²⁷²	-	-	Hydroformylation of 1-hexene	²⁷²
	[HZrRh(CH ₂ PPh ₂) ₂ Cp ₂ (PPh ₃)]	²⁷⁴	-	-	Hydroformylation of 1-hexene	²⁷⁴
	[HZrRh(CH ₂ PPh ₂) ₂ Cp ₂ (CO)(PPh ₃)]	²⁷⁵	-	-	Hydroformylation of 1-hexene	²⁷⁵
	[ZrRh(CH ₂ PPh ₂) ₂ Cp ₂ (COD)][BPh ₄]	^{271,276}	-	-	Hydroformylation of olefins	^{271,276}
	[ZrRh(CH ₂ PPh ₂) ₂ Cp' ₂ (COD)][BPh ₄]	²⁷⁶	-	-	Hydroformylation of olefins	²⁷⁶
	[ZrRh(PPh ₂) ₂ (S- <i>t</i> -Bu)(C ₅ H ₄ SiMe ₃) ₂] ₂	²⁷⁷	-	-	Hydroformylation of 1-hexene	²⁷⁷

Table 4. continued

Metallic Couple ^a	Precursor Cluster	Ref.	Support	Notation of the MMCD catalyst ^b	Catalyzed Reactions	Ref.
		Synth.				Catal.
	[ZrRh(CH ₂ PPPh ₂) ₂ Cp ₂ (acac)(CO) ₂]	²⁷⁸	-	-	Hydroformylation of olefins	278
	[ZrRh(CH ₂ PPPh ₂) ₂ Cp ₂ (acac)(CO)]	²⁷⁸	-	-	Hydroformylation of olefins	278
	[ZrRh(C ₅ H ₄ PPPh ₂) ₂ Me(CO)(PPh ₃)]	²⁸⁰	-	-	Hydroformylation of 1-hexene	280
	[ZrRh{C ₅ H ₄ C(CH ₂) ₄ C ₅ H ₄ }CpCl ₂ (COD)]	³³²	-	-	Polymerization of olefins	332
	[ZrRh((CH ₂ =CH) ₂ Si(C ₅ H ₂ Me ₂) ₂)Cp ^R Cl ₂]	³³⁸	-	-	Polymerization of olefins	338
	(Cp ^R = Cp, Cp*, Ind)					
	[ZrRh{((CH ₂ =CH) ₂ Si(C ₅ Me ₄) ₂)IndCl ₂ }]	³³⁹	-	-	Polymerization of olefins	339
	[ZrRh ₂ (CH ₂ PPPh ₂) ₂ (S-t-Bu) ₂ L ₂ (CO) ₂]	^{259,262}	-	-	Hydroformylation of olefins	273,276
	(L = Cp, Cp')					
	[ZrRh ₂ S ₂ Cp ^{II} ₂ (CO) ₄]	²⁷⁹	-	-	Hydroformylation of 1-octene	279
	(Cp ^{II} = η ⁵ -1,3-di-tertbutylcyclopentadienyl)					
Zr-Ir	[H ₃ ZrIr(CH ₂ SiMe ₃) ₂ Cp*] ₂	⁴¹	-	-	H-D exchange	41
Zr-Ni	[ZrNi{P(SiMe ₃) ₂ } ₂ Cp ₂ (CO) ₂]	³³⁶	-	-	Polymerization of ethylene	336
			-	-	Polymerization of propylene	340
	[ZrNi{((C ₅ Me ₄)SiMe ₂ (C ₅ H ₃)CH ₂ (CH) ₂ CO ₂ CH ₂ (C ₅ H ₃ N)CHN(dipp)}Br ₂ (H ₂ O)]					
		³³⁷	-	-	Polymerization of ethylene	337
Zr-Pd	[ZrPd{((C ₅ Me ₄)SiMe ₂ (C ₅ H ₃)CH ₂ (CH) ₂ CO ₂ CH ₂ (C ₅ H ₃ N)CHN(dipp)}Cl ₄]					
		³³⁷	-	-	Polymerization of ethylene	337
	[ZrPd(C ₅ H ₄ PPPh ₂) ₂ Cl ₄]	²⁸⁰	-	-	Coupling of aryl-Br with alkyl-MgBr	²⁸⁰
Hf-Ru	[HfRu(C ₅ H ₄ PET ₂) ₂ MeCp*]	⁴¹⁵	-	-	Dehydrogenation of amine-boranes	⁴¹⁵
Hf-Co	[HfCo(MesNP-i-Pr) ₂]Cl]	³⁵³	-	-	Kumada coupling	³⁵³
Hf-Rh	[ZrRh{C ₅ H ₄ C(CH ₂) ₄ C ₅ H ₄ }CpCl ₂ (COD)]	³³²	-	-	Polymerization of olefins	332
Hf-Ir	[H ₃ HfIr(CH ₂ SiMe ₃) ₂ Cp*] ₂	⁴¹	-	-	H-D exchange	41
V-Cr	[VCrCp ₃ (CO) ₃]	³⁴¹	SiO ₂	[VCr]	Polymerization of ethylene	341
V-Fe	[NEt ₄][VFe ₃ S ₄ Cl ₃ (DMF) ₃]	⁴⁴⁴	-	-	Reduction of acetylene to ethylene	¹⁰¹
			-	-	Reduction of N ₂ H ₄ to NH ₃	¹⁰¹
V-Co	[VCoOL] ²⁺	²²²	γ-Al ₂ O ₃	[VCo]	Oxidation of cyclohexane	222
	(L = {-NHC ₆ H ₂ MeOCHNC ₆ H ₄ -} ₂)					
V-Rh	[Bu ₄ N] ₂ [V ₄ Rh ₂ (C ₄ H ₇) ₄ O ₁₂] ₂	⁴⁴⁵	SiO ₂	-	Oxidation of propene to acetone	80,223
	[V ₆ Rh ₄ O ₁₉ Cp*] ₄	⁴⁴⁶	SiO ₂	-	Oxidation of propene to acetone	80,223
Nb-Rh	[NbRh(N-t-Bu)(PPh ₂)Cp ₂ Cl]	³⁸¹	-	-	Hydrosilylation of aldehyde/ketone	³⁸¹
	[NbRh(N-t-Bu)(PPh ₂)Cp ₂ Cl(COD)]	³⁸¹	-	-	Hydrosilylation of aldehyde/ketone	³⁸¹
Ta-Re	[Ta ₄ (ReO ₄) ₂ O ₂ (OEt) ₁₄]	⁴⁴⁷	TiO ₂	[Ta ₄ Re ₂]	Oxidation of methanol	235
Ta-Ru	[TaRuLCl ₄ Cp*(p-cymene)]	³¹⁷	-	-	Cyclopropanation of styrene	317
	[TaRuLCl ₃ Cp*(OH)(p-cymene)]Cl	³¹⁷	-	-	Cyclopropanation of styrene	317
	[TaRuLCl ₃ Cp*(O)(p-cymene)]	³¹⁷	-	-	Cyclopropanation of styrene	317

Table 4. continued

Metallic Couple ^a	Precursor Cluster	Ref.	Support	Notation of the MMCD catalyst ^b	Catalyzed Reactions	Ref.
		Synth.				Catal.
$L = C_5H_4(CH_2)_2PR_2$ (R = Ph, Cy)						
Ta-Rh	[TaRh(CH ₂) ₂ Cp ₂ (CO) ₂]	⁴⁸	solid state	[TaRh]	Hydrogenation of alkenes	⁴⁸
	[TaRh(CH ₂) ₂ Cp ₂ (CO)(PPh ₃)]	⁴⁸	-	-	Isomerization of 1-butene,	⁴⁸
			-	-	Hydrogenation of alkenes	⁴⁸
	[TaRh(PEt ₂) ₂ Cp ₂ (C ₂ H ₄)]	³⁸²	-	-	Hydrosilylation of acetophenone	³⁸²
Ta-Ir	[TaIr(CH ₂) ₂ Cp ₂ (CO) ₂]	⁴⁹	-	-	Isomerization of Olefins (>C ₂),	⁴⁹
			-	-	Hydrogenation of alkenes,	⁴⁸⁻⁴⁹
			-	-	Hydrosilylation of ethylene	⁴⁹
	[TaIr(CH ₂) ₂ Cp ₂ (CO)(PPh ₃)]	⁴⁸	-	-	Hydrogenation of alkenes	⁴⁸
	[HTaIr(CH ₂) ₂ Cp ₂ Cp*]	¹⁰²	solid state	[TaIr]	Hydrogenation of ethylene	¹⁰²
Cr-Mo	[CrMo(OAc) ₄ ·2H ₂ O]	⁴⁴⁸	SiO ₂	[CrMo]	Polymerization of olefins	³⁴²
	[(OC) ₄ Mo-CPh(OMe)Cr~SIL]	⁷⁷	SiO ₂	-	Olefin metathesis	⁷⁷
Cr-W	[(OC) ₄ W-CPh(OMe)Cr~SIL]	⁷⁷	SiO ₂	-	Olefin metathesis	⁷⁷
	[(OC) ₄ W-CR ¹ R ² Cr~SIL]	⁷⁷⁻⁷⁸	SiO ₂	-	Olefin metathesis	⁷⁷⁻⁷⁸
	(R ¹ = Ph, Tol, Me; R ² = Ph, OMe)					
	[X(OC) _n W=CPhCr~SIL]	⁷⁹	SiO ₂	-	Olefin metathesis	⁷⁹
	(X = Cl, Br, I, n = 4; X = Cp, n = 2)					
Cr-Fe	[PPN][HCrFe(CO) ₉]	⁴⁴⁹	-	-	Isomerization of alkenes	⁵⁰
Cr-Ru	[CrRu(PPh ₂) ₂ (CO) ₇]	²¹¹	-	-	Hydrogenation of cyclohexanone	²¹¹
	[Ph ₄ P][CrRu(N)O ₄ Me ₂]	²³⁶	-	-	Oxidation of alcohols	²³⁶
	[Bu ₄ N][CrRu(N)O ₄ (CH ₂ SiMe ₃) ₂]	²³⁶	-	-	Oxidation of alcohols	²³⁶
	[PPN] ₂ [Cr ₂ Ru ₃ C(CO) ₁₆]	⁴⁵⁰	SiO ₂	[Cr ₂ Ru ₃]	CO Hydrogenation	¹⁵⁹
Cr-Os	C[CrOs(N)O ₄ (CH ₂ SiMe ₃) ₂]	²³⁶⁻²³⁷	-	-	Oxidation of alcohols	²³⁶⁻²³⁷
	(cation C ⁺ = Bu ₄ N ⁺ , Ph ₄ P ⁺)					
	[Ph ₄ P][CrOs(N)O ₄ Me ₂]	²³⁶⁻²³⁷	-	-	Oxidation of alcohols	²³⁶⁻²³⁷
	[Bu ₄ N][CrOs(N)O ₄ Ph ₂]	²³⁶	-	-	Oxidation of alcohols	²³⁶
	[Ph ₄ P][CrOs(N)O ₄ Me(CH ₂ SiMe ₃)]	²³⁶	-	-	Oxidation of alcohols	²³⁶
	C[CrOs(N)O ₄ (CH ₂ SiMe ₃) ₂ (dppe)]	^{236,250}	-	-	Oxidation of dppe	^{236,250}
	(cation C ⁺ = Bu ₄ N ⁺ , Ph ₄ P ⁺)					
Cr-Co	[CrCo(PhCH ₂)(DH)(CO) ₃ (py)]	¹⁶⁰	-	[CrCo]	CO Hydrogenation	¹⁶⁰
	(DH = monoanion of dimethylglyoxime)					
Cr-Rh	[CrRhInd*(CO) ₅]	⁴⁵¹	-	-	Cyclotrimerization of DMAD	³⁵⁰
	(Ind* = Heptamethylindenyl)					
Cr-Ni	[CrNiLCl ₄]	³⁵⁴	-	-	Coupling of RCHO/alkenyl halides	³⁵⁴
	L = i-Pr-oxazo-Ph(NSO ₂ R)-O(CH ₂) ₄ -phenMe (R = Me, 3,5-chlorophenyl)					

Table 4. continued

Metallic Couple ^a	Precursor Cluster	Ref.	Support	Notation of the MMCD catalyst ^b	Catalyzed Reactions	Ref.
		Synth.				Catal.
Cr-Pd	[Cr ₂ Pd ₂ Cp ₂ (CO) ₆ (PEt ₃) ₂]	452	-	-	Isomerization of 1,5-COD,	51
			-	-	Hydrogenation of 1,5-COD	51
Cr-Pt	[Cr ₂ Pd ₂ Cp ₂ (CO) ₆ (PMe ₃) ₂]	452	γ-Al ₂ O ₃	[Cr ₂ Pd ₂]	Hydrocarbon Rearrangements	82
	[HCrPt(PPh ₃)(CO) ₅ (PPh ₃)]		SiO ₂	[CrPt]	CO ₂ Hydrogenation	161
Mo-W-Fe	K ₈ [P ₂ Mo ₂ W ₁₈ Fe ₂ (H ₂ O)O ₆₈]·MoO ₆	103	γ-Al ₂ O ₃	[Mo ₂ W ₁₈ Fe ₂]	Hydrogenation of cyclohexene	103
			γ-Al ₂ O ₃	[Mo ₂ W ₁₈ Fe ₂]	HDS of thiophene	103
	K ₈ [P ₂ Mo ₂ W ₁₈ Co ₂ (H ₂ O)O ₆₈]·MoO ₆	103	γ-Al ₂ O ₃	[Mo ₂ W ₁₈ Co ₂]	Hydrogenation of cyclohexene	103
			γ-Al ₂ O ₃	[Mo ₂ W ₁₈ Co ₂]	HDS of thiophene	103
Mo-W-Ni	K ₈ [P ₂ Mo ₂ W ₁₈ Ni ₂ (H ₂ O)O ₆₈]·MoO ₆	103	γ-Al ₂ O ₃	[Mo ₂ W ₁₈ Ni ₂]	Hydrogenation of cyclohexene	103
			γ-Al ₂ O ₃	[Mo ₂ W ₁₈ Ni ₂]	HDS of thiophene	103
	[PPN][HMnFe(CO) ₅]	449	-	-	Isomerization of alkenes	50
	[MoFeCp(AsMe ₂)(CO) ₅]	453	-	-	Isomerization of 1-octene,	52
Mo-Fe	[MoFe(Ph ₂ Ppy) ₂ (CO) ₆]	257	-	-	Hydrogenation of 1-octene	52
	[MoFeS ₄ (SCN) ₂ (OMe) ₂] ²⁻	104	-	-	Carbonylation of EtOH	257
	[Et ₄ N] ₂ [MoFe ₃ S ₄ Cl ₃ (Cl ₄ -cat)(MeCN)]	454	-	-	Reduction of acetylene to ethylene	104
			C electrode	-	Reduction of acetylene to ethylene, Reduction of nitrates and nitrites	106 398
			-	-	Reduction of hydrazines	400
	[Et ₄ N] ₂ [Mo ₂ FeS ₄ O ₄]	103	γ-Al ₂ O ₃	[Mo ₂ Fe]	Hydrogenation of cyclohexene	103
			γ-Al ₂ O ₃	[Mo ₂ Fe]	HDS of thiophene	103
	[Mo ₂ FeS ₈ O(OMe) ₂] ³⁻	104	-	-	Reduction of acetylene to ethylene	104
	[Mo ₂ Fe ₂ S ₂ Cp ₂ (CO) ₆]	455	γ-Al ₂ O ₃ , MgO	[Mo ₂ Fe ₂]	CO Hydrogenation	162,164
			γ-Al ₂ O ₃ , MgO, SiO ₂ , TiO ₂	[Mo ₂ Fe ₂]	HDS of thiophene	162,164b,406c
Mo-Fe-Co	[Mo ₂ Fe ₂ S ₄ Cp ₂ (CO) ₆]	456	γ-Al ₂ O ₃	[Mo ₂ Fe ₂]	CO Hydrogenation	164a
	[Et ₄ N] ₃ [Mo ₂ Fe ₆ S ₈ (SPh) ₆ (OMe) ₃]	103	γ-Al ₂ O ₃	[Mo ₂ Fe ₆]	Hydrogenation of cyclohexene	103
			γ-Al ₂ O ₃	[Mo ₂ Fe ₆]	HDS of thiophene	103
	[Et ₄ N] ₃ [Mo ₂ Fe ₆ S ₈ (OMe) ₃ (L ¹) ₃ (L ²) ₃]	105	-	-	Reduction of acetylene to ethylene	105
(L ¹ = L ² = SPh or Cl; L ¹ = SPh, L ² = Cl)						
Mo-Fe-Co	[MoFeCoSCp(CO) ₅]	457	-	-	Hydrosilylation of acetophenone	383
	[HMnFeCo(CMe)Cp(CO) ₅]	107	-	-	Hydrogenation of styrene	107
	[MoFeCoSCp'(CO) ₆ (dppe)]	281	-	-	Hydroformylation of olefins	281
	[Et ₄ N] ₃ [Mo ₂ Fe ₄ Co ₂ S ₈ (SPh) ₆ (OMe) ₃]	105	-	-	Reduction of acetylene to ethylene	105
	[Et ₄ N] ₃ [Mo ₂ Fe ₄ Co ₂ S ₈ (SPh) ₆ (OMe) ₃]	103	γ-Al ₂ O ₃	[Mo ₂ Fe ₄ Co ₂]	Hydrogenation of cyclohexene	103
			γ-Al ₂ O ₃	[Mo ₂ Fe ₄ Co ₂]	HDS of thiophene	103

Table 4. continued

Metallic Couple ^a	Precursor Cluster	Ref.	Support	Notation of the MMCD catalyst ^b	Catalyzed Reactions	Ref.
		Synth.				Catal.
	$[\text{Et}_4\text{N}]_3[\text{Mo}_2\text{Fe}_5\text{CoS}_6(\text{SPh})_6(\text{OMe})_3]$	¹⁰³	$\gamma\text{-Al}_2\text{O}_3$	$[\text{Mo}_2\text{Fe}_5\text{Co}]$	Hydrogenation of cyclohexene	¹⁰³
			$\gamma\text{-Al}_2\text{O}_3$	$[\text{Mo}_2\text{Fe}_5\text{Co}]$	HDS of thiophene	¹⁰³
Mo-Ru	$[\text{MoRuCp}_2(\text{CO})_5]$	⁴⁵⁸	$\gamma\text{-Al}_2\text{O}_3$	$[\text{MoRu}]$	HDS of thiophene	⁴⁰⁷
			-	-	Oxidation of THF	²⁴⁹
	$[\text{MoRuCpInd}(\text{CO})_5]$	^{249a}	-	-	Oxidation of THF	^{249a}
	$[\text{MoRuCp}(\text{C}_5\text{R}_5)(\text{CO})_3(\text{dppm})]$ (R = H, Me)	¹⁶⁵	-	-	CO_2 Hydrogenation	¹⁶⁵
	$[\text{MoRu}(\text{PPh}_2)_2(\text{CO})_7]$	²¹¹	-	-	Hydrogenation of cyclohexanone	²¹¹
	$[\text{Mo}_2\text{RuSCp}_2(\text{CO})_7]$	⁴⁵⁹	-	-	Trimerization of phenylacetylene	³⁵¹
	$[\text{Et}_4\text{N}]_2[\text{Mo}_2\text{Ru}_3\text{C}(\text{CO})_{16}]$	⁴⁵⁰	SiO_2	$[\text{Mo}_2\text{Ru}_3]$	CO Hydrogenation	¹⁵⁹
	$[\text{Mo}_3\text{RuS}_4\text{Cp}'_3(\text{CO})_2][\text{pts}]$	⁴⁶⁰	$\gamma\text{-Al}_2\text{O}_3$	$[\text{Mo}_3\text{Ru}]$	Hydrogenation of naphthalene	¹⁰⁸
			$\gamma\text{-Al}_2\text{O}_3$	$[\text{Mo}_3\text{Ru}]$	Simultaneous HDS, HDN	¹⁰⁸
	$[\text{H}_2\text{Mo}_3\text{RuS}_4\text{Cp}^*_3(\text{PR}_3)][\text{PF}_6]$ (R = Ph, Cy)	⁴⁰²	-	-	Disproportionation of $\text{H}_2\text{N-NH}_2$	⁴⁰²
Mo-Ru-Co	$[\text{HMoRuCo}(\text{CMe})\text{Cp}(\text{CO})_8]$	⁴⁶¹	-	-	Isomerization of fumaric esters	⁵³
	$[\text{MoRuCoSCp}(\text{CO})_8]$	⁴⁶²	-	-	Hydrogenation of styrene	¹⁰⁷
Mo-Os	$[\text{HMoOs}_3\text{Cp}(\text{CO})_{12}]$	⁴⁶³	$\gamma\text{-Al}_2\text{O}_3$	$[\text{MoOs}_3]$	CO Hydrogenation	¹⁶⁶
Mo-Co	$[\text{MoCo}_2(\text{CMe})\text{Cp}(\text{CO})_8]$	⁴⁶⁴	-	-	Hydroformylation of alkenes	¹⁰⁹
			-	-	Hydrosilylation of acetophenone	³⁸³
	$[\text{MoCo}_2(\text{CMe})\text{Cp}(\text{CO})_7\{\text{P}(\text{OMe})_3\}]$	⁴⁶⁴	-	-	Hydroformylation of alkenes	¹⁰⁹
			-	-	Hydrosilylation of acetophenone	³⁸³
	$[\text{MoCo}_2\text{SCp}(\text{CO})_8]$	⁴⁵⁷	-	-	Hydroformylation of alkenes	¹⁰⁹
			-	-	Hydrosilylation of acetophenone	³⁸³
	$[\text{Et}_4\text{N}]_2[\text{Mo}_2\text{CoS}_4\text{O}_4]$	¹⁰³	$\gamma\text{-Al}_2\text{O}_3$	$[\text{Mo}_2\text{Co}]$	Hydrogenation of cyclohexene	¹⁰³
			$\gamma\text{-Al}_2\text{O}_3$	$[\text{Mo}_2\text{Co}]$	HDS of thiophene	¹⁰³
	$[\text{Mo}_2\text{Co}_2\text{S}_3\text{Cp}_2(\text{CO})_4]$	⁴⁵⁶	$\gamma\text{-Al}_2\text{O}_3$	$[\text{Mo}_2\text{Co}_2]$	CO Hydrogenation	¹⁶⁴
			$\gamma\text{-Al}_2\text{O}_3, \text{MgO}$			
			$\text{SiO}_2, \text{TiO}_2$	$[\text{Mo}_2\text{Co}_2]$	HDS of thiophene	^{162,164b,408-409}
	$[\text{Mo}_2\text{Co}_2\text{S}_3\text{Cp}'_2(\text{CO})_4]$	⁴⁵⁶	$\gamma\text{-Al}_2\text{O}_3$		HDS of thiophene and thiophenol	¹⁶²
	$[\text{Mo}_2\text{Co}_2\text{S}_4(\text{C}_5\text{Me}_4\text{Et})_2(\text{CO})_6]$	^{456,465}	-	-	HDS	⁴¹⁰
	$[\text{Mo}_2\text{Co}_2\text{S}_4\text{Cp}_2(\text{CO})_2]$	⁴¹⁷	-	$[\text{Mo}_2\text{Co}_2]$	Coal Conversion	⁴¹⁷
	$[\text{Mo}_2\{\text{Co}_3(\text{CO})_9\text{CCO}_2\}_4]$	^{212a,466}	solid state	$[\text{Mo}_2\text{Co}_3]$	Hydrogenation of crotonaldehyde	²¹²
Mo-Co-Ni	$[\text{MoCoNi}(\text{CMe})\text{Cp}_2(\text{CO})_8]$	⁴⁶⁷	-	-	Hydrogenation of styrene,	¹⁰⁷
			-	-	Hydroformylation of alkenes,	¹⁰⁹
			-	-	Hydrosilylation of acetophenone	³⁸³

Table 4. continued

Metallic Couple ^a	Precursor Cluster	Ref.	Support	Notation of the MMCD catalyst ^b	Catalyzed Reactions	Ref.
		Synth.				Catal.
Mo-Rh	[MoRhCp(CO) ₃ (PPh ₃) ₂] [MoRh(SH) ₂ Cp ₂ (PPh ₃) ₂][PF ₆] [Mo ₂ RhCp ₃ (CO) ₅] [Mo ₂ Rh ₂ S ₂ L ₂ OCP [*] ₂ Cl ₄ (DMF)] (L = S, Se)	110 111 468 469	- γ -Al ₂ O ₃ , SiO ₂ SiO ₂ SiO ₂ -	- [MoRh] [Mo ₂ Rh] [Mo ₂ Rh] -	Hydrogenation of cyclohexene CO and CO ₂ Hydrogenation Hydrogenation of alkynes CO Hydrogenation Hydrogenation of acetaldehyde Hydroformylation of olefins Reduction of hydrazines	110 167 111 168-169 213 168a,213 403
Mo-Ir	[H ₂ MoIr(SH) ₂ Cp ₂ (PPh ₃) ₂][PF ₆] [MoIr ₃ Cp(CO) ₁₁] [Mo ₂ Ir ₂ Cp ₂ (CO) ₁₀] [Mo ₂ Ir ₂ S ₂ L ₂ OCP [*] ₂ Cl ₄ (DMF)] (L = S, Se)	111 472 473 469	- γ -Al ₂ O ₃ γ -Al ₂ O ₃ -	- [Mo ₃ Rh] [Mo ₃ Rh] [Mo ₃ Rh ₂] -	Hydrogenation of alkynes Simultaneous HDS, HDN Propene Metathesis Propene Metathesis Reduction of hydrazines	111 108 108 80 80 403
Mo-Ni	[Et ₄ N] ₂ [Mo ₂ NiS ₄ O ₄] [Mo ₂ Ni ₂ S ₄ Cp ₂ (CO) ₂] [Mo ₂ Ni ₂ S ₄ Cp ₄] [Mo ₃ NiS ₄ Cl(H ₂ O) ₃ ²⁺] [Mo ₃ NiS ₄ Cp [*] ₃ (dmad)][PF ₆] (dmad = dimethyl acetylenedicarboxylate)	103 164a 164a 474 373 373	γ -Al ₂ O ₃ γ -Al ₂ O ₃ γ -Al ₂ O ₃ NaY, HUSY, KL -	[Mo ₂ Ni] [Mo ₂ Ni] [Mo ₂ Ni] -	Hydrogenation of cyclohexene HDS of thiophene CO Hydrogenation CO Hydrogenation HDS of benzothiophenone Cyclization of alkynoic acids	103 103 164a 164a 411-412 373
Mo-Pd	[MoPd(Ph ₂ Ppy) ₂ Cl ₂ (CO) ₃] [MoPd(C ₅ H ₄ PPhBu)I(CO) ₃ L] (L = PPh ₃ , DMF)	475 476 379b	- resin -	- -	Hydrogenation of alkene Hydrogenation of alkene Mo-C=C bond formation	112 112 379b
	[Mo ₂ Pd(CO) ₆ (C ₅ H ₂ Ph ₂ (PPh ₂)) ₂] [Mo ₂ Pd ₂ Cp ₂ (CO) ₆ (PEt ₃) ₂]	379a 452,477	- - - -	- -	Mo-C≡C bond formation Isomerization of 1,5-COD, Hydrogenation of alkene & alkyne, Oligomerization of butadiene Hydrosilylation of 1-pentene,	379a 51 51 51 51

Table 4. continued

Metallic Couple ^a	Precursor Cluster	Ref.	Support	Notation of the MMCD catalyst ^b	Catalyzed Reactions	Ref.
		Synth.				Catal.
[Mo ₂ Pd ₂ Cp ₂ (CO) ₆ (PPh ₃) ₂]		452	-	-	Isomerization of 1,5-COD,	51
			-	-	Hydrogenation of alkene & alkyne	51
			-	-	Oligomerization of butadiene	51
			-	-	Cross coupling aryl halides/triflates	355
			-	-	Hydrosilylation of 1-pentene	51
			γ-Al ₂ O ₃	[Mo ₂ Pd ₂]	Reduction of NO,	395
			γ-Al ₂ O ₃	[Mo ₂ Pd ₂]	Carbonylation of ArNO ₂	361
[Mo ₃ PdS ₄ (tacn) ₃ Cl][PF ₆] ₃	(tacn = 1,4,7-triazacyclononane)	478	-	-	Addition of RCOOH to alkynes,	374
[Mo ₃ PdS ₄ Cp [*] ₃ L][PF ₆]	(L = dba, maleic anhydride)	365	-	-	Cyclization of alkynoic acids	375
[Mo ₃ PdS ₄ Cp' ₃ (PPh ₃)][pts]		479	γ-Al ₂ O ₃	[Mo ₃ Pd]	Hydrogenation of naphthalene	108
			γ-Al ₂ O ₃	[Mo ₃ Pd]	Simultaneous HDS, HDN	108
Na ₂ [Mo ₄ Pd ₄ Cp ₄ (CO) ₁₂]		218,480	-	-	Dehydration of alcohols	218
Mo-Pt [Mo ₂ PtCp ₂ (CO) ₆ (CNCy) ₂]		481	-	-	Hydrogenation of alkynes,	113
			-	-	Polymerization of NBD	345
[Mo ₂ PtCp ₂ (CO) ₆ (CNPh) ₂]		1140,481	MgO	[Mo ₂ Pt]	Hydrogenation of toluene	114
[Mo ₂ PtCp ₂ (CO) ₆ (PEt ₃) ₂]		481-482	-	-	Hydrogenation of alkene & alkyne,	51
			-	-	Hydrosilylation of 1-pentene	51
[Mo ₂ Pt ₂ Cp ₂ (CO) ₆ (PPh ₃) ₂]		481	-	-	Hydrogenation of alkene & alkyne,	51
			-	-	Hydrosilylation of 1-pentene	51
[Mo ₃ PtS ₄ Cp' ₃ (NBE)][pts]		479	γ-Al ₂ O ₃	[Mo ₃ Pt]	Hydrogenation of naphthalene	108
			γ-Al ₂ O ₃	[Mo ₃ Pt]	Simultaneous HDS, HDN	108
[NH ₄] ₄ [H ₄ Mo ₆ PtO ₂₄]		483	MgO	[Mo ₆ Pt]	Dehydrogenation of alkanes	215
Mo-Cu [Mo ₃ CuS ₄ (dmpe) ₃ Cl ₄] ⁺		484	-	-	Cyclopropanation of styrene	318
[Mo ₃ CuS ₄ {(R,R)-Me-BPE} ₃ Cl ₄] ⁺	((R,R)-Me-BPE) = (+)-1,2-bis[(2 <i>R</i> ,5 <i>R</i>)-2,5-(dimethylphospholan-1-yl)]ethane	318	-	-	Cyclopropanation of styrene	318
W-Fe [PPN][HWFe(CO) ₉]		449	-	-	Isomerization of alkenes	50
[Et ₄ N] ₂ [W ₂ FeS ₄ O ₄]		103	γ-Al ₂ O ₃	[W ₂ Fe]	Hydrogenation of cyclohexene	103
			γ-Al ₂ O ₃	[W ₂ Fe]	HDS of thiophene	103
W-Fe-Co [WFeCo(PMe)Cp(CO) ₆]		485	-	-	Hydrogenation of alkenes	107
W-Ru [WRu(PPh ₂) ₂ (CO) ₇]		211	-	-	Hydrogenation of cyclohexanone,	211
			-	-	Hydroformylation of styrene	211
[WRuCp(C ₅ R ₅)(CO) ₃ (dppm)] (R = H, Me)		165	-	-	CO ₂ Hydrogenation	165

Table 4. continued

Metallic Couple ^a	Precursor Cluster	Ref.	Support	Notation of the MMCD catalyst ^b	Catalyzed Reactions	Ref.
		Synth.				Catal.
W-Ru-Co	[HWRuCo(CMe)Cp(CO) ₈]	461	-	-	Isomerization of fumaric esters	53
W-Os	[HWOs ₃ Cp(CO) ₁₂]	463	$\gamma\text{-Al}_2\text{O}_3$	[WOs ₃]	CO Hydrogenation	166
	[PPN][HWOs ₃ (CO) ₁₄]	486	ionic liquids	-	Hydrogenation of alkenes	115
W-Co	[WCo ₂ (CH)Cp(CO) ₈]	464	-	-	Hydrosilylation of acetophenone	383
	[Et ₄ N] ₂ [W ₂ CoS ₄ O ₄]	103	$\gamma\text{-Al}_2\text{O}_3$	[W ₂ Co]	Hydrogenation of cyclohexene	103
			$\gamma\text{-Al}_2\text{O}_3$	[W ₂ Co]	HDS of thiophene	103
W-Rh	[WRhS ₂ Cp ₂ (PPh ₃) ₂][PF ₆]	111	-	-	Hydrogenation of alkynes	111
	[HWRh(PPh ₃)(CO) ₅ (PPh ₃)]	487	-	-	Hydroformylation of alk(e+y)nes	282
	[W ₂ RhCp ₃ (CO) ₅]	468	SiO ₂	[W ₂ Rh]	CO Hydrogenation	169
	[triphos]Rh((CO) ₅ WS(C ₆ H ₄)CH=CH ₂ }]					
	(triphos = MeC(CH ₂ PPh ₂) ₃)	413	-	-	model for benzothiophene HDS	413
W-Ir	[H ₂ WIr(SH) ₂ Cp ₂ (PPh ₃) ₂][PF ₆]	111	-	-	Hydrogenation of alkynes	111
	[WIr ₃ Cp(CO) ₁₁]	84	$\gamma\text{-Al}_2\text{O}_3$	[WIr ₃]	<i>n</i> -Butane Hydrogenolysis,	84
			$\gamma\text{-Al}_2\text{O}_3$	[WIr ₃]	CO Methanation	84
	[W ₂ Ir ₂ Cp ₂ (CO) ₁₀]	84	$\gamma\text{-Al}_2\text{O}_3$	[W ₂ Ir ₂]	<i>n</i> -Butane Hydrogenolysis,	84
			$\gamma\text{-Al}_2\text{O}_3$	[W ₂ Ir ₂]	CO Methanation	84
W-Ni	[Et ₄ N] ₂ [W ₂ NiS ₄ O ₄]	103	$\gamma\text{-Al}_2\text{O}_3$	[W ₂ Ni]	Hydrogenation of cyclohexene	103
			$\gamma\text{-Al}_2\text{O}_3$	[W ₂ Ni]	HDS of thiophene	103
W-Pd	[WPd(PPh ₃) ₂ (CO) ₄ (PPh ₃)]	211	-	-	Hydroformylation of styrene	211
	[W ₂ Pd(CO) ₆ (C ₅ H ₂ Ph ₂ (PPh ₃)) ₂]	379a	-	-	W-C≡C bond formation	379a
	[W ₂ Pd ₂ Cp ₂ (CO) ₆ (PEt ₃) ₂]	452	-	-	Isomerization of 1,5-COD,	51
			-	-	Hydrogenation of alkene & alkyne,	51
			-	-	Oligomerization of butadiene	51
			-	-	Hydrosilylation of 1-pentene	51
	[W ₂ Pd ₂ Cp ₂ (CO) ₆ (PPh ₃) ₂]	452	-	-	Isomerization of 1,5-COD,	51
			$\gamma\text{-Al}_2\text{O}_3$	[W ₂ Pd ₂]	Hydrocarbon Rearrangements	85
			-	-	Hydrogenation of alkene & alkyne,	51
			-	-	Oligomerization of butadiene	51
			-	-	Cross coupling aryl halides/triflates	355
			-	-	Hydrosilylation of 1-pentene,	51
W-Pt	[HWPt(PPh ₃)(CO) ₅ (PPh ₃)]	161	SiO ₂	[WPt]	CO ₂ Hydrogenation	161
	[W ₂ PtCp ₂ (CO) ₆ (NCPh) ₂]	114a,481	MgO, $\gamma\text{-Al}_2\text{O}_3$	[W ₂ Pt]	Hydrogenation of toluene	114a,116
			MgO, $\gamma\text{-Al}_2\text{O}_3$	[W ₂ Pt]	Hydrogenation of crotonaldehyde	116
	[W ₂ PtCp ₂ (CO) ₆ (CNR) ₂]	488	-	-	Polymerization of NBD	345
	(R = Cy, <i>t</i> -Bu)					

Table 4. continued

Metallic Couple ^a	Precursor Cluster	Ref.	Support	Notation of the MMCD catalyst ^b	Catalyzed Reactions	Ref.
		Synth.				Catal.
	[W ₂ Pt ₂ Cp ₂ (CO) ₆ (PEt ₃) ₂]	481-482	-	-	Hydrogenation of alkene & alkyne	51
	[W ₂ Pt ₂ Cp ₂ (CO) ₆ (PPh ₃) ₂]	481	-	-	Hydrogenation of alkene & alkyne,	51
			γ-Al ₂ O ₃	[W ₂ Pt ₂]	Hydrogenation of toluene,	116
			γ-Al ₂ O ₃	[W ₂ Pt ₂]	Hydrogenation of crotonaldehyde	116
Mn-Fe	[MnFe(AsMe ₂)(CO) ₈]	489	-	-	Isomerization of 1-octene,	52
			-	-	Hydrogenation of 1-octene	52
	C[MnFe(CO) ₉] (cation C ⁺ = K ⁺ , Et ₄ N ⁺)	490	carbon	[MnFe]	CO Hydrogenation	173
	[Et ₄ N][MnFe ₂ (CO) ₁₂]	491	γ-Al ₂ O ₃ , SiO ₂ ,			
			MgO, TiO ₂ , ZrO ₂	[MnFe ₂]	CO Hydrogenation	170
			carbon	[MnFe ₂]	CO Hydrogenation	173
	K[MnFe ₂ (CO) ₁₂]	491	SiO ₂	[MnFe ₂]	CO Hydrogenation	171
			γ-Al ₂ O ₃ , MgO,			
			ZrO ₂ + γ-Al ₂ O ₃	[MnFe ₂]	CO Hydrogenation	172
	[MnFe ₂ O(MeCOO) ₆ (H ₂ O) ₃]·2H ₂ O	492	solid state	[MnFe ₂]	NO reduction	396
	[Mn ₂ Fe(CO) ₁₄]	493	carbon	[Mn ₂ Fe]	CO Hydrogenation	173
Mn-Ru	[MnRu(CO) ₆ (PhC=CH-CH=N-i-Pr)]	117	-	-	Hydrogenation of styrene	117
	[Et ₄ N][MnRu ₃ C(CO) ₁₃]	450	SiO ₂	[MnRu ₃]	CO Hydrogenation	159
Mn-Co	[MnCo(CO) ₉]	494	γ-Al ₂ O ₃	[MnCo]	CO Hydrogenation	174
Mn-Rh	[Mn{Rh ₁₂ (CO) ₃₀ }]	175	-	-	CO Hydrogenation	175
	[Mn ₂ Rh ₂ (CPh) ₂ Cp ₂ (CO) ₆]	283	-	-	Hydroformylation of styrene	283
Mn-Pd	[MnPdBr(CO) ₃ (dppm) ₂]	176	-	-	CO ₂ Hydrogenation	176
	[MnPdI(CO) ₃ (dppm) ₂]	176	-	-	Homologation of Methanol	176
Re-Ru	[ReRuCp*(CO) ₅ (dppm)]	376	-	-	Addition of RCOOH to alkynes	376
	[ReRuCp(CO) ₅ (dppm)]	376	-	-	Addition of RCOOH to alkynes	376
	[ReRuCp(CO) ₇]	376	-	-	Addition of RCOOH to alkynes	376
Re-Os	[H ₃ ReOs ₃ (CO) ₁₃]	495	γ-Al ₂ O ₃	[ReOs ₃]	n-Butane Hydrogenolysis	86
			MgO	[ReOs ₃]	CO Methanation	177
Re-Rh	[H ₆ ReRh(PCy ₂) ₂ (PCy ₂ H) ₂]	118	-	-	Hydrogenation of alk(e+y)ne, diene	118
	[Re ₂ {Rh ₁₂ (CO) ₃₀ } ₃]	178	-	-	CO Hydrogenation	178
Re-Ir	C ₂ [Re ₇ IrC(CO) ₂₃] (cation C ⁺ = Et ₄ N ⁺ , PPN ⁺)	496	γ-Al ₂ O ₃	[Re ₇ Ir]	Ethane Hydrogenolysis	87
Re-Pt	[H ₂ RePtCp(CO) ₂ (PPh ₃) ₂]	119	-	-	Hydrogenation of ethylene	119
	[RePt ₃ (CO) ₃ (dppm) ₃][PF ₆]		γ-Al ₂ O ₃	[RePt ₃]	Sulfidation model for RePt/Al ₂ O ₃	423
	[RePt ₃ (CO) ₃ (O)(dppm) ₃][PF ₆]		γ-Al ₂ O ₃	[RePt ₃]	Sulfidation model for RePt/Al ₂ O ₃	423

Table 4. continued

Metallic Couple ^a	Precursor Cluster	Ref.	Support	Notation of the MMCD catalyst ^b	Catalyzed Reactions	Ref.
		Synth.				Catal.
	[RePt ₃ (CO) ₃ (O) ₂ (dppm) ₃][PF ₆] ⁴²³		γ-Al ₂ O ₃	[RePt ₃]	Sulfidation model for RePt/Al ₂ O ₃	423
	[RePt ₃ (O) ₃ (dppm) ₃][PF ₆] ⁴²³		γ-Al ₂ O ₃	[RePt ₃]	Sulfidation model for RePt/Al ₂ O ₃	423
	[Re ₂ Pt(CO) ₁₂] ⁴⁹⁷		γ-Al ₂ O ₃	[Re ₂ Pt]	Cyclopentane Hydrogenolysis, ⁸⁸	
			γ-Al ₂ O ₃	[Re ₂ Pt]	Dehydrogenation of cycloalkane ²¹⁶	
Fe-Ru	[FeRu(PPh ₃) ₂ (CO) ₆] ²¹¹	211	-	-	Hydrogenation of cyclohexanone, ²¹¹	
			-	-	Hydroformylation of styrene ²¹¹	
	[FeRu ₂ (CO) ₁₂] ⁴⁹⁸	498	-	-	Isomerization of <i>cis</i> -stilbene, ⁵⁴	
			γ-Al ₂ O ₃	[FeRu ₂]	Ethane Hydrogenolysis ⁸⁹	
			-	-	Hydrogenation of alkynes, dienes ⁵⁴	
			ZrO ₂	[FeRu ₂]	CO Hydrogenation ¹⁷⁹	
			carbon	[FeRu ₂]	CO Hydrogenation ¹⁸¹	
			-	-	WGSR ^{220a,b}	
			γ-Al ₂ O ₃	[FeRu ₂]	Ethylene Self Homologation ⁸⁹	
	[FeRu ₂ (CO) ₁₁ (PR ₃)] ⁴⁹⁹ (R = Ph, OMe)	499	-	-	WGSR ²²⁰	
[FeRu ₂ (CO) ₁₀ (PR ₃) ₂] ⁴⁹⁹ (R = Ph, OMe)		499	-	-	WGSR ²²⁰	
	[FeRu ₂ (CO) ₁₀ (dppe)] ⁴⁹⁹	499	-	-	WGSR ²²⁰	
	[H ₂ FeRu ₃ (CO) ₁₃] ⁵⁰⁰	500	-	-	Isomerization of alkenes/arenes, ⁵⁴⁻⁵⁶	
			-	-	Hydrogenation of alkynes, dienes ⁵⁴	
			glc Chromosorb	[FeRu ₃]	Hydrogenation of arenes, dienes ¹²⁰	
			borosilicate	[FeRu ₃]	Hydrogenation of alk(en)yes ¹²¹	
			SiO ₂	[FeRu ₃]	CO Hydrogenation ⁸⁵	
			γ-Al ₂ O ₃ , MgO,			
			γ-Al ₂ O ₃ /KOH	[FeRu ₃]	CO and CO ₂ Methanation ¹²²	
			γ-Al ₂ O ₃ , SiO ₂ , NaY	[FeRu ₃]	CO Hydrogenation ¹⁸⁰	
[Fe ₂ Ru(CO) ₁₂] ⁴⁹⁸		498	carbon	[Fe ₂ Ru]	CO Hydrogenation ¹⁸¹	
			-	-	Dehydrogenation of alkenes ¹²⁰	
			-	-	WGSR ^{220a,b}	
			-	-	Isomerization of alkenes, ^{54,56}	
			γ-Al ₂ O ₃	[Fe ₂ Ru]	Ethane Hydrogenolysis ⁸⁹	
			-	-	Hydrogenation of alkynes, dienes ⁵⁴	
			γ-Al ₂ O ₃	[Fe ₂ Ru]	CO Hydrogenation ⁸⁹	
			ZrO ₂	[Fe ₂ Ru]	CO Hydrogenation ¹⁷⁹	
			SiO ₂	[Fe ₂ Ru]	CO Hydrogenation ⁸⁵	
			carbon	[Fe ₂ Ru]	CO Hydrogenation ¹⁸¹	
			-	-	WGSR ^{220a,b}	
			γ-Al ₂ O ₃	[Fe ₂ Ru]	Ethylene Self Homologation ⁸⁹	

Table 4. continued

Metallic Couple ^a	Precursor Cluster	Ref.	Support	Notation of the MMCD catalyst ^b	Catalyzed Reactions	Ref.
		Synth.				Catal.
	[Fe ₂ Ru(CO) ₁₁ (PR ₃)] (R = Ph, OMe)	499	-	-	WGSR	220
	[Fe ₂ Ru(CO) ₁₀ (PR ₃) ₂] (R = Ph, OMe)	499	-	-	WGSR	220
	[Fe ₂ Ru(CO) ₁₀ (dppe)]	499	-	-	WGSR	220
	[Et ₄ N] ₂ [Fe ₃ Ru ₃ C(CO) ₁₃]	450	SiO ₂	[Fe ₃ Ru ₃]	CO Hydrogenation	159,183
Fe-Ru-Co	[HFeRuCo(PMe)(CO) ₈]	501	-	-	Hydrogenation of styrene	107
Fe-Os	[H ₂ FeOs ₃ (CO) ₁₃]	500,502	SiO ₂	[FeOs ₃]	CO Hydrogenation	184
			Al ₂ O ₃	[FeOs ₃]	CO Hydrogenation	185
Fe-Co	[FeCoCp(CO) ₆]	188a	γ-Al ₂ O ₃	[FeCo]	CO Hydrogenation	188
	K[FeCo(CO) ₈]	490	carbon	[FeCo]	CO Hydrogenation	189
	[FeCo(AsMe ₂)(CO) ₇]	453	-	-	Isomerization of 1-octene, Hydrogenation of 1-octene	52
	[FeCo ₂ (PPh)(CO) ₉]	503	-	-	Hydroformylation of alkenes	109
			-	-	Hydrosilylation of acetophenone	383
[HFeCo ₃ (CO) ₁₂]		504	glc Chromosorb	[FeCo ₃]	Hydrogenation of alk(e+y)nes	122
			SiO ₂	[FeCo ₃]	CO Hydrogenation	187
			carbon	[FeCo ₃]	CO Hydrogenation	189
			γ-Al ₂ O ₃ , MgO,			
			γ-Al ₂ O ₃ / KOH	[FeCo ₃]	CO and CO ₂ Methanation	122
			-	-	Dimerization of NBD	346
K[FeCo ₃ (CO) ₁₂]		504	carbon	[FeCo ₃]	CO Hydrogenation	189
[Me ₄ N][FeCo ₃ (CO) ₁₂]		504	-	-	Dimerization of NBD	346
[Et ₄ N][FeCo ₃ (CO) ₁₂]		504	-	-	Hydroformylation of cyclohexene	284
			SiO ₂	[FeCo ₃]	Dimerization of NBD	61
[PPN][FeCo ₃ (CO) ₁₂]		504	-	-	CO Methanation	186
[(PhCH ₂)Me ₃ N][FeCo ₃ (CO) ₁₂]		504	-	-	Hydroformylation of olefins	285
C[FeCo ₃ (CO) ₁₂]		504	-	-	Methanol homologation	251
(cat C ⁺ = Et ₄ N ⁺ or Bu ₄ N ⁺)						
[HFeCo ₃ (CO) ₁₁ (PPh ₃)]		505	-	-	PKR	322
[Fe ₂ CoCp(CO) ₉]		506	-	-	Isomerization of 1-pentene	57
[Fe ₂ Co(Ph ₂ PCH ₂ L) ₂ (CO) ₈ Cl ₂]		343	-	-	Oligomerization of ethylene	343
(L = oxazoline)						
[Fe ₂ CoO(MeCOO) ₆ (H ₂ O) ₃]·2H ₂ O		492	solid state	[Fe ₂ Co]	NO reduction	396
[Fe ₂ Co ₂ (PPh) ₂ (CO) ₁₁]		507	-	-	Hydroformylation of olefins	286
[Fe ₂ Co ₂ OSae ₂]·4DMF·H ₂ O		225	-	-	Oxidation of alkanes	225
(H ₂ Sae = salicylidene-2-ethanolamine)						

Table 4. continued

Metallic Couple ^a	Precursor Cluster	Ref.	Support	Notation of the MMCD catalyst ^b	Catalyzed Reactions	Ref.
		Synth.				Catal.
	[PPN][Fe ₃ Co(CO) ₁₃]	508	-	-	CO Methanation	186
	C[Fe ₃ Co(CO) ₁₃] (cation C ⁺ = K ⁺ , Et ₄ N ⁺)	508	carbon	[Fe ₃ Co]	CO Hydrogenation	189
	[Et ₄ N][Fe ₃ Co(CO) ₁₃]	508	-	-	Methanol homologation	251b,c
			-	-	Hydroformylation of cyclohexene	284
Fe-Co-Cu	[FeCuCo(L) ₃ (NCS) ₂ (MeOH)] ₂ (H ₂ L = diethanolamine)	226	-	-	Oxidation of cycloalkanes	226
Fe-Rh	[FeRh(P <i>t</i> -Bu ₂)(CO) ₄ (dpmm)]	287	-	-	Hydroformylation of ethylene	287
	[FeRh(Ph ₂ Ppy) ₂ (CO) ₄ Cl]	257	-	-	Carbonylation of EtOH	257
	[Me ₄ N] ₂ [FeRh ₄ (CO) ₁₅]	509	SiO ₂	[FeRh ₄]	CO Hydrogenation,	191
			SiO ₂	[FeRh ₄]	Hydroformylation of olefins	97,191,290
	[PPN] ₂ [FeRh ₄ (CO) ₁₅]	509	-	-	Carbonylation of nitrobenzene	362
	[TMBA][FeRh ₅ (CO) ₁₆]	509	SiO ₂	[FeRh ₅]	CO Hydrogenation,	191
			SiO ₂	[FeRh ₅]	Hydroformylation of olefins	97,191,290
	C ₂ [Fe ₂ Rh ₄ (CO) ₁₆] (cation C ⁺ = [Me ₃ (CH ₂ Ph)N] ⁺ , TBPA)	509	NaY zeolite	[Fe ₂ Rh ₄]	<i>n</i> -Alkane Hydrogenolysis,	90
					CO Hydrogenation	90,190
	[TMBA] ₂ [Fe ₂ Rh ₄ (CO) ₁₆]	509	SiO ₂	[Fe ₂ Rh ₄]	CO Hydrogenation,	191
			SiO ₂	[Fe ₂ Rh ₄]	Hydroformylation of olefins	97,191,290
			γ-Al ₂ O ₃ , TiO ₂ ,			
			ZrO ₂	[Fe ₂ Rh ₄]	Cycloaddition of propyne + CO ₂	377
	[HFe ₃ Rh(C=CHPh)(CO) ₁₁]	58	-	-	Isomerization of 1-heptene	58
		-	-	-	Hydrogenation of 1-heptene	58
		-	-	-	Hydroformylation of 1-pentene	58
	[Ph ₄ P][Fe ₃ Rh ₂ (MeC=C=CH ₂)(CO) ₁₃]	59	-	-	Isomerization of alkenes	59
	[Fe ₃ Rh ₂ C(CO) ₁₄]	510	SiO ₂	[Fe ₃ Rh ₂]	CO Hydrogenation,	191
			SiO ₂	[Fe ₃ Rh ₂]	Hydroformylation of olefins	97,191,290
	[Et ₄ N][Fe ₃ Rh ₃ C(CO) ₁₅]	511	SiO ₂	[Fe ₃ Rh ₃]	Hydroformylation of propene	193
	[Ph ₄ P][Fe ₃ Rh ₃ C(CO) ₁₅]	289	-	-	Hydroformylation of 1-pentene	289
	[Et ₄ N][Fe ₄ RhC(CO) ₁₄]	512	SiO ₂	[Fe ₄ Rh]	CO Hydrogenation,	193
			SiO ₂	[Fe ₄ Rh]	Hydroformylation of propene	193
	[Ph ₄ P][Fe ₄ RhC(CO) ₁₄]	289,512	-	-	Hydroformylation of 1-pentene	289
	[Ph ₄ P][Fe ₄ Rh ₂ (N)(CO) ₁₅]	288	-	-	Hydroformylation of 1-pentene	288
	[Fe ₄ Rh ₂ C(CO) ₁₆]	289	-	-	Hydroformylation of 1-pentene	289
	[Ph ₄ P] ₂ [Fe ₅ Rh(N)(CO) ₁₅]	288	-	-	Hydroformylation of 1-pentene	288
	[Ph ₄ P][Fe ₅ RhC(CO) ₁₆]	512	-	-	Hydroformylation of 1-pentene	289
	[Et ₄ N][Fe ₅ RhC(CO) ₁₆]	512	SiO ₂	[Fe ₅ Rh]	CO Hydrogenation,	193
			SiO ₂	[Fe ₅ Rh]	Hydroformylation of propene	193

Table 4. continued

Metallic Couple ^a	Precursor Cluster	Ref.	Support	Notation of the MMCD catalyst ^b	Catalyzed Reactions	Ref.
		Synth.				Catal.
	[Me ₄ N][Fe ₅ RhC(CO) ₁₆]	512	-	-	Hydrosilylation of phenylacetylene	384
Fe-Ir	Na ₂ [FeIr ₄ (CO) ₁₅]	513	-	-	WGSR	220d
	[TMBA] ₂ [FeIr ₄ (CO) ₁₅]	513	SiO ₂	[FeIr ₄]	CO Hydrogenation,	97,195
			SiO ₂	[FeIr ₄]	Hydroformylation of ethylene	191a,195
	[Et ₄ N] ₂ [Fe ₂ Ir ₂ (CO) ₁₂]	514	MgO	[Fe ₂ Ir ₂]	CO Hydrogenation	194
	[Et ₄ N] ₂ [Fe ₂ Ir ₄ (CO) ₁₆]	515	MgO	[Fe ₂ Ir ₄]	CO Hydrogenation	194
Fe-Ni	[FeNi(Ph ₂ Ppy) ₂ (CO) ₃ (NCS) ₂]	257	-	-	Carbonylation of EtOH	257
	[Fe ₂ NiO(MeCOO) ₆ (H ₂ O) ₃]·2H ₂ O	492	solid state	[Fe ₂ Ni]	NO reduction	396
Fe-Pd	[FePdCl(PPh ₂)(CO) ₄] ₂	60	-	-	Isomerization of 1-octene,	60
			SiO ₂	[Fe ₂ Pd ₂]	Isomerization of 1-octene	61
			-	-	Hydrogenation of 1-hexyne,	60
			-	-	Carbonylation of alkenes	60
			-	-	Cross coupling aryl halides/triflates	356
	[FePd{SiR ₂ (OR')}(CO) ₃ (dppm)(allyl)]	424	-	-	Coupling of organotin hydrides	424
	(R = OMe, Me, OSiMe ₃ , OSiHMe ₂ ; R' = Me, SiMe ₃ , SiHMe ₂)					
	[FePdCl{Si(OR) ₃ }(CO) ₃ (dppm)]	424	-	-	Coupling of organotin hydrides	424
	(R = Me, SiMe ₃)					
	[FePd{SiR ₃ }(CO) ₃ L(allyl)]	426	-	-	Coupling of organotin hydrides	426
	(R ₃ = (OMe) ₃ , Me(OSiMe ₃) ₂ ; L = dppa, dppm, or Ph ₂ Ppy)					
	[FePd ₂ (CO) ₄ (dppm)]	18b	SiO ₂	[FePd ₂]	Carbonylation of ArNO ₂	18b,c,516
	[Fe ₂ Pd ₂ (CO) ₅ (NO) ₂ (dppm)]	516-517	SiO ₂	[Fe ₂ Pd ₂]	Carbonylation of ArNO ₂	18b,c,516
	[TMBA] ₂ [Fe ₄ Pd(CO) ₁₆]	518	SiO ₂	[Fe ₄ Pd]	CO Methanation,	191,195
			SiO ₂	[Fe ₄ Pd]	Hydroformylation of olefins	191a
	[TMBA] ₃ [HFe ₆ Pd ₆ (CO) ₂₄]	518	SiO ₂	[Fe ₆ Pd ₆]	CO Hydrogenation,	191,195
			SiO ₂	[Fe ₆ Pd ₆]	Hydroformylation of olefins	195
Fe-Pt	[FePt(SiMe ₂)Cp ₂ (COD)]	427	-	-	ROP of [Fe(<i>n</i> -C ₅ H ₄) ₂ SiMe ₂]	427
	[FePt ₂ (PhC ₂ Ph)(CO) ₅ (PPh ₃) ₂]	385	-	-	Hydrosilylation of alkynes	385
	[Fe ₂ Pt(CO) ₉ (PPh ₃) ₂]	73	polymer	-	Hydrogenation of ethylene	73
	[Fe ₂ Pt(NO) ₂ (CO) ₆ (CNR) ₂]	488,519	-	-	Polymerization of NBD	345
	(R = Cy, <i>t</i> -Bu)					
	[Fe ₂ Pt(CO) ₆ (NO) ₂ (CN <i>t</i> -Bu) ₂]	488,519	γ-Al ₂ O ₃	[Fe ₂ Pt]	Methylcyclopentane Demethylation	85,91
	[Fe ₂ Pt(COD)(CO) ₈]	520	SiO ₂	[Fe ₂ Pt]	Oxidation of CO in air and H ₂	245
	[Fe ₂ Pt ₃ (COD) ₂ (CO) ₁₂]	520	SiO ₂	[Fe ₂ Pt ₃]	Oxidation of CO in air and H ₂	245a,246
	[TMBA] ₂ [Fe ₃ Pt ₃ (CO) ₁₆]	521	SiO ₂	[Fe ₃ Pt ₃]	CO Hydrogenation,	97,191
			SiO ₂	[Fe ₃ Pt ₃]	Hydroformylation of olefins	191a
	[TMBA] ₂ [Fe ₄ Pt(CO) ₁₆]	518	SiO ₂	[Fe ₄ Pt]	CO Methanation,	97,191
			SiO ₂	[Fe ₄ Pt]	Hydroformylation of olefins	191a

Table 4. continued

Metallic Couple ^a	Precursor Cluster	Ref.	Support	Notation of the MMCD catalyst ^b	Catalyzed Reactions	Ref.
		Synth.				Catal.
Fe-Cu	[FeCu(Ph ₂ Ppy) ₂ (CO) ₃ Cl]	257	-	-	Carbonylation of EtOH	257
	[FeCuL ₂ (CO) ₃]BF ₄] (L = (2-oxazoline-2-ylmethyl)diphenylphosphine)	320	-	-	Cyclopropanation of styrene	320
			-	-	Diels-Alder	320
	[FeCuL](NO ₃) ₂ ·4H ₂ O (L = {-NCHC ₆ H ₂ MeOCHN(CH ₂) ₃ -} ₂)	227	Zr-clay	-	Oxidation of cyclohexane	227
	[FeCuL](NO ₃) ₂ (L = {-NCHC ₆ H ₂ MeOCHNC ₆ H ₄ -} ₂)	228	γ-Al ₂ O ₃	-	Oxidation of cyclohexane	228
Fe-Au	[Et ₄ N][Fe ₄ Au(CO) ₁₆] [Et ₄ N] ₄ [Fe ₄ Au ₄ (CO) ₁₆]	522 523	TiO ₂ , CeO ₂ CeO ₂ , SBA-15 TiO ₂ , CeO ₂ TiO ₂	[Fe ₄ Au] [Fe ₄ Au] [Fe ₄ Au] [Fe ₄ Au ₄]	Toluene combustion Methanol combustion Oxidation of CO in H ₂ (PROX) Toluene combustion	229-231 231,238 247 229-230
Fe-Hg	[FeHg(Ph ₂ Ppy) ₂ (CO) ₃ (SCN) ₂]	257	-	-	Carbonylation of EtOH	257
Ru-Os	[H ₂ RuOs ₃ (CO) ₁₃] [Ph ₄ As][H ₃ RuOs ₃ (CO) ₁₂]	500 63	γ-Al ₂ O ₃ γ-Al ₂ O ₃ γ-Al ₂ O ₃ polymer polymer	[RuOs ₃] [RuOs ₃] [RuOs ₃] -	Isomerization of 1-butene, Hydrogenation of ethylene CO Hydrogenation, Isomerization of 1-hexene, Hydroformylation of 1-hexene	62 62 196 63 63
Ru-Co	[RuCoCp(CO) ₄ (PPh ₃) ₂] [RuCo ₂ (CO) ₁₁] [RuCo ₂ S(CO) ₉] [RuCo ₂ Se(CO) ₉] [RuCo ₂ (PR)(CO) ₉] (R = Me, Ph) [HRuCo ₃ (CO) ₁₂]	251a 524 462,525 525 525 251c	- SiO ₂ - carbon, γ-Al ₂ O ₃ - - - SiO ₂ γ-Al ₂ O ₃ , NaY, SiO ₂ γ-Al ₂ O ₃ , MgO, γ-Al ₂ O ₃ /KOH carbon - carbon	[RuCo ₂] [RuCo ₃] -	Homologation of MeOH CO Hydrogenation Isomerization of 1-hexene, Hydrogenation of alkenes HDS of thiophene Isomerization of 1-hexene, Hydrogenation of 1-hexene Hydrogenation of alkenes Hydrogenation of alk(e+y)nes CO Hydrogenation CO Hydrogenation CO and CO ₂ Methanation Homologation of MeOH Hydrocarbylation of MeOH Hydroformylation of alkenes Hydroformylation of olefins,	253 159,183,197 64 414 64 64 107 120,122 159,183,197-199 201-202 251c,254 261 254a,284 292

Table 4. continued

Metallic Couple ^a	Precursor Cluster	Ref.	Support	Notation of the MMCD catalyst ^b	Catalyzed Reactions	Ref.
		Synth.		MMCD catalyst ^b		Catal.
	C[RuCo ₃ (CO) ₁₂]	251c,254b	-	-	Homologation of MeOH	251c,254
	(cation C ⁺ = Na ⁺ , Cs ⁺ , Et ₃ N ⁺ , Ph ₄ P ⁺ , PPN ⁺)					
	C'[RuCo ₃ (CO) ₁₂]	505	-	-	PKR	322
	(cation C ⁺ = H ⁺ , Et ₄ N ⁺ , bmim ⁺)					
	[Et ₃ N][RuCo ₃ (CO) ₁₂]	251c	-	-	Homologation of methylacetate	252
	[Et ₃ N][RuCo ₃ (PhC ₂ Ph)(CO) ₁₀]	255	-	-	Homologation of MeOH	255
	[HRu ₂ CoS(CO) ₉]	414	carbon, γ-Al ₂ O ₃	[Ru ₂ Co]	HDS of thiophene	414
	[HRu ₂ Co(PMe)(CO) ₉]	501	-	-	Hydrogenation of alkenes	107
	[Ru ₂ Co ₂ (CO) ₁₃]	524a	SiO ₂	[Ru ₂ Co ₂]	CO Hydrogenation,	198-199
			carbon	[Ru ₂ Co ₂]	Hydrocarbonylation of MeOH	261
	[H ₂ Ru ₂ Co ₂ (CO) ₁₂]	526	SiO ₂	[Ru ₂ Co ₂]	CO Hydrogenation	198-199
	[Et ₃ N][Ru ₃ Co(CO) ₁₃]	508	-	-	Homologation of methylacetate	252
			carbon	[Ru ₃ Co]	Hydroformylation of olefins	292
	[PPN][Ru ₃ Co(CO) ₁₃]	508	-	-	CO Methanation	186
			NaY, SiO ₂			
			γ-Al ₂ O ₃	[Ru ₃ Co]	CO and CO ₂ Hydrogenation	180
	[HRu ₃ Co(CO) ₁₃]	202	NaY zeolite	[Ru ₃ Co]	CO Hydrogenation	202
		508	carbon	[Ru ₃ Co]	Hydrocarbonylation of MeOH	261
	[H ₃ Ru ₃ Co(CO) ₁₂]	527	SiO ₂	[Ru ₃ Co]	CO Hydrogenation	197-199
			-	-	WGSR	220d,221
			carbon	[Ru ₃ Co]	Hydroformylation of olefins	292
	[Ru ₃ Co ₃ C(CO) ₁₄]	508	SiO ₂	[Ru ₃ Co ₃]	CO Hydrogenation	159,183
Ru-Co-Cu	[RuCo ₃ (CuPPh ₃)(CO) ₁₂]	255	-	-	Homologation of MeOH	255
Ru-Co-Au	[Au(PPh ₃) ₂][RuCo ₃ (CO) ₁₂]	255	-	-	Homologation of MeOH	255
Ru-Rh	[RuRhCl(CO) ₃ (dppm) ₂]	293	-	-	Hydroformylation of pentene	293
	[HRuRh(bim)(CO)(COD)(PPh ₃) ₂]	123	-	-	Hydrogenation of alkenes	123-124
	(bim = 2,2'-bi-imidazolato)		-	-	Hydrogenation of ketones	123-124
	[HRuRhCl(pz)(CO)(diolefin)(PPh ₃) ₂]	214	-	-	Hydrogenation of ketones	214
	(pz = pyrazolate; diolefin = COD or TFB (TFB = tetrafluorobenzobarrelene))					
	[RuRh ₂ (CO) ₁₂]	203	-	-	CO Hydrogenation	203
	[HRuRh ₃ (CO) ₁₂]	528	-	-	Homologation of MeOH	256
	[HRuRh ₃ (CO) ₁₀ (PPh ₃) ₂]	528	-	-	Homologation of MeOH	256
	[PPN] ₂ [RuRh ₄ (CO) ₁₅]	529	-	-	Carbonylation of nitrobenzene	362
	[PPN][RuRh ₅ (CO) ₁₆]	530	-	-	WGSR,	220d
			-	-	Homologation of MeOH	256
			-	-	Hydroformylation of 1-hexene	294

Table 4. continued

Metallic Couple ^a	Precursor Cluster	Ref.	Support	Notation of the MMCD catalyst ^b	Catalyzed Reactions	Ref.
		Synth.				Catal.
	[H ₂ Ru ₂ Rh ₂ (CO) ₁₂]	531	-	-	Hydrogenation of alkene,	125
			-	-	WGSR,	220d
			-	-	Homologation of MeOH	256
	[Et ₄ N][Ru ₃ Rh ₃ C(CO) ₁₅]	450	SiO ₂	[Ru ₃ Rh ₃]	CO hydrogenation	159
Ru-Ir	[HRuIr(bim)(CO)(COD)(PPh ₃) ₂] (bim = 2,2'-bi-imidazolato)	123	-	-	Hydrogenation of alkenes	123-124
	[HRuIrCl(pz)(CO)(diolefin)(PPh ₃) ₂] (pz = pyrazolate; diolefin = COD or TFB (TFB = tetrafluorobenzobarrelene))	214	-	-	Hydrogenation of ketones	123-124
	[HIrRu ₃ (CO) ₁₃]	532	-	-	Hydrogenation of PhC ₂ Ph	126
	[HIrRu ₃ (CO) ₁₁ (RC ₂ R)] (R = Ph, Me)	126	-	-	Hydrogenation of PhC ₂ Ph	126
	[IrRu ₃ (CO) ₁₀ (RC ₂ R)(RC ₂ HR)] (R = Ph, Me)	126	-	-	Hydrogenation of PhC ₂ Ph	126
Ru-Ni	[Ru ₂ NiS ₂ (N) ₂ Me ₄ (dppe)]	239	-	-	Oxidation of benzyl alcohol	239
	[H ₃ Ru ₃ NiCp(CO) ₉]	140,533	-	-	Isomerization of alkenes,	65
			-	-	Alkane Hydrogenolysis,	65
			-	-	Hydrogenation of alkenes, dienes	65,127
			Chromosorb P	[Ru ₃ Ni]	Hydrogenation of arenes, dienes	128
			Chromosorb P	[Ru ₃ Ni]	Dehydrogenation of alcohols	128
			γ-Al ₂ O ₃	[Ru ₃ Ni]	Ammonia synthesis	404-405
	[H ₃ Ru ₃ NiCp(CO) ₈ (PR ₃)] (R = Ph, Cy)	66	-	-	Isomerization of dienes	66
	[H ₃ Ru ₃ NiCp(CO) ₇ (PPh ₃) ₂]	66	-	-	Isomerization of dienes	66
	[Et ₄ N] ₂ [Ru ₃ Ni ₃ C(CO) ₁₃]	450	SiO ₂	[Ru ₃ Ni ₃]	CO Hydrogenation	159
Ru-Pd	[PPh ₄][RuPd(N)O ₂ Me ₂ (N-N)] (N-N = (-)-sparteine)	240	-	-	Oxidation of alcohols,	240
	[Ru ₂ PdS ₂ (N) ₂ Me ₄ (dppe)]	534	-	-	Oxidation of PPh ₃	240
	[Ru ₂ PdL ₂ (phen) ₄](ClO ₄) ₂	357	-	-	Oxidation of benzyl alcohol	239
	[Ru ₂ PdL ₂ (bpy) ₄](ClO ₄) ₂ (L = N,N'-(4-amino-1-benzyl piperidine)-glyoxime)	357	-	-	Suzuki-Miyaura coupling	357
	[Et ₄ N][Ru ₆ Pd ₆ (CO) ₂₄]	535	MCM-41	[Ru ₆ Pd ₆]	Suzuki-Miyaura coupling	357
Ru-Pt	[RuPt ₅ (CO) ₅ (PPh ₃) ₃]	73	polymer	-	Hydrogenation of alkenes	129-130
	[RuPt ₅ (PhC ₂ Ph)(CO) ₅ (PPh ₃) ₂]	385	-	-	Hydrosilylation of alkynes	385
	[Ru ₂ Pt(PhC ₂ Ph)(CO) ₇ (PPh ₃) ₂]	385	-	-	Hydrosilylation of alkynes	385
	[Ru ₂ Pt(PhC ₂ Ph)(CO) ₈ (dppe)]	536	-	-	Hydrosilylation of PhC ₂ Ph	386
	[Ru ₂ PtS ₂ (N) ₂ Me ₄ (dppe)]	534	-	-	Oxidation of benzyl alcohol	239

Table 4. continued

Metallic Couple ^a	Precursor Cluster	Ref.	Support	Notation of the MMCD catalyst ^b	Catalyzed Reactions	Ref.
		Synth.		[Ru _x Pt]		Catal.
	[H ₂ Ru ₂ Pt ₂ (CO) ₈ (PPh ₃) ₂]	385	-	-	Hydrosilylation of alkynes	385
	[H ₂ Ru ₂ Pt ₂ (CO) ₉ (Sn- <i>t</i> -Bu ₃) ₂]	399	SiO ₂	[Ru ₂ Pt ₂]	Hydrogenation of nitrobenzene	399
	[Ru ₃ Pt(CO) ₁₂ py ₃]	92	oxides, carbon	[Ru ₃ Pt]	Hydrocarbon Conversion	92
	[Ru ₄ Pt ₂ (CO) ₁₈]	537	carbon	[Ru ₄ Pt ₂]	Oxidation of methanol	241
	[Ru ₅ PtC(CO) ₁₆]	538	SiO ₂	[Ru ₅ Pt]	Hydrogenation of alkenes	133
			SiO ₂	[Ru ₅ Pt]	Hydrogenation of C=O bonds	133
			SiO ₂	[Ru ₅ Pt]	Hydrogenation of nitrobenzene	399
	[Ru ₅ PtC(CO) ₁₅ (P- <i>t</i> -Bu ₃)]	539	-	-	Hydrogenation of PhC ₂ H	131
	[Ph ₄ P] ₂ [Ru ₅ PtC(CO) ₁₅]	540	SiO ₂	[Ru ₅ Pt]	Hydrogenation of alkenes	129e, 130
			SiO ₂	[Ru ₅ Pt]	Hydrogenation of C=O bonds	129e
			γ-Al ₂ O ₃	[Ru ₅ Pt]	Ethanol steam reforming	242
	[Ru ₅ PtC(GePh ₂)(CO) ₁₅]	541	SiO ₂	[Ru ₅ Pt]	Hydrogenation of alkenes	133
			SiO ₂	[Ru ₅ Pt]	Hydrogenation of C=O bonds	133
	[Ru ₅ PtC(SnPh ₂)(CO) ₁₅]	541	SiO ₂	[Ru ₅ Pt]	Hydrogenation of alkenes	133
			SiO ₂	[Ru ₅ Pt]	Hydrogenation of C=O bonds	133
			MgO, SiO ₂	[Ru ₅ Pt]	Hydrogenation of citral (C=C+C=O)	134-135
			SiO ₂	[Ru ₅ Pt]	Hydrogenation of nitrobenzene	399
	[Ru ₅ PtC(PhC ₂ H)(CO) ₁₃ (P- <i>t</i> -Bu ₃)]	132	-	-	Hydrogenation of PhC ₂ H	132
	[H ₄ Ru ₆ Pt ₃ (CO) ₂₁]	93b	MgO, γ-Al ₂ O ₃	[Ru ₆ Pt ₃]	<i>n</i> -Butane Hydrogenolysis	93
			MgO, γ-Al ₂ O ₃	[Ru ₆ Pt ₃]	Hydrogenation of ethylene	93
	[H ₂ Ru ₆ Pt ₃ (PhC ₂ Ph)(CO) ₂₀]	136b	-	-	Hydrogenation of PhC ₂ Ph,	136
			-	-	Hydrosilylation of PhC ₂ Ph	386
	[H ₂ Ru ₆ Pt ₃ (TolC ₂ Tol)(CO) ₂₀]	136a	-	-	Hydrosilylation of PhC ₂ Ph	386
	[H ₂ Ru ₆ Pt ₃ (PhC ₂ Ph)(SMe ₂)(CO) ₁₉]	137	-	-	Hydrogenation of PhC ₂ Ph	137
	[Bu ₄ N][HRu ₆ Pt ₃ (PhC ₂ Ph)(CO) ₂₀]	386	-	-	Hydrosilylation of PhC ₂ Ph	386
	[PPN] ₂ [Ru ₁₀ Pt ₂ (C) ₂ (CO) ₂₈]	542	SiO ₂	[Ru ₁₀ Pt ₂]	Hydrogenation of alkenes	129e, 130
			SiO ₂	[Ru ₁₀ Pt ₂]	Hydrogenation of C=O bonds	129e
Ru-Cu	[H ₃ Ru ₄ {Cu(PPh ₃)}(CO) ₁₂]	67	-	-	Isomerization of 1-pentene	67
	[H ₂ Ru ₄ {Cu(PPh ₃) ₂ }(CO) ₁₂]	67	-	-	Isomerization of 1-pentene	67
	[Ru ₆ (CuL) ₂ C(CO) ₁₆]	204	-	-	CO Hydrogenation	204
	(L = organonitrile)					
	[PPN] ₂ [Ru ₁₂ Cu ₄ (C) ₂ Cl ₂ (CO) ₃₂]	138	SiO ₂	[Ru ₁₂ Cu ₄]	Hydrogenation of alk(e+y)nes	129c, 129e, 130, 138
Ru-Ag	[Ru ₆ (AgL) ₂ C(CO) ₁₆]	204	-	-	CO Hydrogenation	204
	(L = organonitrile)					
	[Ph ₄ As] ₂ [Ru ₁₀ Ag ₃ (C) ₂ Cl(CO) ₂₈]	139	SiO ₂	[Ru ₁₀ Ag ₃]	Hydrogenation of 1-hexene	139

Table 4. continued

Metallic Couple ^a	Precursor Cluster	Ref.	Support	Notation of the MMCD catalyst ^b	Catalyzed Reactions	Ref.
		Synth.				Catal.
Ru-Au	[H ₂ RuAu(CO)(PPh ₃) ₄][PF ₆]	68a	-	-	Isomerization of 1-hexene	68
	[H ₂ Ru ₄ {Au(PPh ₃)}(CO) ₁₂]	67	-	-	Isomerization of 1-pentene	67
	[H ₂ Ru ₄ {Au(PPh ₃) ₂ }(CO) ₁₂]	67	-	-	Isomerization of 1-pentene	67
	[Ru ₆ (AuL) ₂ C(CO) ₁₆] (L = organonitrile)	204	-	-	CO Hydrogenation	204
Os-Co	[Et ₄ N][OsCo ₃ (CO) ₁₂]	251b	-	-	Homologation of MeOH	251b
	[PPN] ₂ [OsRh ₄ (CO) ₁₅]	543	-	-	Carbonylation of nitrobenzene	362
Os-Rh	[H ₃ Os ₃ Rh(CO) ₁₂]	544	-	-	Isomerization of 1-octene	69
	[H ₂ Os ₃ Rh(acac)(CO) ₁₀]	545	polymer	-	Isomerization of 1-butene,	70
			polymer	-	Hydrogenation of ethylene	70
			γ-Al ₂ O ₃	[Os ₃ Rh]	CO Hydrogenation	185
Os-Ir	[PPN][Os ₃ Ir(CO) ₁₃]	258	-	-	Carbonylation of MeOH	258
Os-Ni	[H ₃ Os ₃ NiCp(CO) ₉]	140,533,546	-	-	Isomerization of alkenes,	65,71
			Chromosorb-P	[Os ₃ Ni]	Hydrogenation of alkenes	141,143
			γ-Al ₂ O ₃	[Os ₃ Ni]	Hydrogenation of alk(e+y)nes	142,144
			γ-Al ₂ O ₃	[Os ₃ Ni]	CO and CO ₂ Hydrogenation	142,144
			Chromosorb-P	[Os ₃ Ni]	Hydrogenation of acetone	143
			Chromosorb-P	[Os ₃ Ni]	Dehydrogenation of alcohols	128
			Chromosorb-P	[Os ₃ Ni]	Dehydration of isopropanol	143
			γ-Al ₂ O ₃	[Os ₃ Ni]	Ammonia synthesis	404-405
	[H ₃ Os ₃ NiCp(CO) ₈ L] (L = PPh ₂ H or P(C ₆ H ₄ Me-o) ₃)	547	-	-	Isomerization of alkenes,	71
			-	-	Hydrogenation of alk(e+y)nes	71
Os-Ni-Cu	[Os ₃ Ni ₃ Cp ₃ (CO) ₉]	140,548	-	-	Hydrogenation of alk(e+y)nes	140
			γ-Al ₂ O ₃	[Os ₃ Ni ₃]	Hydrogenation of alk(e+y)nes	144
			γ-Al ₂ O ₃	[Os ₃ Ni ₃]	CO and CO ₂ Hydrogenation	142,144
	[H ₂ Os ₃ NiCuCp(CO) ₉ (PPh ₃)]	128a	Chromosorb-P	[Os ₃ NiCu]	Hydrogenation of dienes	128a
			Chromosorb-P	[Os ₃ NiCu]	Dehydrogenation of alcohols	128
Os-Pt	[OsPt ₂ (PhC ₂ Ph)(CO) ₅ (PPh ₃) ₂]	385	-	-	Hydrosilylation of alkynes	385
Os-Au	[HOs ₃ Au(CO) ₁₀ (PPh ₃)]	72	SiO ₂	-	Isomerization of 1-butene	73
	[ClOs ₃ Au(CO) ₁₀ (PPh ₃)]	72	SiO ₂	-	Isomerization of 1-butene	73
			polymer	-	Hydrogenation of ethylene	145
	[Os ₄ AuH ₃ (CO) ₁₂ (PPh ₃)]	363	-	-	Oxidative carbonylation of aniline	363-364
	[Os ₄ Au ₄ H ₂ (CO) ₁₁ (PPh ₃) ₄]	364	-	-	Oxidative carbonylation of aniline	364

Table 4. continued

Metallic Couple ^a	Precursor Cluster	Ref.	Support	Notation of the MMCD catalyst ^b	Catalyzed Reactions	Ref.
		Synth.				Catal.
Co-Rh	[CoRh(CO) ₇]	262b,549	-	-	Hydrocarbonylation of diketenes	262
			-	-	Hydroformylation of alkenes	295-296
	[CoRh(CO) ₆ (PPh ₃)]	298	-	-	Hydroformylation of DCPD	298
	[CoRh(CO) ₅ (PPh ₃) ₂]	298	-	-	Hydroformylation of DCPD	298
	[CoRh(<i>t</i> -BuNC)(CO) ₄] _n	550	-	-	Silylformylation of internal alkynes	392
			-	-	Silylcarbocyclization of enynes	393
	[HCoRh{P(<i>t</i> -Bu) ₂ } ₂ (CO) ₂ (HP <i>t</i> -Bu ₂)L]	297	-	-	Hydroformylation of olefins	297
	(L = CO, HP <i>t</i> -Bu ₂)					
	[Co{Rh ₁₂ (CO) ₃₀ }]	175	-	-	CO Hydrogenation	175
	[Co ₂ Rh ₂ (CO) ₁₂]	551	alumina	[Co ₂ Rh ₂]	Isomerization of allylbenzene	74
			γ-Al ₂ O ₃	[Co ₂ Rh ₂]	Hydrocarbon Rearrangements	94-95
			-	-	Hydrogenation of styrene	146
			SiO ₂	[Co ₂ Rh ₂]	Hydrogenation of alkenes,	61,147-149
			SiO ₂	[Co ₂ Rh ₂]	CO Hydrogenation	198
			ZrO ₂	[Co ₂ Rh ₂]	CO Hydrogenation	206
			resin	-	CO Hydrogenation	207
			-	-	WGSR	220d
			-	-	Homologation of MeOH	251b,c,253c,254b
			-	-	Hydroformylation of alkenes	295b,299-300
			γ-Al ₂ O ₃ , SiO ₂ ,			
			MgSiO ₃	[Co ₂ Rh ₂]	Hydroformylation of 1-hexene	299
			resin	-	Hydroformylation of olefins	301
			SiO ₂	[Co ₂ Rh ₂]	Hydroformylation of olefins	149,303-304
			ZnO, carbon	[Co ₂ Rh ₂]	Hydroformylation of olefins	305
			γ-Al ₂ O ₃ , SiO ₂ ,			
			MgO, NaY	[Co ₂ Rh ₂]	Hydroformylation of 1-hexene	301c,306
			carbon	[Co ₂ Rh ₂]	Hydroformylation of olefins	307
			-	-	Hydroformylation of formaldehyde	313
			-	-	Hydroformylation of amides	314
			carbon	[Co ₂ Rh ₂]	PKR and PKR-like	323-326
			solid state	[Co ₂ Rh ₂]	Aminocarbonylation of alkynes	366-367
			carbon	[Co ₂ Rh ₂]	Oxidative carbonylation of amine	368
			-	-	Silylformylation of alkynes	389-390,392
			-	-	Silylcarbocyclization of alkynes	389,391,393
			solid state	[Co ₂ Rh ₂]	Silylcarbocyclization of enynes	394
			SiO ₂	[Co ₂ Rh ₂]	Hydrogenation of nitrobenzene	61

Table 4. continued

Metallic Couple ^a	Precursor Cluster	Ref.	Support	Notation of the MMCD catalyst ^b	Catalyzed Reactions	Ref.
		Synth.				Catal.
[Co ₃ Rh(CO) ₁₂] ⁵⁵¹	γ-Al ₂ O ₃	[Co ₂ Rh ₂]	Disproportionation of dihydroarenes ⁷⁴			
	solid state	[Co ₂ Rh ₂]	Synthesis of coumarins ²⁶⁴			
	solid state	[Co ₂ Rh ₂]	Cyclocarbonylation of alkynes ²⁶⁵			
	-	-	Hydrogenation of styrene ¹⁴⁶			
	SiO ₂	[Co ₃ Rh]	CO Hydrogenation ¹⁹⁸			
	ZrO ₂	[Co ₃ Rh]	CO Hydrogenation ²⁰⁶			
	resin	-	CO Hydrogenation ²⁰⁷			
	-	-	WGSR ^{220d}			
	-	-	Homologation of MeOH ^{251b,c,253c,254b}			
	-	-	Hydroformylation of 1-hexene ^{295b}			
[Co ₃ Rh ₉ (CO) ₃₀] ²⁻ ²⁰⁵	resin	-	Hydroformylation of olefins ³⁰¹			
	SiO ₂	-	Hydroformylation 1-hexene ³⁰²			
	SiO ₂	[Co ₃ Rh]	Hydroformylation of olefins ³⁰³⁻³⁰⁴			
	ZnO, carbon	[Co ₃ Rh]	Hydroformylation of olefins ³⁰⁵			
	carbon	[Co ₃ Rh]	PKR and PKR-like ³²³⁻³²⁴			
	-	-	Silylformylation of alkynes ³⁸⁹			
	-	-	Silylcarbocyclization reactions ³⁸⁹			
	-	-	CO Hydrogenation ²⁰⁵			
Co-Ir	[Co ₂ Ir ₂ (CO) ₁₂] ⁵⁵¹	-	WGSR ^{220d}			
Co-Ni	[Co ₂ Ni(CMe)Cp(CO) ₆] ⁴⁶⁷	-	Hydroformylation of olefins ^{109a}			
Co-Pd	-	-	Hydrosilylation of acetophenone ³⁸³			
	[Co ₂ Ni ₂ (OMe) ₄ (acac) ₄ (OAc) ₂] ²⁴³	NaY	[Co ₂ Ni ₂]	Oxidation of methanol ²⁴³		
	[CoPdAc(CO) ₄ (bpy)] ⁵⁵²	-	-	CO + aziridine copolymerization ²⁶⁶		
	[CoPd(CRO)(CO) ₄ L] ²⁶⁷	-	-	CO + aziridine copolymerization ²⁶⁷		
	(L = bpy, TMEDA, phen; R = Me, Ph)					
	[CoPd(OAc) ₄] ⁵⁵³	-	-	Amination + aziridination reactions ³⁶⁹		
	[Co ₂ Pd(CO) ₇ (dppe)] ^{254b}	-	-	Homologation of MeOH ^{251b,254b}		
		carbon	[Co ₂ Pd]	Hydrocarbonylation of MeOH ²⁶¹		
		-	-	Cross-coupling aryl halides/triflates ³⁵⁶		
Co-Pt	[CoPtMe(CO) ₄ (dppe)] ⁵⁵⁴	-	-	Carbonylation of thietanes ²⁶⁸		
[Co ₂ Pt(CO) ₈ (CNCy) ₂] ^{488,519}	γ-Al ₂ O ₃	[Co ₂ Pt]	Methylcyclopentane Demethylation ^{81,96}			
	-	-	Hydrogenation of 1-hexyne ⁵¹			
	-	-	Hydroformylation of 1-pentene ⁵¹			
	-	-	Dimerization of NBD ³⁴⁵			
	[Co ₂ Pt(CO) ₈ (CN- <i>t</i> -Bu) ₂] ⁴⁸⁸	-	-	Dimerization of NBD ³⁴⁵		

Table 4. continued

Metallic Couple ^a	Precursor Cluster	Ref.	Support	Notation of the MMCD catalyst ^b	Catalyzed Reactions	Ref.
		Synth.				Catal.
[Co ₂ Pt(CO) ₇ (dppe)]		555	-	-	Hydrogenation of 1-hexyne	51
			-	-	Homologation of MeOH	251b,254b
			-	-	Hydroformylation of 1-pentene	51
[Co ₂ Pt(CO) ₇ (dpae)]		555	-	-	Hydrogenation of 1-hexyne	51
[Co ₂ Pt(CO) ₇ (PNP)]		556	-	-	PKR	322
(PNP = dppe, C ₆ H ₁₃ S(CH ₂) ₂ N(PPh ₂) ₂ , PhN(PPh ₂) ₂)						
[Co ₂ Pt ₂ (CO) ₈ (PPh ₃) ₂]		557	-	-	Isomerization of 1,3-butadiene	75
			γ-Al ₂ O ₃	[Co ₂ Pt ₂]	Methylcyclopentane Demethylation	81,96
			-	-	Hydrogenation of alk(e+y)nes	113
		150	polymer	-	Hydrogenation of olefins	150
			-	-	Hydroformylation of olefins	51,310
			-	-	Oligomerization of 1,3-butadiene	75
			-	-	Dimerization of NBD	345
[Co ₂ Pt ₂ (CO) ₈ (PEt ₃) ₂]		558	-	-	Dimerization of NBD	345
[Co ₂ Pt ₂ (CO) ₈ (AsPh ₃) ₂]		113	-	-	Hydrogenation of PhC ₂ Ph	113
			-	-	Dimerization of NBD	345
[Co ₂ Pt ₃ (CO) ₉ (PEt ₃) ₃]		558	γ-Al ₂ O ₃	[Co ₂ Pt ₃]	Methylcyclopentane Demethylation	81,96
			-	-	Dimerization of NBD	345
[Co ₂ Pt ₃ (CO) ₉ (PPh ₃) ₃]		345	-	-	Dimerization of NBD	345
Co-Cu	[CoCu(CO) ₄ (TMED)]	559	SiO ₂	[CuCo]	CO Hydrogenation	27g
			SiO ₂	[CuCo]	Hydroformylation of ethylene	27g
	[Co ₃ CuCl ₃ (MeDea) ₃ (solv.)]	232	-	-	Oxidation of cycloalkanes	232
	(H ₂ Dea = diethanolamine, solv. = (MeOH) _{0.55} (H ₂ O) _{0.45})					
	[Co ₁₂ Cu ₂ (CCO) ₈ (CO) ₃₆]	466	solid state	[Co ₁₂ Cu ₂]	Hydrogenation of crotonaldehyde	212
Co-Cu-Zn	[CoCuZn ₂ Cl ₃ (MeDea) ₃ (solv.)]	232	-	-	Oxidation of cycloalkanes	232
	(H ₂ Dea = diethanolamine, solv. = (MeOH) _{0.74} (H ₂ O) _{0.26} or DMF)					
Co-Zn	[CoZnEt ₂ L]	359	-	-	Alkylation of benzaldehyde	359
	L = (ROC ₆ H ₃ (O)CHNCH ₂ C ₆ H ₃ Me) ₂ (R = Me, Et)					
	[CoZn ₂ (O ₂ CPh) ₆ n(bpa) _n	378	-	-	Transesterification	378
	(bpa = 1,2-bis(4-pyridyl)ethane)					
	[Co ₂ Zn(CO) ₈]	560	-	-	Dimerization of NBD	347
	[Co ₄ Zn ₂ (CO) ₁₅]	348	-	-	Dimerization of NBD	348
	[Co ₁₈ Zn ₄ O(CC ₂ O) ₁₂ (CO) ₅₄]	561	solid state	[Co ₁₈ Zn ₄]	Hydrogenation of crotonaldehyde	212
Co-Cd	[Co ₂ Cd(CO) ₆]	560	-	-	Dimerization of NBD	349
	[Co ₂ Cd(O ₂ CPh) ₆ n(bpa) _n	378	-	-	Transesterification	378
	(bpa = 1,2-bis(4-pyridyl)ethane)					

Table 4. continued

Metallic Couple ^a	Precursor Cluster	Ref.	Support	Notation of the MMCD catalyst ^b	Catalyzed Reactions	Ref.
		Synth.				Catal.
Co-Hg	[Co ₂ Hg(CO) ₈]	560	-	-	Dimerization of NBD	349
Rh-Ir	[Rh ₂ Ir ₄ (CO) ₁₆]	90,97	NaY	[Rh ₂ Ir ₄]	<i>n</i> -Alkane Hydrogenolysis	90,97
	[Rh ₃ Ir ₃ (CO) ₁₆]	90,97	NaY	[Rh ₃ Ir ₃]	<i>n</i> -Alkane Hydrogenolysis	90,97
	[Rh ₄ Ir ₂ (CO) ₁₆]	90,97	NaY	[Rh ₄ Ir ₂]	<i>n</i> -Alkane Hydrogenolysis	90,97
	[Rh ₅ Ir(CO) ₁₆]	90,97	NaY	[Rh ₅ Ir]	<i>n</i> -Alkane Hydrogenolysis	90,97
	[Rh ₆ Ir ₆ (CO) ₃₀] ²⁻	205	-	-	CO Hydrogenation	205
	[Rh ₉ Ir ₃ (CO) ₃₀] ²⁻	205	-	-	CO Hydrogenation	205
	[Ir ₂ {Rh ₁₂ (CO) ₃₀ }]	208	-	-	CO Hydrogenation	208
	[Ir ₂ {Rh ₁₂ (CO) ₃₀ }] ₃	178	-	-	CO Hydrogenation	178
Rh-Pt	[PPN] ₂ [Rh ₄ Pt(CO) ₁₂]	562	-	-	CO Hydrogenation	209
	[Et ₄ N][Rh ₅ Pt(CO) ₁₅]	151	resin	-	Hydrogenation of arene derivatives	151
	[PPN][Rh ₅ Pt(CO) ₁₅]	562	-	-	CO Hydrogenation	209
	Na[Rh ₅ Pt(CO) ₁₅]	563	MgO	[Rh ₅ Pt]	Hydrogenation of toluene	152
	[Pt{Rh ₁₂ (CO) ₃₀ }]	175	-	-	CO Hydrogenation	175
Rh-Cu	[Cu ₂ {Rh ₁₂ (CO) ₃₀ }]	208	-	-	CO Hydrogenation	208
Rh-Ag	[Ag ₂ {Rh ₁₂ (CO) ₃₀ }]	208	-	-	CO Hydrogenation	208
Rh-Au	[RhAu{HC(PPPh ₂) ₃ }(COD)(PPPh ₃)][BF ₄] ₂	153	-	-	Hydrogenation of alk(e+y)nes	153
	[Au ₂ {Rh ₁₂ (CO) ₃₀ }]	208	-	-	CO Hydrogenation	208
Rh-Zn	[RhZnCl ₂ (CO)(NOP)][BF ₄]	311	-	-	Hydroformylation of olefins (NOP = 2,6-bis[(3-(diphenylphosphino)propoxy)methyl]pyridine)	311
	[Zn{Rh ₁₂ (CO) ₃₀ }]	175	-	-	CO hydrogenation	175
Ir-Pd	[Ir ₂ PdCp [*] ₂ Cl ₂ S ₂]	371	-	-	Addition of alcohols to alkynes	371
Ir-Pt	[PPN][IrPtMeI ₅ (CO) ₃]	10,259	-	-	Carbonylation of MeOH	10,259
	[IrPt(SRS)Cp [*] Cl(PPPh ₃) ₂][SbF ₆]	387	-	-	Hydrosilylation of alkynes (R = <i>cis</i> -C ₈ H ₁₄ , <i>trans</i> -C ₈ H ₁₄)	387
	[Ir ₂ PtCp [*] ₂ Cl ₂ S ₂]	371	-	-	Addition of alcohols to alkynes	371
	[Ir ₂ Pt(CO) ₇ py ₂]	92	oxides, carbon	[Ir ₂ Pt]	Hydrocarbon Conversion	92
			oxides, carbon	[Ir ₂ Pt]	Naphtha Reforming	92
	[Ir ₂ Pt ₂ (CO) ₇ (PPPh ₃) ₃]	154	-	-	Hydrogenation of olefins	154
	[Ir ₆ Pt(CO) ₁₅ py ₂]	92	oxides, carbon	[Ir ₆ Pt]	Hydrocarbon Conversion	92
			oxides, carbon	[Ir ₆ Pt]	Naphtha Reforming	92
Ir-Cu	[IrCu(Ph ₂ Ppy) ₂ Cl(CO)][BF ₄]	312	-	-	Hydroformylation of styrene	312
Pd-Pt	[PdPtCl ₄ (dmappm)]	358	-	-	Heck coupling iodobenzene/styrene (dmappm = 1,1-bis[di(<i>o</i> - <i>N,N</i> -dimethylanilinyl)phosphino]methane)	358
Pd-Cu	[PdCuCl ₄ L ₄ -PdCl ₂] _n (L = pyrrolidin-2-one)	234	-	-	Oxidation of cyclohexene	234
	[Pd ₆ Cu ₄ Cl ₁₂ O ₄ (HMPA) ₄]	233	-	-	Oxidation of alkenes	233

Table 4. continued

Metallic Couple ^a	Precursor Cluster	Ref.	Support	Notation of the MMCD catalyst ^b	Catalyzed Reactions	Ref.
		Synth.				Catal.
Pd-Ag	[PdAg(OAc) ₃]	370	-	-	Aromatic C-H bond amination	370
Pd-Zn	[PdZn(OOCMe) ₄ (OH ₂)]	564	γ -Al ₂ O ₃	[PdZn]	Dehydration of alcohols	219
Pt-Cu	[Pt ₂ Cu ₄ (C ₂ -t-Bu) ₈]	565	SiO ₂	[Pt ₂ Cu ₄]	Hexane conversion	98
			SiO ₂	[Pt ₂ Cu ₄]	Hydrogenation of toluene	155
Pt-Au	[Pt(AuPPh ₃) ₂ (PPh ₃) ₂](NO ₃) ₂	566	SiO ₂	[PtAu ₂]	Alkane dehydrogenation	217
	[Pt(AuPPh ₃) ₃ (PPh ₃) ₂](NO ₃)	566b	solid state	[PtAu ₃]	H ₂ -D ₂ Equilibration	42
	[Pt(AuPPh ₃) ₄ (PPh ₃) ₂](NO ₃) ₂	566b	solid state	[PtAu ₄]	H ₂ -D ₂ Equilibration	42
	[Pt(AuPPh ₃) ₆ (PPh ₃) ₂](NO ₃) ₂	567	solid state	[PtAu ₆]	H ₂ -D ₂ Equilibration	42-43
			γ -Al ₂ O ₃ , SiO ₂	[PtAu ₆]	H ₂ -D ₂ Equilibration	45
			SiO ₂	[PtAu ₆]	H ₂ -D ₂ Equilibration,	46
			SiO ₂	[PtAu ₆]	Hydrogenation of ethylene,	46a
			SiO ₂	[PtAu ₆]	Oxidation of CO	46a
	[HPt(AuPPh ₃) ₇ (PPh ₃) ₂](NO ₃) ₂	568	solid state	[PtAu ₇]	H ₂ -D ₂ Equilibration	42-43
			γ -Al ₂ O ₃ , SiO ₂	[PtAu ₇]	H ₂ -D ₂ Equilibration	45
	[Pt(AuPPh ₃) ₈](NO ₃) ₂	569	solid state	[PtAu ₈]	H ₂ -D ₂ Equilibration	42-43
			γ -Al ₂ O ₃ , SiO ₂	[PtAu ₈]	H ₂ -D ₂ Equilibration	45
			solid state	[PtAu ₈]	Hydrogenation of ethylene	43b, 46b
			solid state	[PtAu ₈]	Hydrogenation of O ₂	43b
			SiO ₂	[PtAu ₈]	Alkane dehydrogenation	217
	[HPt(AuPPh ₃) ₉](NO ₃) ₂	44	-	-	H ₂ -D ₂ Equilibration	44
	[Pt ₂ Au ₄ (C ₂ -t-Bu) ₈]	565	SiO ₂	[Pt ₂ Au ₄]	Homoexchange of ¹⁶ O- ¹⁸ O	47
			SiO ₂	[Pt ₂ Au ₄]	Hexane conversion	98-99
			SiO ₂	[Pt ₂ Au ₄]	Hydrogenation of alkenes	155-156
			SiO ₂	[Pt ₂ Au ₄]	Oxidation of propylene	47
			SiO ₂ , TiO ₂	[Pt ₂ Au ₄]	Oxidation of CO	248
			SiO ₂	[Pt ₂ Au ₄]	Reduction of NO	47, 397
Cu-Zn	[CuZn{Ph ₂ PC ₁₀ H ₅ (O)} ₂ Cl] ₂	360	-	-	Asymmetric alkylation of enones	360
Zn-Cd	[Zn ₂ Cd(O ₂ CPh) ₆] _n (bpa) _n	378	-	-	Transesterification	378
	(bpa = 1,2-bis(4-pyridyl)ethane)					

^aThe metals are listed with increasing number of their group. ^bThis notation is meant to indicate the core composition of the molecular precursor but has no implication as far as the particle size, shape, or composition of the catalyst is concerned. Therefore, when there is no such notation, it means that the reported compound is a homogeneous catalyst.

such as organic polymers or inorganic oxides or onto the pores of well-defined micro- and mesoporous materials, functionalized or not (with, e.g., oxygen-donating ligands, with groups having a greater affinity for low oxidation-state metal carbonyls), has made much progress in recent years. The development of such systems was originally motivated by the hope to overcome the limitations and difficulties encountered in both homogeneous catalysis (catalyst recovery and cluster fragmentation) and heterogeneous catalysis (limited selectivity

tuning due to frequently ill-defined active sites, reduced effectiveness of components of a multimetallic catalyst, and often severe reaction conditions). At the same time, it was hoped that such immobilized systems would give rise to a successful combination of the advantages inherent to homogeneous catalysis (molecular understanding of the mechanisms and catalytic cycles, mild reaction conditions, high atom efficiency, and easier tuning by the ligands electronic and steric properties) with those specific to heterogeneous

catalysis (higher catalyst stability, applicability to a wide range of reactions, technological versatility, and easier separation from the reaction products).

Supported mixed-metal cluster-derived (MMCD) heterogeneous catalysts may have been considered initially as curiosities,^{18b,c,361} but this is no longer the case, and they constitute a very promising class of catalytic materials. This development has been greatly facilitated by the huge diversity of bimetallic molecular precursors known, their availability often in gram scale, and the established synthetic strategies allowing access to new bimetallic couples. Numerous studies have concluded that bimetallic metal particles, obtained by thermal treatment of supported molecular clusters and removal of their ligands, often have unique catalytic properties. The use of molecular precursors containing metals in low oxidation state is highly desirable because lower activation temperatures are required than when reduction of the metals is necessary. Severe activation conditions may lead to segregation of the different metals and jeopardize synergistic interactions. The use of carbonyl clusters is particularly appropriate, also because the CO ligands are cleanly and irreversibly eliminated, in contrast to, for example, phosphines that may become the source of desirable or undesirable phosphide phases.^{18d,436} It is generally observed that the use of well-defined bimetallic molecular precursors leads to metal particles of much better controlled size and composition than those obtained from mixtures of monometallic salts, because of the close proximity of the atoms in the precursors and the existence of metal–metal bonding. The large number of experimental parameters involved in catalytic studies (solvent, temperature, pressure), the nature of the support, the impregnation method used, the thermal decomposition, and activation procedures of the catalysts all need to be considered, and making comparisons between results from different research groups is very difficult, if not meaningless. Despite all of the results already available, which provide interesting directions for future work, there is a need for more systematic comparisons and critical testing allowing a clear-cut evaluation of the advantages brought about by MMCD catalysts. Comparisons with the properties of mixtures of the corresponding homometallic complexes or of bimetallic colloids would be highly desirable from a fundamental point of view as well as because of their potential industrial relevance. We also anticipate that “heterometal-sensitive reactions”, that is, reactions that require at least two different metals to proceed with high activity and selectivity, should be particularly worthwhile to study as their results will be very informative, even if only qualitatively, about the specificity of MMCD catalysts. Their study should, in general, help improve our understanding of fundamental aspects of catalytic chemistry. Particularly important in this respect are the new powerful analytical techniques, such as *in situ* TEM (transmission electron microscopy), Z-contrast imaging in TEM, or ultrahigh-resolution aberration-corrected STEM (scanning transmission electron microscopy), which allow atomic scale observations of materials and have already provided researchers with new and most valuable insights.^{21,437}

We hope to have provided an incentive for more studies on multimetallic catalysis based on heterometallic clusters. The potential of heterometallic complexes is considerable, and several bimetallic associations remain poorly or not at all investigated, and therefore are absent from this Review. Clear trends have already been identified in a number of cases concerning catalytic performances as a function of the bi- or

trimetallic association and of the intermetallic ratio in the molecular precursor, but more research should provide better comparative evaluations of catalysts under similar conditions.

AUTHOR INFORMATION

Corresponding Authors

*Tel.: +33 3 68851308. E-mail: paulin.buchwalter@hotmail.fr.

*E-mail: rose@unistra.fr.

*E-mail: braunstein@unistra.fr.

Notes

The authors declare no competing financial interest.

Biographies



Paulin Buchwalter received his Master's degree from the Université de Strasbourg in 2009 in the field of materials chemistry. During these studies, he first joined the group of Dr. P. Braunstein in the Laboratoire de Chimie de Coordination, Strasbourg, where he worked on the synthesis of Prussian blue analogues. He then joined the group of Prof. S. Bégin in the Institut de Physique et Chimie des Matériaux de Strasbourg, and worked on the synthesis and magnetic applications of functionalized iron oxide nanoparticles for the preparation of self-assembled monolayers on inorganic surfaces. He received his Ph.D. in 2013 under the supervision of Dr. J.-L. Paillaud (Institut de Science des Matériaux de Mulhouse), Dr. P. Rabu (Institut de Physique et Chimie des Matériaux de Strasbourg), and Dr. P. Braunstein, working on the study of the thermal behavior of organometallic molecular clusters and on the synthesis and applications of confined cobalt phosphide nanoparticles starting from such precursors. His main research interests are in the preparation and characterization of metal nanoparticles and their applications in catalysis.



Jacky Rosé obtained his Ph.D. in 1985 in Organometallic Chemistry from the University of Strasbourg under the supervision of Prof. P. Braunstein. His current interests encompass synthetic methodologies

for the preparation of low oxidation-state heterometallic complexes and clusters containing ligands such as CO, phosphines, and hydrocarbons, the formation of new metal–metal bonds, the electronic behavior of metal carbonyl building blocks as a function of their structural environment, the application of the isolobal analogy, and the use of assembling ligands for the rational synthesis of heterometallic clusters.



Pierre Braunstein graduated from the Ecole Nationale Supérieure de Chimie de Mulhouse (1969) and obtained his Dr. Ing. (1971) and Doctorat d'Etat (1974) from the Université Louis Pasteur (ULP) in Strasbourg. He spent the academic years 1971/72 as a postdoctoral fellow at University College London (with R. S. Nyholm and R. J. H. Clark) and 1974/75 as A. von Humboldt fellow at the TU Munich (with E. O. Fischer). He remained within the CNRS where he became Director of Research Except. Class at the University of Strasbourg. His main research interests lie in the inorganic and organometallic chemistry of the transition and main group elements (where he has (co)authored over 500 scientific publications and review articles) and include the synthesis and coordination/organometallic chemistry of metal–metal bonded (hetero)dinuclear and cluster complexes, of coordination clusters, of heterofunctional ligands, of quinonoid zwitterions, and the study of hemilabile metal–ligand systems. Applications range from, for example, homogeneous catalytic ethylene oligomerization to nanosciences. He has received numerous national and international awards and is a member of various academies, including the french Académie of Sciences and the German National Academy of Sciences Leopoldina. He has been featured in *Angewandte Chemie* (<http://onlinelibrary.wiley.com/doi/10.1002/anie.201000183/abstract>).

ACKNOWLEDGMENTS

This work is dedicated to Profs. E. Sappa (Torino), A. Tiripicchio (Parma), and H. Vahrenkamp (Freiburg) for a decades-long friendship triggered by cluster chemistry. We thank the Région Alsace (Ph.D. grant to P. Buchwalter), the Centre National de la Recherche Scientifique, the Ministère de la Recherche, the University of Strasbourg, and the ic-FRC of Strasbourg (<http://www.icfrc.fr>) for support. We are most grateful to the co-workers and collaborators who have been involved in our own research and whose names appear in the references. We thank Drs. J.-L. Paillaud, B. Lebeau (IS2M, UHA Mulhouse), and P. Rabu (IPCMS Strasbourg) for fruitful interactions.

ABBREVIATIONS

acac	acetylacetone
Ar	aromatic
bmim	1-butyl-3-methylimidazolium
Bn	benzyl
bpy	2,2'-bipyridine
Bu	butyl
cat	catecholate
COA	cyclooctane
COD	cyclooctadiene
COE	cyclooctene
Cp	η^5 -cyclopentadienyl ($\eta^5\text{-C}_5\text{H}_5$)
Cp'	η^5 -methylcyclopentadienyl ($\eta^5\text{-MeC}_5\text{H}_4$)
Cp ^t	η^5 -tertbutylcyclopentadienyl ($\eta^5\text{-C}_5\text{H}_4\text{-}t\text{-Bu}$)
Cp*	η^5 -pentamethylcyclopentadienyl ($\eta^5\text{-C}_5\text{Me}_5$)
Cy	cyclohexyl
DCPD	dicyclopentadiene
depe	1,2-bis(diethylphosphino)ethane
dmpe	1,2-bis(dimethylphosphino)ethane
dpae	1,2-bis(diphenylarsino)ethane
dppa	1,2-bis(diphenylphosphino)amine
dppe	1,2-bis(diphenylphosphino)ethane
dppm	1,2-bis(diphenylphosphino)methane
ee	enantiomeric excess
Et	ethyl
HDN	hydrodenitrogenation
HDS	hydrodesulfurization
HMPA	hexamethylphosphoramide [(Me ₂ N)PO]
Ind	indenyl
MAO	methylaluminoxane (Al(CH ₃) _x O _y) _n
Me	methyl
Mes	mesityl
MMCD	mixed-metal cluster-derived catalyst
NBD	norbornadiene
NBE	norbornene
NP	nanoparticle
pts	p-toluenesulfonate
Ph	phenyl
phen	phenanthroline
PPN	bis(triphenylphosphine)iminium
Pr	propyl
PROX	Preferential Oxidation
py	pyridine
scCO ₂	supercritical CO ₂
TBPA	tris(4-bromophenyl)ammonium
TMBA	trimethyl(benzyl)ammonium
TMED	tetramethyl(ethylenediamine)
TOF	turnover frequency
[M _x M' _y]	heterogeneous catalyst prepared from a molecular cluster of metal core composition M _x M' _y

REFERENCES

- (a) Cotton, F. A.; Curtis, N. F.; Harris, C. B.; Johnson, B. F. G.; Lippard, S. J.; Mague, J. T.; Robinson, W. R.; Wood, J. S. *Science* **1964**, *145*, 1305. (b) Cotton, F. A. *Inorg. Chem.* **1965**, *4*, 334. (c) Cotton, F. A. *Q. Rev., Chem. Soc.* **1966**, *20*, 389.
- (a) Braunstein, P.; Rosé, J. In *Stereochemistry of Organometallic and Inorganic Compounds*; Bernal, I., Ed.; Elsevier: Amsterdam, 1989; Vol. III. (b) Süss-Fink, G.; Meister, G. In *Advances in Organometallic Chemistry*; Stone, F. G. A., Robert, W., Eds.; Academic Press: New York, 1993; Vol. 35. (c) Braunstein, P.; Rosé, J. In *Comprehensive Organometallic Chemistry II*; Abel, E. W., Stone, F. G. A., Wilkinson, G., Eds.; Pergamon Press: Oxford, 1995; Vol. 10. (d) Braunstein, P.; Rosé, J. In *Catalysis by Di- and Polynuclear Metal Cluster Complexes*; Adams, R. D., Cotton, F. A., Eds.; Wiley-VCH: New York, 1998. (e) Braunstein, P.; Rosé, J. In *Clusters in Chemistry*; Braunstein, P., Oro, L. A.; Raithby, P. R., Eds.; Wiley-VCH: Weinheim, 1999, Vol. 2.

- 616–677. (f) Dyson, P. J. *Coord. Chem. Rev.* **2004**, *248*, 2443. (g) Kamijo, S.; Yamamoto, Y. *Multimetallic Catalysts in Organic Synthesis*; Wiley-VCH Verlag GmbH & Co. KGaA: New York, 2004. (h) Jiang, H.-L.; Xu, Q. *J. Mater. Chem.* **2011**, *21*, 13705. (i) Sankar, M.; Dimitratos, N.; Miedziak, P. J.; Wells, P. P.; Kiely, C. J.; Hutchings, G. J. *Chem. Soc. Rev.* **2012**, *41*, 8099. (j) Tao, F. *Chem. Soc. Rev.* **2012**, *41*, 7977. (k) Singh, A. K.; Xu, Q. *ChemCatChem* **2013**, *5*, 652. (l) Thomas, J. M.; Ducati, C.; Leary, R.; Midgley, P. A. *ChemCatChem* **2013**, *5*, 2560. (m) Wang, Z.-C.; Liu, J.-W.; Schlangen, M.; Weiske, T.; Schröder, D.; Sauer, J.; Schwarz, H. *Chem.—Eur. J.* **2013**, *19*, 11496 and references cited therein.
- (3) Ponec, V. *Appl. Catal., A* **2001**, *222*, 31.
- (4) Bond, G. C.; Louis, C.; Thompson, D. T. *Catalysis by Gold*; Imperial College Press: London, 2006.
- (5) (a) Hutchings, G. J. *Catal. Today* **2014**, *238*, 69. (b) Edwards, J. K.; Freakley, S. J.; Carley, A. F.; Kiely, C. J.; Hutchings, G. J. *Acc. Chem. Res.* **2014**, *47*, 845.
- (6) (a) Dobbek, H.; Svetlichnyi, V.; Gremer, L.; Huber, R.; Meyer, O. *Science* **2001**, *293*, 1281. (b) Fontecilla-Camps, J. C.; Volbeda, A.; Cavazza, C.; Nicolet, Y. *Chem. Rev.* **2007**, *107*, 4273. (c) Jiang, W.; Yun, D.; Saleh, L.; Barr, E. W.; Xing, G.; Hoffart, L. M.; Maslak, M.-A.; Krebs, C.; Bollinger, J. M. *Science* **2007**, *316*, 1188. (d) Jiang, W.; Bollinger, J. M.; Krebs, C. *J. Am. Chem. Soc.* **2007**, *129*, 7504. (e) Ragsdale, S. W. *J. Inorg. Biochem.* **2007**, *101*, 1657. (f) *Biological Inorganic Chemistry: Structure and Reactivity*; Bertini, I., Gray, H. B., Stiefel, E. I., Valentine, J. S., Eds.; University Science Books: Sausalito, CA, 2007. (g) Kung, Y.; Drennan, C. L. *Curr. Opin. Chem. Biol.* **2011**, *15*, 276. (h) Seino, H.; Hidai, M. *Chem. Sci.* **2011**, *2*, 847. (i) Dance, I. *Chem. Commun.* **2013**, *49*, 10893. (j) MacLeod, K. C.; Holland, P. L. *Nat. Chem.* **2013**, *5*, 559. (k) Tereniak, S. J.; Carlson, R. K.; Clouston, L. J.; Young, V. G.; Bill, E.; Maurice, R.; Chen, Y.-S.; Kim, H. J.; Gagliardi, L.; Lu, C. C. *J. Am. Chem. Soc.* **2013**, *136*, 1842. (l) Wombwell, C.; Reisner, E. *Dalton Trans.* **2014**, *43*, 4483.
- (7) (a) Artero, V.; Fontecave, M. *Coord. Chem. Rev.* **2005**, *249*, 1518. (b) Bouwman, E.; Reedijk, J. *Coord. Chem. Rev.* **2005**, *249*, 1555. (c) Ogo, S.; Kabe, R.; Uehara, K.; Kure, B.; Nishimura, T.; Menon, S. C.; Harada, R.; Fukuzumi, S.; Higuchi, Y.; Ohhara, T.; Tamada, T.; Kuroki, R. *Science* **2007**, *316*, 585. (d) Rauchfuss, T. B. *Science* **2007**, *316*, 553. (e) Gloaguen, F.; Rauchfuss, T. B. *Chem. Soc. Rev.* **2009**, *38*, 100. (f) Ogo, S. *Chem. Commun.* **2009**, 3317. (g) Canaguier, S.; Vaccaro, L.; Artero, V.; Ostermann, R.; Pécaut, J.; Field, M. J.; Fontecave, M. *Chem.—Eur. J.* **2009**, *15*, 9350. (h) Barton, B. E.; Olsen, M. T.; Rauchfuss, T. B. *Curr. Opin. Biotechnol.* **2010**, *21*, 292. (i) Canaguier, S.; Field, M.; Oudart, Y.; Pécaut, J.; Fontecave, M.; Artero, V. *Chem. Commun.* **2010**, *46*, 5876. (j) Canaguier, S.; Fourmond, V.; Perotto, C. U.; Fize, J.; Pécaut, J.; Fontecave, M.; Field, M. J.; Artero, V. *Chem. Commun.* **2013**, *49*, 5004. (k) Ogo, S.; Ichikawa, K.; Kishima, T.; Matsumoto, T.; Nakai, H.; Kusaka, K.; Ohhara, T. *Science* **2013**, *339*, 682. (l) Kaur-Ghumaaan, S.; Stein, M. *Dalton Trans.* **2014**, *43*, 9392.
- (8) (a) Sunley, G. J.; Watson, D. J. *Catal. Today* **2000**, *58*, 293. (b) Jones, J. H. *Platinum Met. Rev.* **2000**, *44*, 94. (c) Thomas, C. M.; Süss-Fink, G. *Coord. Chem. Rev.* **2003**, *243*, 125. (d) Haynes, A.; Maitlis, P. M.; Morris, G. E.; Sunley, G. J.; Adams, H.; Badger, P. W.; Bowers, C. M.; Cook, D. B.; Elliott, P. I. P.; Ghaffar, T.; Green, H.; Griffin, T. R.; Payne, M.; Pearson, J. M.; Taylor, M. J.; Vickers, P. W.; Watt, R. J. *J. Am. Chem. Soc.* **2004**, *126*, 2847. (e) Haynes, A. In *Catalytic Carbonylation Reactions*; Beller, M., Ed.; Springer: Berlin, Heidelberg, 2006; Vol. 18. (f) Kalck, P.; Serp, P. *Iridium Complexes in Organic Synthesis*; Wiley-VCH Verlag GmbH & Co. KGaA: New York, 2008.
- (9) Whyman, R.; Wright, A. P.; Iggo, J. A.; Heaton, B. T. *J. Chem. Soc., Dalton Trans.* **2002**, 771.
- (10) Gautron, S.; Lassauque, N.; Berre, C.; Azam, L.; Giordano, R.; Serp, P.; Laurenczy, G.; Thiébaut, D.; Kalck, P. *Top. Catal.* **2006**, *40*, 83.
- (11) Chianelli, R. R. *Catal. Rev.* **1984**, *26*, 361.
- (12) Shum, V. K.; Butt, J. B.; Sachtler, W. M. H. *J. Catal.* **1985**, *96*, 371.
- (13) (a) *Metal Clusters in Chemistry*; Braunstein, P., Oro, L. A., Raithby, P. R., Eds.; Wiley-VCH: Weinheim, 1999. (b) Severin, K. *Chem.—Eur. J.* **2002**, *8*, 1514. (c) Bardajia, M.; Laguna, A. *Eur. J. Inorg. Chem.* **2003**, 3069. (d) Li, Y.; Wong, W.-T. *Coord. Chem. Rev.* **2003**, *243*, 191. (e) Skopenko, V. V.; Kokozei, V. N.; Vasil'eva, O. Y.; Petrusenko, S. R. *Theor. Exp. Chem.* **2003**, *39*, 269. (f) Adams, R. D.; Captain, B. *J. Organomet. Chem.* **2004**, *689*, 4521. (g) Shapley, P. A. *Activation and Functionalization of C-H Bonds*; American Chemical Society: Washington, DC, 2004; Vol. 885. (h) Affronte, M.; Garretta, S.; Timco, G. A.; Winpenny, R. E. P. *Chem. Commun.* **2007**, 1789. (i) Antonova, A. B. *Coord. Chem. Rev.* **2007**, *251*, 1521. (j) Ritleng, V.; Chetcuti, M. *J. Chem. Rev.* **2007**, *107*, 797. (k) Adams, R. D.; Captain, B. *Angew. Chem., Int. Ed.* **2008**, *47*, 252. (l) Melnik, M.; Garaj, J.; Holloway, C. *E. J. Coord. Chem.* **2008**, *61*, 3021. (m) Adams, R. D.; Captain, B. *Acc. Chem. Res.* **2009**, *42*, 409. (n) Drobot, D. V.; Seisenbaeva, G. A.; Kessler, V. G.; Scheglov, P. A.; Nikanova, O. A.; Michnevich, S. N.; Petrakova, O. V. *J. Cluster Sci.* **2009**, *20*, 23. (o) Maggini, S. *Coord. Chem. Rev.* **2009**, *253*, 1793. (p) Mandal, S. K.; Roesky, H. W. *Acc. Chem. Res.* **2009**, *43*, 248. (q) Haak, R. M.; Wezenberg, S. J.; Kleij, A. W. *Chem. Commun.* **2010**, *46*, 2713. (r) Suzuki, N.; Hashizume, D. *Coord. Chem. Rev.* **2010**, *254*, 1307. (s) Clemente-Leon, M.; Coronado, E.; Marti-Gastaldo, C.; Romero, F. M. *Chem. Soc. Rev.* **2011**, *40*, 473. (t) Sculfert, S.; Braunstein, P. *Chem. Soc. Rev.* **2011**, *40*, 2741. (u) Komiya, S. *Coord. Chem. Rev.* **2012**, *256*, 556. (v) Sokolov, M. N.; Abramov, P. A. *Coord. Chem. Rev.* **2012**, *256*, 1972. (w) Timco, G. A.; McInnes, E. J. L.; Winpenny, R. E. P. *Chem. Soc. Rev.* **2013**, *42*, 1796. (x) Gervasio, G.; Sappa, E.; Secco, A. J. *Organomet. Chem.* **2014**, *751*, 111.
- (14) (a) Delferro, M.; Marks, T. J. *Chem. Rev.* **2011**, *111*, 2450. (b) Park, J.; Hong, S. *Chem. Soc. Rev.* **2012**, *41*, 6931. (c) Bratko, I.; Gomez, M. *Dalton Trans.* **2013**, *42*, 10664.
- (15) (a) Braunstein, P.; Naud, F. *Angew. Chem., Int. Ed.* **2001**, *40*, 680. (b) Zhang, W.-H.; Chien, S. W.; Hor, T. S. A. *Coord. Chem. Rev.* **2011**, *255*, 1991.
- (16) Rösch, N.; Pacchioni, G. In *Clusters and Colloids*; Schmid, G., Ed.; Wiley-VCH: Weinheim, 1994.
- (17) (a) Muettterties, E. L.; Rhodin, T. N.; Band, E.; Brucker, C. F.; Pretzer, W. R. *Chem. Rev.* **1979**, *79*, 91. (b) Gomez-Sal, M. P.; Johnson, B. F. G.; Lewis, J.; Raithby, P. R.; Wright, A. H. *J. Chem. Soc., Chem. Commun.* **1985**, 1682. (c) Wadeohl, H. *Angew. Chem., Int. Ed. Engl.* **1992**, *31*, 247. (d) Braga, D.; Dyson, P. J.; Grepioni, F.; Johnson, B. F. G. *Chem. Rev.* **1994**, *94*, 1585. (e) Bradshaw, A. M. *Surf. Sci.* **1995**, *331*–*333*, 978. (f) Brait, S.; Deabate, S.; Knox, S. R.; Sappa, E. J. *Cluster Sci.* **2001**, *12*, 139. (g) Monakhov, K. Y.; Gourlaouen, C.; Braunstein, P. *Chem. Commun.* **2012**, *48*, 8317.
- (18) (a) Braunstein, P.; Bender, R.; Kervennal, J. *Organometallics* **1982**, *1*, 1236. (b) Braunstein, P.; Kervennal, J.; Richert, J.-L. *Angew. Chem., Int. Ed. Engl.* **1985**, *24*, 768. (c) Braunstein, P.; Devenish, R.; Gallezot, P.; Heaton, B. T.; Humphreys, C. J.; Kervennal, J.; Mulley, S.; Ries, M. *Angew. Chem., Int. Ed. Engl.* **1988**, *27*, 927. (d) Grosshans-Vièles, S.; Croizat, P.; Paillaud, J.-L.; Braunstein, P.; Ersen, O.; Rosé, J.; Lebeau, B.; Rabu, P.; Estournès, C. *J. Cluster Sci.* **2008**, *19*, 73.
- (19) Schwank, J. *Gold Bull.* **1985**, *18*, 2.
- (20) (a) Salter, I. D. In *Comprehensive Organometallic Chemistry II*; Abel, E. W., Stone, F. G. A., Wilkinson, G., Eds.; Pergamon Press: Oxford, 1995; Vol. 10. (b) Salter, I. D. In *Metal Clusters in Chemistry*; Braunstein, P.; Oro, L. A.; Raithby, P. R., Eds.; Wiley-VCH Verlag GmbH: New York, 1999; Vol. 1, 509–534.
- (21) (a) Ramos, A.; Otten, E.; Stephan, D. W. *J. Am. Chem. Soc.* **2009**, *131*, 15610. (b) Green, A. G.; Kiesz, M. D.; Oria, J. V.; Elliott, A. G.; Buechler, A. K.; Hohenberger, J.; Meyer, K.; Zink, J. I.; Diaconescu, P. L. *Inorg. Chem.* **2013**, *52*, 5603.
- (22) (a) Atkinson, R. C. J.; Long, N. J. In *Ferrocenes: Ligands, Materials and Biomolecules*; Stepnicka, P., Ed.; John Wiley & Sons Ltd.: Chichester, UK, 2008. (b) Chien, S. W.; Hor, T. S. A. In *Ferrocenes: Ligands, Materials and Biomolecules*; Stepnicka, P., Ed.; John Wiley & Sons Ltd.: Chichester, UK, 2008. (c) Colacot, T. J.; Parisel, S. In *Ferrocenes: Ligands, Materials and Biomolecules*; Stepnicka, P., Ed.; John Wiley & Sons Ltd.: Chichester, UK, 2008. (d) Stepnicka, P. In

- Ferrocenes: Ligands, Materials and Biomolecules*; Stepnicka, P., Ed.; John Wiley & Sons Ltd.: Chichester, UK, 2008. (e) Blaser, H.-U.; Chen, W.; Camponovo, F.; Togni, A. In *Ferrocenes: Ligands, Materials and Biomolecules*; Stepnicka, P., Ed.; John Wiley & Sons Ltd.: Chichester, UK, 2008. (f) Stepnicka, P.; Lamac, M. In *Ferrocenes: Ligands, Materials and Biomolecules*; Stepnicka, P., Ed.; John Wiley & Sons Ltd.: Chichester, UK, 2008. (g) Xia, J.-B.; Jamison, T. F.; You, S.-L. *Chiral Ferrocenes in Asymmetric Catalysis*; Wiley-VCH Verlag GmbH & Co. KGaA: New York, 2009. (h) Blaser, H.-U.; Lotz, M. *Chiral Ferrocenes in Asymmetric Catalysis*; Wiley-VCH Verlag GmbH & Co. KGaA: New York, 2009. (i) Zhou, Y. G.; Hou, X. L. *Chiral Ferrocenes in Asymmetric Catalysis*; Wiley-VCH Verlag GmbH & Co. KGaA: New York, 2009. (j) Zhang, W.; Liu, D. *Chiral Ferrocenes in Asymmetric Catalysis*; Wiley-VCH Verlag GmbH & Co. KGaA: New York, 2009. (k) You, S.-L. *Chiral Ferrocenes in Asymmetric Catalysis*; Wiley-VCH Verlag GmbH & Co. KGaA: New York, 2009. (l) Carretero, J. C.; Adrio, J.; Rivero, M. R. *Chiral Ferrocenes in Asymmetric Catalysis*; Wiley-VCH Verlag GmbH & Co. KGaA: New York, 2009. (m) Kuwano, R. *Chiral Ferrocenes in Asymmetric Catalysis*; Wiley-VCH Verlag GmbH & Co. KGaA: New York, 2009. (n) Marion, N.; Fu, G. C. *Chiral Ferrocenes in Asymmetric Catalysis*; Wiley-VCH Verlag GmbH & Co. KGaA: New York, 2009. (o) Richards, C. J. *Chiral Ferrocenes in Asymmetric Catalysis*; Wiley-VCH Verlag GmbH & Co. KGaA: New York, 2009.
- (23) (a) Lee, J. H.; Son, S. U.; Chung, Y. K. *Tetrahedron: Asymmetry* **2003**, *14*, 2109. (b) Nomura, H.; Richards, C. J. *Chem.—Eur. J.* **2007**, *13*, 10216. (c) Kirsch, S. F.; Overman, L. E.; White, N. S. *Org. Lett.* **2007**, *9*, 911. (d) Li, X.; Li, Q.; Wu, X.; Gao, Y.; Xu, D.; Kong, L. *Tetrahedron: Asymmetry* **2007**, *18*, 629. (e) Fadini, L.; Togni, A. *Tetrahedron: Asymmetry* **2008**, *19*, 2555.
- (24) Liu, S.; Motta, A.; Delferro, M.; Marks, T. J. *J. Am. Chem. Soc.* **2013**, *135*, 8830.
- (25) Mata, J. A.; Hahn, E. F.; Peris, E. *Chem. Sci.* **2014**, *5*, 1723.
- (26) Holt, M. S.; Wilson, W. L.; Nelson, J. H. *Chem. Rev.* **1989**, *89*, 11.
- (27) (a) Coloma, F.; Llorca, J.; Hom, N.; Ramirez de la Piscina, P.; Rodriguez-Reinoso, F.; Sepulveda-Escribano, A. *Phys. Chem. Chem. Phys.* **2000**, *2*, 3063. (b) Hom, N.; Llorca, J.; Ramirez de la Piscina, P.; Rodriguez-Reinoso, F.; Sepulveda-Escribano, A.; Silvestre-Albero, J. *Phys. Chem. Chem. Phys.* **2001**, *3*, 1782. (c) Hom, N.; Clos, N.; Muller, G.; Sales, J.; Ramirez de la Piscina, P.; Fierro, J.-L. G. *J. Mol. Catal.* **1992**, *74*, 401. (d) Llorca, J.; Ramirez de la Piscina, P.; Fierro, J.-L. G.; Sales, J.; Hom, N. *J. Mol. Catal. A: Chem.* **1997**, *118*, 101. (e) Llorca, J.; Ramirez de la Piscina, P.; Sales, J.; Hom, N. *J. Chem. Soc., Chem. Commun.* **1994**, 2555. (f) Llorca, J.; Hom, N.; Sales, J.; Ramirez de la Piscina, P. In *Studies in Surface Science and Catalysis*; Parmaliana, A., Sanfilippo, D., Frusteri, F., Vaccari, A., Arena, F., Eds.; Elsevier: New York, 1998; Vol. 119. (g) Llorca, J.; Hom, N.; Rossell, O.; Seco, M.; Fierro, J.-L. G.; Ramirez de la Piscina, P. *J. Mol. Catal. A: Chem.* **1999**, *149*, 225. (h) Llorca, J.; Ramirez de la Piscina, P.; Sales, J.; Hom, N. In *Studies in Surface Science and Catalysis*; Inui, T., Anpo, M., Izui, K., Yanagida, S., Yamaguchi, T., Eds.; Elsevier: New York, 1998; Vol. 114.
- (28) (a) Choudhury, J.; Podder, S.; Roy, S. *J. Am. Chem. Soc.* **2005**, *127*, 6162. (b) Choudhury, J.; Roy, S. *J. Mol. Catal. A: Chem.* **2008**, *279*, 37. (c) Guidotti, M.; Dal Santo, V.; Gallo, A.; Gianotti, E.; Peli, G.; Psaro, R.; Sordelli, L. *Catal. Lett.* **2006**, *112*, 89. (d) Gallo, A.; Psaro, R.; Guidotti, M.; Dal Santo, V.; Della Pergola, R.; Masih, D.; Izumi, Y. *Dalton Trans.* **2013**, *42*, 12714.
- (29) (a) Hermans, S.; Raja, R.; Thomas, J. M.; Johnson, B. F. G.; Sankar, G.; Gleeson, D. *Angew. Chem., Int. Ed.* **2001**, *40*, 1211. (b) Adams, R. D.; Boswell, E. M.; Captain, B.; Hungria, A. B.; Midgley, P. A.; Raja, R.; Thomas, J. M. *Angew. Chem., Int. Ed.* **2007**, *46*, 8182.
- (30) Thomas, J. M.; Adams, R. D.; Boswell, E. M.; Captain, B.; Gronbeck, H.; Raja, R. *Faraday Discuss.* **2008**, *138*, 301.
- (31) Goel, A. B.; Throckmorton, P. E.; Grimm, R. A. *Inorg. Chim. Acta* **1986**, *117*, L15.
- (32) Raja, R.; Adams, R. D.; Blom, D. A.; Pearl, W. C.; Gianotti, E.; Thomas, J. M. *Langmuir* **2009**, *25*, 7200.
- (33) Li, B.; Zhang, H.; Huynh, L.; Diverchy, C.; Hermans, S.; Devillers, M.; Dikarev, E. V. *Inorg. Chem.* **2009**, *48*, 6152.
- (34) Adams, R. D.; Chen, M.; Elpitiya, G.; Potter, M. E.; Raja, R. *ACS Catal.* **2013**, *3*, 3106.
- (35) (a) Snytnikov, P. V.; Yusenko, K.; Korenev, S.; Shubin, Y. V.; Sobyanin, V. A. *Kinet. Catal.* **2007**, *48*, 276. (b) Potemkin, D. I.; Filatov, E. Y.; Zadesenets, A. V.; Snytnikov, P. V.; Shubin, Y. V.; Sobyanin, V. A. *Chem. Eng. J.* **2012**, *207–208*, 683.
- (36) Putaj, P.; Lefebvre, F. *Coord. Chem. Rev.* **2011**, *255*, 1642.
- (37) (a) Wang, Z.; Chen, G.; Ding, K. *Chem. Rev.* **2008**, *109*, 322. (b) Farrusseng, D.; Aguado, S.; Pinel, C. *Angew. Chem., Int. Ed.* **2009**, *48*, 7502. (c) Lee, J.; Farha, O. K.; Roberts, J.; Scheidt, K. A.; Nguyen, S. T.; Hupp, J. T. *Chem. Soc. Rev.* **2009**, *38*, 1450. (d) Corma, A.; García, H.; Llabrés i Xamena, F. X. *Chem. Rev.* **2010**, *110*, 4606. (e) Ranocchiai, M.; van Bokhoven, J. A. *Phys. Chem. Chem. Phys.* **2011**, *13*, 6388. (f) Yoon, M.; Srirambalaji, R.; Kim, K. *Chem. Rev.* **2011**, *112*, 1196.
- (38) Wang, Z.-C.; Dietl, N.; Kretschmer, R.; Weiske, T.; Schlangen, M.; Schwarz, H. *Angew. Chem., Int. Ed.* **2011**, *50*, 12351.
- (39) Leithall, R. M.; Shetti, V. N.; Maurelli, S.; Chiesa, M.; Gianotti, E.; Raja, R. *J. Am. Chem. Soc.* **2013**, *135*, 2915.
- (40) Luo, G.; Luo, Y.; Zhang, W.; Qu, J.; Hou, Z. *Organometallics* **2014**, *33*, 1126.
- (41) Oishi, M.; Kato, T.; Nakagawa, M.; Suzuki, H. *Organometallics* **2008**, *27*, 6046.
- (42) (a) Aubart, M. A.; Chandler, B. D.; Gould, R. A. T.; Krogstad, D. A.; Schoondergang, M. F. J.; Pignolet, L. H. *Inorg. Chem.* **1994**, *33*, 3724. (b) Aubart, M. A.; Pignolet, L. H. *J. Am. Chem. Soc.* **1992**, *114*, 7901.
- (43) (a) Pignolet, L. H.; Aubart, M. A.; Craighead, K. L.; Gould, R. A. T.; Krogstad, D. A.; Wiley, J. S. *Coord. Chem. Rev.* **1995**, *143*, 219. (b) Kappen, T. G. M. M.; Bour, J. J.; Schlebos, P. P. J.; Roelofsen, A. M.; van der Linden, J. G. M.; Steggerda, J. J.; Aubart, M. A.; Krogstad, D. A.; Schoondergang, M. F. J.; Pignolet, L. H. *Inorg. Chem.* **1993**, *32*, 1074.
- (44) Rubinstein, L. I.; Pignolet, L. H. *Inorg. Chem.* **1996**, *35*, 6755.
- (45) Graf, I. V. G.; Bacon, J. W.; Consugar, M. B.; Curley, M. E.; Ito, L. N.; Pignolet, L. H. *Inorg. Chem.* **1996**, *35*, 689.
- (46) (a) Yuan, Y.; Asakura, K.; Wan, H.; Tsai, K.; Yasuhiro, I. *J. Mol. Catal. A: Chem.* **1997**, *122*, 147. (b) Yuan, Y.; Asakura, K.; Wan, H.; Tsai, K.; Iwasawa, Y. *Chem. Lett.* **1996**, 129.
- (47) Mihut, C.; Descorme, C.; Duprez, D.; Amirdis, M. D. *J. Catal.* **2002**, *212*, 125.
- (48) Hostetler, M. J.; Butts, M. D.; Bergman, R. G. *J. Am. Chem. Soc.* **1993**, *115*, 2743.
- (49) Hostetler, M. J.; Bergman, R. G. *J. Am. Chem. Soc.* **1990**, *112*, 8621.
- (50) Tooley, P. A.; Arndt, L. W.; Darenbourg, M. Y. *J. Am. Chem. Soc.* **1985**, *107*, 2422.
- (51) Pittman, C. U., Jr.; Honnick, W.; Absi-Halabi, M.; Richmond, M. G.; Bender, R.; Braunstein, P. *J. Mol. Catal.* **1985**, *32*, 177.
- (52) Casey, C. P.; Bullock, R. M. *J. Mol. Catal.* **1982**, *14*, 283.
- (53) Schacht, H. T.; Vahrenkamp, H. *Chem. Ber.* **1989**, *122*, 2253.
- (54) (a) Giordano, R.; Sappa, E. *J. Organomet. Chem.* **1993**, *448*, 157. (b) Michelin Lausarot, P.; Vaglio, G. A.; Valle, M. *J. Organomet. Chem.* **1984**, *275*, 233.
- (55) Fox, J. R.; Gladfelter, W. L.; Geoffroy, G. L.; Tavaresipour, I.; Abdel-Mequid, S.; Day, V. W. *Inorg. Chem.* **1981**, *20*, 3230.
- (56) Castiglioni, M.; Giordano, R.; Sappa, E. *J. Organomet. Chem.* **1995**, *491*, 111.
- (57) Cirjak, L. M.; Sutherland, L. U.S. Patent 4,504,371, 1985.
- (58) Attali, S.; Mathieu, R. *J. Organomet. Chem.* **1985**, *291*, 205.
- (59) Attali, S.; Dahan, F.; Mathieu, R. *Organometallics* **1986**, *5*, 1376.
- (60) Thompson, D. T. *Platinum Met. Rev.* **1975**, *19*, 88.
- (61) Blum, J.; Gelman, F.; Abu-Reiq, R.; Miloslavski, I.; Schumann, H.; Avnir, D. *Polyhedron* **2000**, *19*, 509.
- (62) Scott, J. P.; Budge, J. R.; Rheingold, A.; Gates, B. C. *J. Am. Chem. Soc.* **1987**, *109*, 7736.

- (63) Marrakchi, H.; Haimeur, M.; Escalant, P.; Lieto, J.; Aune, J. P. *Nouv. J. Chim.* **1986**, *10*, 159.
- (64) Li, Q.; Ding, E.; Liu, S.; Yin, Y. *Gaodeng Xuexiao Huaxue Xuebao* **1997**, *18*, 1007.
- (65) Castiglioni, M.; Giordano, R.; Sappa, E. *J. Organomet. Chem.* **1987**, *319*, 167.
- (66) Castiglioni, M.; Giordano, R.; Sappa, E. *J. Organomet. Chem.* **1988**, *342*, 111.
- (67) Evans, J.; Jingxing, G. *J. Chem. Soc., Chem. Commun.* **1985**, 39.
- (68) (a) Alexander, B. D.; Gomez-Sal, M. P.; Gannon, P. R.; Blaine, C. A.; Boyle, P. D.; Muetting, A. M.; Pignolet, L. H. *Inorg. Chem.* **1988**, *27*, 3301. (b) Muetting, A. M.; Bos, W.; Alexander, B. D.; Boyle, P. D.; Casalnuovo, J. A.; Balaban, S.; Ito, L. N.; Johnson, S. M.; Pignolet, L. H. *New. J. Chem.* **1988**, *12*, 505.
- (69) Po-Kwan Lau, J.; Wong, W.-T. *J. Organomet. Chem.* **2002**, *659*, 151.
- (70) Lieto, J.; Wolf, M.; Maatrana, B. A.; Prochazka, M.; Tesche, B.; Knözinger, H.; Gates, B. C. *J. Phys. Chem.* **1985**, *89*, 991.
- (71) Castiglioni, M.; Giordano, R.; Sappa, E.; Tiripicchio, A.; Tiripicchio Camellini, M. *J. Chem. Soc., Dalton Trans.* **1986**, 23.
- (72) Wolf, M.; Knözinger, H.; Tesche, B. *J. Mol. Catal.* **1984**, *25*, 273.
- (73) Pierantozzi, R.; McQuade, K. J.; Gates, B. C.; Wolf, M.; Knözinger, H.; Ruhmann, W. *J. Am. Chem. Soc.* **1979**, *101*, 5436.
- (74) Eliau, N.; Avnir, D.; Eisen, M. S.; Blum, J. *J. Sol-Gel Sci. Technol.* **2005**, *35*, 159.
- (75) Li, D.; Zhai, W.; Chen, Z.; Sun, Y.; Zhao, X.; Wang, Z. *Huaxue Xuebao* **1986**, *44*, 990.
- (76) Le Gendre, P.; Picquet, M.; Richard, P.; Moïse, C. *J. Organomet. Chem.* **2002**, *643–644*, 231.
- (77) (a) Weiss, K.; Guthmann, W.; Denzner, M.; Maisuls, S. *Nato ASI Ser., Ser. C* **1990**, *26*, 517. (b) Weiss, K.; Guthmann, W.; Maisuls, S. *Angew. Chem.* **1988**, *100*, 268.
- (78) Weiss, K.; Guthmann, W.; Denzner, M. *J. Mol. Catal.* **1988**, *46*, 341.
- (79) Weiss, K.; Denzner, M. *J. Organomet. Chem.* **1988**, *355*, 273.
- (80) Ichikawa, M.; Pan, W.; Imada, Y.; Yamaguchi, M.; Isobe, K.; Shido, T. *J. Mol. Catal. A: Chem.* **1996**, *107*, 23.
- (81) Maire, G.; Zahraa, O.; Garin, F.; Crouzet, C.; Aeiyach, S.; Legaré, P.; Braunstein, P. *J. Chim. Phys.* **1981**, *78*, 951.
- (82) Esteban Puges, P.; Garin, F.; Girard, P.; Bernhardt, P.; Maire, G. *Proceeding, Iberoamerican Congress on Catalysis*, Lisbon, Portugal, 1984; p 1111.
- (83) Shapley, J. R.; Uchiyama, W. S.; Scott, R. A. *J. Phys. Chem.* **1990**, *94*, 1190.
- (84) Shapley, J. R.; Hardwick, S. J.; Foose, D. S.; Stucky, G. D.; Churchill, M. R.; Bueno, C.; Hutchinson, J. P. *J. Am. Chem. Soc.* **1981**, *103*, 7383.
- (85) Guczi, L. In *Studies in Surface Science and Catalysis*; Gates, B. C., Guczi, L., Knözinger, H., Eds.; Elsevier Science Publishers: Amsterdam, 1986; Vol. 29.
- (86) Fung, A. S.; Tooley, P. A.; McDevitt, M. R.; Gates, B. C.; Kelley, M. *J. Polyhedron* **1988**, *7*, 2421.
- (87) Nashner, M. S.; Somerville, D. M.; Lane, P. D.; Adler, D. L.; Shapley, J. R.; Nuzzo, R. G. *J. Am. Chem. Soc.* **1996**, *118*, 12964.
- (88) Augustine, S. M.; Nacheff, M. S.; Tsang, C. M.; Butt, J. B.; Sachtl, W. M. H. *Proc. 9th Int. Congr. Catal.* **1988**, *3*, 1190.
- (89) Iwasawa, Y.; Yamada, M. *J. Chem. Soc., Chem. Commun.* **1985**, 675.
- (90) Ichikawa, M.; Rao, L.; Ito, T.; Fukuoka, A. *Faraday Discuss. Chem. Soc.* **1989**, *87*, 321.
- (91) Zahraa, O. Ph.D. Thesis, Université Louis Pasteur, 1980.
- (92) (a) McVicker, G. B. U.S. Patent, 4,217,249, 1980, Exxon Research and Engineering Co. (b) McVicker, G. B. U.S. Patent 4,302,400, 1981, Exxon Research and Engineering Co.
- (93) (a) Chotisawan, S.; Wittayakun, J.; Lobo-Lapidus, R.; Gates, B. C. *Catal. Lett.* **2007**, *115*, 99. (b) Chotisawan, S.; Wittayakun, J.; Gates, B. C. *J. Phys. Chem. B* **2006**, *110*, 12459.
- (94) Anderson, J. R.; Mainwaring, D. E. *J. Catal.* **1974**, *35*, 162.
- (95) Ichikawa, M. *Adv. Catal.* **1992**, *38*, 283.
- (96) Maire, G. *Studies in Surface Science and Catalysis*; Elsevier Science Publishers: Amsterdam, 1986; Vol. 29.
- (97) Ichikawa, M.; Rao, L.; Kimura, T.; Fukuoka, A. *J. Mol. Catal.* **1990**, *62*, 15.
- (98) (a) Chandler, B. D.; Schabel, A. B.; Pignolet, L. H. *J. Catal.* **2000**, *193*, 186. (b) Chandler, B. D.; Pignolet, L. H. *Catal. Today* **2001**, *65*, 39.
- (99) Chandler, B. D.; Schabel, A. B.; Blanford, C. F.; Pignolet, L. H. *J. Catal.* **1999**, *187*, 367.
- (100) (a) Thomas, J. M.; Johnson, B. F. G.; Raja, R.; Sankar, G.; Midgley, P. A. *Acc. Chem. Res.* **2002**, *36*, 20. (b) Weller, A. S.; McIndoe, J. S. *Eur. J. Inorg. Chem.* **2007**, 4411.
- (101) (a) Coucovanis, D.; Mosier, P. E.; Malinak, S. M.; Laughlin, L. J.; Demadis, K. D. *Curr. Plant Sci. Biotechnol. Agric.* **1995**, *27*, 137. (b) Coucovanis, D.; Demadis, K. D.; Malinak, S. M.; Mosier, P. E.; Tyson, M. A.; Laughlin, L. J. *J. Mol. Catal. A: Chem.* **1996**, *107*, 123. (c) Coucovanis, D.; Demadis, K. D.; Malinak, S. M.; Mosier, P. E.; Tyson, M. A.; Laughlin, L. J. *ACS Symp. Ser.* **1996**, *653*, 117. (d) Coucovanis, D. *J. Biol. Inorg. Chem.* **1996**, *1*, 594.
- (102) Butts, M. D.; Bergman, R. G. *Organometallics* **1994**, *13*, 2668.
- (103) Niu, S.; Zhang, Z.; Xu, J.; Zhang, H.; Xin, Q.; Wei, Z. *Cuihua Xuebao* **1995**, *16*, 464.
- (104) Xu, J.; Liu, X.; Zhou, X.; Liu, L.; Li, S.; Wang, T. *Jilin Daxue Ziran Kexue Xuebao* **1984**, 97.
- (105) Nan, Y.; Xu, J.; Cai, H. *Fenzi Cuihua* **1996**, *10*, 461.
- (106) Laughlin, L. J.; Coucovanis, D. *J. Am. Chem. Soc.* **1995**, *117*, 3118.
- (107) Mani, D.; Vahrenkamp, H. *J. Mol. Catal.* **1985**, *29*, 305.
- (108) Herbst, K.; Brorson, M.; Carlsson, A. *J. Mol. Catal. A: Chem.* **2010**, *325*, 1.
- (109) (a) Richmond, M. G.; Absi-Halabi, M.; Pittman, C. U., Jr. *J. Mol. Catal.* **1984**, *22*, 367. (b) Pittman, C. U., Jr.; Ryan, R. C.; Wilson, W. D.; Wileman, G.; Absi-Halabi, M. *Prepr.-Am. Chem. Soc., Div. Pet. Chem.* **1980**, *25*, 714.
- (110) Carlton, L.; Lindsell, W. E.; McCullough, K. J.; Preston, P. N. *J. Chem. Soc., Dalton Trans.* **1984**, 1693.
- (111) Kato, H.; Seino, H.; Mizobe, Y.; Hidai, M. *J. Chem. Soc., Dalton Trans.* **2002**, 1494.
- (112) Zhang, Z.-Z.; Cheng, H. *Coord. Chem. Rev.* **1996**, *147*, 1.
- (113) Fusi, A.; Ugo, R.; Psaro, R.; Braunstein, P.; Dehand, J. *Philos. Trans. R. Soc. London, Ser. A* **1982**, *308*, 125.
- (114) (a) Alexeev, O.; Shelef, M.; Gates, B. C. *J. Catal.* **1996**, *164*, 1. (b) Alexeev, O.; Kawi, S.; Shelef, M.; Gates, B. C. *J. Phys. Chem.* **1996**, *100*, 253.
- (115) Zhao, D.; Dyson, P. J.; Laurenczy, G.; McIndoe, J. S. *J. Mol. Catal. A: Chem.* **2004**, *214*, 19.
- (116) Alexeev, O. S.; Graham, G. W.; Shelef, M.; Gates, B. C. *J. Catal.* **2000**, *190*, 157.
- (117) Beers, O. C. P.; Bouman, M. M.; Komen, A. E.; Vrieze, K.; Elsevier, C. J.; Horn, E.; Spek, A. L. *Organometallics* **1993**, *12*, 315.
- (118) Baker, R. T.; Glassman, T. E.; Overall, D. W.; Calabrese, J. C. *Isr. J. Chem.* **1991**, *31*, 33.
- (119) Casey, C. P.; Rutter, E. W., Jr. *J. Am. Chem. Soc.* **1989**, *111*, 8917.
- (120) Castiglioni, M.; Deabate, S.; Garrone, E.; Giordano, R.; Onida, B.; Predieri, G.; Sappa, E. *J. Cluster Sci.* **1997**, *8*, 381.
- (121) Bonelli, B.; Brait, S.; Deabate, S.; Garrone, E.; Giordano, R.; Sappa, E.; Verre, F. *J. Cluster Sci.* **2000**, *11*, 307.
- (122) Deabate, S.; Giordano, R.; Sappa, E.; Predieri, G. *The Sixth International Conference on the Chemistry of the Platinum Group Metals*; The Royal Society of Chemistry, University of York: UK, 1996; p 100.
- (123) Garcia, M. P.; Lopez, A. M.; Esteruelas, M. A.; Laboz, F. J.; Oro, L. A. *J. Chem. Soc., Chem. Commun.* **1988**, 793.
- (124) Esteruelas, M. A.; Garcia, M. P.; Lopez, A. M.; Oro, L. A. *Organometallics* **1991**, *10*, 127.
- (125) Piacenti, F.; Matteoli, U.; Bianchi, M.; Frediani, P.; Menchi, G. *Gazz. Chim. Ital.* **1988**, *118*, 305.
- (126) Ferrand, V.; Süss-Fink, G.; Neels, A.; Stoeckli-Evans, H. *J. Chem. Soc., Dalton Trans.* **1998**, 3825.

- (127) Castiglioni, M.; Giordano, R.; Sappa, E. *J. Organomet. Chem.* **1984**, *275*, 119.
- (128) (a) Castagno, F.; Castiglioni, M.; Sappa, E.; Tiripicchio, A.; Tiripicchio Camellini, M.; Braunstein, P.; Rosé, J. *J. Chem. Soc., Dalton Trans.* **1989**, *1477*. (b) Castiglioni, M.; Castagno, F.; Giordano, R.; Sappa, E. *J. Mol. Catal.* **1989**, *55*, 311.
- (129) (a) Raja, R.; Hermans, S.; Shephard, D. S.; Johnson, B. F. G.; Sankar, G.; Bromley, S.; Thomas, J. M. *Chem. Commun.* **1999**, *1571*. (b) Raja, R.; Sankar, G.; Hermans, S.; Shephard, D. S.; Bromley, S.; Thomas, J. M.; Johnson, B. F. G.; Maschmeyer, T. *Chem. Commun.* **1999**, *2131*. (c) Raja, R.; Thomas, J. M. *J. Mol. Catal. A: Chem.* **2002**, *181*, 3. (d) Johnson, B. F. G.; Raynor, S. A.; Brown, D. B.; Shephard, D. S.; Mashmeyer, T.; Thomas, J. M.; Hermans, S.; Raja, R.; Sankar, G. *J. Mol. Catal. A: Chem.* **2002**, *182–183*, 89. (e) Raja, R.; Khimyak, T.; Thomas, J. M.; Hermans, S.; Johnson, B. F. G. *Angew. Chem., Int. Ed.* **2001**, *40*, 4638.
- (130) Thomas, J. M.; Raja, R.; Johnson, B. F. G.; O'Connell, T. J.; Sankar, G.; Khimyak, T. *Chem. Commun.* **2003**, *1126*.
- (131) Adams, R. D.; Captain, B.; Zhu, L. *J. Am. Chem. Soc.* **2004**, *126*, 3042.
- (132) Adams, R. D.; Captain, B.; Zhu, L. *J. Organomet. Chem.* **2006**, *691*, 3122.
- (133) Hungria, A. B.; Raja, R.; Adams, R. D.; Captain, B.; Thomas, J. M.; Midgley, P. A.; Golovko, V.; Johnson, B. F. G. *Angew. Chem., Int. Ed.* **2006**, *45*, 4782.
- (134) Uffalussy, K. J.; Captain, B. K.; Adams, R. D.; Hungria, A. B.; Monnier, J. R.; Amiridis, M. D. *ACS Catal.* **2011**, *1*, 1710.
- (135) Muraza, O.; Rebrov, E. V.; Berenguer-Murcia, A.; de Croon, M. H. J. M.; Schouten, J. C. *Appl. Catal., A* **2009**, *368*, 87.
- (136) (a) Adams, R. D.; Barnard, T. S.; Li, Z.; Wu, W.; Yamamoto, J. H. *J. Am. Chem. Soc.* **1994**, *116*, 9103. (b) Adams, R. D.; Li, Z.; Swepston, P.; Wu, W.; Yamamoto, J. H. *J. Am. Chem. Soc.* **1992**, *114*, 10657.
- (137) Adams, R. D.; Barnard, T. S. *Organometallics* **1998**, *17*, 2885.
- (138) Shephard, D. S.; Maschmeyer, T.; Sankar, G.; Thomas, J. M.; Ozkaya, D.; Johnson, B. F. G.; Raja, R.; Oldroyd, R. D.; Bell, R. G. *Chem.—Eur. J.* **1998**, *4*, 1214.
- (139) Shephard, D. S.; Maschmeyer, T.; Johnson, B. F. G.; Thomas, J. M.; Sankar, G.; Ozkaya, D.; Zhou, W.; Oldroyd, R. D.; Bell, R. G. *Angew. Chem., Int. Ed. Engl.* **1997**, *36*, 2242.
- (140) Castiglioni, M.; Sappa, E.; Valle, M.; Lanfranchi, M.; Tiripicchio, A. *J. Organomet. Chem.* **1983**, *241*, 99.
- (141) Castiglioni, M.; Giordano, R.; Sappa, E.; Volpe, P. *J. Chromatogr.* **1985**, *349*, 173.
- (142) Moggi, P.; Albanesi, G.; Predieri, G.; Sappa, E. *J. Organomet. Chem.* **1983**, *252*, C89.
- (143) Castiglioni, M.; Giordano, R.; Sappa, E. *J. Mol. Catal.* **1986**, *37*, 287.
- (144) Albanesi, G.; Bernardi, R.; Moggi, P.; Predieri, G.; Sappa, E. *Gazz. Chim. Ital.* **1986**, *116*, 385.
- (145) Pierantozzi, R.; McQuade, K. J.; Gates, B. C. *Proceedings of the 7th International Congress on Catalysis, Tokyo 1981, Part B*; Elsevier: Amsterdam, 1981.
- (146) Labroue, D.; Poilblanc, R. *J. Mol. Catal.* **1977**, *2*, 329.
- (147) Gelman, F.; Avnir, D.; Schumann, H.; Blum, J. *J. Mol. Catal. A: Chem.* **2001**, *171*, 191.
- (148) Gelman, F.; Blum, J.; Avnir, D. *J. Am. Chem. Soc.* **2002**, *124*, 14460.
- (149) Gelman, F.; Blum, J.; Schumann, H.; Avnir, D. *J. Sol-Gel Sci. Technol.* **2003**, *26*, 43.
- (150) Gates, B. C. *NSF-CNRS International Seminar on the Relationship Between Metal Cluster Compounds, Surface Science and Catalysis*, Asilomar, 1979.
- (151) Bhaduri, S.; Sharma, K. R. *J. Chem. Soc., Dalton Trans.* **1984**, *2309*.
- (152) Shirai, M.; Yang, O. B.; Weber, W. A.; Gates, B. C. *J. Catal.* **1999**, *182*, 274.
- (153) El-Amouri, H.; Bahsoun, A. A.; Fischer, J.; Osborn, J. A.; Youinou, M. T. *Organometallics* **1991**, *10*, 3582.
- (154) Bhaduri, S.; Sharma, K. R.; Clegg, W.; Sheldrick, G. M.; Stalke, D. *J. Chem. Soc., Dalton Trans.* **1984**, *2851*.
- (155) Chandler, B. D.; Schabel, A. B.; Pignolet, L. H. *J. Phys. Chem. B* **2001**, *105*, 149.
- (156) Ortiz-Soto, L. B.; Monnier, J. R.; Amirdis, M. D. *Catal. Lett.* **2006**, *107*, 13.
- (157) Braunstein, P.; Matt, D.; Nobel, D. *Chem. Rev.* **1988**, *88*, 747.
- (158) Ojeda, M.; Fandos, R.; Fierro, J. L. G.; Otero, A.; Pastor, C.; Rodríguez, A.; Ruiz, M. J.; Terreros, P. *J. Mol. Catal. A: Chem.* **2006**, *247*, 44.
- (159) Xiao, F. S.; Fukuoka, A.; Ichikawa, M.; Henderson, W.; Shriver, D. F. *J. Mol. Catal.* **1992**, *74*, 379.
- (160) Domingo, M. R.; Irving, A.; Liao, Y.-H.; Moss, J. R.; Nash, A. J. *Organomet. Chem.* **1993**, *443*, 232.
- (161) Shao, C.; Fan, L.; Fujimoto, K.; Iwasawa, Y. *Appl. Catal.* **1995**, *128*, L1.
- (162) Curtis, M. D.; Penner-Hahn, J. E.; Schwank, J.; Baralt, O.; McCabe, D. J.; Thompson, L.; Waldo, G. *Polyhedron* **1988**, *7*, 2411.
- (163) (a) Curtis, M. D.; Schwank, J. W.; Thompson, L.; Williams, P. D.; Baralt, O. *Prepr.-Am. Chem. Soc., Div. Fuel Chem.* **1986**, *31*, 44. (b) Curtis, M. D.; Schwank, J.; Penner-Hahn, E.; Thompson, L.; Baralt, O.; Waldo, G. *Mater. Res. Soc. Symp. Proc.* **1988**, *111*, 331.
- (164) (a) Curtis, M. D.; Schwank, J.; Thompson, L. T.; Williams, P. D. U.S. Patent 4,605,751, 1986. (b) Curtis, M. D. *Report of the International Seminar on Organic Chemistry on Metal Clusters and Surfaces*, S. Vittoria d'Alba, 1992; p 50.
- (165) Man, M. L.; Zhou, Z.; Ng, S. M.; Lau, C. P. *Dalton Trans.* **2003**, 3727.
- (166) Shapley, J. R.; Hardwick, S. J.; Foose, D. S.; Stucky, G. D. *Prepr.-Am. Chem. Soc., Div. Pet. Chem.* **1980**, *25*, 780.
- (167) Te, M.; Lowenthal, E. E.; Foley, H. C. *J. Catal.* **1994**, *146*, 591.
- (168) (a) Trunschke, A.; Ewald, H.; Miessner, H.; Fukuoka, A.; Ichikawa, M.; Böttcher, H.-C. *Mater. Chem. Phys.* **1991**, *29*, 503. (b) Trunschke, A.; Ewald, H.; Miessner, H.; Marengo, S.; Martinengo, S.; Pinna, F.; Zanderighi, L. *J. Mol. Catal.* **1992**, *74*, 365. (c) Mueller, H.; Trunschke, A.; Miessner, H.; Böttcher, H.-C.; Scheer, M.; Walther, B. *Ger. Offen.* **296 227**, 1991.
- (169) Trunschke, A.; Ewald, H.; Gutschick, D.; Miessner, H.; Skupin, M.; Walther, B.; Böttcher, H.-C. *J. Mol. Catal.* **1989**, *56*, 95.
- (170) Kuznetsov, V. L.; Danilyuk, A. F.; Kolosova, I. E.; Yermakov, Y. I. *React. Kinet. Catal. Lett.* **1982**, *21*, 249.
- (171) Bruce, L.; Hope, G.; Turney, T. W. *React. Kinet. Catal. Lett.* **1982**, *20*, 175.
- (172) Pierantozzi, R. *J. Catal.* **1987**, *106*, 323.
- (173) (a) Venter, J.; Kaminsky, M.; Geoffroy, G. L.; Vannice, M. A. *J. Catal.* **1987**, *103*, 155. (b) Venter, J.; Kaminsky, M.; Geoffroy, G. L.; Vannice, M. A. *J. Catal.* **1987**, *103*, 450.
- (174) Vanhove, D.; Makambo, L.; Blanchard, M. *J. Chem. Res., Synop.* **1980**, 335.
- (175) Walker, W. E.; Brown, E. S.; Pruett, R. L. U.S. Patent 3,878,290, 1975, Union Carbide Co.
- (176) Hoskins, B. F.; Steen, R. J.; Turney, T. W. *Inorg. Chim. Acta* **1983**, *77*, L 69.
- (177) Fung, A. S.; Kelley, M. J.; Gates, B. C. *J. Mol. Catal.* **1992**, *71*, 215.
- (178) Walker, W. E.; Brown, E. S.; Pruett, R. L. U.S. Patent 3,378,214, 1975, Union Carbide Co.
- (179) (a) Guo, Z.; Xu, H.; Shi, J.; Wang, Q. *Shiyou Huagong* **1996**, *25*, 395. (b) Xu, H.; Guo, Z.; Wang, H.; Lin, Z. *Cuihua Xuebao* **1995**, *16*, 341.
- (180) (a) Ferkul, H. E.; Berlie, J. M.; Stanton, D. J.; McCowan, J. D.; Baird, M. C. *Can. J. Chem.* **1983**, *61*, 1306. (b) Ferkul, H. E.; Stanton, D. J.; McCowan, J. D.; Baird, M. C. *J. Chem. Soc., Chem. Commun.* **1982**, 955.
- (181) Kaminsky, M.; Yoon, K. J.; Geoffroy, G. L.; Vannice, M. A. *J. Catal.* **1985**, *91*, 338.
- (182) Vannice, M. A.; Lam, Y.; Garten, R. L. *Hydrocarbon Synthesis*; ACS Symposium Series 178; American Chemical Society: Washington, DC, 1979; p 26.

- (183) Xiao, F. S.; Fukuoka, A.; Ichikawa, M. *J. Catal.* **1992**, *138*, 206.
- (184) Choplin, A.; Leconte, M.; Bassett, J. M.; Shore, S. G.; Hsu, W. L. *J. Mol. Catal.* **1983**, *21*, 389.
- (185) Budge, J. R.; Lücke, B. F.; Gates, B. C.; Toran, J. *J. Catal.* **1985**, *91*, 272.
- (186) Drezdzon, M. A.; Whitmire, K. H.; Bhattacharyya, A. A.; Hsu, W. L.; Nagel, C. C.; Shore, S. G.; Shriver, D. F. *J. Am. Chem. Soc.* **1982**, *104*, 5630.
- (187) Hemmerich, R.; Keim, W.; Röper, M. *J. Chem. Soc., Chem. Commun.* **1983**, 428.
- (188) (a) Khomenko, T. I.; Kutyreva, N.; Kadushin, A. A.; Maksimov, Y. V.; Matveev, V. V.; Slinkin, A.; Fedorovskaja, E. *J. Mol. Catal.* **1989**, *56*, 61. (b) Maksimov, Y. V.; Matveev, V. V.; Suzdalev, I. P.; Khomenko, T. I.; Kadushin, A. A. *Hyperfine Interact.* **1990**, *57*, 1987.
- (189) Chen, A. A.; Kaminsky, M.; Geoffroy, G. L.; Vannice, M. A. *J. Phys. Chem.* **1986**, *90*, 4810.
- (190) (a) Ichikawa, M.; Rao, L. F.; Fukuoka, A. *Proceedings of the 1st Congress of Catalysis Science and Technology 1990*, Kodansha, Tokyo, 1991; p 111. (b) Fukuoka, A.; Rao, L. F.; Ichikawa, M. *Nippon Kagaku Kaishi* **1989**, *S61*. (c) Rao, L. F.; Fukuoka, A.; Ichikawa, M. *J. Chem. Soc., Chem. Commun.* **1988**, 458.
- (191) (a) Fukuoka, A.; Kimura, T.; Kosugi, N.; Kuroda, H.; Minai, Y.; Sakai, Y.; Tominaga, T.; Ichikawa, M. *J. Catal.* **1990**, *126*, 434. (b) Ichikawa, M. *Polyhedron* **1988**, *7*, 2351.
- (192) Brizuela, G. P.; Damiani, D. E. *Lat. Am. Appl. Res.* **1991**, *21*, 93.
- (193) Kovalchuk, V. I.; Mikova, N. M.; Chesnokov, N. V.; Naimushina, L. V.; Kuznetsov, B. N. *J. Mol. Catal. A: Chem.* **1996**, *107*, 329.
- (194) (a) Marengo, S.; Psaro, R.; Dossi, C.; Calmotti, S.; Della Pergola, R. *Stud. Surf. Sci. Catal.* **1996**, *101*, 1411. (b) Ugo, R.; Dossi, C.; Psaro, R. *J. Mol. Catal. A: Chem.* **1996**, *107*, 13.
- (195) Kimura, T.; Fukuoka, A.; Fumagalli, A.; Ichikawa, M. *Catal. Lett.* **1989**, *2*, 227.
- (196) Budge, J. R.; Lücke, B. F.; Scott, J. P.; Gates, B. C. *Proceedings, 8th International Congress on Catalysis, Berlin (Ger.)*; Verlag Chemie: Weinheim, 1984; p 89.
- (197) Xiao, F.; Guo, X.; Masaru, I. *Chin. Sci. Bull.* **1992**, *37*, 347.
- (198) Kiviaho, J.; Reinikainen, M.; Niemelä, M. K.; Kataja, K.; Jääskeläinen, S. *J. Mol. Catal. A: Chem.* **1996**, *106*, 187.
- (199) (a) Kiviaho, J.; Niemelä, M. K.; Reinikainen, M.; Pakkanen, T. A. *Appl. Catal., A* **1997**, *149*, 353. (b) Reinikainen, M.; Kiviaho, J.; Kröger, M.; Niemelä, M.; Jaeaeskelaainen, S. *J. Mol. Catal. A: Chem.* **1997**, *118*, 137.
- (200) Wu, L.; Suo, Q.; Tao, K. *Neimenggu Daxue Xuebao, Ziran Kexueban* **1995**, *26*, 441.
- (201) Shen, G. C.; Liu, A. M.; Shido, T.; Ichikawa, M. *Top. Catal.* **1995**, *2*, 141.
- (202) Shen, J. G. C.; Ichikawa, M. *J. Phys. Chem. B* **1998**, *102*, 5602.
- (203) Knifton, J. F. *J. Chem. Soc., Chem. Commun.* **1983**, 729.
- (204) (a) Pruett, R. L.; Bradley, J. S. U.S. Patent 4,301,086, 1982, Exxon Research and Engineering Co. (b) Pruett, R. L.; Bradley, J. S. U.S. Patent 4,342,838, 1982, Exxon Research and Engineering Co.
- (205) (a) Brown, E. S.; U.S. Patent 3,989,799, 1976. (b) Brown, E. S. U.S. Patent 3,929,969, 1975.
- (206) Ichikawa, M. *Chem. Technol.* **1982**, 674.
- (207) Alvila, L.; Pakkanen, T. A.; Krause, O.; Joutsimo, M. U.S. Patent 4,777,320, 1988.
- (208) Walker, W. E.; Brown, E. S.; Pruett, R. L. U.S. Patent 3,878,292, 1975, Union Carbide Co.
- (209) Röper, M.; Schieren, M.; Fumagalli, A. *J. Mol. Catal.* **1986**, *34*, 173.
- (210) Keim, W.; Berger, M.; Schlupp, J. *J. Catal.* **1980**, *61*, 359.
- (211) He, Z.; Lugan, N.; Neibecker, D.; Mathieu, R.; Bonnet, J. *J. Organomet. Chem.* **1992**, *426*, 247.
- (212) (a) Banares, M.; Patil, A. N.; Fehlner, T. P.; Wolf, E. E. *Catal. Lett.* **1995**, *34*, 251. (b) Patil, A. N.; Banares, M.; Lei, X.; Fehlner, T. P.; Wolf, E. E. *J. Catal.* **1996**, *159*, 458.
- (213) Trunschke, A.; Böttcher, H.-C.; Fukuoka, A.; Ichikawa, M.; Miessner, H. *Catal. Lett.* **1991**, *8*, 221.
- (214) Garcia, M. P.; Lopez, A. M.; Esteruelas, M. A.; Lahoz, F. J.; Oro, L. A. *J. Organomet. Chem.* **1990**, *388*, 365.
- (215) Kondarides, D. I.; Tomishige, K.; Nagasawa, Y.; Lee, U.; Iwasawa, Y. *J. Mol. Catal. A: Chem.* **1996**, *111*, 145.
- (216) Fung, A. S.; Kelley, M. J.; Koningsberger, D. C.; Gates, B. C. *J. Am. Chem. Soc.* **1997**, *119*, 5877.
- (217) Chandler, B. D.; Rubinstein, L. I.; Pignolet, L. H. *J. Mol. Catal. A: Chem.* **1998**, *133*, 267.
- (218) Stromnova, T. A.; Busygina, I. N.; Katser, S. B.; Antsyshkina, A. S.; Porai-Koshits, M. A.; Moiseev, I. I. *Izv. Akad. Nauk SSSR, Ser. Khim.* **1987**, *6*, 1435.
- (219) Chistyakov, A.; Tsodikov, M.; Murzin, V.; Yandieva, F.; Zubavichus, Y.; Kozitsyna, N.; Gekhman, A.; Kriventsov, V.; Moiseev, I. *Kinet. Catal.* **2011**, *52*, 258.
- (220) (a) Ungermann, C.; Landis, V.; Moya, S. A.; Cohen, H.; Walker, H.; Pearson, R. G.; Rinker, R. G.; Ford, P. C. *J. Am. Chem. Soc.* **1979**, *101*, 5922. (b) Ford, P. C.; Rinker, R. G.; Unkermann, C.; Laine, R. M.; Landis, V.; Moya, S. A. *J. Am. Chem. Soc.* **1978**, *100*, 4595. (c) Venäläinen, T. *Ann. Acad. Sci. Fenn., Ser. A2* **1987**, *211*, 1. (d) Venäläinen, T.; Iiskola, E.; Pursiainen, J.; Pakkanen, T. A.; Pakkanen, T. T. *J. Mol. Catal.* **1986**, *34*, 293.
- (221) Pursiainen, J. *Ann. Acad. Sci. Fenn., Ser. A2* **1986**, *209*, 46.
- (222) Kishore, M. J. L.; Mishra, G. S.; Kumar, A. *J. Mol. Catal. A: Chem.* **2005**, *230*, 35.
- (223) Takahashi, K.; Yamaguchi, M.; Shido, T.; Ohtani, H.; Isobe, K.; Ichikawa, M. *J. Chem. Soc., Chem. Commun.* **1995**, 1301.
- (224) Berentsveig, V. V.; Nga, C. B.; Rudenko, A. P. *Vestn. Mosk. Univ., Ser. 2: Khim.* **1986**, *27*, 583.
- (225) Nesterov, D. S.; Chygorin, E. N.; Kokozay, V. N.; Bon, V. V.; Boča, R.; Kozlov, Y. N.; Shul'pina, L. S.; Jezierska, J.; Ozarowski, A.; Pombeiro, A. J. L.; Shul'pin, G. B. *Inorg. Chem.* **2012**, *51*, 9110.
- (226) Nesterov, D. S.; Kokozay, V. N.; Dyakonenko, V. V.; Shishkin, O. V.; Jezierska, J.; Ozarowski, A.; Kirillov, A. M.; Kopylovich, M. N.; Pombeiro, A. J. L. *Chem. Commun.* **2006**, *0*, 4605.
- (227) Anisia, K. S.; Kumar, A. *J. Mol. Catal. A: Chem.* **2007**, *271*, 164.
- (228) Kishore, M. J. L.; Kumar, A. *Ind. Eng. Chem. Res.* **2007**, *46*, 4787.
- (229) Albonetti, S.; Bonelli, R.; Epoupa Mengou, J.; Femoni, C.; Tiozzo, C.; Zacchini, S.; Trifirò, F. *Catal. Today* **2008**, *137*, 483.
- (230) Albonetti, S.; Bonelli, R.; Delaigle, R.; Femoni, C.; Gaigneaux, E. M.; Morandi, V.; Ortolani, L.; Tiozzo, C.; Zacchini, S.; Trifirò, F. *Appl. Catal., A* **2010**, *372*, 138.
- (231) Bonelli, R.; Albonetti, S.; Morandi, V.; Ortolani, L.; Riccobene, P. M.; Scirè, S.; Zacchini, S. *Appl. Catal., A* **2011**, *395*, 10.
- (232) Nesterov, D. S.; Kokozay, V. N.; Jezierska, J.; Pavlyuk, O. V.; Boča, R.; Pombeiro, A. J. L. *Inorg. Chem.* **2011**, *50*, 4401.
- (233) Hosokawa, T.; Takano, M.; Murahashi, S.-I. *J. Am. Chem. Soc.* **1996**, *118*, 3990.
- (234) Hosokawa, T.; Takano, M.; Murahashi, S.; Ozaki, H.; Kitagawa, Y.; Sakaguchi, K.; Katsube, Y. *J. Chem. Soc., Chem. Commun.* **1994**, 1433.
- (235) Nikanova, O. A.; Capron, M.; Fang, G.; Faye, J.; Mamede, A.-S.; Jalowiecki-Duhamel, L.; Dumeignil, F.; Seisenbaeva, G. A. *J. Catal.* **2011**, *279*, 310.
- (236) Shapley, P. A.; Zhang, N.; Allen, J. L.; Pool, D. H.; Liang, H.-C. *J. Am. Chem. Soc.* **2000**, *122*, 1079.
- (237) Zhang, N.; Mann, C. M.; Shapley, P. A. *J. Am. Chem. Soc.* **1988**, *110*, 6591.
- (238) Bonelli, R.; Lucarelli, C.; Pasini, T.; Liotta, L. F.; Zacchini, S.; Albonetti, S. *Appl. Catal., A* **2011**, *400*, 54.
- (239) Kuiper, J. L.; Shapley, P. A.; Rayner, C. M. *Organometallics* **2004**, *23*, 3814.
- (240) Kuiper, J. L.; Shapley, P. A. *J. Organomet. Chem.* **2007**, *692*, 1653.
- (241) García, B.; Captain, B.; Adams, R. D.; Hungria, A. R.; Midgley, P. A.; Thomas, J. M.; Weidner, J. *J. Cluster Sci.* **2007**, *18*, 121.

- (242) (a) Koh, A. C. W.; Leong, W. K.; Chen, L.; Ang, T. P.; Lin, J.; Johnson, B. F. G.; Khimyak, T. *Catal. Commun.* **2008**, *9*, 170. (b) Koh, A. C. W.; Chen, L.; Leong, W. K.; Ang, T. P.; Johnson, B. F. G.; Khimyak, T.; Lin, J. *Int. J. Hydrogen Energy* **2009**, *34*, 5691.
- (243) Kessler, V. G.; Gohil, S.; Kritikos, M.; Korsak, O. N.; Knyazeva, E. E.; Moskovskaya, I. F.; Romanovsky, B. V. *Polyhedron* **2001**, *20*, 915.
- (244) (a) Ghenciu, A. F. *Curr. Opin. Solid State Mater. Sci.* **2002**, *6*, 389. (b) Trimm, D. L. *Appl. Catal., A* **2005**, *296*, 1. (c) Bion, N.; Epron, F.; Moreno, M.; Mariño, F.; Duprez, D. *Top. Catal.* **2008**, *51*, 76. (d) Liu, K.; Wang, A.; Zhang, T. *ACS Catal.* **2012**, *2*, 1165. (e) Wei, Z.; Sun, J.; Li, Y.; Datye, A. K.; Wang, Y. *Chem. Soc. Rev.* **2012**, *41*, 7994.
- (245) (a) Siani, A.; Captain, B.; Alexeev, O. S.; Stafyla, E.; Hungria, A. B.; Midgley, P. A.; Thomas, J. M.; Adams, R. D.; Amiridis, M. D. *Langmuir* **2006**, *22*, 5160. (b) Siani, A.; Captain, B.; Adams, R. D.; Alexeev, O. S.; Amiridis, M. D. *Top. Catal.* **2011**, *54*, 318.
- (246) Siani, A.; Alexeev, O. S.; Captain, B.; Lafaye, G.; Marécot, P.; Adams, R. D.; Amiridis, M. D. *J. Catal.* **2008**, *255*, 162.
- (247) Bonelli, R.; Zucchini, S.; Albonetti, S. *Catalysts* **2012**, *2*, 1.
- (248) Ortiz-Soto, L. B.; Alexeev, O. S.; Amiridis, M. D. *Langmuir* **2006**, *22*, 3112.
- (249) (a) Straub, T.; Koskinen, A. M. P. *Inorg. Chem. Commun.* **2002**, *5*, 1052. (b) Straub, T.; Koskinen, A. M. P. WO Patent 033391, 2004.
- (250) Allen, J. L.; Shapley, P. A.; Wilson, S. R. *Organometallics* **1994**, *13*, 3749.
- (251) (a) Doyle, G. *J. Mol. Catal.* **1981**, *13*, 237. (b) Uchida, Y. *Rep. Asahi Glass Found. Ind. Technol.* **1982**, *40*, 49. (c) Hidai, M.; Orisaku, M.; Ue, M.; Koyasu, Y.; Kodama, T.; Uchida, Y. *Organometallics* **1983**, *2*, 292. (d) Centritto, N.; Barriola, A. M. *Acta Cient. Venez.* **1984**, *35*, 346.
- (252) Hidai, M.; Koyasu, Y.; Yokota, M.; Orisaku, M.; Uchida, Y. *Bull. Chem. Soc. Jpn.* **1982**, *55*, 3951.
- (253) (a) Gauthier-Lafaye, J.; Perron, R. *Methanol et Carbonylation*; Rhône-Poulenc Recherches: Paris, 1986; and references cited therein. (b) Gauthier-Lafaye, J.; Perron, R.; Colleuille, Y. *Actual. Chim.* **1983**, *9*, 11. (c) Matsuzaka, H.; Hidai, M. *Kagaku Kogyo* **1987**, *38*, 495. (d) Doyle, G. *J. Mol. Catal.* **1983**, *18*, 251. (e) Doyle, G. Eur. Patent 30434, 1981, Exxon Research and Engineering Co.
- (254) (a) Hidai, M.; Fukuoka, A.; Koyasu, Y.; Uchida, Y. *J. Mol. Catal.* **1986**, *35*, 29. (b) Hidai, M.; Orisaku, M.; Ue, M.; Uchida, Y.; Yasufuku, K.; Yamazaki, H. *Chem. Lett.* **1981**, 143.
- (255) Rosé, J. Ph.D. Thesis, Université Louis Pasteur, 1985.
- (256) Pursiainen, J.; Karjalainen, K.; Pakkanen, T. A. *J. Organomet. Chem.* **1986**, *314*, 227.
- (257) Zhang, Z. Z.; Xi, H. P.; Zhao, W. J.; Jiang, K. Y.; Wang, R. J.; Wang, H. G.; Wu, Y. *J. Organomet. Chem.* **1993**, *454*, 221.
- (258) Süss-Fink, G.; Haak, S.; Ferrand, V.; Stoeckli-Evans, H. *J. Mol. Catal. A: Chem.* **1999**, *143*, 163.
- (259) Gautron, S.; Lassauque, N.; Le Berre, C.; Azam, L.; Giordano, R.; Serp, P.; Laurenczy, G.; Daran, J.-C.; Duhayon, C.; Thiébaut, D.; Kalck, P. *Organometallics* **2006**, *25*, 5894.
- (260) Gautron, S.; Lassauque, N.; Le Berre, C.; Serp, P.; Azam, L.; Giordano, R.; Laurenczy, G.; Thiébaut, D.; Kalck, P. *Eur. J. Inorg. Chem.* **2006**, *1121*.
- (261) Bischoff, S.; Weigt, A.; Fujimoto, K.; Lücke, B. *J. Mol. Catal.* **1995**, *95*, 259.
- (262) (a) Spindler, F. H. Dissertation ETH Zurich, no. 7012, 1982. (b) Spindler, F. H.; Bor, G.; Dietler, U. K.; Pino, P. *J. Organomet. Chem.* **1981**, *213*, 303. (c) Pino, P.; von Bézard, D. Ger. Offen. 2,807,251, 1978.
- (263) Kalck, P.; Serra, C.; Machet, C.; Broussier, R.; Gautheron, B.; Delmas, G.; Trouvé, G.; Kubicki, M. *Organometallics* **1993**, *12*, 1021.
- (264) Park, K. H.; Jung, I. G.; Chung, Y. K. *Synlett* **2004**, 2541.
- (265) Park, K. H.; Kim, S. Y.; Chung, Y. K. *Org. Biomol. Chem.* **2005**, *3*, 395.
- (266) Komine, N.; Tanaka, S.-i.; Tsutsuminai, S.; Akahane, Y.; Hirano, M.; Komiya, S. *Chem. Lett.* **2004**, *33*, 858.
- (267) Tanaka, S.-i.; Hoh, H.; Akahane, Y.; Tsutsuminai, S.; Komine, N.; Hirano, M.; Komiya, S. *J. Organomet. Chem.* **2007**, *692*, 26.
- (268) Furuya, M.; Tsutsuminai, S.; Nagasawa, H.; Komine, N.; Hirano, M.; Komiya, S. *Chem. Commun.* **2003**, 2046.
- (269) (a) Li, C.; Widjaja, E.; Garland, M. *J. Am. Chem. Soc.* **2003**, *125*, 5540. (b) Li, C.; Widjaja, E.; Garland, M. *Organometallics* **2004**, *23*, 4131. (c) Li, C.; Chen, L.; Garland, M. *J. Am. Chem. Soc.* **2007**, *129*, 13327. (d) Li, C.; Chen, L.; Garland, M. *Adv. Synth. Catal.* **2008**, *350*, 679. (e) Li, C.; Cheng, S.; Tjahjono, M.; Schreyer, M.; Garland, M. *J. Am. Chem. Soc.* **2010**, *132*, 4589.
- (270) Casado, M. A.; Pérez-Torrente, J. J.; Ciriano, M. A.; Oro, L. A.; Orejón, A.; Claver, C. *Organometallics* **1999**, *18*, 3035.
- (271) Choukroun, R.; Iraqi, A.; Rifai, C.; Gervais, D. *J. Organomet. Chem.* **1988**, *353*, 45.
- (272) Gelmini, L.; Stephan, D. W. *Organometallics* **1988**, *7*, 849.
- (273) (a) Senocq, F.; Randrianalimanana, C.; Thorez, A.; Kalck, P.; Choukroun, R.; Gervais, D. *J. Chem. Soc., Chem. Commun.* **1984**, 376. (b) Senocq, F.; Randrianalimanana, C.; Thorez, A.; Kalck, P.; Choukroun, R.; Gervais, D. *J. Mol. Catal.* **1986**, *35*, 213. (c) Choukroun, R.; Gervais, D.; Rifai, C. *Polyhedron* **1989**, *8*, 1760. (d) Choukroun, R.; Gervais, D.; Iraqi, A.; Daran, J.-C.; Jeannin, Y. *Organometallics* **1987**, *6*, 1197.
- (275) Choukroun, R.; Gervais, D.; Kalck, P.; Senocq, F. *J. Organomet. Chem.* **1987**, *335*, C9.
- (276) Choukroun, R.; Dahan, F.; Gervais, D.; Rifai, C. *Organometallics* **1990**, *9*, 1982.
- (277) Larsson, A.-M.; Choukroun, R.; Daran, J.-C.; Cuenca, T.; Flores, J. C.; Royo, P. *J. Organomet. Chem.* **1993**, *444*, 83.
- (278) Trzeciak, A. M.; Ziolkowski, J. J.; Choukroun, R. *J. Mol. Catal. A: Chem.* **1996**, *110*, 135.
- (279) Hernandez-Gruel, M. A. F.; Pérez-Torrente, J. J.; Ciriano, M. A.; Rivas, A. B.; Lahoz, F. J.; Dobrinovitch, I. T.; Oro, L. A. *Organometallics* **2003**, *22*, 1237.
- (280) Bosch, B. E.; Brümmer, I.; Kunz, K.; Erker, G.; Fröhlich, R.; Kotila, S. *Organometallics* **2000**, *19*, 1255.
- (281) Wang, Q.-L.; Chen, S.-N.; Wang, X.; Wu, G.-M.; Sun, W.-H.; Wang, H.-Q.; Yang, S.-Y. *Polyhedron* **1996**, *15*, 2613.
- (282) Dickson, R. S.; De Simone, T.; Campi, E. M.; Jackson, W. R. *Inorg. Chim. Acta* **1994**, *220*, 187.
- (283) Zhu, B.-H.; Zhang, L.; Xiao, N.; Chen, J.-B.; Yin, Y.-Q.; Sun, J. *Inorg. Chim. Acta* **2004**, *357*, 864.
- (284) Hidai, M.; Fukuoka, A.; Koyasu, Y.; Uchida, Y. *J. Chem. Soc., Chem. Commun.* **1984**, 516.
- (285) (a) Li, H.; Luo, Y.; Fu, H. *Fenzi Cuihua* **1988**, *2*, 50. (b) Luo, Y.; Fu, H.; Xue, S.; Ma, Y. *Fenzi Cuihua* **1989**, *3*, 130. (c) Re, X.; Luo, Y.; Fu, H. *Fenzi Cuihua* **1987**, *1*, 111.
- (286) (a) Pittman, C. U., Jr.; Hilal, H.; Don, M. J.; Richmond, M. G. *Chem. Ind. (London)* **1992**, *47*, 307. (b) Richmond, M. G. *J. Mol. Catal.* **1989**, *54*, 199.
- (287) Böttcher, H.-C.; Merzweiler, K.; Bruhn, C. *Z. Naturforsch., B: Chem. Sci.* **1997**, *52*, 810.
- (288) Della Pergola, R.; Cinquantini, A.; Diana, E.; Garlaschelli, L.; Laschi, F.; Luzzini, P.; Manassero, M.; Repossi, A.; Sansoni, M.; Stanghellini, P. L.; Zanello, P. *Inorg. Chem.* **1997**, *36*, 3761.
- (289) Alami, M. K.; Dahan, F.; Mathieu, R. *J. Chem. Soc., Dalton Trans.* **1987**, 1983.
- (290) Fukuoka, A.; Ichikawa, M.; Hriljac, J. A.; Shriver, D. F. *Inorg. Chem.* **1987**, *26*, 3643.
- (291) (a) Zong, H.; Qi, T.; Chen, Z.; Jiang, Y. *Chin. J. Polym. Sci.* **1991**, *9*, 171. (b) Tang, Q.; Zong, H.; Chen, Z.; Jiang, Y. *Chin. J. Polym. Sci.* **1991**, *9*, 39.
- (292) Fukuoka, A.; Matsuzaka, H.; Hidai, M.; Ichikawa, M. *Chem. Lett.* **1987**, 941.
- (293) Chaudret, B.; Delavaux, B.; Poilblanc, R. *Nouv. J. Chim.* **1983**, *7*, 679.
- (294) Alvila, L.; Pakkanen, T. A.; Pakkanen, T. T.; Krause, O. *J. Mol. Catal.* **1992**, *73*, 325.
- (295) (a) Ojima, I.; Okabe, M.; Kato, K.; Kwon, H. B.; Horvath, I. T. *J. Am. Chem. Soc.* **1988**, *110*, 150. (b) Garland, M. *Organometallics* **1993**, *12*, 535.

- (296) Ojima, L. *J. Mol. Catal.* **1986**, *37*, 25.
- (297) Walther, B.; Böttcher, H.-C.; Scheer, M.; Fischer, G.; Fenske, D.; Süss-Fink, G. *J. Organomet. Chem.* **1992**, *437*, 307.
- (298) Garlaschelli, L.; Marchionna, M.; Iapalucci, M. C.; Longoni, G. *J. Mol. Catal.* **1991**, *68*, 7.
- (299) Alvila, L.; Pakkanen, T. A.; Pakkanen, T. T.; Krause, O. *J. Mol. Catal.* **1992**, *75*, 333.
- (300) Ceriotti, A.; Garlaschelli, L.; Longoni, G.; Malatesta, M. C.; Strumolo, D.; Fumagalli, A.; Martinengo, S. *J. Mol. Catal.* **1984**, *24*, 309.
- (301) (a) Garrou, P. E. U.S. Patent 4,374,999, 1983. (b) Hartwell, G. E.; Garrou, P. E. U.S. Patent 4,144,191, 1979; Dow Chemical Co. (c) Alvila, L.; Pakkanen, T. A.; Krause, O.; Joutsimo, M. EP 253 827 B1, 1991. (d) Alvila, L.; Krause, O.; Pakkanen, T. A.; Joutsimo, M. U.S. Patent 4,652,539, 1987.
- (302) Su, G.; Chen, Y.; Yang, S.; Luo, S.; Xie, W.; Yang, Z. *China-Japan-US Symposium Heterogeneous Catalysis and Related Energy Problems*; Chinese Academy of Science, Dalian Institute Chemical Physics: Dalian, Peoples Republic of China, 1982.
- (303) Huang, L.; Xu, Y.; Piao, G.; Liu, A.; Zhang, W. *Catal. Lett.* **1994**, *23*, 87.
- (304) (a) Huang, L. *J. Mol. Catal. A: Chem.* **1997**, *125*, 47. (b) Huang, L.; Liu, A.; Xu, Y. *J. Mol. Catal. A: Chem.* **1997**, *124*, 57. (c) Huang, L.; Xu, Y. *Catal. Lett.* **1996**, *40*, 203. (d) Huang, L. *Bull. Soc. Chim. Fr.* **1996**, *133*, 359.
- (305) (a) Ichikawa, M. *J. Catal.* **1979**, *59*, 67. (b) Ichikawa, M. *J. Catal.* **1979**, *56*, 127.
- (306) Alvila, L. Dissertation, University of Joensuu, Finland, 1992.
- (307) Kim, J. Y.; Park, J. H.; Jung, O.-S.; Chung, Y. K.; Park, K. H. *Catal. Lett.* **2009**, *128*, 483.
- (308) Moroz, B. L.; Semikolenov, V. A.; Likholobov, V. A.; Yemakov, Y. I. *J. Chem. Soc., Chem. Commun.* **1982**, 1286.
- (309) Moroz, B. L.; Shumilo, O. N.; Paukstis, E.; Likholobov, V. A.; Bulgakov, N. N.; Yurchenko, E. N.; Ermakov, Y. I. *Homogeneous Heterogeneous Catalysis, Proceedings of the 5th International Symposium on Relations between Homogeneous and Heterogeneous Catalysis*; VNU Science Press: Utrecht, 1986.
- (310) Zhai, W.; Li, D.; Ma, Y.; Zhao, Z. *Youji Huaxue* **1983**, *3*, 180.
- (311) Lockmeyer, J. R.; Rheingold, A. L.; Bulkowski, J. E. *Organometallics* **1993**, *12*, 256.
- (312) Franciò, G.; Scopelliti, R.; Arena, C. G.; Bruno, G.; Drommi, D.; Faraone, F. *Organometallics* **1998**, *17*, 338.
- (313) Marchionna, M.; Longoni, G. *J. Mol. Catal.* **1986**, *35*, 107.
- (314) Ojima, I.; Zhang, Z. *J. Org. Chem.* **1988**, *53*, 4425.
- (315) Morgan, J. P.; Kundu, K.; Doyle, M. P. *Chem. Commun.* **2005**, 3307.
- (316) Goux, J.; Le Gendre, P.; Richard, P.; Moïse, C. *J. Organomet. Chem.* **2005**, *690*, 301.
- (317) Goux, J.; Le Gendre, P.; Richard, P.; Moïse, C. *J. Organomet. Chem.* **2006**, *691*, 3239.
- (318) Feliz, M.; Guillamón, E.; Llusar, R.; Vicent, C.; Stiriba, S.-E.; Pérez-Prieto, J.; Barberis, M. *Chem.—Eur. J.* **2006**, *12*, 1486.
- (319) Guillamón, E.; Llusar, R.; Pérez-Prieto, J.; Stiriba, S.-E. *J. Organomet. Chem.* **2008**, *693*, 1723.
- (320) Braunstein, P.; Clerc, G.; Morise, X. *New J. Chem.* **2003**, *27*, 68.
- (321) (a) Gibson, S. E.; Stevenazzi, A. *Angew. Chem., Int. Ed.* **2003**, *42*, 1800. (b) Gibson, S. E.; Mainolfi, N. *Angew. Chem., Int. Ed.* **2005**, *44*, 3022. (c) Gibson, S. E.; Lewis, S. E.; Mainolfi, N. *J. Organomet. Chem.* **2004**, *689*, 3873. (d) Gibson, S. E.; Kaufmann, K. A. C.; Loch, J. A.; Miyazaki, A. *Pure Appl. Chem.* **2008**, *80*, 903.
- (322) Paolillo, R.; Gallo, V.; Mastorilli, P.; Nobile, C. F.; Rosé, J.; Braunstein, P. *Organometallics* **2008**, *27*, 741.
- (323) Park, K. H.; Jung, I. G.; Chung, Y. K. *Org. Lett.* **2004**, *6*, 1183.
- (324) Park, K. H.; Chung, Y. K. *Adv. Synth. Catal.* **2005**, *347*, 854.
- (325) Park, J. H.; Kim, S. Y.; Kim, S. M.; Lee, S. I.; Chung, Y. K. *Synlett* **2007**, 453.
- (326) Park, J. H.; Kim, E.; Kim, H.-M.; Choi, S. Y.; Chung, Y. K. *Chem. Commun.* **2008**, 2388.
- (327) Liu, S.; Motta, A.; Mouat, A. R.; Delferro, M.; Marks, T. J. *J. Am. Chem. Soc.* **2014**, *136*, 10460.
- (328) Wang, J.; Li, H.; Guo, N.; Li, L.; Stern, C. L.; Marks, T. J. *Organometallics* **2004**, *23*, 5112.
- (329) Gurubasavaraj, P. M.; Roesky, H. W.; Sharma, P. M. V.; Oswald, R. B.; Dolle, V.; Herbst-Irmer, R.; Pal, A. *Organometallics* **2007**, *26*, 3346.
- (330) Mandal, S. K.; Gurubasavaraj, P. M.; Roesky, H. W.; Schwab, G.; Stalke, D.; Oswald, R. B.; Dolle, V. *Inorg. Chem.* **2007**, *46*, 10158.
- (331) Mitani, M.; Ouchi, K.; Hayakawa, M.; Yamada, T.; Mukaiyama, T. *Polym. Bull.* **1995**, *35*, 677.
- (332) Yan, X.; Chernega, A.; Green, M. L. H.; Sanders, J.; Souter, J.; Ushioda, T. *J. Mol. Catal. A: Chem.* **1998**, *128*, 119.
- (333) (a) Ishino, H.; Takemoto, S.; Hirata, K.; Kanaizuka, Y.; Hidai, M.; Nabika, M.; Seki, Y.; Miyatake, T.; Suzuki, N. *Organometallics* **2004**, *23*, 4544. (b) Hidai, M.; Nabika, M. U.S. Patent 0158355, 2003. (c) Hidai, M.; Nabika, M. EP 1205494, 2001.
- (334) Mokuolu, Q. F.; Duckmant, P. A.; Hitchcock, P. B.; Wilson, C.; Blake, A. J.; Shukla, L.; Love, J. B. *Dalton Trans.* **2004**, 1960.
- (335) Green, M. L. H.; Popham, N. H. *J. Chem. Soc., Dalton Trans.* **1999**, 1049.
- (336) Lindenberg, F.; Shribman, T.; Sieler, J.; Hey-Hawkins, E.; Eisen, M. S. *J. Organomet. Chem.* **1996**, *515*, 19.
- (337) Kuwabara, J.; Takeuchi, D.; Osakada, K. *Chem. Commun.* **2006**, 3815.
- (338) Yamaguchi, Y.; Suzuki, N.; Mise, T.; Wakatsuki, Y. *Organometallics* **1999**, *18*, 996.
- (339) Takayama, C.; Yamaguchi, Y.; Mise, T.; Suzuki, N. *J. Chem. Soc., Dalton Trans.* **2001**, 948.
- (340) Shribman, T.; Kurz, S.; Senff, U.; Lindberg, F.; Hey-Hawkins, E.; Eisen, M. S. *J. Mol. Catal. A: Chem.* **1998**, *129*, 191.
- (341) Dawkins, G. M. EP 255 296, 1988, BP Chemicals Ltd.
- (342) Krauss, H. L.; Amberger, E.; Bohley, T. *3rd International School on Homogeneous Catalysis*, Lagow, Poland, 1998.
- (343) Braunstein, P.; Clerc, G.; Morise, X.; Welter, R.; Mantovani, G. *Dalton Trans.* **2003**, 1601.
- (344) Mitani, M.; Hayakawa, M.; Yamada, T.; Mukaiyama, T. *Bull. Chem. Soc. Jpn.* **1996**, *69*, 2967.
- (345) Barbier, J.-P. Ph.D. Thesis, Université Louis Pasteur, 1978.
- (346) Catton, G. A.; Jones, G. F. C.; Mays, M. J.; Howell, J. A. S. *Inorg. Chim. Acta* **1976**, *20*, L41.
- (347) Schrauzer, G. N.; Ho, R. K. Y.; Schlesinger, G. *Tetrahedron Lett.* **1970**, 543.
- (348) Burlitch, J. M.; Hayes, S. E.; Lemley, J. T. *Organometallics* **1985**, *4*, 167.
- (349) Schrauzer, G. N.; Bastian, B. N.; Fosselius, G. A. *J. Am. Chem. Soc.* **1966**, *88*, 4890.
- (350) Mantovani, L.; Ceccon, A.; Gambaro, A.; Santi, S.; Ganis, P.; Venzo, A. *Organometallics* **1997**, *16*, 2682.
- (351) (a) Adams, R. D.; Babin, J. E.; Tasi, M. *Organometallics* **1987**, *6*, 2247. (b) Adams, R. D.; Babin, J. E.; Tasi, M.; Wang, J. G. *Organometallics* **1988**, *7*, 755.
- (352) Zhou, W.; Napoline, J. W.; Thomas, C. M. *Eur. J. Inorg. Chem.* **2011**, 2029.
- (353) Setty, V. N.; Zhou, W.; Foxman, B. M.; Thomas, C. M. *Inorg. Chem.* **2011**, *50*, 4647.
- (354) Liu, X.; Henderson, J. A.; Sasaki, T.; Kishi, Y. *J. Am. Chem. Soc.* **2009**, *131*, 16678.
- (355) Shenglof, M.; Molander, G. A.; Blum, J. *Synthesis* **2006**, 111.
- (356) Shenglof, M.; Gelman, D.; Heymer, B.; Schumann, H.; Molander, G. A.; Blum, J. *Synthesis* **2003**, 0302.
- (357) Kilic, A.; Yilmaz, I.; Ulusoy, M.; Tas, E. *Appl. Organomet. Chem.* **2008**, *22*, 494.
- (358) Jones, N. D.; James, B. R. *Adv. Synth. Catal.* **2002**, *344*, 1126.
- (359) Keller, F.; Rippert, A. *J. Helv. Chim. Acta* **1999**, *82*, 125.
- (360) Endo, K.; Ogawa, M.; Shibata, T. *Angew. Chem., Int. Ed.* **2010**, *49*, 2410.
- (361) (a) Braunstein, P.; Bender, R.; Kervennal, J. *Organometallics* **1982**, *1*, 1236. (b) Kervennal, J.; Cognion, J.-M.; Braunstein, P. *French*

- Pat. 2,515,640, 1982, U.S. Patent 4,478,757, 1982, PCUK (Produits Chimiques Ugine Kuhlmann).
- (362) Ragaini, F.; Cenini, S.; Fumagalli, A.; Crotti, C. *J. Organomet. Chem.* **1992**, *428*, 401.
- (363) Li, Y.; Pan, W.-X.; Wong, W.-T. *J. Cluster Sci.* **2002**, *13*, 223.
- (364) Li, Y.; Wong, W.-T. *Eur. J. Inorg. Chem.* **2003**, 2651.
- (365) Takei, I.; Enta, Y.; Wakebe, Y.; Suzuki, T.; Hidai, M. *Chem. Lett.* **2006**, *35*, 590.
- (366) Park, J. H.; Kim, E.; Chung, Y. K. *Org. Lett.* **2008**, *10*, 4719.
- (367) Park, J. H.; Kim, S. Y.; Kim, S. M.; Chung, Y. K. *Org. Lett.* **2007**, *9*, 2465.
- (368) Park, J. H.; Yoon, J. C.; Chung, Y. K. *Adv. Synth. Catal.* **2009**, *351*, 1233.
- (369) Huang, G.-H.; Li, J.-M.; Huang, J.-J.; Lin, J.-D.; Chuang, G. J. *Chem.—Eur. J.* **2014**, *20*, 5240.
- (370) Anand, M.; Sunoj, R. B.; Schaefer, H. F. *J. Am. Chem. Soc.* **2014**, *136*, 5535.
- (371) (a) Masui, D.; Ishii, Y.; Hidai, M. *Chem. Lett.* **1998**, *27*, 717. (b) Masui, D.; Kochi, T.; Tang, Z.; Ishii, Y.; Mizobe, Y.; Hidai, M. *J. Organomet. Chem.* **2001**, *620*, 69.
- (372) Le Gendre, P.; Comte, V.; Michelot, A.; Moïse, C. *Inorg. Chim. Acta* **2003**, *350*, 289.
- (373) Takei, I.; Wakebe, Y.; Suzuki, K.; Enta, Y.; Suzuki, T.; Mizobe, Y.; Hidai, M. *Organometallics* **2003**, *22*, 4639.
- (374) Wakabayashi, T.; Ishii, Y.; Murata, T.; Mizobe, Y.; Hidai, M. *Tetrahedron Lett.* **1995**, *36*, 5585.
- (375) Wakabayashi, T.; Ishii, Y.; Ishikawa, K.; Hidai, M. *Angew. Chem., Int. Ed. Engl.* **1996**, *35*, 2123.
- (376) Ye, S.; Leong, W. K. *J. Organomet. Chem.* **2006**, *691*, 1216.
- (377) (a) Pillai, S. M.; Ohnishi, R.; Ichikawa, M. *React. Kinet. Catal. Lett.* **1992**, *48*, 201. (b) Pillai, S. M.; Ohnishi, R.; Ichikawa, M. *J. Chem. Soc., Chem. Commun.* **1990**, 246.
- (378) Lee, Y. M.; Song, Y. J.; Poong, J. I.; Kim, S. H.; Koo, H. G.; Lee, J. A.; Kim, C.; Kim, S.-J.; Kim, Y. *Inorg. Chem. Commun.* **2010**, *13*, 101.
- (379) (a) Angelucci, F.; Ricci, A.; Lo Sterzo, C.; Masi, D.; Bianchini, C.; Bocelli, G. *Organometallics* **2002**, *21*, 3001. (b) Angelucci, F.; Ricci, A.; Masi, D.; Bianchini, C.; Lo Sterzo, C. *Organometallics* **2004**, *23*, 4105.
- (380) Comte, V.; Le Gendre, P.; Richard, P.; Moïse, C. *Organometallics* **2005**, *24*, 1439.
- (381) Leelasubcharoen, S.; Zhizhko, P. A.; Kuzmina, L. G.; Churakov, A. V.; Howard, J. A. K.; Nikonorov, G. I. *Organometallics* **2009**, *28*, 4500.
- (382) Findlay, A. E.; Leelasubcharoen, S.; Kuzmina, L. G.; Howard, J. A. K.; Nikonorov, G. I. *Dalton Trans.* **2010**, *39*, 9264.
- (383) Pittman, C. U., Jr.; Richmond, M. G.; Absi-Halabi, M.; Beurich, H.; Richter, F.; Vahrenkamp, H. *Angew. Chem., Int. Ed. Engl.* **1982**, *21*, 786.
- (384) Kopylova, L. I.; Pukhnarevich, V. B.; Gurevskaya, L. B.; Tsybenov, M. T.; Voronkov, M. G. *Zh. Obshch. Khim.* **1992**, *62*, 346.
- (385) Adams, R. D.; Bunz, U.; Captain, B.; Fu, W.; Steffen, W. J. *Organomet. Chem.* **2000**, *614–615*, 75.
- (386) Adams, R. D.; Barnard, T. S. *Organometallics* **1998**, *17*, 2567.
- (387) Nakata, N.; Sakashita, M.; Komatsubara, C.; Ishii, A. *Eur. J. Inorg. Chem.* **2010**, 447.
- (388) Zhou, W.; Marquardt, S. L.; Bezpaliko, M. W.; Foxman, B. M.; Thomas, C. M. *Organometallics* **2013**, *32*, 1766.
- (389) Ojima, I.; Li, Z. In *Catalysis by Di- and Polynuclear Metal Cluster Complexes*; Adams, R. D., Cotton, F. A., Eds.; Wiley-VCH: New York, 1998.
- (390) Yoshikai, N.; Yamanaka, M.; Ojima, I.; Morokuma, K.; Nakamura, E. *Organometallics* **2006**, *25*, 3867.
- (391) Ojima, I.; Vu, A. T.; McCullagh, J. V.; Kinoshita, A. *J. Am. Chem. Soc.* **1999**, *121*, 3230.
- (392) Ojima, I.; Vidal, E. S. *Organometallics* **1999**, *18*, 5103.
- (393) Ojima, I.; Vu, A. T.; Lee, S.-Y.; McCullagh, J. V.; Moralee, A. C.; Fujiwara, M.; Hoang, T. H. *J. Am. Chem. Soc.* **2002**, *124*, 9164.
- (394) Park, K. H.; Jung, I. G.; Kim, S. Y.; Chung, Y. K. *Org. Lett.* **2003**, *5*, 4967.
- (395) Hoost, T. E.; Graham, G. W.; Shelef, M.; Alexeev, O.; Gates, B. C. *Catal. Lett.* **1996**, *38*, 57.
- (396) Gavrilenko, K. S.; Mironyuk, T. V.; Il'in, V. G.; Orlik, S. N.; Pavlyshchuk, V. V. *Theor. Exp. Chem.* **2002**, *38*, 118.
- (397) Mihut, C.; Chandler, B. D.; Amiridis, M. D. *Catal. Commun.* **2002**, *3*, 91.
- (398) Wang, H.; Belanger, D. *Proc.-Electrochem. Soc.* **1997**, *97–6*, 216.
- (399) Manzoli, M.; Shetti, V. N.; Blaine, J. A. L.; Zhu, L.; Isrow, D.; Yempally, V.; Captain, B.; Coluccia, S.; Raja, R.; Gianotti, E. *Dalton Trans.* **2012**, *41*, 982.
- (400) Malinak, S. M.; Simeonov, A.; Mosier, P. E.; McKenna, C. E.; Coucovanis, D. *J. Am. Chem. Soc.* **1997**, *119*, 1662.
- (401) (a) Demadis, K. D.; Malinak, S. M.; Coucovanis, D. *Inorg. Chem.* **1996**, *35*, 4038. (b) Belonogova, O. V.; Likhtenstein, G. I. *Bioorg. Khim.* **1996**, *22*, 907. (c) Pohlmann, C. *Wiss. Ber.-Forschungszent. Karlsruhe* **1997**, *FZKA 5871*, 1. (d) Xu, J.; Nan, Y.; Liu, Y.; Zhou, X.; Chen, Y.; Niu, S.; Wang, T.; Huang, J.; Luo, A.; Wang, Z.; Zhong, Z.; Li, J. *Chin. Sci. Bull.* **1997**, *42*, 868. (e) Dance, I. *Chem. Commun.* **1997**, 165.
- (402) Takei, I.; Dohki, K.; Kobayashi, K.; Suzuki, T.; Hidai, M. *Inorg. Chem.* **2005**, *44*, 3768.
- (403) Seino, H.; Masumori, T.; Hidai, M.; Mizobe, Y. *Organometallics* **2003**, *22*, 3424.
- (404) Armigliato, A.; Bigi, S.; Moggi, P.; Papadopoulos, S.; Predieri, G.; Salvati, G.; Sappa, E. *Mater. Chem. Phys.* **1991**, *29*, 251.
- (405) Predieri, G.; Moggi, P.; Papadopoulos, S.; Armigliato, A.; Bigi, S.; Sappa, E. *J. Chem. Soc., Chem. Commun.* **1990**, 1736.
- (406) (a) Curtis, M. D. *Appl. Organomet. Chem.* **1992**, *6*, 429. (b) Druker, S. D.; Curtis, M. D. *J. Am. Chem. Soc.* **1995**, *117*, 6366. (c) Curtis, M. D. *J. Cluster Sci.* **1996**, *7*, 247.
- (407) Pinto, P.; Calhorda, M. J.; Straub, T.; Miikkulainen, V.; Räty, J.; Suvanto, M.; Pakkanen, T. A. *J. Mol. Catal. A: Chem.* **2001**, *170*, 209.
- (408) (a) Curtis, M. D. *Chem. Ind. (Dekker)* **1996**, *67*, 129. (b) Curtis, M. D. *ACS Symp. Ser.* **1996**, *653*, 154.
- (409) Curtis, M. D.; Druker, S. H. *J. Am. Chem. Soc.* **1997**, *119*, 1027.
- (410) (a) Mansour, M. A.; Curtis, M. D.; Kampf, J. W. *Organometallics* **1995**, *14*, 5460. (b) Mansour, M. A.; Curtis, M. D.; Kampf, J. W. *Organometallics* **1997**, *16*, 3363.
- (411) (a) Tatsumi, T.; Taniguchi, M.; Yasuda, S.; Ishii, Y.; Murata, T.; Hidai, M. *Appl. Catal., A* **1996**, *139*, L5. (b) Tatsumi, T.; Taniguchi, M.; Ishige, H.; Ishii, Y.; Murata, T.; Hidai, M. *Appl. Surf. Sci.* **1997**, *121/122*, 500.
- (412) Taniguchi, M.; Imamura, D.; Ishige, H.; Ishii, Y.; Murata, T.; Hidai, M.; Tatsumi, T. *J. Catal.* **1999**, *187*, 139.
- (413) Bianchini, C.; Jiménez, M. V.; Meli, A.; Moneti, S.; Patinec, V.; Vizza, F. *Organometallics* **1997**, *16*, 5696.
- (414) Markel, E. J.; Van Zee, J. W. *J. Mol. Catal.* **1992**, *73*, 335.
- (415) Miyazaki, T.; Tanabe, Y.; Yuki, M.; Miyake, Y.; Nishibayashi, Y. *Organometallics* **2011**, *30*, 2394.
- (416) Nikitinskii, A. V.; Bochkarev, L. N.; Voronin, R. V.; Khorshev, S. Y.; Kurskii, Y. A.; Bochkarev, M. N. *Russ. J. Gen. Chem.* **2004**, *74*, 1194.
- (417) Song, C.; Parfitt, D. S.; Schobert, H. H. *Prep. Pap.-Am. Chem. Soc., Div. Fuel Chem.* **1993**, *38*, 546.
- (418) (a) Piers, W. E. *Organometallics* **2011**, *30*, 13. (b) Joya, K. S.; de Groot, H. J. M. *Int. J. Hydrogen Energy* **2012**, *37*, 8787. (c) Swierk, J. R.; Mallouk, T. E. *Chem. Soc. Rev.* **2013**, *42*, 2357.
- (419) (a) Suntivich, J.; May, K. J.; Gasteiger, H. A.; Goodenough, J. B.; Shao-Horn, Y. *Science* **2011**, *334*, 1383. (b) Liang, Y.; Wang, H.; Zhou, J.; Li, Y.; Wang, J.; Regier, T.; Dai, H. *J. Am. Chem. Soc.* **2012**, *134*, 3517.
- (420) Tsui, E. Y.; Kanady, J. S.; Agapie, T. *Inorg. Chem.* **2013**, *52*, 13833.
- (421) Tsui, E. Y.; Tran, R.; Yano, J.; Agapie, T. *Nat. Chem.* **2013**, *5*, 293.

- (422) Tsui, E. Y.; Agapie, T. *Proc. Natl. Acad. Sci. U.S.A.* **2013**, *110*, 10084.
- (423) (a) Hao, L.; Xiao, J.; Vittal, J. J.; Puddephatt, R. J. *Organometallics* **1997**, *16*, 2165. (b) Puddephatt, R. J.; Xiao, J. *NATO ASI, Ser. C* **1996**, *474*, 407.
- (424) (a) Braunstein, P.; Morise, X. *Organometallics* **1998**, *17*, 540. (b) Braunstein, P.; Morise, X. *Chem. Rev.* **2000**, *100*, 3541.
- (425) Braunstein, P.; Morise, X.; Blin, J. *J. Chem. Soc., Chem. Commun.* **1995**, 1455.
- (426) Braunstein, P.; Durand, J.; Morise, X.; Tiripicchio, A.; Uguzzoli, F. *Organometallics* **2000**, *19*, 444.
- (427) Sheridan, J. B.; Temple, K.; Lough, A. J.; Manners, I. *J. Chem. Soc., Dalton Trans.* **1997**, 711.
- (428) Ragaini, F. *Dalton Trans.* **2009**, 6251.
- (429) (a) Haber, F.; van Oordt, G. Z. *Anorg. Chem.* **1905**, *44*, 341. (b) Smil, V. *Nature* **1999**, *400*, 415. (c) Kandemir, T.; Schuster, M. E.; Senyshyn, A.; Behrens, M.; Schlögl, R. *Angew. Chem., Int. Ed. Engl.* **2013**, *52*, 12723.
- (430) (a) Shima, T.; Hu, S.; Luo, G.; Kang, X.; Luo, Y.; Hou, Z. *Science* **2013**, *340*, 1549. (b) Sivasankar, C.; Baskaran, S.; Tamizmani, M.; Ramakrishna, K. *J. Organomet. Chem.* **2014**, *752*, 44. (c) Jia, H.-P.; Quadrelli, E. A. *Chem. Soc. Rev.* **2014**, *43*, 547.
- (431) (a) Powers, D. C.; Ritter, T. *Acc. Chem. Res.* **2011**, *45*, 840. (b) Bonney, K. J.; Proutiere, F.; Schoenebeck, F. *Chem. Sci.* **2013**, *4*, 4434.
- (432) Das, R. K.; Saha, B.; Rahaman, S. M. W.; Bera, J. K. *Chem.—Eur. J.* **2010**, *16*, 14459.
- (433) Braunstein, P.; Chetcuti, M. J.; Welter, R. *Chem. Commun.* **2001**, 2508.
- (434) Braunstein, P.; Durand, J.; Knorr, M.; Strohmann, C. *Chem. Commun.* **2001**, 211.
- (435) Sappa, E.; Tiripicchio, A.; Braunstein, P. *Coord. Chem. Rev.* **1985**, *65*, 219.
- (436) (a) Schweyer-Tihay, F.; Braunstein, P.; Estournès, C.; Guille, J. L.; Lebeau, B.; Paillaud, J.-L.; Richard-Plouet, M.; Rosé, J. *Chem. Mater.* **2002**, *15*, 57. (b) Buchwalter, P.; Rosé, J.; Lebeau, B.; Ersen, O.; Girleanu, M.; Rabu, P.; Braunstein, P.; Paillaud, J.-L. *J. Nanopart. Res.* **2013**, *15*, 1. (c) Buchwalter, P.; Rosé, J.; Lebeau, B.; Rabu, P.; Braunstein, P.; Paillaud, J.-L. *Inorg. Chim. Acta* **2014**, *409*, 330.
- (437) (a) Yang, J. C.; Small, M. W.; Grieshaber, R. V.; Nuzzo, R. G. *Chem. Soc. Rev.* **2012**, *41*, 8179. (b) Browning, N. D.; Aydin, C.; Lu, J.; Kulkarni, A.; Okamoto, N. L.; Ortalan, V.; Reed, B. W.; Uzun, A.; Gates, B. C. *ChemCatChem* **2013**, *5*, 2673. (c) DeLaRiva, A. T.; Hansen, T. W.; Challa, S. R.; Datye, A. K. *J. Catal.* **2013**, *308*, 291.
- (438) Fandos, R.; Hernández, C.; Otero, A.; Rodríguez, A.; Ruiz, M. J.; Terreros, P. *Chem.—Eur. J.* **2003**, *9*, 671.
- (439) Atencio, R.; Casado, M. A.; Ciriano, M. A.; Lahoz, F. J.; Pérez-Torrente, J. J.; Tiripicchio, A.; Oro, L. A. J. *Organomet. Chem.* **1996**, *514*, 103.
- (440) Lindenberg, F.; Gelbrich, T.; Hey-Hawkins, E. Z. *Anorg. Allg. Chem.* **1995**, *621*, 771.
- (441) Senff, U.; Kurz, S.; Hey-Hawkins, E. Z. *Anorg. Allg. Chem.* **1997**, *623*, 1255.
- (442) Greenwood, B. P.; Forman, S. I.; Rowe, G. T.; Chen, C.-H.; Foxman, B. M.; Thomas, C. M. *Inorg. Chem.* **2009**, *48*, 6251.
- (443) Greenwood, B. P.; Rowe, G. T.; Chen, C.-H.; Foxman, B. M.; Thomas, C. M. *J. Am. Chem. Soc.* **2010**, *132*, 44.
- (444) Kovacs, J. A.; Holm, R. H. *J. Am. Chem. Soc.* **1986**, *108*, 340.
- (445) Akashi, H.; Isobe, K.; Ozawa, Y.; Yagasaki, A. *J. Cluster Sci.* **1991**, *2*, 291.
- (446) Hayashi, Y.; Ozawa, Y.; Isobe, K. *Chem. Lett.* **1989**, *18*, 425.
- (447) (a) Nikanova, O. A.; Seisenbaeva, G. A.; Kessler, V. G.; Shcheglov, P. A.; Drobot, D. V. *Russ. J. Inorg. Chem.* **2007**, *52*, 1687. (b) Nikanova, O. A.; Kessler, V. G.; Drobot, D. V.; Shcheglov, P. A.; Seisenbaeva, G. A. *Polyhedron* **2007**, *26*, 862.
- (448) Garner, C. D.; Senior, R. G. *J. Chem. Soc., Chem. Commun.* **1974**, 580.
- (449) Arndt, L.; Delord, T.; Darensbourg, M. Y. *J. Am. Chem. Soc.* **1984**, *106*, 456.
- (450) Jensen, M. P.; Henderson, W.; Johnston, D. H.; Sabat, M.; Shriner, D. F. *J. Organomet. Chem.* **1990**, *394*, 121.
- (451) Bonifaci, C.; Ceccon, A.; Gambaro, A.; Ganis, P.; Mantovani, L.; Santi, S.; Venzo, A. *J. Organomet. Chem.* **1994**, *475*, 267.
- (452) Bender, R.; Braunstein, P.; Jud, J.-M.; Dusausoy, Y. *Inorg. Chem.* **1983**, *22*, 3394.
- (453) Ehrl, W.; Vahrenkamp, H. *Chem. Ber.* **1973**, *106*, 2563.
- (454) Palermo, R. E.; Singh, R.; Bashkin, J. K.; Holm, R. H. *J. Am. Chem. Soc.* **1984**, *106*, 2600.
- (455) (a) Braunstein, P.; Jud, J.-M.; Tiripicchio, A.; Tiripicchio-Camellini, M.; Sappa, E. *Angew. Chem., Int. Ed. Engl.* **1982**, *21*, 307. (b) Williams, P. D.; Curtis, M. D.; Duffy, D. N.; Butler, W. M. *Organometallics* **1983**, *2*, 165.
- (456) Curtis, M. D.; Williams, P. D. *Inorg. Chem.* **1983**, *22*, 2661.
- (457) Richter, F.; Vahrenkamp, H. *Angew. Chem., Int. Ed. Engl.* **1978**, *17*, 864.
- (458) Straub, T.; Haukka, M.; Pakkanen, T. A. *J. Organomet. Chem.* **2000**, *612*, 106.
- (459) (a) Richter, F.; Roland, E.; Vahrenkamp, H. *Chem. Ber.* **1984**, *117*, 2429. (b) Adams, R. D.; Babin, J. E.; Tasi, M. *Angew. Chem., Int. Ed. Engl.* **1987**, *26*, 685.
- (460) Herbst, K.; Monari, M.; Brorson, M. *Inorg. Chem.* **2001**, *40*, 2979.
- (461) Schacht, H.-T.; Vahrenkamp, H. *Chem. Ber.* **1989**, *122*, 2239.
- (462) Roland, E.; Vahrenkamp, H. *Chem. Ber.* **1984**, *117*, 1039.
- (463) Churchill, M. R.; Hollander, F. J.; Shapley, J. R.; Foose, D. S. J. *Chem. Soc., Chem. Commun.* **1978**, 534.
- (464) Beurich, H.; Vahrenkamp, H. *Angew. Chem., Int. Ed. Engl.* **1978**, *17*, 863.
- (465) Brunner, H.; Wachter, J. *J. Organomet. Chem.* **1982**, *240*, C41.
- (466) Banares, M. A.; Dauphin, L.; Lei, X.; Cen, W.; Shang, M.; Wolf, E. E.; Fehlner, T. P. *Chem. Mater.* **1995**, *7*, 553.
- (467) Beurich, H.; Vahrenkamp, H. *Angew. Chem., Int. Ed. Engl.* **1981**, *20*, 98.
- (468) Walther, B.; Scheer, M.; Böttcher, H.-C.; Trunschke, A.; Ewald, H.; Gutschick, D.; Miessner, H.; Skupin, M.; Vorbeck, G. *Inorg. Chim. Acta* **1989**, *156*, 285.
- (469) Seino, H.; Hidai, M.; Mizobe, Y. *Chem. Lett.* **2002**, *31*, 920.
- (470) Do, Y.; You, X. Z.; Zhang, C.; Ozawa, Y.; Isobe, K. *J. Am. Chem. Soc.* **1991**, *113*, 5892.
- (471) Hayashi, Y.; Toriumi, K.; Isobe, K. *J. Am. Chem. Soc.* **1988**, *110*, 3666.
- (472) Churchill, M. R.; Bueno, C.; Hutchinson, J. P. *J. Organomet. Chem.* **1986**, *312*, 121.
- (473) Lucas, N. T.; Humphrey, M. G.; Hockless, D. C. R. *J. Organomet. Chem.* **1997**, *535*, 175.
- (474) Dimmock, P. W.; Lamprecht, G. J.; Sykes, A. G. *J. Chem. Soc., Dalton Trans.* **1991**, 955.
- (475) Wang, X.; Zhang, Z. *Jiegou Huaxue* **1987**, *6*, 1.
- (476) Zhao, W.; Fang, Y.; Zhang, S.; Li, Y.; Zhang, Z.; Wang, X. *Lizi Jiaohuan Yu Xifu* **1992**, *8*, 39.
- (477) Bender, R.; Braunstein, P.; Dusausoy, Y.; Protas, J. *Angew. Chem., Int. Ed. Engl.* **1978**, *17*, 596.
- (478) Murata, T.; Gao, H.; Mizobe, Y.; Nakano, F.; Motomura, S.; Tanase, T.; Yano, S.; Hidai, M. *J. Am. Chem. Soc.* **1992**, *114*, 8287.
- (479) Herbst, K.; Rink, B.; Dahlenburg, L.; Brorson, M. *Organometallics* **2001**, *20*, 3655.
- (480) Stromnova, T. A.; Busygina, I. N.; Katser, S. B.; Antsyshkina, A. S.; Porai-Koshits, M. A.; Moiseev, I. I. *J. Chem. Soc., Chem. Commun.* **1988**, *114*.
- (481) Bender, R.; Braunstein, P.; Jud, J.-M.; Dusausoy, Y. *Inorg. Chem.* **1984**, *23*, 4489.
- (482) Bender, R.; Braunstein, P.; Dusausoy, Y.; Protas, J. *J. Organomet. Chem.* **1979**, *172*, C51.
- (483) Lee, U.; Sasaki, Y. *Chem. Lett.* **1984**, *13*, 1297.
- (484) Feliz, M.; Garriga, J. M.; Llusar, R.; Uriel, S.; Humphrey, M. G.; Lucas, N. T.; Samoc, M.; Luther-Davies, B. *Inorg. Chem.* **2001**, *40*, 6132.
- (485) Müller, M.; Vahrenkamp, H. *Chem. Ber.* **1983**, *116*, 2322.

- (486) Fajardo, M.; Gómez-sal, M. P.; Johnson, B. F. G.; Lewis, J.; Raithby, P. R. *J. Organomet. Chem.* **1984**, 272, C57.
- (487) Shulman, P. M.; Burkhardt, E. D.; Lundquist, E. G.; Pilato, R. S.; Geoffroy, G. L.; Rheingold, A. L. *Organometallics* **1987**, 6, 101.
- (488) Barbier, J.-P.; Braunstein, P. *J. Chem. Res., Synop.* **1978**, 412.
- (489) Ehrl, W.; Vahrenkamp, H. *Chem. Ber.* **1973**, 106, 2556.
- (490) Ruff, J. K. *Inorg. Chem.* **1968**, 7, 1818.
- (491) Anders, U.; Graham, W. A. G. *Chem. Commun. (London)* **1966**, 291.
- (492) Blake, A. B.; Yavari, A.; Hatfield, W. E.; Sethulekshmi, C. N. J. *Chem. Soc., Dalton Trans.* **1985**, 2509.
- (493) Evans, G. O.; Wozniak, W. T.; Sheline, R. K. *Inorg. Chem.* **1970**, 9, 979.
- (494) Joshi, K. K.; Pauson, P. L. Z. *Naturforsch.* **1962**, 17b, 565.
- (495) Knight, J.; Mays, M. J. *J. Chem. Soc., Dalton Trans.* **1972**, 1022.
- (496) Ma, L.; Wilson, S. R.; Shapley, J. R. *J. Am. Chem. Soc.* **1994**, 116, 787.
- (497) Urbancic, M. A.; Wilson, S. R.; Shapley, J. R. *Inorg. Chem.* **1984**, 23, 2954.
- (498) Yawney, D. B. W.; Stone, F. G. A. *J. Chem. Soc. A* **1969**, 502.
- (499) Venäläinen, T.; Pakkanen, T. *J. Organomet. Chem.* **1984**, 266, 269.
- (500) Geoffroy, G. L.; Fox, J. R.; Burkhardt, E.; Foley, H. C.; Harley, A. D.; Rosen, R.; *Inorganic Syntheses*; John Wiley & Sons, Inc.: New York, 1982, 21, 57.
- (501) Müller, M.; Vahrenkamp, H. *Chem. Ber.* **1983**, 116, 2311.
- (502) Churchill, M. R.; Bueno, C.; Hsu, W. L.; Plotkin, J. S.; Shore, S. G. *Inorg. Chem.* **1982**, 21, 1958.
- (503) Richter, F.; Beurich, H.; Vahrenkamp, H. *J. Organomet. Chem.* **1979**, 166, CS.
- (504) Chini, P.; Colli, L.; Paraldo, M. *Gazz. Chim. Ital.* **1960**, 90, 1005.
- (505) Braunstein, P.; Rosé, J.; Granger, P.; Raya, J.; Bouaoud, S. E.; Grandjean, D. *Organometallics* **1991**, 10, 3686.
- (506) Knight, J.; Mays, M. J. *J. Chem. Soc. A* **1970**, 654.
- (507) Vahrenkamp, H.; Wucherer, E. *J. Angew. Chem., Int. Ed. Engl.* **1981**, 20, 680.
- (508) Steinhardt, P. C.; Gladfelter, W. L.; Harley, A. D.; Fox, J. R.; Geoffroy, G. L. *Inorg. Chem.* **1980**, 19, 332.
- (509) Ceriotti, A.; Longoni, G.; Della Pergola, R.; Heaton, B. T.; Smith, D. O. *J. Chem. Soc., Dalton Trans.* **1983**, 1433.
- (510) Hriljac, J. A.; Holt, E. M.; Shriver, D. F. *Inorg. Chem.* **1987**, 26, 2943.
- (511) Gubin, S. P.; Mikova, N. M.; Tsybenov, M. T.; Lopatin, V. E. *Koord. Khim.* **1984**, 10, 625.
- (512) Lopatin, V. E.; Mikova, N. M.; Gubin, S. P. *Izv. Akad. Nauk SSSR, Ser. Khim.* **1983**, 1407.
- (513) Fumagalli, A., private communication.
- (514) Della Pergola, R.; Garlaschelli, L.; Demartin, F.; Manassero, M.; Masciocchi, N.; Sansoni, M. *J. Chem. Soc., Dalton Trans.* **1990**, 127.
- (515) Della Pergola, R.; Ceriotti, A.; Garlaschelli, L.; Demartin, F.; Manassero, M.; Masciocchi, N.; Sansoni, M. *Inorg. Chem.* **1993**, 32, 3277.
- (516) Braunstein, P.; Kervennal, J.; Richert, J.-L.; Ries, M. FR Patent 2,558,074, 1985, U.S. Patent 4,609,639, 1985, ATOCHEM.
- (517) Braunstein, P.; de Méric de Bellefon, C.; Ries, M.; Fischer, J. *Organometallics* **1988**, 7, 332.
- (518) Longoni, G.; Manassero, M.; Sansoni, M. *J. Am. Chem. Soc.* **1980**, 102, 3242.
- (519) Barbier, J.-P.; Braunstein, P. *J. Chem. Res., Miniprint* **1978**, 5029.
- (520) Adams, R. D.; Arafa, I.; Chen, G.; Lii, J. C.; Wang, J. G. *Organometallics* **1990**, 9, 2350.
- (521) Longoni, G.; Manassero, M.; Sansoni, M. *J. Am. Chem. Soc.* **1980**, 102, 7973.
- (522) Albano, V. G.; Aureli, R.; Iapalucci, M. C.; Laschi, F.; Longoni, G.; Monari, M.; Zanello, P. *J. Chem. Soc., Chem. Commun.* **1993**, 1501.
- (523) Albano, V. G.; Calderoni, F.; Iapalucci, M. C.; Longoni, G.; Monari, M. *J. Chem. Soc., Chem. Commun.* **1995**, 433.
- (524) (a) Roland, E.; Vahrenkamp, H. *Angew. Chem., Int. Ed. Engl.* **1981**, 20, 679. (b) Roland, E.; Vahrenkamp, H. *Chem. Ber.* **1985**, 118, 1133.
- (525) (a) Roland, E.; Vahrenkamp, H. *Organometallics* **1983**, 2, 1048. (b) Roland, E.; Bernhardt, W.; Vahrenkamp, H. *Chem. Ber.* **1986**, 119, 2566.
- (526) Roland, E.; Vahrenkamp, H. *Organometallics* **1983**, 2, 183.
- (527) Gladfelter, W. L.; Geoffroy, G. L.; Calabrese, J. C. *Inorg. Chem.* **1980**, 19, 2569.
- (528) Pursiainen, J.; Pakkanen, T. A.; Jääskeläinen, J. *J. Organomet. Chem.* **1985**, 290, 85.
- (529) Fumagalli, A.; Ciani, G. *J. Organomet. Chem.* **1984**, 272, 91.
- (530) Pursiainen, J.; Pakkanen, T. A.; Smolander, K. *J. Chem. Soc., Dalton Trans.* **1987**, 781.
- (531) (a) Pursiainen, J.; Pakkanen, T. A. *J. Chem. Soc., Chem. Commun.* **1984**, 252. (b) Pursiainen, J.; Pakkanen, T. A.; Heaton, B. T.; Seregni, C.; Goodfellow, R. G. *J. Chem. Soc., Dalton Trans.* **1986**, 681.
- (532) Süss-Fink, G.; Haak, S.; Ferrand, V.; Stoeckli-Evans, H. *J. Chem. Soc., Dalton Trans.* **1997**, 3861.
- (533) Lavigne, G.; Papageorgiou, F.; Bergounhou, C.; Bonnet, J. J. *Inorg. Chem.* **1983**, 22, 2485.
- (534) Shapley, P. A.; Liang, H.-C.; Dopke, N. C. *Organometallics* **2001**, 20, 4700.
- (535) Brivio, E.; Ceriotti, A.; Della Pergola, R.; Garlaschelli, L.; Demartin, F.; Manassero, M.; Sansoni, M.; Zanello, P.; Laschi, F.; Heaton, B. T. *J. Chem. Soc., Dalton Trans.* **1994**, 3237.
- (536) Adams, R. D.; Wu, W. *Organometallics* **1993**, 12, 1248.
- (537) Adams, R. D.; Chen, G.; Wu, W. *J. Cluster Sci.* **1993**, 4, 119.
- (538) Adams, R. D.; Wu, W. *J. Cluster Sci.* **1991**, 2, 271.
- (539) (a) Adams, R. D.; Captain, B.; Fu, W.; Pellechia, P. J.; Smith, M. D. *Inorg. Chem.* **2003**, 42, 2094. (b) Adams, R. D.; Captain, B.; Fu, W.; Pellechia, P. J.; Smith, M. D. *Angew. Chem., Int. Ed.* **2002**, 41, 1951.
- (540) Khimyak, T.; Johnson, B. F. G.; Hermans, S.; Bond, A. D. *Dalton Trans.* **2003**, 2651.
- (541) Adams, R. D.; Captain, B.; Fu, W. *J. Organomet. Chem.* **2003**, 671, 158.
- (542) Johnson, B. F. G.; Hermans, S.; Khimyak, T. *Eur. J. Inorg. Chem.* **2003**, 1325.
- (543) Fumagalli, A.; Garlaschelli, L.; Della Pergola, R. *J. Organomet. Chem.* **1989**, 362, 197.
- (544) Sundberg, P.; Norén, B.; Johnson, B. F. G.; Lewis, J.; Raithby, P. R. *J. Organomet. Chem.* **1988**, 353, 383.
- (545) Farrugia, L. J.; Howard, J. A. K.; Mitrprachachon, P.; Stone, F. G. A.; Woodward, P. *J. Chem. Soc., Dalton Trans.* **1981**, 171.
- (546) Shore, S. G.; Hsu, W. L.; Weisenberger, C. R.; Caste, M. L.; Churchill, M. R.; Bueno, C. *Organometallics* **1982**, 1, 1405.
- (547) Sappa, E.; Valle, M.; Predieri, G.; Tiripicchio, A. *Inorg. Chim. Acta* **1984**, 88, L23.
- (548) Sappa, E.; Lanfranchi, M.; Tiripicchio, A.; Camellini, M. T. *J. Chem. Soc., Chem. Commun.* **1981**, 995.
- (549) Horvath, I. T.; Bor, G.; Garland, M.; Pino, P. *Organometallics* **1986**, 5, 1441.
- (550) Ojima, I.; Clos, N.; Donovan, R. J.; Ingallina, P. *Organometallics* **1991**, 10, 3211.
- (551) Martinengo, S.; Chini, P.; Albano, V. G.; Cariati, F.; Salvatori, T. *J. Organomet. Chem.* **1973**, 59, 379.
- (552) Komine, N.; Hoh, H.; Hirano, M.; Komiya, S. *Organometallics* **2000**, 19, 5251.
- (553) Davies, H. M. L.; Dick, A. R. *Top. Curr. Chem.* **2010**, 292, 303.
- (554) Fukuoka, A.; Sadashima, T.; Sugiura, T.; Wu, X.; Mizuho, Y.; Komiya, S. *J. Organomet. Chem.* **1994**, 473, 139.
- (555) Dehand, J.; Nennig, J. F. *Inorg. Nucl. Chem. Lett.* **1974**, 10, 875.
- (556) Gallo, V.; Mastorilli, P.; Nobile, C. F.; Braunstein, P.; Englert, U. *Dalton Trans.* **2006**, 2342.
- (557) Braunstein, P.; Dehand, J.; Nennig, J. F. *J. Organomet. Chem.* **1975**, 92, 117.
- (558) Barbier, J.-P.; Braunstein, P.; Fischer, J.; Ricard, L. *Inorg. Chim. Acta* **1978**, 31, L361.

- (559) Doyle, G.; Eriksen, K. A. *Organometallics* **1985**, *4*, 877.
- (560) Hieber, W.; Teller, U. Z. *Anorg. Allg. Chem.* **1942**, *249*, 43.
- (561) Cen, W.; Haller, K. J.; Fehlner, T. P. *Inorg. Chem.* **1991**, *30*, 3120.
- (562) Fumagalli, A.; Martinengo, S.; Chini, P.; Galli, D.; Heaton, B. T.; Della Pergola, R. *Inorg. Chem.* **1984**, *23*, 2947.
- (563) Xu, Z.; Kawi, S.; Rheingold, A. L.; Gates, B. C. *Inorg. Chem.* **1994**, *33*, 4415.
- (564) Kozitsyna, N. Y.; Nefedov, S. E.; Dolgushin, F. M.; Cherkashina, N. V.; Vargaftik, M. N.; Moiseev, I. I. *Inorg. Chim. Acta* **2006**, *359*, 2072.
- (565) Espinet, P.; Fornies, J.; Martinez, F.; Tomas, M.; Lalinde, E.; Moreno, M. T.; Ruiz, A.; Welch, A. J. *J. Chem. Soc., Dalton Trans.* **1990**, 791.
- (566) (a) Boyle, P. D.; Johnson, B. J.; Alexander, B. D.; Casalnuovo, J. A.; Gannon, P. R.; Johnson, S. M.; Larka, E. A.; Mueting, A. M.; Pignolet, L. H. *Inorg. Chem.* **1987**, *26*, 1346. (b) Ito, L. N.; Felicissimo, A. M. P.; Pignolet, L. H. *Inorg. Chem.* **1991**, *30*, 387.
- (567) Ito, L. N.; Sweet, J. D.; Mueting, A. M.; Pignolet, L. H.; Schoondergang, M. F. J.; Steggerda, J. J. *Inorg. Chem.* **1989**, *28*, 3696.
- (568) Kanters, R. P. F.; Bour, J. J.; Schlebos, P. P. J.; Bosman, W. P.; Behm, H.; Steggerda, J. J.; Ito, L. N.; Pignolet, L. H. *Inorg. Chem.* **1989**, *28*, 2591.
- (569) Kanters, R. P. F.; Schlebos, P. P. J.; Bour, J. J.; Bosman, W. P.; Behm, H. J.; Steggerda, J. J. *Inorg. Chem.* **1988**, *27*, 4034.